

ELASTODYNAMIC SOURCE THEORY

Thesis by

Charles B. Archambeau

In Partial Fulfillment of the Requirements

For the Degree of

Doctor of Philosophy

California Institute of Technology

Pasadena, California

1964

(Submitted June 8, 1964)

ACKNOWLEDGMENTS

The author most gratefully acknowledges the guidance and support of Dr. Frank Press throughout this study. Dr. Leon Knopoff also read portions of the work and supplied helpful comments and encouragement.

To many colleagues, particularly Drs. D. L. Anderson, A. Ben-Menahem, D. G. Harkrider, S. W. Smith and M. N. Toksoz, the author is indebted for many stimulating and useful discussions on various aspects of this work.

The author is especially grateful to Mr. Laszlo Lenches for preparation of the figures and to Mrs. A. Tingley for the difficult task of typing the manuscript.

During a period of this research the author held the Sinclair Oil Company Fellowship. In addition this research was partially supported by Contract AF-49(638)-1337. The author is most grateful for the support from all these sources.

ABSTRACT

The mathematical formulation and evaluation of the radiation field for general elastodynamic sources is given and applications of the theory to the description of source fields of geophysical interest are treated. The study was primarily undertaken to provide a theoretical basis for estimating the properties of the tectonic stress field and parameters of rupture phenomenon in the earth through observations of the radiation field from earthquakes and other tectonic sources.

Thus the description of the tectonic source is particularly emphasized, both as to its physical origins and with respect to the radiation field to be expected from it. The mathematical description of the tectonic source field is achieved in terms of an elastic relaxation theory of radiation which corresponds to a generalized initial value problem involving the initial prestress field. As a consequence, the radiation field is obtained in terms of the rupture expansion rate (velocity of rupture), the rupture dimensions and orientation and the magnitude and orientation of the initial stress field. Inertial conditions are inherent in the relaxation theory so that the time dependence of the field is automatically specified. Careful attention is given to causality relationships so that the resulting field expressions contain the complicated space-time relationships associated with a tectonic source field. Energy and equilibrium relations are considered and expressions are obtained for the estimated energy release and the final static field in terms of the source parameters.

Detailed properties of the radiation field are given in the form of source field amplitude and phase spectra. Spatial radiation patterns are obtained showing the direction properties as functions of frequency, prestress and other source parameters. Similar results are given for shock induced rupture under prestress conditions, along with estimates of tectonic energy release.

It is concluded that the theoretical predictions for the properties of the radiation field from a spontaneous rupture source are in general agreement with the actual observations of the field from such a source, but that accurate estimates of the prestress and rupture parameters require a more complete coverage and analysis of the field than is usually the case. It is concluded from a preliminary analysis of the Ranier nuclear explosion that tectonic energy release did occur and that the anomalous radiation observed would correspond to a prestress shear field of the order of 20 bars.

The most likely mechanism of rupture at depth in the earth is considered to be unstable creep phenomenon resulting in phase change (melting) and the rupture source models adopted are not inconsistent with this hypothesis.

TABLE OF CONTENTS

	<u>Page</u>
Chapter 1	
Elastodynamic Source Theory and its Application to Tectonic Sources.....	1
(1. 1) Historical Development.....	1
(1. 2) Scope, Objectives and Methods of the Present Study.....	3
Chapter 2	
Mathematical Theory of Elastodynamic Sources.....	12
(2. 1) Introduction.....	12
(2. 2) Fundamental Relations.....	14
(2. 3) Elementary Multipole Representations..... for Stationary Sources.....	33
(2. 4) Multipole Representations of Arbitrary (non-stationary) Sources.....	38
(2. 5) Evaluation of the Static Displacement Field.....	41
(2. 6) Evaluation of the Primary Dynamic Radiation Field: The Propagation Function.....	45
(2. 7) Representations for Initial Value (Relaxation) Sources.....	54
(2. 8) Transformations of the Primary Field for the Initial Value Source.....	63
(2. 9) General Representations for Finite Volume Sources.....	70
(2. 10) Summary of Theoretical Results.....	77
Chapter 3	
Tectonic Source Theory.....	79
(3. 1) Introduction.....	79
(3. 2) Macroscopic Mechanisms of Seismic Rupture.....	80
(3. 3) A Comparative Review of Tectonic Source Theory.....	88

	<u>Page</u>
(3.4) The Physics of Dislocation Rupture in the Earth.....	104
(3.5) Compatibility of the Macroscopic and Microscopic Mechanisms of Seismic Rupture.....	114
(3.6) Approximations for Dynamical Models of the Tectonic Source.....	118
(3.7) Basic Equilibrium Relationships.....	124
(3.8) Radiation Energy from Elastic Relaxation Sources.....	131
(3.9) Dynamical Elastic Relaxation.....	141
(3.10) Rupture Propagation and Growth Effects....	154
(3.11) Primary Field Potentials for Natural Tectonic Sources: Expanding Ellipsoidal Ruptures.....	173
(3.12) Primary Field Potentials for Natural Tectonic Sources: Propagating Ruptures.....	189
(3.13) Shock Induced Tectonic Radiation from a Homogeneously Prestrained Medium.....	210
(3.14) Tectonic Radiation due to Spontaneous Rupture in a Homogeneously Prestrained Medium.....	224
 Chapter 4	
Preliminary Applications of the Theory.....	238
(4.1) Introduction.....	238
(4.2) The Radiation Field from Natural Tectonic Sources as a Function of Rupture Dynamics and Geometry.....	243
(4.3) Energy from Tectonic Sources.....	251
(4.4) Scaling Laws for Tectonic Energy Release Associated with Explosive Sources.....	255
(4.5) The Anomalous Tectonic Radiation from an Explosive Source in a Homogeneously Prestrained Medium and Comparisons with Spontaneous Rupture	267
 Chapter 5	
Conclusions.....	272
(5.1) A Resume of Results and Conclusions.....	272

	<u>Page</u>
References.....	276
Appendices.....	282
(1) Multipole Coefficients.....	282
(2) A Theorem for Harmonic Functions.....	291
(3) Transformations of the Static Source Field....	294
(4) Transformations of the Cartesian Vector Displacement Field to Curvilinear Coordinates.....	304
(5) Solution Coefficients for Expanding Ellipsoidal Ruptures.....	309
(6) Solution Coefficients for Propagating Rupture Models.	314
(7) Stress-strain Relations in Ellipsoidal Coordinates as Functions of the Harmonic Potentials ϕ and ω	318
(8) Ellipsoidal Harmonics.....	328
(9) Expansion of Ellipsoidal Harmonics in Terms of Spherical Harmonics.....	336
(10) Strain coefficients P_{ij} , Q_{ij}	340
(11) Table of Symbols and Special Functions.....	341
Figure Captions.....	350
Illustrations.....	359

Chapter 1

ELASTODYNAMIC SOURCE THEORY AND ITS APPLICATION TO TECTONIC SOURCES

1.1. Historical Development

The basis for a theory of elastic sources was already well developed by the middle of the last century (see for example Love, 1944). Indeed a complete mathematical statement of the theory describing elastodynamic source radiation has been known since that time and can be set down, at least formally, in a single line in terms of a Green's function formulation (e. g. , Morse and Feshbach, 1953). In a logical sense then, successive theoretical work has constituted various applications of this formulation.

In contrast to the activity in electromagnetic source theory however, there seems to have been no very great motivation to apply the formal theory to the study of natural sources of elastic radiation, even though there were no doubt as many earthquakes in the last century as in this. It is perhaps the aura of mystery that yet surrounds this particular phenomenon (e. g. , the belief that it is chaotic), even in the scientific mind, that precluded more profound work on this subject. Certainly such an investigation was within the capabilities and fields of interest of many scientists of the day. In any event, current interest in Geophysics, particularly seismology, seems to be rapidly changing the situation toward a more deterministic point of view.

Thus Love's work, undertaken at the beginning of this century

and based on the consideration of various simple point forces and couples within or on the surface of an elastic medium, using methods developed by Kelvin and Lorenz (Love, 1944), was utilized twenty years later as a means of describing the source mechanism of an earthquake. (For reviews and extensive bibliographies, see Honda (1957, 1962) or Balakina, Savarenski and Vvedenskaya (1961) wherein the original work of Byerly, Hodgson, Nakano and others is discussed.)

While the first approach appears to be inadequate in many respects, it does nevertheless provide some information concerning the character of this source. In the last decade or two a host of theories and models have been proposed and compared to the facts with varying degrees of success. By and large they are of two types, either based on the dislocation theory (e. g., Knopoff and Gilbert (1959, 1960); Balakina, Savarenski and Vvedonskaya (1961); Steketee (1958); Droste and Teisseyre (1956, 1960); Housner (1955)), first proposed by Volterra (1907), or are generalized point source theories employing propagation of the source to describe the phenomenon of rupture (Ben Menahem, 1961). These recent source theories have generally attempted to model the rupture phenomenon in order to predict the radiation field while earlier models were in the nature of equivalent sources, deduced from incomplete observations of the radiation field. Most of these models and theories are summarized in section 3.3 where they are compared to some of the results and conclusions of the present study.

1. 2. Scope, Objectives and Methods of the Present Study

The Chapters following the present introduction are relatively self contained, as in fact are most of the sections into which they are divided. The intention is to present a definitive study of the elastodynamic source in a form which lends itself to direct practical application with respect to natural and induced sources within the earth. In this regard the most important consideration to be undertaken is a description of tectonic sources, both as to their probable cause and with respect to the radiation field to be expected from them.

The present study provides a dual result in that the purely mathematical formulation and evaluation of the source field for a group of very general sources is given and second a detailed and explicit dynamical field theory for tectonic sources is obtained. The latter incorporates the important physical properties of the rupture expansion rate or velocity, the physical orientation, location and dimensions of the rupture, the time dependence of the radiation field and the magnitude and orientation of the initial stress field in the vicinity of the rupture. This tectonic source theory is considered in the light of what is known and implied by experimental work concerning the physics of the rupture processes within the earth and several detailed models are adopted, consistent with these implications. Evaluation and numerical investigation of the resulting solutions as functions of the source parameters, particularly the initial stress field and rate of rupture expansion,

is given in order to clearly delineate the complicated radiation properties of this source. In addition, a theory of induced tectonic radiation, resulting from an explosive source in prestressed media, is proposed and considered simultaneously with the theory of spontaneous rupture. Thus, expressions for the dynamic and static fields to be expected from these tectonic source types are given along with numerical examples and theoretical energy estimates.

An ultimate objective of this study is to provide the theoretical basis for a detailed study of the stress field within the earth through observations of the radiation field from both earthquakes and large nuclear or chemical explosions in a prestressed medium. A more immediate objective is to provide the means for a better understanding of the mechanisms of spontaneous rupture through observations of the radiation field. In the realization of these goals it is intended that explosive induced tectonic sources assume the role of controlled experiments wherein most of the source parameters are known beforehand. A demonstration of the approach is given in chapter 4 of this study. The second and third chapters are devoted to the detailed evaluation of the radiation field from general elastodynamic sources along with an explanation and formulation of the tectonic source as an elastic relaxation phenomenon associated with the initial elastic stress field. Chapter 4 then presents some of the properties of the tectonic source in the form of radiation patterns and *spectra* along with some preliminary

applications.

In total the study constitutes a very detailed investigation of the elastodynamic source from the theoretical point of view. With due regard to previous theories of the tectonic source, it is concluded that this particular type of source arises from the relaxation of an initial shear stress field in response to the growth of a rupture within which the rigidity modulus is vanishingly small, implying that phase change (melting) is the mechanism of tectonic rupture or is, at least, intimately associated with it. In this case a condition of vanishing shear stress at the expanding rupture boundary applies and the initial stress field must adjust to this boundary condition, so that elastic radiation from the stressed medium exterior to the rupture ensues and thereby the stress is reduced to the required levels. The phenomenon is formulated as a generalized initial value problem thereby allowing the resulting radiation field to be described and investigated in complete detail. By this approach both the final static field and the total energy radiated are also obtained in terms of the initial stress field and the other source and medium parameters.

The initial chapter in this investigation serves, in part, as a mathematical introduction to the remaining discussion. In particular the basic formulation of the source problem is reviewed (section 2.2) and emphasis is placed upon the initial value problem and its relationship to elastodynamic source theory. The basic relationship of the radiation field to the equilibrium field of the

elastic medium is emphasized, in particular for cases in which the medium is initially in a prestressed condition. The essentials of the boundary value problem arising in practical applications of the source theory to determine the excitation of layered models of the earth is also given and the form of the solutions is specified. Next the sources are classified as to their mathematical form, that is according to whether the source function appearing in the equations of motion is a separable function of the spatial coordinates and time or not. Elementary multipole expansions are obtained for the two general types of source by a technique corresponding to a generalization of that used by Love, Kelvin and Lorenz (Love, 1944) for more specialized sources (sections 2.3-2.6). Interestingly enough it is shown that a rather simple relationship exists between the dynamic and static displacement fields due to an externally applied force field. The effect of non-separability of the source function is deduced and comparison made with the case in which the source function is separable. This phase of the investigation is meant to provide a degree of insight to the general source problem as well as explicit expressions for the field due to an externally applied force system, as opposed to a relaxation source. An alternate expansion for such a force system is given in section (2.9) in a form more amenable to practical use. Consideration is also given to sources of the relaxation type (section 2.7), where an elementary initial value source, suitable for later generalization in the description of the tectonic source, is evaluated by making

use of the special properties of the equilibrium field to which the dynamical field is, for this source, directly and intimately related. The essential results of the chapter are summarized briefly in section (2.10) as an aid to rapid comprehension of the theoretical discussion.

The following chapter (3) deals in detail with the tectonic source as the central problem of this study. The general physical concepts leading to the description of the tectonic source in terms of elastic relaxation are discussed in section (3.2) while the following section (3.3) is devoted to a review of previous theories and models of the tectonic source. These earlier ideas and models are compared to the preliminary results of chapter 2 and the general physical concepts advanced from the viewpoint of the present study.

The next three sections are concerned with the physical realizability of the various models and theories of tectonic rupture, including those of the present study. Underlying the discussion is the contention that the macroscopic *theory* advanced to model the rupture phenomenon, to the extent necessary for a description of the radiation field, be at least compatible with the following conditions:

- (1) The physical mechanism of rupture implied by the theory must result in a net reduction of stored elastic energy within the medium.
- (2) The mechanism must restore the system (the finite medium) to a final state of equilibrium.

- (3) The mechanism must be more likely to occur under the thermodynamic (and stress) conditions within the earth than other competing mechanisms.

While the mechanism of rupture is undoubtedly nonlinear it is clear that these conditions are independent of this particular detail.

On the basis of the first of these conditions, most of the dislocation theories are rejected as physical models since the potential energy of the system can be shown to increase upon their creation. They are therefore in the classification of the largely arbitrary "equivalent sources" along with the equivalent point forces and couples often used to model an earthquake, the meaning and validity of which are considered, in this study at least, to be in serious doubt. From a review of the microscopic theory of deformation and rupture as well as from a review of the experimental evidence (section 3.4) it is concluded along with Orowan, Handin and Griggs (1960), on the basis of the condition (3) above, that unstable creep resulting in strain concentration and eventual phase change is the most likely mechanism of rupture at depths below a few kilometers in the earth, while ordinary fracture phenomenon is rejected as a much less likely competing mechanism. The macroscopic manifestations of the creep mechanism are also considered as they relate to aftershock phenomenon, the observations of reduced rigidity in long linear fault zones at the surface and the like.

With this background the present theory is discussed in

terms of its compatibility with the microscopic physical theory of rupture (section 3.5) and found to be adequate. The following section (3.6) discusses some of the approximations nevertheless inherent in the present theory and concludes that the effects neglected are likely to be small. The likelihood of fracture phenomenon at shallow depths is noted and special detailed source models are advanced to deal with this contingency.

Sections (3.7) and (3.8) show that the first and second of the conditions indicated above are satisfied by an elastic relaxation source theory. In addition, theoretical expressions for the energy released by such a source are obtained and the mathematical formulation of the basic equilibrium problem for the source is given for later application in the dynamical theory. These sections provide the essential physical insight to the theory as well as its formal justification.

The following sections (3.9) and (3.10) give the detailed formulation of the dynamical theory for the source and these constitute the main theoretical results of the present study. Throughout, careful attention is given to causality relationships and inertial effects so that the resulting expressions contain the complicated space-time relationships inherent in such a source. The remaining sections of the chapter give the detailed evaluations of the fields for models of rupture consistent with either spontaneous rupture or shock induced rupture. The results are expressed in forms which lend themselves to the explicit computations required for

the detailed investigations considered in chapter 4.

Chapter 4 takes up a preliminary investigation of the source theory given in the preceding sections. Many of the important properties of the radiation field are graphically illustrated (in the form of radiation patterns and spectra) and it is found from these numerical studies that the source theory is in agreement with what is already known or suspected concerning the radiation fields from earthquakes, while also providing additional precise theoretical predictions. In particular the effects of rupture expansion are clearly evident in the directional asymmetry of the radiation field. The directional properties of the phase and amplitude spectra are observed to be frequency dependent. The directional properties of the amplitude are similar to those obtained by Ben Menahem (1961) for wavelengths approaching the length of rupture. The properties of the source field are investigated for wavelengths both shorter than, equal to and much longer than the rupture length and the character of the source is discussed for each of those ranges. Both the amplitude and phase characteristics of the source field are found to be sensitive functions of the initial stress field magnitude and orientation. Rupture orientation with respect to the earth's free surface is investigated in a preliminary manner and it is found that there are considerable differences to be expected between "strike slip" and "dip slip" ruptures due to differences in the direction of rupture expansion and in the orientation of the initial stress field.

By virtue of this effort, a means of automatic computation of the source field exists so that additional, more extensive numerical studies and applications can be made in future studies with relative ease.

A basic theoretical study of the question of tectonic energy release by explosions producing shock induced rupture is initiated by considerations of energy release from a tectonic stress field. A means of estimating the tectonic energy release as a function of the explosive energy and the initial prestress field is devised on the combined basis of the work of Haskell (1961) and Press and Archambeau (1962), and applied to a particular case. The anomalous radiation field associated with the tectonic energy release is also computed and compared to that obtained for spontaneous rupture from a source of similar energy.

Since a very large number of symbols and special functions are used, an appendix listing most of these quantities is included (Appendix (11)). The symbols and functions are therein defined and reference is given to the equation or section in which they are first introduced or defined.

The conclusions of the study are summarized in the final chapter.

Chapter 2

MATHEMATICAL THEORY OF ELASTODYNAMIC SOURCES

2.1. Introduction

The present chapter is devoted primarily to a formal logical development of the source theory and its relationship to general boundary value problems of interest. The representations are effected in terms of potential fields, since the potential method is found to be the most flexible in the representation of very complicated sources. In this regard the dilatation and rotation vector are found to be most usefully employed.

The formalism of an initial value problem, first given by Poisson (Love, 1944) for elastic wave propagation, is used in a somewhat generalized form to describe a relaxation source of an elementary type. This elementary source solution will be used to generate a rupture source field by a superposition technique in chapter 3.

The practicality of the present investigations are enhanced by the successful formulation of the direct field from the source in terms of eigenfunction expansions in spherical, rectangular and cylindrical coordinates. These expansions of the source field allow computation of the radiation field to be extended throughout a layered model of the earth, so that both "body wave" and "surface wave" excitation may be predicted. Such a capability is of course required for the experimental determination of source properties inasmuch as the prediction of the elastic field at the earth's

surface depends upon it.

There have been many previous mathematical treatments of elastodynamic sources. From a purely mathematical standpoint, every representation is or may be obtained from a Green's function integral solution, although it is often difficult to perceive clearly that this formulation underlies the theory in many particular cases. The basic integral formulation can vary of course, depending on whether vector or scalar equations are used, among other variables. In particular, the vector equation of motion can be treated directly or vector wave equations may be used, in either case the Green's function is a tensor (Morse and Feshbach, 1953, chapter 13). If scalar wave equations are used, the Green's function is a scalar function.

Thus, for example, in the present study potentials are introduced and only scalar wave equations are considered, so that a simple scalar Green's function is involved. On the other hand, Knopoff (1956) and deHoop (1958) consider the vector wave equations of elastodynamics using a tensor Green's function. The resulting representation theory is a very general one and is most appropriate to problems of diffraction. For source representation problems, however, the scalar theory is much more convenient. In addition, the initial value problem associated with stress relaxation is simply formulated, applied, and finally evaluated, through use of the properties of the potentials and the scalar Green's function.

2.2. Fundamental Relations

The equations of motion for a homogeneous, isotropic elastic solid may be written in the vector form

$$(\lambda + \mu)\nabla(\nabla \cdot \underline{u}) + \mu\nabla^2 \underline{u} + \rho \underline{f} = \rho \frac{\partial^2 \underline{u}}{\partial t^2} \quad (2.2.1)$$

where \underline{f} denotes the body force density and \underline{u} the displacement vector. The vector $\underline{f} = \rho \underline{f}$ may be used to represent a source within or on the boundary of the elastic solid, as is well known. Therefore, letting τ denote a source volume, B_τ a surface enclosing τ which will be called the source boundary, take \underline{f} to be constrained according to

$$\begin{aligned} \underline{f}(\underline{r}, t) &\neq 0, \quad \underline{r} \text{ within or on } B_\tau \\ \underline{f}(\underline{r}, t) &= 0, \quad \underline{r} \text{ exterior to } B_\tau \end{aligned} \quad (2.2.2)$$

In this representation, the source boundary need not be fixed in space (or time), nor need this 'boundary' necessarily represent a physical discontinuity in the medium.

Now, \underline{f} is a spatial and time dependent field and may be decomposed into the potential form

$$\underline{f} = \nabla\Phi + \nabla \times \underline{B} \quad (2.2.3)$$

where Φ and \underline{B} are scalar and vector functions of the spatial coordinates. For an unbounded medium, where the source boundary $B(\tau)$ is not a physical discontinuity or is 'at infinity', then (Love,

1944)

$$\begin{aligned}\Phi &= \frac{1}{4\pi} \iiint_{\tau} \left[\underline{f}' \cdot \nabla \left(\frac{1}{r^*} \right) \right] d\tau \\ \mathbf{B} &= \frac{1}{4\pi} \iiint_{\tau} \left[\underline{f}' \times \nabla \left(\frac{1}{r^*} \right) \right] d\tau\end{aligned}\tag{2.2.4}$$

The integration is over the primed coordinates throughout the whole space, \underline{f}' is the vector field as a function of the primed coordinates and

$$r^* = |\underline{r} - \underline{r}'|$$

with \underline{r} denoting the fixed distance from the origin of source coordinates to the point of observation (Figure 1). The relations (2.2.3) and (2.2.4) clearly hold whether \underline{f} is time dependent or not. Note that from (2.2.4), $\nabla \cdot \underline{B} = 0$.

Introducing the decomposition (2.2.3) into the equations of motion (2.2.1), and by decomposing the vector field \underline{u} to the form

$$\underline{u} = \nabla \delta + \nabla \times \psi$$

as is always possible, then it is found that (2.2.1) is satisfied, provided the potentials δ and ψ are solutions of

$$\begin{aligned}\nabla^2 \delta + \frac{\Phi}{\lambda + 2\mu} &= \frac{1}{v_p^2} \frac{\partial^2 \delta}{\partial t^2} \\ \nabla^2 \psi + \frac{1}{\mu} \underline{B} &= \frac{1}{v_s^2} \frac{\partial^2 \psi}{\partial t^2}\end{aligned}\tag{2.2.5}$$

where v_s and v_p are the shear and compressional wave velocities given by

$$v_p = \left[\frac{\lambda + 2\mu}{\rho} \right]^{1/2}, \quad v_s = \left[\frac{\mu}{\rho} \right]^{1/2}$$

Alternately, equation (2.2.1) may be written in the form

$$(\lambda + 2\mu)\nabla(\nabla \cdot \underline{u}) - \mu\nabla \times \nabla \times \underline{u} + \rho \underline{f} = \rho \frac{\partial^2}{\partial t^2} \underline{u} \quad (2.2.6)$$

Operating on this equation with the divergence and curl operators, defining

$$\begin{aligned} \Theta &= \nabla \cdot \underline{u} \\ \Omega &= \frac{1}{2} \nabla \times \underline{u} \end{aligned} \quad (2.2.7)$$

the dilatation and rotation, then (2.2.6) is satisfied if

$$\begin{aligned} \nabla^2 \Theta - \frac{1}{v_p^2} \frac{\partial^2 \Theta}{\partial t^2} &= - \frac{1}{\lambda + 2\mu} (\nabla \cdot \underline{f}) \\ \nabla^2 \underline{\Omega} - \frac{1}{v_s^2} \frac{\partial^2 \underline{\Omega}}{\partial t^2} &= - \frac{1}{2\mu} (\nabla \times \underline{f}) \end{aligned} \quad (2.2.8)$$

These equations are valid irrespective of the physical nature of the source boundary B_T and clearly, $\nabla \cdot \underline{\Omega} = 0$.

Invariably the source function \underline{f} will be assumed to obey the constraints previously imposed, in particular that the function vanishes outside some finite source volume. Consequently, if the equations (2.2.8) are considered as the fundamental relations, and

solutions for Θ and $\underline{\Omega}$ are obtained, then the equation of motion (2.2.6) can be used to obtain the corresponding acceleration field, thus

$$\rho \frac{\partial^2}{\partial t^2} \underline{u} = (\lambda + 2\mu)\nabla\Theta - 2\mu \nabla \times \underline{\Omega} \quad (2.2.9)$$

with \underline{r} exterior to $B(\tau)$. This relationship allows the transform of the displacement field to be computed as well. Due to the similarity of the relationship (2.2.9) with that between the ordinary scalar and vector potentials and the displacement field, the dilatation and rotation will be termed physical potentials.

From a purely mathematical point of view, the problem of source representation reduces to a consideration of the solutions of the inhomogeneous scalar and vector wave equations, of equations (2.2.5) or (2.2.8). If the Cartesian components of the vectors $\underline{\psi}$ or $\underline{\Omega}$ are used, then the equations (2.2.5) and (2.2.8) correspond, in each case, to a set of four inhomogeneous scalar wave equations of the general form

$$\nabla^2 \chi - \frac{1}{v^2} \frac{\partial^2 \chi}{\partial t^2} = -S(\underline{r}, t) \quad (2.2.10)$$

Thus, the solutions of the equations of motion with a source term may be reduced to a consideration of solutions for the inhomogeneous scalar wave equation (2.2.10).

A Green's function solution of (2.2.10) affords a completely general integral relationship between the source function $S(\underline{r}, t)$

the initial values of χ and $\partial\chi/\partial t$, and the potential field χ , at all points and at any time. It is possible to generalize the usual formulation slightly. In particular, the time at which the initial values of χ and $\partial\chi/\partial t$ are defined, need not be taken to be the same at every point within the source region. Thus if the initial values of the potentials χ and $\partial\chi/\partial t$ are defined at a time $\tau^* \geq 0$, where τ^* may depend on the source coordinates \underline{r}_0 , then (1)

$$\begin{aligned} \chi(\underline{r}, t) = & \frac{1}{4\pi} \int_0^{t^+} dt_0 \iiint G(\underline{r}, t/\underline{r}_0, t_0) S(\underline{r}_0, t_0) d\underline{r}_0 \\ & + \frac{1}{4\pi} \int_0^{t^+} dt_0 \iint d\underline{s}_0 \cdot (G \nabla_0 \chi - \chi \nabla G) \\ & - \frac{1}{4\pi v^2} \iiint \left[\left(\frac{\partial G}{\partial t_0} \chi \right)_{t_0 = \tau^*} - \left(G \frac{\partial \chi}{\partial t_0} \right)_{t_0 = \tau^*} \right] d\underline{r}_0 \end{aligned}$$

$$t^+ = t + \epsilon, \quad 0 < \epsilon \ll 1 \quad (2.2.11)$$

the Green's function $G(\underline{r}, t/\underline{r}_0, t_0)$ being a solution of the inhomogeneous wave equation

$$\begin{aligned} \nabla^2 G(\underline{r}, t/\underline{r}_0, t_0) - \frac{1}{v^2} \frac{\partial^2}{\partial t^2} G(\underline{r}, t/\underline{r}_0, t_0) \\ = - 4\pi \delta(\underline{r} - \underline{r}_0) \delta(t - t_0) \end{aligned} \quad (2.2.12)$$

(1) In section (3.9) a detailed derivation of a result equivalent to (2.2.11) will be obtained through the use of transform methods. The formula of (2.2.11) is a slight generalization of the classical Green's function integral solution (e.g., Morse and Feshbach, pp. 834-837, 1953). The actual proof of its validity rests on the derivation in section (3.9).

with \underline{r}_0 and t_0 denoting the source coordinates and time respectively.

The surface integral in (2.2.11) corresponds to a general solution of the homogeneous wave equation, without source terms or initial values. The remaining volume integrals taken together correspond to a particular solution of the inhomogeneous equation (2.2.10) and are of the most immediate interest in the present study. These particular solutions will be termed the primary source field and will be denoted as the potential $\chi^{(1)}(\underline{r}, t)$. Following this decomposition of the solution, the homogeneous part of the general solution can be expressed in terms of a superposition of eigenfunctions with variable coefficients appropriate for combination with the primary field solutions in problems involving sources in a medium with boundaries, rather than as surface integrals over the boundaries. This technique of combining general eigenfunction solutions of the homogeneous wave equations with the particular solutions $\chi^{(1)}(\underline{r}, t)$ is particularly appropriate for consideration of wave propagation in a layered half space or sphere and is commonly used (e. g., Ewing, Jardetzky and Press, 1957). Thus, if the source is located in a particular layer in a layered earth model, which may be a half space or sphere, then the equation of motion for the material points of the layer is the inhomogeneous equation (2.2.1) with elastic constants and density appropriate for the layer. Considering only a single source in a particular layer, then the equations of motion for the remaining layers are all homo-

geneous equations. The general solution for the source layer is therefore given by

$$\chi_n(\underline{r}, t) = \chi_n^{(1)}(\underline{r}, t) + \chi_n^{(0)}(\underline{r}, t) \quad (2.2.13)$$

where n denotes the n^{th} layer or source layer and $\chi_n^{(0)}$ denotes the general solution of the homogeneous equation in that layer. In the remaining $(N-1)$ layers, the solutions are simply

$$\chi_j(\underline{r}, t) = \chi_j^{(0)}(\underline{r}, t) ; \quad j = 1, 2, \dots, N, \quad j \neq n \quad (2.2.14)$$

The required solution for elastic wave propagation in such a medium is obtained by adjustment of the undetermined coefficients in the homogeneous eigenfunction solutions $\chi_j^{(0)}$, $j = 1, 2, \dots, N$, so as to satisfy the boundary conditions of stress and displacement continuity at the layer interfaces and source boundary. In this manner, the classical modal solutions are obtained. Typical examples of the procedure for point source problems in layered media are given by Gilbert and MacDonald (1960) for a spherical earth and by Harkrider (Thesis, C.I. T., 1963) for a layered half space. The involved computations required for the solution of the characteristic equation and subsequent evaluation of the amplitudes of the functions $\chi_j^{(0)}$ is effected by use of the Thomson-Haskell matrix technique (Haskell, 1953).

This technique is not as general as the integral Green's function method, but, when applicable, does of course give an equivalent result in an interpretively simple form. In practice it suffers

from fairly severe geometrical restrictions which effectively limit its applicability to problems involving media such that all the boundaries correspond to coordinate surfaces of a single coordinate, in a system in which the wave equation is separable.⁽¹⁾ Most of the following applications correspond to one of the following three cases:

- (1). All the boundaries are planes and are parallel.
- (2). All the boundaries are coaxial cylinders.
- (3). All the boundaries are spherical with a common origin.

These conditions do not include the source boundary, if it represents a physical discontinuity in the elastic properties, since it is susceptible to special treatment and can therefore be considered separately.

In view of the practical boundary constraints listed, it is clear that only three possible coordinate systems are utilized, namely, the Cartesian, cylindrical and spherical systems. Thus the eigenfunction expansions of importance for $\chi_j^{(0)}$, $j = 1, 2, \dots, N$ are

⁽¹⁾ A less restrictive condition is that every boundary must correspond to some coordinate surface in one of the coordinate systems in which the wave equation is separable and that the eigenfunctions in any one of the separable systems can be expanded in terms of the eigenfunctions of all and any of the other systems. The required eigenfunction expansions are known only in a few cases (i. e., Cartesian, cylindrical and spherical systems) and even in these cases, the "mixed" boundary problem becomes very complicated and algebraically cumbersome. Usually the solution cannot be expressed in closed form in such cases.

$$\chi_j^{(0)} = \frac{1}{2\pi} \int_{-\infty}^{+\infty} e^{i\omega t} d\omega \int_{-\infty}^{+\infty} \int_{-\infty}^{+\infty} \left\{ G_j(k_1, k_2, \omega) e^{-i(\kappa_j^2 - k_3^2)^{1/2} z} + \beta_j(k_1, k_2, \omega) e^{i(\kappa_j^2 - k_3^2)^{1/2} z} \right\} \exp \{ ik_1 x + ik_2 y \} dk_1 dk_2 ;$$

$$j = 1, 2, \dots, N-1$$

$$\chi_N^{(0)} = \frac{1}{2\pi} \int_{-\infty}^{+\infty} e^{i\omega t} d\omega \int_{-\infty}^{+\infty} \int_{-\infty}^{+\infty} \beta_N(k_1, k_2, \omega) e^{-(\kappa_3^2 - \kappa_N^2)^{1/2} z} \times \exp \{ ik_1 x + ik_2 y \} dk_1 dk_2 \quad (2.2.15)$$

with

$$\kappa_j = \frac{\omega}{v_j}, \quad v_j^2 = \left(\frac{\lambda_j + 2\mu_j}{\rho_j}, \frac{\mu_j}{\rho_j} \right); \quad \kappa_3 = [k_1^2 + k_2^2]^{1/2},$$

in Cartesian coordinates, and

$$\chi_j^{(0)} = \frac{1}{2\pi} \int_{-\infty}^{+\infty} e^{i\omega t} d\omega \sum_{m=0}^{\infty} \int_0^{\infty} \left[\left\{ c_m^{(j)}(k, \omega) e^{-i(\kappa_j^2 - k^2)^{1/2} z} + \mathfrak{D}_m^{(j)}(k, \omega) e^{i(\kappa_j^2 - k^2)^{1/2} z} \right\} \cos m\phi + \left\{ e_m^{(j)}(k, \omega) e^{-i(\kappa_j^2 - k^2)^{1/2} z} + \mathfrak{F}_m^{(j)}(k, \omega) e^{i(\kappa_j^2 - k^2)^{1/2} z} \right\} \sin m\phi \right] J_m(k\rho) dk$$

$$j = 1, 2, \dots, N-1 \quad (2.2.16)$$

$$\chi_N^{(0)} = \frac{1}{2\pi} \int_{-\infty}^{+\infty} e^{i\omega t} d\omega \sum_{m=0}^{\infty} \int_0^{\infty} \left[\mathfrak{D}_m^{(N)}(k, \omega) e^{-(\kappa^2 - \kappa_N^2)^{1/2} z} \cos m\phi + \mathfrak{F}_m^{(N)}(k, \omega) e^{-(\kappa^2 - \kappa_N^2)^{1/2} z} \sin m\phi \right] J_m(k\rho) dk$$

in cylindrical coordinates. Both of these expansions are appropriate to layered half space models of the earth, where the N^{th} layer extends to unbounded values of z . The radiation condition has been applied to the expansion for the N^{th} layer in each system.

The expansion in spherical coordinates for a finite, spherically layered earth model is

$$\begin{aligned} \chi_j^{(0)} = & \frac{1}{2\pi} \int_{-\infty}^{+\infty} e^{i\omega t} d\omega \sum_{\ell=0}^{\infty} \sum_{m=0}^{\ell} \left\{ \left[A_{\ell m}^{(j)}(\omega) j_{\ell}(\kappa_j r) + B_{\ell m}^{(j)}(\omega) n_{\ell}(\kappa_j r) \right] \cos m\phi \right. \\ & \left. + \left[C_{\ell m}^{(j)}(\omega) j_{\ell}(\kappa_j r) + D_{\ell m}^{(j)}(\omega) n_{\ell}(\kappa_j r) \right] \sin m\phi \right\} P_{\ell}^m(\cos \theta) \\ & j = 1, 2, \dots, N-1 \end{aligned} \quad (2.2.17)$$

$$\begin{aligned} \chi_N^{(0)} = & \frac{1}{2\pi} \int_{-\infty}^{+\infty} e^{i\omega t} d\omega \sum_{\ell=0}^{\infty} \sum_{m=0}^{\ell} \left\{ A_{\ell m}^{(N)}(\omega) \cos m\phi \right. \\ & \left. + C_{\ell m}^{(N)}(\omega) \sin m\phi \right\} j_{\ell}(\kappa_N r) P_{\ell}^m(\cos \theta) \end{aligned}$$

where the spherical Bessel and Neumann functions $j_{\ell}(\zeta)$ and $n_{\ell}(\zeta)$ may be replaced by spherical Hankel functions $h_{\ell}^{(1)}(\zeta)$ and $h_{\ell}^{(2)}(\zeta)$, since

$$h_{\ell}^{(1)}(\zeta) = j_{\ell}(\zeta) + in_{\ell}(\zeta)$$

$$h_{\ell}^{(2)}(\zeta) = j_{\ell}(\zeta) - in_{\ell}(\zeta)$$

The expansion 2.2.17 is appropriate for a layered sphere with $j = N$ denoting the inner layer containing the origin of the coordinates.

Only if the primary radiation field $\chi_n^{(1)}$ is expressed in terms of one of the eigenfunction expansions (2.2.15)-(2.2.17) is this superposition method feasible, since only in this case do the boundary conditions at the interfaces of the n^{th} (source) layer reduce to algebraic expressions independent of the variable coordinates on the boundary. However, when the source representation is expressed in such a form, then the usual techniques, such as those used by the previously mentioned authors, may be utilized to obtain the complete solution at any point in the medium. Therefore, a requirement for the representation is the expansion of the source field in terms of the previously noted eigenfunction representations.

It is clear that the solutions $\chi_j^{(0)}$ represent the reflected, refracted and diffracted radiation field associated with the presence of boundaries. As a consequence of this fact, one observes that the direct radiation from the sources, $\chi^{(1)}$, is the infinite space solution of the inhomogeneous wave equation and is obtained by taking the Green's function solution of (2.2.12) for an infinite space. One has

$$G(\underline{r}, t / \underline{r}_0, t_0) = \frac{\delta\left\{\frac{r^*}{v} - (t - t_0)\right\}}{r^*} ; \quad r^* = |\underline{r} - \underline{r}_0|, \quad t - t_0 > 0$$

as the appropriate solution. After substitution into (2.2.11), followed by integration over the source time t_0 , then $\chi^{(1)}(\underline{r}, t)$ is given by

$$\begin{aligned}
 \chi^{(1)}(\underline{r}, t) = & \frac{1}{4\pi} \iiint \frac{S(\underline{r}_o, t - \frac{r^*}{v})}{r^*} d\underline{r}_o \\
 & - \frac{1}{4\pi v^2} \iiint d\underline{r}_o \left\{ \chi(\underline{r}_o, \tau^*) \frac{\delta_1(\frac{r^*}{v} + \tau^* - t)}{r^*} \right. \\
 & \left. - \left(\frac{\partial \chi(\underline{r}_o, t_o)}{\partial t_o} \right)_{t_o = \tau^*} \frac{\delta(\frac{r^*}{v} + \tau^* - t)}{r^*} \right\} \quad (2.2.18)
 \end{aligned}$$

where

$$\delta_1\left(\frac{r^*}{v} + \tau^* - t\right) = \frac{\partial}{\partial t} \left\{ \delta\left(\frac{r^*}{v} + \tau^* - t\right) \right\}$$

and $\delta(x - x_o)$ is the Dirac Delta function.

The initial value of the potential and its first time derivative ("velocity") are clearly source terms which arise due to a pre-existing condition of the medium. In the present context, this condition may be associated with the existence of a prestressed condition of the medium due to the existence of tectonic forces in the earth. The creation of a rupture in such a medium will alter the boundary conditions for the stress field and requires a readjustment of this static stress field so as to maintain equilibrium. The amount of readjustment or relaxation required will define an initial value for the ensuing dynamical readjustment in which radiation of elastic energy is the primary mechanism. The initial values defined by the rupture will naturally be complicated functions of position relative to the rupture. In addition, since the rupture will change its dimensions with time, the equilibrium value of the potential will

actually vary with time so that the term "initial value" is only meaningful as a limit concept corresponding to the change in the equilibrium field due to a differential increment of rupture growth. The formulation of the initial value problem included in (2. 2.18), therefore relates only to the radiation field due to a differential increment of rupture. However this elementary source is capable of generalization to include the complications of finite rupturing. These considerations will be taken up more fully in chapter 3. For the present, only the properties of the elementary source will be investigated, the resulting solution playing the role of a Green's function for the rupture source.

Thus the initial value source term in (2. 2.18) will, in the present theory, be of relatively greater importance than the usual source term involving $S(\underline{r}, t)$. It is of some importance to note that the source term associated with the initial values, to be termed a relaxation source hereafter, is independent of the source factor associated with $S(\underline{r}, t)$. In particular, the source potential field is a superposition of these distinct source mechanisms, and each factor may be treated independently in a formal mathematical theory. Furthermore, the initial values associated with a relaxation source do not appear explicitly in the equations of motion as does $S(\underline{r}, t)$, but may be introduced by the usual procedures involving a Fourier transformation to the equations of motion. For this reason and in order to obtain expansions of the source field similar to (2. 2.15) - (2. 2.17), it is convenient to transform (2. 2.18) to the frequency

domain, using the Fourier transform operator

$$\mathfrak{F}\{\chi^{(1)}(\underline{r}, t)\} \equiv \int_{-\infty}^{+\infty} \chi^{(1)}(\underline{r}, t) e^{-i\omega t} dt \equiv \tilde{\chi}^{(1)}(\underline{r}, \omega)$$

Thus, the primary radiation field has the transformed solution,

with $\kappa = \omega/v$,

$$\begin{aligned} \chi^{(1)}(\underline{r}, \omega) &= \frac{1}{4\pi} \iiint \tilde{\mathfrak{S}}(\underline{r}_0, \omega) \left(\frac{e^{-i\kappa r^*}}{r^*} \right) d\underline{r}_0 \\ &+ \frac{1}{4\pi v} \iiint \left\{ \left(\frac{\partial \chi}{\partial t} \right)_{t_0 = \tau^*} - i\omega \chi(\underline{r}_0, \tau^*) \right\} \frac{e^{-i(\kappa r^* + \omega \tau^*)}}{r^*} d\underline{r}_0 \end{aligned}$$

and it is quite clear that the integrals may be combined to provide a single source term

$$\begin{aligned} \chi^{(1)}(\underline{r}, \omega) &= \frac{1}{4\pi} \iiint \left\{ \tilde{\mathfrak{S}}(\underline{r}_0, \omega) + \frac{1}{v} \left(\frac{\partial \chi}{\partial t} \right)_{t_0 = \tau^*} e^{-i\omega \tau^*} \right. \\ &\left. - \frac{i\omega}{v} \chi(\underline{r}_0, \tau^*) e^{-i\omega \tau^*} \right\} \left(\frac{e^{-i\kappa r^*}}{r^*} \right) d\underline{r}_0 \quad (2.2.19) \end{aligned}$$

From the previous brief discussion of the relaxation source mechanism, it is reasonably obvious that the only term involved in the representation of such a source will be the initial value $\chi(\underline{r}_0, \tau^*)$. In the following mathematical considerations of this equation, the factors $\tilde{\mathfrak{S}}(\underline{r}_0, \omega)$ and $-\frac{i\omega}{v} \chi(\underline{r}_0, \tau^*) \exp\{-i\omega \tau^*\}$ will be considered separately on some occasions, since it is of considerable advantage to make use of the special properties of the

initial value function $\chi(\underline{r}_0, \tau^*)$. In particular, this function is the difference between the equilibrium field before the creation of a boundary element in the medium and the equilibrium field with the boundary. It is not difficult to show (see section 3.7) that the difference field $\chi(\underline{r}_0, \tau^*)$ satisfies the equations of equilibrium without a body force term, corresponding to the tectonic forces, or any other force field such as gravity. It follows, then that if the potential χ represents one of the potentials \mathfrak{S} or ψ_j , $j = 1, 2, 3$, then $\chi(\underline{r}_0, \tau)$ is a biharmonic function, while if χ represents one of the physical potentials Θ or Ω_j , $j = 1, 2, 3$, then the initial value $\chi(\underline{r}_0, \tau^*)$ is a harmonic function. A detailed investigation and substantiation of these properties of the initial value function will be provided in chapter 3, wherein all of the foregoing remarks will be expanded. In view of the mathematical simplicity of harmonic functions, it will be most convenient to treat the so-called physical potentials rather than the regular scalar and vector potentials in problems associated with a relaxation source. Thus, due to their relative simplicity and physical significance, the dilatation and rotation are considered the fundamental potentials for source representations.

The transformed wave equations appropriate to the source problem are, from equations (2.2.5)

$$\begin{aligned} \nabla^2 \tilde{s} + k_p^2 \tilde{s} = & -\frac{1}{(\lambda+2\mu)} \tilde{\Phi} + \left[\frac{i\omega}{v_p} \tilde{s}(\underline{r}, \tau_1^*) \right. \\ & \left. - \frac{1}{v_p} \left(\frac{\partial \tilde{s}(\underline{r}, t)}{\partial t} \right)_{t=\tau_1^*} \right] e^{-i\omega\tau_1^*} \end{aligned} \quad (2.2.20)$$

$$\begin{aligned} \nabla^2 \tilde{\psi}_\ell + k_s^2 \tilde{\psi}_\ell = & -\left(\frac{1}{\mu}\right) \tilde{B}_\ell + \left[\frac{i\omega}{v_s} \tilde{\psi}_\ell(\underline{r}, \tau_2^*) \right. \\ & \left. - \frac{1}{v_s} \left(\frac{\partial \tilde{\psi}_\ell(\underline{r}, t)}{\partial t} \right)_{t=\tau_2^*} \right] e^{-i\omega\tau_2^*} \end{aligned}$$

where

$$\tilde{\Phi}(\underline{r}, \omega) = \frac{1}{4\pi} \iiint_V \left[\tilde{f}(\underline{r}', \omega) \cdot \nabla \left(\frac{1}{r^*} \right) \right] dV' \quad (2.2.21)$$

$$\tilde{B}_\ell(\underline{r}, \omega) = \frac{1}{4\pi} \iiint_V \left[\tilde{f}(\underline{r}', \omega) \times \nabla \left(\frac{1}{r^*} \right) \right] dV'$$

with $k_p = \omega/v_p$ and $k_s = \omega/v_s$. The primary source field appropriate to these equations is from (2.2.19)

$$\begin{aligned} \tilde{s}^{(1)}(\underline{r}, \omega) = & \frac{1}{4\pi(\lambda+2\mu)} \iiint \left[\tilde{\Phi}(\underline{r}_o, \omega) + \left\{ \rho \left(\frac{\partial \tilde{s}}{\partial t} \right)_{t=\tau_1^*} \right. \right. \\ & \left. \left. - i\omega \tilde{s}(\underline{r}_o, \tau_1^*) \right\} e^{-i\omega\tau_1^*} \right] \left(\frac{e^{-ik_p r^*}}{r^*} \right) d\underline{r}_o \end{aligned} \quad (2.2.22)$$

$$\begin{aligned} \tilde{\psi}_\ell^{(1)}(\underline{r}, \omega) = & \frac{1}{4\pi\mu} \iiint \left[\tilde{B}_\ell(\underline{r}_o, \omega) + \left\{ \rho \left(\frac{\partial \tilde{\psi}_\ell}{\partial \tau} \right)_{t_o=\tau_2^*} \right. \right. \\ & \left. \left. - i\omega \tilde{\psi}_\ell(\underline{r}_o, \tau_2^*) \right\} e^{-i\omega\tau_2^*} \right] \left(\frac{e^{-ik_s r^*}}{r^*} \right) d\underline{r}_o \end{aligned}$$

where the general delay time τ^* is taken to have the value τ_1^* or τ_2^* for the two different potentials. These solutions are seen to be the source terms from a generalized Kirchhoff solution of the inhomogeneous Helmholtz equations of (2.2.20). It is clear that, in general, the source terms in (2.2.20) and in the solution (2.2.22) may be written in an abbreviated notational form, for example as

$$\tilde{\Phi}'(\underline{r}, \omega) = \tilde{\Phi}(\underline{r}, \omega) + \left[\rho \left(\frac{\partial \mathcal{S}}{\partial t} \right)_{t=\tau_1^*} - i\omega \rho \mathcal{S}(\underline{r}, \tau_1^*) \right] e^{-i\omega \tau_1^*} \quad (2.2.23)$$

where various of the source terms may be set to zero in (2.2.23) for the consideration of special sources.

Corresponding to this dynamical solution, one has the static or equilibrium relations

$$\begin{aligned} \mathcal{S}^{(1)}(\underline{r}) &= \frac{1}{4\pi(\lambda+2\mu)} \iiint \frac{\Phi(\underline{r}_0)}{r^*} d\underline{r}_0 \\ \psi_{\ell}^{(1)}(\underline{r}) &= \frac{1}{4\pi\mu} \iiint \frac{B_{\ell}(\underline{r}_0)}{r^*} d\underline{r}_0 \end{aligned} \quad (2.2.24)$$

which provide solutions to (2.2.5) or (2.2.1) when the inertial term is absent. The source potentials Φ and \underline{B} are

$$\begin{aligned} \Phi(\underline{r}) &= \frac{1}{4\pi} \iiint \left[\underline{f}(\underline{r}') \cdot \nabla \left(\frac{1}{r^*} \right) \right] d\underline{r}' \\ \underline{B}(\underline{r}) &= \frac{1}{4\pi} \iiint \left[\underline{f}(\underline{r}') \times \nabla \left(\frac{1}{r^*} \right) \right] d\underline{r}' \end{aligned} \quad (2.2.25)$$

This formulation, in terms of the potentials δ and $\underline{\psi}$, will be investigated under the condition $\Phi' = \Phi$ for the relationship of the dynamic to the static source field.

The problem may also be formulated in terms of the physical potentials, the dilatation Θ and rotation $\underline{\Omega}$, as

$$\begin{aligned} \nabla^2 \tilde{\Theta} + k_p^2 \tilde{\Theta} = & - \left(\frac{1}{\lambda + 2\mu} \right) \nabla \cdot \tilde{\underline{f}} \\ & + \left[\frac{i\omega}{v_p} \Theta(\underline{r}, \tau_1^*) - \frac{1}{v_p} \left(\frac{\partial \Theta(\underline{r}, t)}{\partial t} \right)_{t=\tau_1^*} \right] e^{-i\omega\tau_1^*} \end{aligned}$$

$$\begin{aligned} \nabla^2 \tilde{\underline{\Omega}} + k_s^2 \tilde{\underline{\Omega}} = & - \frac{1}{2\mu} \nabla \times \tilde{\underline{f}} \\ & + \left[\frac{i\omega}{v_s} \underline{\Omega}(\underline{r}, \tau_2^*) - \frac{1}{v_s} \left(\frac{\partial \underline{\Omega}}{\partial t} \right)_{t=\tau_2^*} \right] e^{-i\omega\tau_2^*} \end{aligned}$$

Now, since the initial values $\Theta(\underline{r}, \tau_1^*)$ and $\underline{\Omega}(\underline{r}, \tau_2^*)$ are also equilibrium values in applications to relaxation sources, it is convenient to use the definitions

$$\Theta(\underline{r}, \tau_1^*) = \nabla \cdot \underline{u}^*(\underline{r})$$

$$\underline{\Omega}(\underline{r}, \tau_2^*) = \frac{1}{2} \nabla \times \underline{u}^*(\underline{r})$$

with $\underline{u}^*(\underline{r})$ representing an equilibrium displacement field, and to set the initial time derivative term to zero under these conditions.

Then (2.2.26) becomes

$$\begin{aligned} \nabla^2 \tilde{\Theta} + k_p^2 \tilde{\Theta} &= - \left(\frac{1}{\lambda + 2\mu} \right) \left[\nabla \cdot \tilde{\underline{f}} - i\omega\rho \nabla \cdot \underline{\underline{u}}^* e^{-i\omega\tau_1^*} \right] \\ \nabla^2 \underline{\underline{\Omega}} + k_s^2 \underline{\underline{\Omega}} &= - \frac{1}{2\mu} \left[\nabla \times \tilde{\underline{f}} - i\omega\rho \nabla \times \underline{\underline{u}}^* e^{-i\omega\tau_2^*} \right] \end{aligned} \quad (2.2.27)$$

Solutions for the primary source field are therefore, from (2.2.19)

$$\begin{aligned} \tilde{\Theta}(\underline{\underline{r}}, \omega) &= \frac{1}{4\pi(\lambda + 2\mu)} \iiint \left[\nabla \cdot \tilde{\underline{f}} - i\omega\rho \nabla \cdot \underline{\underline{u}}^* e^{-i\omega\tau_1^*} \right] \frac{e^{-ik_p r^*}}{r^*} d\underline{\underline{r}}' \\ \underline{\underline{\Omega}}(\underline{\underline{r}}, \omega) &= \frac{1}{8\pi\mu} \iiint \left[\nabla \times \tilde{\underline{f}} - i\omega\rho \nabla \times \underline{\underline{u}}^* e^{-i\omega\tau_2^*} \right] \frac{e^{-ik_s r^*}}{r^*} d\underline{\underline{r}}' \end{aligned} \quad (2.2.28)$$

The source terms involving $\tilde{\underline{f}}$ and $i\omega\rho \underline{\underline{u}}^*$ are again seen to give a superposition field so that each may be considered separately in the following evaluation of (2.2.28).

In order to effect a useful source representation, it will be necessary to evaluate the integral solutions (2.2.21) and (2.2.28) for general spatial distributions of the source function $\tilde{\underline{f}}$ and initial values, such as $\underline{\underline{u}}^*$, and to express the results in terms of the eigenfunction expansions previously considered. These essentially mathematical considerations will be taken up in the following sections of the present chapter.

2.3. Elementary Multipole Representation for Stationary Sources

Let the source function in the dynamic case be of the separable form

$$\underline{f}(\underline{r}, t) = S(t)\underline{R}(\underline{r}) \quad (2.3.1)$$

Such a separable source function will be termed a 'stationary source'. The equivalent static source will be defined as

$$\underline{f}(\underline{r}) \equiv \underline{R}(\underline{r}) \quad (2.3.2)$$

Therefore, the source potentials are, from (2.2.21)

$$\tilde{\Phi}(\underline{r}, \omega) = \frac{\tilde{S}(\omega)}{4\pi} \int \int \int_{\tau} \underline{R}(\underline{r}') \cdot \nabla \left(\frac{1}{r^*} \right) d\tau' = \Phi(\underline{r})\tilde{S}(\omega) \quad (2.3.3)$$

$$\tilde{\underline{B}}(\underline{r}, \omega) = \frac{\tilde{S}(\omega)}{4\pi} \int \int \int_{\tau} \underline{R}(\underline{r}') \times \nabla \left(\frac{1}{r^*} \right) d\tau' = \underline{B}(\underline{r})\tilde{S}(\omega)$$

where $\Phi(\underline{r})$ and $\underline{B}(\underline{r})$ are the potentials for the equivalent static problem. Since

$$r^* = \left[r^2 - 2rr' \cos \gamma + r'^2 \right]^{1/2}$$

then $(r^*)^{-1}$ may be expanded as

$$\frac{1}{r^*} = \begin{cases} \sum_{n=0}^{\infty} \frac{r'^n}{r^{n+1}} P_n(\cos \gamma); & r > r' \\ \sum_{n=0}^{\infty} \frac{r^n}{r'^{n+1}} P_n(\cos \gamma); & r < r' \end{cases}$$

The potentials $\tilde{\Phi}$ and \tilde{B} are to be specified in the region outside the source volume, thus $r > r'$. The expansion of $(\frac{1}{r})$ with $r > r'$ is most conveniently expressed in the operational form

$$\frac{1}{r} = \sum_{n=0}^{\infty} \frac{(-1)^n}{n!} (r' \cdot \nabla)^n \left(\frac{1}{r} \right); \quad r > r'$$

in view of the form of the integrands in (2.3.3). Here, the components \underline{r}' are $\{x'_i\}$ and those of \underline{r} are denoted by $\{x_i\}$. This expansion implies that the source is distributed within a finite volume. On the other hand, once the representation is achieved in terms of the 'source potentials' $\Phi(\underline{r})$ and $B(\underline{r})$, $|\underline{r}| > |r'|$, then these potentials represent a 'source' distributed throughout the infinite space, since these potentials are source terms for the solutions of (2.2.5).

Therefore, the source potentials are, after interchanging summation and integration, where it may be noted that the integration is with respect to the primed coordinates only

$$\tilde{\Phi}(\underline{r}, \omega) = \frac{\tilde{S}(\omega)}{4\pi} \sum_{n=0}^{\infty} \frac{(-1)^n}{n!} \int \int \int_{\tau} \underline{R}(r') \cdot \nabla (r' \cdot \nabla) \left(\frac{1}{r} \right) d\tau'$$

$$\tilde{B}(\underline{r}, \omega) = \frac{\tilde{S}(\omega)}{4\pi} \sum_{n=0}^{\infty} \frac{(-1)^n}{n!} \int \int \int_{\tau} \underline{R}(r') \times \nabla (r' \cdot \nabla)^n \left(\frac{1}{r} \right) d\tau'$$

Now, expansion of the operator $\underline{R} \cdot \nabla (r' \cdot \nabla)^n$ gives:

$$(\underline{R} \cdot \nabla)(\underline{r}' \cdot \nabla)^n \left(\frac{1}{r} \right) = R_{i_0} x'_{i_1} x'_{i_2} \dots x'_{i_n} \frac{\partial^{(n+1)} r^{-1}}{\partial x_{i_0} \dots \partial x_{i_n}}$$

where the summation convention over the repeated indices is employed and $i_v = 1, 2, 3$ for all $v = 0, 1, \dots, n$.

A similar expansion of the operator $\underline{R} \times \nabla(\underline{r}' \cdot \nabla)^n$ gives:

$$(\underline{R} \times \nabla)(\underline{r}' \cdot \nabla)^n \left(\frac{1}{r} \right) = \epsilon_{i_0 j k} R_j x'_{i_1} \dots x'_{i_n} \frac{\partial^{(n+1)} r^{-1}}{\partial x_k \partial x_{i_1} \dots \partial x_{i_n}} e_{i_0}$$

with

$$\epsilon_{i_0 j k} = \begin{cases} +1 & \text{if } i_0, j, k \text{ an even permutation of } 1, 2, 3 \\ -1 & \text{if } i_0, j, k \text{ an odd permutation of } 1, 2, 3 \\ 0 & \text{if any of the indices } i_0, j, k \text{ are equal} \end{cases}$$

$\hat{e}_{i_0} = (\hat{e}_1, \hat{e}_2, \hat{e}_3)$, basis vectors in the unprimed coordinate system

Finally, substituting these expressions into the potential equations, interchanging summation and integration and setting:

$$R^{(n+1)}(i_0, i_1, \dots, i_n) = \int \int \int_{\tau} R_{i_0} x'_{i_1} \dots x'_{i_n} d\tau' \quad (2.3.4)$$

corresponding to a tensor of rank $(n+1)$, gives:

$$\begin{aligned} \tilde{\Phi}(\underline{r}, \omega) &= \frac{\tilde{S}(\omega)}{4\pi} \sum_{n=0}^{\infty} \frac{(-1)^n}{n!} R^{(n+1)}(i_0, \dots, i_n) \frac{\partial^{(n+1)} r^{-1}}{\partial x_{i_0} \dots \partial x_{i_n}} \\ \tilde{\underline{B}}(\underline{r}, \omega) &= \frac{\tilde{S}(\omega)}{4\pi} \sum_{n=0}^{\infty} \frac{(-1)^n}{n!} (\epsilon_{i_0 j k} R^{(n+1)}(j, i_1 \dots i_n) \frac{\partial^{(n+1)} r^{-1}}{\partial x_k \partial x_{i_1} \dots \partial x_{i_n}}) \hat{e}_{i_0} \end{aligned} \quad (2.3.5)$$

Thus, the $R^{(n+1)}(i_0 \dots i_n)$ correspond to multipole moments. For example, if $n = 0$:

$$R^{(1)}(i_0) = \int \int \int_{\tau} \mathbb{R}_{i_0}(\underline{r}') d\tau', \quad i_0 = 1, 2, 3$$

and this is just the resultant vector force for the source with components $(R^{(1)}(1), R^{(1)}(2), R^{(1)}(3))$. Thus, if we set $R = \{R^{(1)}(i_0)\}$ denoting this resultant, then from the equations (2.3.5)

$$\tilde{\Phi}(\underline{r}, \omega) = \frac{\tilde{S}(\omega)}{4\pi} \underline{R} \cdot \nabla \left(\frac{1}{r} \right) = \tilde{S}(\omega) \Phi(\underline{r})$$

$$\tilde{\underline{B}}(\underline{r}, \omega) = \frac{\tilde{S}(\omega)}{4\pi} \underline{R} \times \nabla \left(\frac{1}{r} \right) = \tilde{S}(\omega) \underline{B}(\underline{r})$$

This corresponds to a result obtained by Love (1944, p. 304). This simple case (i. e., $n = 0$) is used as a basis for much of the present source representation theory.

Since r^{-1} is a solution of Laplace's equation, then it is seen that any derivative $\frac{\partial^{(p+q+s)}}{\partial x_1^p \partial x_2^q \partial x_3^s} \left(\frac{1}{r} \right)$ is another. These

quantities are therefore solid harmonics of the type $r^{-n-1} S_n(\theta, \phi)$ with $n = p + q + s$ and where:

$$S_n(\theta, \phi) = \sum_{m=0}^n (a_{mn} \cos m\phi + b_{mn} \sin m\phi) P_n^m(\cos \theta)$$

denotes a surface harmonic. The associated Legendre function $P_n^m(\cos \theta)$ introduced here may be defined by

$$P_n^m(\xi) = \frac{(-1)^n}{2^n n!} (1 - \xi^2)^{m/2} \frac{d^{m+n}}{d\xi^{m+n}} \{1 - \xi^2\}^n$$

The derivatives of different order (n) in (2.3.5) may be written as a single harmonic function by combining the linearly dependent functions of the series in (2.3.5). Thus

$$P^{(n+1)} \frac{S_{n+1}(\theta, \phi)}{r^{n+2}} = \frac{(-1)^{n+1}}{n!} R^{n+1}(i_0, i_1, \dots, i_n) \frac{\partial^{(n+1)} r^{-1}}{\partial x_{i_0} \dots \partial x_{i_n}} \quad (2.3.6)$$

$$P^{(n+1)} \frac{g_{n+1}^{(i_0)}(\theta, \phi)}{r^{n+2}} = \frac{(-1)^{n+1}}{n!} \epsilon_{i_0 j k} R^{(n+1)}(j, i_1 \dots i_n) \frac{\partial^{(n+1)} r^{-1}}{\partial x_j \partial x_{i_1} \dots \partial x_{i_n}}$$

with $P^{(n+1)}$ defined as the magnitude of the multipole

$$P^{(n+1)} = (n+1) \left\{ \sum_{i_0=1}^3 \dots \sum_{i_n=1}^3 [R^{(n+1)}(i_0 \dots i_n)]^2 \right\}^{1/2} \quad (2.3.7)$$

and where the angular functions $S_{n+1}(\theta, \phi)$ and $g_{n+1}^{(i_0)}(\theta, \phi)$ are of the form

$$S_n(\theta, \phi) = \sum_{m=0}^n (\alpha_{nm} \cos m\phi + \beta_{nm} \sin m\phi) P_n^m(\cos \theta)$$

$$g_n^{(i)}(\theta, \phi) = \sum_{m=0}^n (\gamma_{nm}^{(i)} \cos m\phi + g_{nm}^{(i)} \sin m\phi) P_n^m(\cos \theta)$$

corresponding to surface harmonics. The coefficients α_{mn} etc. are combinations of the factors $R^{(n+1)}(k, i_1 \dots i_n) / P^{(n+1)}$ which may

be interpreted as generalized direction cosines. A compilation of these coefficients for the cases $n = 0, 1$ is given in Appendix 1.

Thus, if

$$\underline{s}_{n+1}(\theta, \phi) \equiv s_{n+1}^{(i_0)} \hat{e}_{i_0}$$

then the potentials of (2.3.3) may be written as

$$\begin{aligned} \tilde{\Phi}(\underline{r}, \omega) &= -\frac{\tilde{S}(\omega)}{4\pi} \sum_{n=0}^{\infty} \rho^{(n+1)} \frac{S_{n+1}(\theta, \phi)}{r^{n+2}} = \tilde{S}(\omega) \Phi(\underline{r}) \\ \tilde{B}(\underline{r}, \omega) &= -\frac{\tilde{S}(\omega)}{4\pi} \sum_{n=0}^{\infty} \frac{\rho^{(n+1)}}{r^{n+2}} \underline{s}_{n+1}(\theta, \phi) = \tilde{S}(\omega) B(\underline{r}) \end{aligned} \tag{2.3.8}$$

2.4. Multipole Representations of Arbitrary (Non-Stationary) Sources

If the source function cannot be expressed in a separable form, as in (2.3.1), then the connection between the static and dynamic source potentials is not of the simple form given by (2.3.8). However, the formal development of the dynamic source potential is not altered by the essentially more complicated nature of an arbitrary volume source. In particular, if the source function is of an unseparable form, $\underline{f}(\underline{r}, t)$, then the equivalent static source is given by

$$\underline{f}(\underline{r}) = \lim_{t \rightarrow \infty} \underline{f}(\underline{r}, t) \quad \text{or} \quad \underline{f}(\underline{r}) = \lim_{\omega \rightarrow \infty} \tilde{\underline{f}}(\underline{r}, \omega)$$

and the transformed dynamic source potentials are

$$\tilde{\Phi}(\underline{r}, \omega) = \frac{1}{4\pi} \int \int \int_{\tau} \underline{f}(\underline{r}', \omega) \cdot \nabla \left(\frac{1}{r} \right) d\tau' \quad (2.4.1)$$

$$\tilde{\underline{B}}(\underline{r}, \omega) = \frac{1}{4\pi} \int \int \int_{\tau} \underline{f}(\underline{r}', \omega) \times \nabla \left(\frac{1}{r} \right) d\tau'$$

Quite clearly, these potentials may be expanded into a multipole representation by the same methods used for the stationary source.

Thus, the general representation is

$$\tilde{\Phi}(\underline{r}, \omega) = -\frac{1}{4\pi} \sum_{n=0}^{\infty} \rho^{(n+1)}(\omega) \frac{S_{n+1}(\theta, \phi)}{r^{n+2}} \quad (2.4.2)$$

$$\tilde{\underline{B}}(\underline{r}, \omega) = -\frac{1}{4\pi} \sum_{n=0}^{\infty} \frac{\rho^{(n+1)}(\omega)}{r^{n+2}} \underline{g}_{-n+1}(\theta, \phi)$$

with

$$S_n(\theta, \phi) = \sum_{m=0}^n (\alpha_{nm}(\omega) \cos m\phi + \beta_{nm}(\omega) \sin m\phi) P_n^m(\cos \theta) \quad (2.4.3)$$

$$\underline{g}_n^{(i)}(\theta, \phi) = \sum_{m=0}^n (\gamma_{nm}^i(\omega) \cos m\phi + \delta_{nm}^i(\omega) \sin m\phi) P_n^m(\cos \theta)$$

and as before

$$\rho^{(n+1)}(\omega) = (n+1) \left\{ \sum_{i_0=1}^3 \dots \sum_{i_n=1}^3 \left[\mathcal{R}^{(n+1)}(i_0, \dots, i_n; \omega) \right]^2 \right\}^{1/2}$$

The multipole coefficients are now frequency dependent and are linear combinations of the tensor components

$$\mathcal{R}^{(n+1)}(i_0, i_1, \dots, i_n) = \int \int \int_{\tau} f_{i_0}(\underline{r}', \omega) x_{i_1}' \dots x_{i_n}' d\tau' \quad (2.4.4)$$

The source potentials $\tilde{\Phi}$ and $\tilde{\underline{B}}$ are formally invariant to the detailed properties of \underline{f} , the expressions (2.4.2) being valid for all \underline{f} . Therefore, the precise character of the source does not alter the formal development of the theory and it is clearly possible to proceed to obtain formal expressions of the displacement field in the medium without considering the detailed nature of the source. In the following sections, all formal expression of the dependence of the multipole coefficients on the angular frequency (ω) will be suppressed, but may, nevertheless, be considered as implied in all the results. In later sections, multipole coefficients for specific sources of interest will be computed, and it will be shown that in general they are frequency dependent.

For purposes of reference, sources which may only be described by non-separable source functions $\underline{f}(\underline{r}, t)$ will be termed non-stationary, since their non-separability is due, primarily, to allowance for the propagation of the source boundary. This should occur, for example, if the boundary is controlled by a propagating rupture surface or shock front.

2.5. Evaluation of the Static Displacement Field

By way of a preliminary approach to the dynamic problem, it will be useful to consider the displacement potential in the static limit. As has been indicated, these potentials are given by

$$\begin{aligned} \nabla^2 \underline{\mathfrak{s}} + \frac{\Phi}{\lambda+2\mu} &= 0 \\ \nabla^2 \underline{\Psi} + \frac{1}{\mu} \underline{\mathfrak{B}} &= 0 \end{aligned} \tag{2.5.1}$$

where $\Phi(\underline{r})$ and $\underline{\mathfrak{B}}(\underline{r})$ are given by (2.2.25). From (2.3.8) then, infinite space solutions, analogous to the primary radiation field in the dynamic case, are

$$\underline{\mathfrak{s}}^{(1)}(\underline{r}) = - \frac{1}{16\pi^2(\lambda+2\mu)} \sum_{n=0}^{\infty} \rho^{(n+1)} \left[\iiint_V \frac{1}{r^*} \left(\frac{S_{n+1}(\theta', \phi')}{r'^{n+2}} \right) dV' \right] \tag{2.5.2}$$

$$\underline{\Psi}^{(1)}(\underline{r}) = - \frac{1}{16\pi^2\mu} \sum_{n=0}^{\infty} \rho^{(n+1)} \left[\iiint_V \frac{1}{r^*} (S_{n+1}(\theta', \phi')) r'^{1-n-2} dV' \right] \tag{2.5.3}$$

Since components of the vector potential $\underline{\Psi}^{(1)}$ arise from integrals identical, except for constant factors, to that generating $\underline{\mathfrak{s}}^{(1)}$, it will be sufficient to consider only $\underline{\mathfrak{s}}^{(1)}$. (Here, the evaluation of the volume integrals depends only on the fact that the integrand is a harmonic function multiplied by $1/r^*$, as will be shown below.)

Making use of a method which was also used by Love (pp. 304-5) in similar circumstances, we may partition the space into

spherical shells with origin at the point of observation and of radius r^* (Figure 2). Then the volume integral in (2.5.2) may be written in the form:

$$\iiint_V \frac{1}{r^*} \left(\frac{S_{n+1}(\theta', \phi')}{r'^{n+2}} \right) dV' = \int_0^\infty \frac{dr^*}{r^*} \iint_S \frac{S_{n+1}(\theta', \phi')}{r'^{n+2}} da$$

It is not difficult to show (see Appendix (2)) that for harmonic functions of the type $S_{n+1}(\theta', \phi')/r'^{n+2}$ with $n \geq 0$

$$\iint_S \frac{S_{n+1}(\theta', \phi')}{r'^{n+2}} da = \begin{cases} 4\pi r^{*2} \left(\frac{S_{n+1}(\theta, \phi)}{r^{n+2}} \right) ; & \text{for } r^* < r \\ 0 ; & r^* > r \end{cases} \quad (2.5.4)$$

The proof of this statement follows directly from the mean value theorem for harmonic functions (Brand, 1955). Therefore:

$$\begin{aligned} \iiint_V \frac{1}{r^*} \left(\frac{S_{n+1}(\theta', \phi')}{r'^{n+2}} \right) dV' &= 4\pi \left(\frac{S_{n+1}(\theta, \phi)}{r^{n+2}} \right) \int_0^r r^* dr^* \\ &= 2\pi \left(\frac{S_{n+1}(\theta, \phi)}{r^n} \right) \end{aligned}$$

Using this result in (2.5.2) and for the components of $\underline{\psi}^{(1)}$ in (2.5.3) as well

$$\begin{aligned} \mathcal{J}^{(1)}(\underline{r}) &= - \frac{1}{8\pi(\lambda+2\mu)} \sum_{n=0}^{\infty} \frac{\rho^{(n+1)}}{r^n} S_{n+1}(\theta, \phi) \\ \underline{\psi}^{(1)}(\underline{r}) &= - \frac{1}{8\pi\mu} \sum_{n=0}^{\infty} \frac{\rho^{(n+1)}}{r^n} \underline{g}_{n+1}(\theta, \phi) \end{aligned} \quad (2.5.5)$$

The displacement field corresponding to these potentials is:

$$\begin{aligned} \underline{u}^{(1)}(\underline{r}) &= \nabla \mathcal{S}^{(1)}(\underline{r}) + \nabla \times \underline{\psi}^{(1)}(\underline{r}) \\ \underline{u}^{(1)}(\underline{r}) &= -\frac{1}{8\pi} \sum_{n=0}^{\infty} \rho^{(n+1)} \left[\frac{1}{\lambda+2\mu} \nabla \left(\frac{S_{n+1}(\theta, \phi)}{r^n} \right) \right. \\ &\quad \left. + \frac{1}{\mu} \nabla \times \left(\frac{1}{r^n} \mathfrak{S}_{-n+1}(\theta, \phi) \right) \right] \end{aligned} \quad (2.5.6)$$

For the case of a horizontal point force taken in the x^1 direction, one observes that the source integrals giving the multipole coefficients (2.3.4) go to zero with the exception of $R^{(1)}(1)$ which has the simple form

$$R^{(1)}(1) = \iiint_{\tau} M \delta(x) \delta(y) \delta(z) dx dy dz = M$$

with M a constant. Using the results of Appendix (1), the Cartesian components of the displacement field are found to be

$$\begin{aligned} u_1^{(1)}(\underline{r}) &= \frac{M}{8\pi} \left[\frac{1}{\lambda+2\mu} \frac{\partial}{\partial x^1} (\cos \phi P_1^1(\cos \theta)) \right. \\ &\quad \left. + \frac{1}{\mu} \left\{ \frac{\partial}{\partial x^2} (\sin \phi P_1^1(\cos \theta)) - \frac{\partial}{\partial x^3} (-P_1^0(\cos \theta)) \right\} \right] \\ u_2^{(1)}(\underline{r}) &= \frac{M}{8\pi} \left[\frac{1}{\lambda+2\mu} \frac{\partial}{\partial x^2} (\cos \phi P_1^1(\cos \theta)) - \frac{1}{\mu} \frac{\partial}{\partial x^3} (\sin \phi P_1^1(\cos \theta)) \right] \end{aligned}$$

$$u_3^{(1)}(\underline{r}) = \frac{M}{8\pi} \left[\frac{1}{\lambda+2\mu} \frac{\partial}{\partial x_3} (\cos \phi P_1^1(\cos \theta)) - \frac{1}{\mu} \frac{\partial}{\partial x_1} (P_1^0(\cos \theta)) \right]$$

and observing that

$$\frac{\partial r}{\partial x_1} = \cos \phi P_1^1(\cos \theta); \quad \frac{\partial r}{\partial x_2} = \sin \phi P_1^1(\cos \theta); \quad \frac{\partial r}{\partial x_3} = P_1^0(\cos \theta)$$

$$\sum_{j=1}^3 \frac{\partial^2 r}{\partial x^j{}^2} = \frac{2}{r}; \quad \sum_{j=1}^3 \left(\frac{\partial r}{\partial x^j} \right)^2 = 1$$

then these components may be written as

$$u_1^{(1)}(\underline{r}) = -\frac{M(\lambda+\mu)}{8\pi\mu(\lambda+2\mu)} \frac{\partial^2 r}{\partial x_1^2} + \frac{M}{4\pi\mu r}$$

$$u_2^{(1)}(\underline{r}) = -\frac{M(\lambda+\mu)}{8\pi\mu(\lambda+2\mu)} \frac{\partial^2 r}{\partial x_1 \partial x_3}$$

$$u_3^{(1)}(\underline{r}) = -\frac{M(\lambda+\mu)}{8\pi\mu(\lambda+2\mu)} \frac{\partial^2 r}{\partial x_1 \partial x_2}$$

These are precisely the results given by Love (p. 185) for this simple source and provide a check on the methods used to obtain (2.5.6).

In order to apply these results to geophysical problems of interest, it is necessary to consider various transformations of the potentials to coordinates other than that with an origin at the source. In particular, an important transformation is a simple translation from the source to the center of a spherical earth model. The Appendix (3) gives the potentials in terms of coordi-

nates translated along the z axis of the source coordinates with no relative rotations of the two systems. For Geophysical applications, such a coordinate change is sufficiently general, since the source coordinates may usually be chosen with the z axis normal to the earth's surface. In addition, it is often more convenient to express the components of displacement as spherical components rather than as Cartesian components. The relationship of curvilinear components of displacement to the scalar potential and the Cartesian components of the vector potential is given in Appendix (4). Application of these relations to the transformed potentials provides, finally, expressions for the spherical components of the displacement field in terms of spherical coordinates at the center of the earth. These results are given in Appendix (3) as well.

2.6. Evaluation of the Primary Dynamic Radiation Field: The Propagation Function

Turning to the dynamic problem for the stationary source, equations (2.2.21), (2.2.22), and (2.3.8) provide the potentials in terms of the integrals

$$\tilde{\mathcal{S}}^{(1)}(\underline{r}, \omega) = - \frac{\tilde{S}(\omega)}{16\pi^2(\lambda+2\mu)} \sum_{n=0}^{\infty} \rho^{(n+1)} \left[\iiint_V \frac{e^{-ik_p r^*}}{r^*} \frac{S_{n+1}(\theta, \phi)}{r'^{n+2}} dV' \right] \quad (2.6.1)$$

$$\tilde{\Psi}^{(1)}(\underline{r}, \omega) = - \frac{\tilde{S}(\omega)}{16\pi^2\mu} \sum_{n=0}^{\infty} \rho^{(n+1)} \left[\iiint_V \frac{e^{-ik_s r^*}}{r^*} \frac{1}{r'^{n+2}} \underline{g}(\theta', \phi') dV' \right]$$

Here again, the volume integrals for $\underline{\psi}^{(1)}$ are of the same form as those for $\underline{s}^{(1)}$. It is seen that the integrations may be performed in exactly the same manner as were those in the static case. Therefore, from (2.5.4), one has immediately

$$\tilde{s}^{(1)}(\underline{r}, \omega) = - \frac{\tilde{S}(\omega)}{4\pi(\lambda+2\mu)} \sum_{n=0}^{\infty} \frac{\rho^{(n+1)}}{r^{(n+2)}} S_{n+1}(\theta, \phi) \int_0^r \pi^* e^{-ik_p r^*} dr^*$$

Integration by parts therefore gives

$$\begin{aligned} \tilde{s}^{(1)}(\underline{r}, \omega) = & - \frac{\tilde{S}(\omega)}{8\pi(\lambda+2\mu)} \sum_{n=0}^{\infty} \frac{\rho^{(n+1)}}{r^n} S_{n+1}(\theta, \phi) \\ & \times \left\{ \frac{2}{k_p^2 r^2} \left[e^{-ik_p r} (ik_p r + 1) - 1 \right] \right\} \end{aligned} \quad (2.6.2)$$

Likewise

$$\begin{aligned} \underline{\psi}^{(1)}(\underline{r}, \omega) = & - \frac{S(\omega)}{8\pi\mu} \sum_{n=0}^{\infty} \frac{\rho^{(n+1)}}{r^n} \underline{s}_{n+1}(\theta, \phi) \left\{ \frac{2}{k_s^2 r^2} \left[e^{-ik_s r} (ik_s r + 1) - 1 \right] \right\} \end{aligned} \quad (2.6.3)$$

Introducing the function

$$\Omega(kr) = \frac{2}{k^2 r^2} \left[e^{-ikr} (ikr + 1) - 1 \right] \quad (2.6.4)$$

which will be termed a propagation function, the potentials may be written:

$$\tilde{\mathfrak{S}}^{(1)}(\underline{\mathbf{r}}, \omega) = -\frac{\tilde{\mathfrak{S}}(\omega)}{8\pi(\lambda+2\mu)} \Omega(\mathbf{k}_p \mathbf{r}) \sum_{n=1}^{\infty} \frac{\rho^{(n)}}{r^{n-1}} S_n(\theta, \phi) = \tilde{\mathfrak{S}}(\omega) \Omega(\mathbf{k}_p \mathbf{r}) \mathfrak{S}^{(1)}(\underline{\mathbf{r}}) \quad (2.6.5)$$

$$\tilde{\underline{\Psi}}^{(1)}(\underline{\mathbf{r}}, \omega) = -\frac{\tilde{\mathfrak{S}}(\omega)}{8\pi\mu} \Omega(\mathbf{k}_s \mathbf{r}) \sum_{n=1}^{\infty} \frac{\rho^{(n)}}{r^{n-1}} \underline{\mathfrak{S}}_n(\theta, \phi) = \tilde{\mathfrak{S}}(\omega) \Omega(\mathbf{k}_s \mathbf{r}) \underline{\Psi}^{(1)}(\underline{\mathbf{r}})$$

Here, $\mathfrak{S}^{(1)}(\underline{\mathbf{r}})$ and $\underline{\Psi}^{(1)}(\underline{\mathbf{r}})$ are the static potentials, equations (2.6.5) showing the relationship between the static and dynamic fields.

Further, the dynamic potentials of (2.6.5) may also be expressed in terms of the source potentials given by (2.3.8), and the propagation functions. Finally, the transform of the dynamic displacement field $\tilde{\underline{\mathbf{u}}}^{(1)}(\underline{\mathbf{r}}, \omega)$ has the form

$$\begin{aligned} \tilde{\underline{\mathbf{u}}}^{(1)}(\underline{\mathbf{r}}, \omega) = \tilde{\mathfrak{S}}(\omega) \left[\nabla \mathfrak{S}^{(1)}(\underline{\mathbf{r}}) \Omega(\mathbf{k}_p \mathbf{r}) + \Omega(\mathbf{k}_s \mathbf{r}) \nabla \times \underline{\Psi}^{(1)}(\underline{\mathbf{r}}) \right. \\ \left. + (\nabla \Omega(\mathbf{k}_p \mathbf{r})) \mathfrak{S}^{(1)}(\underline{\mathbf{r}}) + \nabla \Omega(\mathbf{k}_s \mathbf{r}) \times \underline{\Psi}^{(1)}(\underline{\mathbf{r}}) \right] \quad (2.6.6) \end{aligned}$$

expressed in terms of the static potentials.

For the more general non-stationary source, the potentials $\mathfrak{S}^{(1)}$ and $\underline{\Psi}^{(1)}$ are formally given by the equations (2.6.2) and (2.6.3), provided the multipole coefficients are taken to be frequency dependent. Furthermore, the transform $\tilde{\mathfrak{S}}(\omega)$ must be considered to be unity if these equations are to be used for the non-stationary source, unless it happens that the multipoles have a common frequency factor, in which case a function $\tilde{\mathfrak{S}}(\omega)$ could be factored out. In any case, the solutions $\tilde{\mathfrak{S}}^{(1)}$ and $\tilde{\underline{\Psi}}^{(1)}$ for any source whatsoever, are given formally by

$$\tilde{\zeta}^{(1)}(\underline{x}, \omega) = - \frac{\Omega(k_p, r)}{8\pi(\lambda+2\mu)} \sum_{n=0}^{\infty} \frac{\rho^{(n+1)}(\omega)}{r^n} S_{n+1}(\theta, \phi)$$

(2. 6. 7)

$$\tilde{\psi}^{(1)}(\underline{x}, \omega) = - \frac{\Omega(k_s, r)}{8\pi\mu} \sum_{n=0}^{\infty} \frac{\rho^{(n+1)}(\omega)}{r^n} \underline{g}_{n+1}(\theta, \phi)$$

As has been shown for the stationary source, these solutions may be expressed in terms of the static solutions in special cases; but in general, it is important to note that the multipole coefficients are linearly independent functions of frequency and that consequently any simple relationship to the static solution will be fortuitous. In the developments to follow, both stationary and non-stationary sources can be considered simultaneously, since the results are seen to be at least formally similar.

The results expressed in the equations (2. 6. 2) through (2. 6. 7) constitute an expansion of the source radiation field in a form not previously discovered. Its chief value lies in the insight to be gained from the demonstrated relationship between the static and dynamic fields in the case of the stationary source and from the simple properties of the multipole coefficients and the propagation functions in the general case. It thereby provides the means of relating the radiation fields from complicated sources through a simple common field expansion. In a more practical sense it is clear that the representation of (2. 6. 7) may be used to compute the body wave radiation field. This evaluation of the direct radiation

field thus reduces to the computation of the multipole factors from (2.4.4) for the appropriate force system. In addition, the formulation developed here allows some investigation of the more abstract properties of the dynamic source. Thus it is clear from (2.6.7) that the independent time dependence of the multipole factors renders the convolution technique, for generalizing the time variation at the source, ineffective except for a stationary source. Investigation of the properties of the propagation function will demonstrate other characteristics of the field.

The propagation functions $\Omega(\kappa r)$, $\kappa = k_p, k_s$, may be expressed in a number of different ways. In particular, the spherical Hankel and Bessel functions may be defined by (Jeffreys, p. 558),

$$j_n(\zeta) = \sqrt{\frac{\pi}{2}} \zeta^{-1/2} J_{n+\frac{1}{2}}(\zeta) = (-1)^n \zeta^n \left(\frac{d}{\zeta d\zeta} \right)^n \left(\frac{\sin \zeta}{\zeta} \right)$$

$$h_n^{(2)}(\zeta) = \sqrt{\frac{\pi}{2}} \zeta^{-1/2} H_{n+\frac{1}{2}}(\zeta) = (-1)^n \zeta^n \left(\frac{d}{\zeta d\zeta} \right)^n \left(\frac{e^{-i\zeta}}{-i\zeta} \right)$$

one has, for example,

$$\Omega(\kappa r) = -2 \left(\frac{1}{\kappa r} \right)^2 + ih_1^{(2)}(\kappa r) \quad (2.6.8)$$

On the other hand, if $\Omega(\kappa r)$ is expanded in a power series, then, with ${}_1F_1(a;b;z)$ denoting a hypergeometric function

$$\Omega(\kappa r) = \sum_{v=0}^{\infty} \left(\frac{1}{1+\frac{v}{2}} \right) \frac{(-i\kappa r)^v}{v!} = {}_1F_1(2;3;-i\kappa r) \quad (2.6.9)$$

Therefore, since κ takes on the values $k_s = \frac{\omega}{v_s}$ and $k_p = \frac{\omega}{v_p}$, then in the limit as $\omega \rightarrow 0$ (i. e., the static limit), $\kappa \rightarrow 0$ also, and from the series

$$\lim_{\omega \rightarrow 0} \Omega(\kappa r) = 1 ; \quad \lim_{\omega \rightarrow 0} \nabla \Omega(\kappa r) = 0$$

Hence, the transformed dynamic field, $\underline{u}^{(1)}(\underline{r}, \omega)$ given by (2. 6. 6), reduces to the static result (2. 5. 6) in the limit $\omega \rightarrow 0$, as it should, provided of course that $\tilde{S}(\omega)$ is properly behaved.

The reduction of the dynamic field to the static field in the zero frequency limit has not been previously demonstrated. Further the properties of the propagation function indicate that in the near source region, where $\kappa r \ll 1$, the source field behaves like a static field insofar as its dependence on the spatial coordinates is concerned. On the other hand, for $\kappa r \gg 1$, the field behaves as a true radiation field, having a radial dependence of essentially the form $\exp\{-i\kappa r\}/\kappa r$. The situation is perfectly analogous to the case for an electromagnetic source of radiation (e. g., Jackson, 1962). In the latter case the intermediate field, where $\kappa r \sim 1$, is called the induction field and has the same formal properties as does the elastic field in this range.

Again, consider the special problem of a point force in the x^1 direction, as was done in the static case. It is seen that equation (2. 6. 6) written in its component form as

$$\begin{aligned} \tilde{u}_i(\underline{r}, \omega) = \tilde{S}(\omega) \left[\frac{\partial \tilde{\delta}^{(1)}}{\partial x^i} \Omega(k_p r) + \epsilon_{ijk} \frac{\partial \tilde{\psi}_i}{\partial x^k} \Omega(k_s r) + \tilde{\delta}^{(1)} \frac{\partial \Omega(k_p r)}{\partial x^i} \right. \\ \left. + \epsilon_{ijk} \frac{\partial \Omega(k_s r)}{\partial x^i} \tilde{\psi}_k(\underline{r}) \right] \end{aligned}$$

is most convenient, since the previous results for the static problem may be utilized. As was previously indicated, all the multipole coefficients vanish except

$$R^{(1)}(1) = M$$

and since

$$\frac{\partial \Omega(kr)}{\partial x^j} = -\frac{4}{k^2 r^3} \left[e^{-ikr} (ikr + 1) - 1 \right] \frac{\partial r}{\partial x^j} + \frac{2}{r} e^{-ikr} \left(\frac{\partial r}{\partial x^j} \right)$$

then $u_1^{(1)}(\underline{r}, \omega)$, for example, is found to be

$$\begin{aligned} u_1^{(1)}(\underline{r}, \omega) = -\frac{\tilde{S}(\omega)M}{4\pi\rho} \left(\frac{\partial^2 r^{-1}}{\partial x'^2} \right) \left[\frac{1}{\omega^2} \left\{ e^{-ik_p r} (ik_p r + 1) - e^{-ik_s r} (ik_s r + 1) \right\} \right] \\ + \frac{\tilde{S}(\omega)M}{4\pi\rho r} \left(\frac{\partial r}{\partial x'} \right)^2 \left\{ \frac{1}{v_p^2} e^{-ik_p r} - \frac{1}{v_s^2} e^{-ik_s r} \right\} + \frac{\tilde{S}(\omega)M}{4\pi\rho v_s^2} \left(\frac{e^{-ik_s r}}{r} \right) \end{aligned} \quad (2.6.10)$$

Comparing this result with that given by Love (p. 305) as

$$\begin{aligned} u_1^{(1)}(\underline{r}, t) = \frac{1}{4\pi\rho} \left(\frac{\partial^2 r^{-1}}{\partial x'^2} \right) \int_{r/v_p}^{r/v_s} t' \chi(t-t') dt' + \frac{1}{4\pi\rho r} \left(\frac{\partial r}{\partial x'} \right)^2 \left\{ \frac{\chi(t-r/v_p)}{v_p^2} \right. \\ \left. - \frac{\chi(t-r/v_s)}{v_s^2} \right\} + \frac{1}{4\pi\rho v_s^2} \left(\frac{\chi(t-r/v_s)}{r} \right) \end{aligned}$$

where

$$\mathcal{F}\{\chi(t)\} = M \cdot \tilde{S}(\omega)$$

one observes that

$$\mathcal{F}\left\{\int_{r/v_p}^{r/v_s} t' \chi(t-t') dt'\right\} = -\tilde{S}(\omega) \cdot M \left[\frac{1}{\omega} \left\{ e^{-ik_p r} (ik_p r+1) - e^{-ik_s r} (ik_s r+1) \right\} \right]$$

$$\mathcal{F}\left\{\chi\left(t - \frac{r}{v}\right)\right\} = \tilde{S}(\omega) \cdot M e^{-i\kappa r} ; \quad \kappa = \omega/v \quad \text{with } v = v_s \text{ or } v_p$$

and therefore that (2.6.10) is the Fourier transform of Love's result. The other components $\tilde{u}_2^{(1)}$ and $\tilde{u}_3^{(0)}$ can likewise be shown to be equivalent to those obtained by Love. This provides a simple check on the dynamic solutions in equations (2.6.2) and (2.6.3).

Although the representation obtained and expressed by either equations (2.6.5) or (2.6.7) is a relatively simple one, an application of these results in all but the simplest boundary value problems of interest proves to be very awkward. This is particularly true for wave propagation in a layered half space or sphere. The difficulty can, in principle, be resolved by a suitable transformation of coordinates, the particular transformation to be used depends upon the geometry of the boundaries.

As with the static solution, the difficulties encountered in the application of these solutions in a spherically inhomogeneous body may be resolved, at least in theory, by simply translating the reference system. In particular, if the inhomogeneities of a spherical earth are approximated by a layered sphere, then the boundary value problem for the forced motion of the body may be solved, provided

the source potentials are expressed in a form compatible with the solutions of the homogeneous equations in each layer. Thus, it is necessary that the source potentials be expressed in terms of spherical coordinates with origin at the center of the earth. In addition, the potentials must be expressed in terms of a linear combination of the angular eigenfunctions, $P_n^m(\cos \theta)e^{\pm im\phi}$, of the homogeneous wave equation. Under these conditions, the boundary conditions give a set of algebraic equations defining the characteristic equation for the system.

A translation of the coordinates to an arbitrary origin of coordinates, in particular that at the center of a spherically layered earth model, can be accomplished by more or less the same procedures used for the static case in Appendix (3). In addition, the resulting transformed source potentials may be expressed in terms of the appropriate angular eigenfunctions. The transformed potentials are, however, found to be expressible only as a rather complicated series and the series is not, unfortunately, rapidly convergent under normal circumstances. For this reason, the results will not be reproduced here. It seems sufficient, in fact, to simply state that all attempts to transform the source potentials obtained above to a more widely⁽¹⁾ useful form have been, in any practical sense, unsuccessful. Thus it appears that one must be content primarily with the insight to be gained from the particular solutions rather than

(1) That is, to forms suitable for the computation of the resonance spectrum for a layered model of the earth.

with any great utility that they might possess.⁽¹⁾ For the stated purposes of this study, this result is quite adequate, especially since other representations are readily available and will be developed in the following sections. An important special case will be considered in the following section.

2.7 Representations for Initial Value (Relaxation) Sources

Consider now the 'physical potentials' of the form (2.2.28)

$$\tilde{\Theta}^{(1)}(\underline{r}, \omega) = \frac{1}{4\pi(\lambda+2\mu)} \iiint_V [\nabla' \cdot \tilde{f}' - i\omega\rho \nabla' \cdot \underline{u}'^* e^{-i\omega\tau_1}] \frac{e^{-ik_p r^*}}{r^*} d\underline{r}' \quad (2.7.1)$$

$$\Omega^{(1)}(\underline{r}, \omega) = \frac{1}{8\pi\mu} \iiint_V [\nabla' \times \tilde{f}' - i\omega\rho \nabla' \times \underline{u}'^* e^{-i\omega\tau_2}] \frac{e^{-ik_s r^*}}{r^*} d\underline{r}'$$

For the important case in which only the initial value factor $-i\omega\rho \underline{u}'^*$ is considered, then the source factors $\nabla' \cdot \underline{u}'^*$ and the components of $\nabla' \times \underline{u}'^*$ are harmonic. The harmonic nature of these initial value functions follows from the fact that they correspond to differences in equilibrium values of dilatation and rotation, which are themselves harmonic. In particular, with the initial value function \underline{u}'^* defined throughout the whole space and constrained to vanish with distance as $r^{-\alpha}$, $\alpha \geq 2$, then

⁽¹⁾The solutions can of course be used for the prediction of body wave radiation. This, however, is of marginal importance from the point of view of the present study.

$$\Theta^* \equiv \nabla \cdot \underline{u}^* = O(r^{-\alpha}) ; \quad 2\Omega^* \equiv \nabla \times \underline{u}^* = O(r^{-\alpha}) ; \quad \alpha \geq 2$$

and it follows that Θ^* and Ω_i^* , $i = 1, 2, 3$ are of the form

$$\Theta^* = \sum_{n=1}^{\infty} \left(\frac{1}{r}\right)^{n+1} \sum_{m=0}^n \left\{ a_{nm} \cos m\phi + b_{nm} \sin m\phi \right\} P_n^m(\cos \theta)$$

$$\Omega_j^* = \sum_{n=1}^{\infty} \left(\frac{1}{r}\right)^{n+1} \sum_{m=0}^n \left\{ c_{nm}^{(j)} \cos m\phi + d_{nm}^{(j)} \sin m\phi \right\} P_n^m(\cos \theta)$$

These properties will be shown to follow directly from the definition of the initial values for these potentials in section 3.7. For the developments of the present section these results will be anticipated beforehand.

In order to maintain generality in the evaluation of the relaxation field it is necessary to introduce, explicitly, a causality relationship between the relaxation of the equilibrium field and the physical phenomenon initiating this effect. More specifically, taking the origin of the source coordinates at the point at which an elementary rupture increment, or any perturbation in the physical properties of the medium, is introduced, one may conclude that no relaxation of the potentials at a point \underline{r}' is possible until information concerning the existence of the perturbation has propagated over the distance interval r' . Thus the "initial value", Θ^* , for the dilatation is not defined until a time

$$\tau_1^* = r'/v_p$$

after the creation of the rupture. By the same reasoning

$$\tau_2^* = r'/v_s$$

is the delay time for the rotation. Now since the dynamic field is at least of the order $(1/r)$ while the initial values Θ^* and Ω_j^* are of the order $(1/r^2)$, then for $1/r \ll 1$, it is reasonable to approximate the initial field by taking Θ^* and Ω_j^* to be zero outside a spherical region of radius R_s , with $(1/R_s)^2 \ll 1$. Thus in this approximation, one has, for example,

$$\begin{aligned} \tilde{\Theta}^{(1)}(\underline{r}, \omega) = & \frac{-i\omega\rho}{4\pi(\lambda+2\mu)} \int_0^{R_s} \int_0^{2\pi} \int_0^\pi \left[\sum_{n=0}^{\infty} \left(\frac{1}{r}\right)^{n+1} S_n(\theta', \phi') \right] \\ & \times \frac{e^{-ik_p r^{**}}}{r^*} r'^2 \sin \theta' d\theta' d\phi' dr' \end{aligned}$$

with $r^{**} = r^* + r'$. Now since

$$\frac{e^{-ik_p r^*}}{r^*} = -ik_p \sum_{l=0}^{\infty} (2l+1) P_l(\cos \gamma) j_l(k_p r') h_l^{(2)}(k_p r) ; r > R_s \geq r'$$

and

$$\int_0^{2\pi} \int_0^\pi P_l(\cos \gamma) S_n(\theta', \phi') \sin \theta' d\theta' d\phi' = \frac{4\pi}{2n+1} S_n(\theta, \phi) \delta_{ln}$$

then making use of these relations in the previous integral for $\tilde{\Theta}^{(1)}$, gives

$$\tilde{\Theta}^{(1)}(\underline{r}, \omega) = -\frac{k_p^2}{v_p} \sum_{n=1}^{\infty} h_n^{(2)}(k_p r) S_n(\theta, \phi) \int_0^{R_s} \left(\frac{1}{r'}\right)^{n+1} e^{-ik_p r'} j_n(k_p r') r'^2 dr'$$

The integral over the radial coordinates may be evaluated as a Mellin transform (Erdelyi et al., 1954, Vol. 1, p. 328); and therefore one has⁽¹⁾

$$\int_0^{R_s} \left(\frac{1}{r'}\right)^{n+1} e^{-ik_p r'} j_n(k_p r') r'^2 dr' = \left(\frac{\pi}{2}\right)^{1/2} \frac{k_p^n R_s^2}{2^{n+3/2} \Gamma(n+3/2)} {}_2F_2(n+1, 2; 3, 2n+2; -2ik_p R_s) \quad (2.7.2)$$

so that

$$\tilde{\Theta}^{(1)}(\underline{r}, \omega) = \sum_{n=1}^{\infty} \sum_{m=0}^n \left\{ A_{nm} \cos m\phi + B_{nm} \sin m\phi \right\} h_n^{(2)}(k_p r) P_n^m(\cos \theta) \quad (2.7.3a)$$

$$\tilde{\Omega}_j^{(1)}(\underline{r}, \omega) = \sum_{n=1}^{\infty} \sum_{m=0}^n \left\{ C_{nm}^{(j)} \cos m\phi + D_{nm}^{(j)} \sin m\phi \right\} h_n^{(2)}(k_s r) P_n^m(\cos \theta)$$

with

$$\begin{pmatrix} A_{nm} \\ B_{nm} \end{pmatrix} = -\left(\frac{\pi}{2}\right)^{1/2} \frac{k_p^n}{2^{n+3/2} \Gamma(n+3/2)} (k_p R_s)^2 {}_2F_2(n+1, 2; 3, 2n+2; -2ik_p R_s) \begin{pmatrix} a_{nm} \\ b_{nm} \end{pmatrix} \quad (2.7.3b)$$

$$\begin{pmatrix} C_{nm}^{(j)} \\ D_{nm}^{(j)} \end{pmatrix} = -\left(\frac{\pi}{2}\right)^{1/2} \frac{k_s^n}{2^{n+3/2} \Gamma(n+3/2)} (k_s R_s)^2 {}_2F_2(n+1, 2; 3, 2n+2; -ik_s R_s) \begin{pmatrix} c_{nm}^{(j)} \\ d_{nm}^{(j)} \end{pmatrix}$$

⁽¹⁾ Alternate evaluations of the radial integral in question are possible. In this regard see Erdelyi et al., 1954, Vol. 2, p. 335-336; No. 16 and 26.

The function ${}_2F_2$ is a hypergeometric function given by (Erdelyi et al., 1954b; Higher Transcendental Functions (H. T. F.), vol. 1)

$${}_2F_2(n+1, 2; 3, 2n+2; -2ik_p R_s) = \sum_{r=0}^{\infty} \frac{\Gamma(n+r+1)\Gamma(2n+2)}{\Gamma(2n+r+2)\Gamma(n+1)} \left(\frac{2}{r+2}\right) \frac{(-2ik_p R_s)^r}{\Gamma(r+1)}$$

convergent for all values of its argument. It is not difficult to see that the series (2.7.3a) converges and that the convergence is very rapid for $\kappa < 1$.

Therefore the coefficients of the dynamic field are seen to be related to those of the equilibrium field in a rather complicated, yet calculable, manner. Added complications arise in applications of this elementary source solution to the analytical description of a nonsymmetrically propagating rupture. These problems will be taken up in the following chapter.

It is clear from the preceding manipulations that a physical interpretation of the radial factor R_s can be made by introducing the notion of an effective source volume. This simply amounts to a recognition of the fact that the overwhelming preponderance of radiated energy arises from the region immediately surrounding a rupture or other strong perturbation. Thus, in a demonstrable mathematical sense, an effective boundary to the source region can be justifiably introduced and further, the parameter R_s , arising from this procedure has physical significance.

For long period radiation satisfying the conditions

$$k_p R_s < k_s R_s \ll 1 \quad (2.7.4)$$

the integrals over the radial coordinate may be approximated as

$$\int_0^{R_s} \left(\frac{1}{r'}\right)^{n-1} e^{-iKr'} j_n(Kr') dr' \simeq \int_0^{R_s} \left(\frac{1}{r'}\right)^{n-1} j_n(Kr') dr' \quad (2.7.5)$$

where $K = k_p$ or k_s . The approximation implies that, although the stress release throughout the region bounded by a sphere of radius R_s is not instantaneous throughout the volume, the difference in phase between the long wave length radiation from even the most distantly separated points is negligible. In this case one has, after evaluation of the integral of (2.7.5) as a Hankle transform (Erdelyi et al. (1954), vol. 2, p. 22, No. 4)

$$\begin{pmatrix} A_{nm} \\ B_{nm} \end{pmatrix} = -\left(\frac{k_p}{v_p}\right) \left[\frac{\sqrt{\pi} k_p^{n-1}}{2^n \Gamma(n+1/2)} - \frac{j_{n-1}(k_p R_s)}{R_s^{n-1}} \right] \begin{pmatrix} a_{nm} \\ b_{nm} \end{pmatrix} \quad (2.7.6)$$

$$\begin{pmatrix} C_{nm}^{(j)} \\ D_{nm}^{(j)} \end{pmatrix} = -\left(\frac{k_s}{v_s}\right) \left[\frac{\sqrt{\pi} k_s^{n-1}}{2^n \Gamma(n+1/2)} - \frac{j_{n-1}(k_s R_s)}{R_s^{n-1}} \right] \begin{pmatrix} c_{nm}^{(j)} \\ d_{nm}^{(j)} \end{pmatrix}$$

This simpler relationship between the coefficients for the radiation field and those for the change in the equilibrium field are applicable to the calculation of the long wave length radiation, such as for long period surface waves and lower order modes of oscillation for a finite body.

If the effective source volume is very large, then the limiting values of the coefficients given by (2.7.3) may be determined by taking

$$\int_0^{R_s} \left(\frac{1}{r'}\right)^{n-1} e^{-i\kappa r'} j_n(\kappa r') dr' \simeq \int_0^{\infty} \left(\frac{1}{r'}\right)^{n-1} e^{-i\kappa' r'} j_n(\kappa r') dr' \quad (2.7.7)$$

when $\kappa R_s \gg 1$. For this approximation the parameter κ' in the exponential is taken to be greater than κ , corresponding to an initiation of the relaxation mechanism at times determined by velocities which are lower than the P and S wave velocities. Thus

$$\kappa' > \kappa \quad (2.7.8)$$

for the evaluation of the integral of (2.7.7). The limiting case $\kappa' \rightarrow \kappa$ can then be considered. Thus from Erdelyi et al. (1954), vol. 2, p. 37, No. 32 and p. 33, No. 7 ,

$$\begin{aligned} \int_0^{\infty} \left(\frac{1}{r'}\right)^{n-1} e^{-i\kappa' r'} j_n(\kappa r') dr' \\ = \frac{-\sqrt{\pi} \kappa^{n-2}}{2^{n+1} \Gamma(n+3/2)} {}_2F_1(1, 3/2; n+3/2; (\kappa/\kappa')^2) \end{aligned} \quad (2.7.9)$$

However, the hypergeometric function ${}_2F_1$ has the limiting value

$${}_2F_1(1, 3/2; n+3/2; 1) = \frac{\Gamma(n+3/2)\Gamma(n-1)}{\Gamma(n+1/2)\Gamma(n)} \quad , \text{ for } n > 1$$

thus, if $n > 1$ then

$$\int_0^{\infty} \left(\frac{1}{r'}\right)^{n-1} e^{-i\kappa r'} j_n(\kappa r') dr' = \frac{-\sqrt{\pi} \kappa^{n-2}}{2^{n+1} (n-1) \Gamma(n+1/2)} \quad (2.7.10)$$

Since it will be shown in a later section (3.14) that the relaxation will require $n \geq 2$, then (2.7.10) will be generally applicable. In addition from the previous study of the static field and its interpretation in terms of multipoles or equivalent force systems in section 2.5, it is seen that the case $n = 1$ corresponds to an unbalanced force at the source. Since a naturally induced source, such as that associated with rupture and stress relaxation, can have no net unbalanced force (or moment), inasmuch as there are no suddenly applied forces (or torques) to maintain the equilibrium of the body after rupture, then for such sources the coefficients corresponding to $n = 1$ in the expressions for the change in the equilibrium field must vanish. Thus by this argument alone the assertion that $n > 1$ for a relaxation source becomes quite plausible. In Chapter 3 the assertion will be shown to be valid by direct computation.

In any case, for $\kappa R_s \gg 1$ and $n > 1$, the dynamic field coefficients in (2.7.3) have the limiting values

$$\begin{pmatrix} A_{nm} \\ B_{nm} \end{pmatrix} \approx \frac{1}{v_p} \left\{ \frac{\sqrt{\pi} k_p^n}{2^{n+1} (n-1) \Gamma(n+1/2)} \right\} \begin{pmatrix} a_{nm} \\ b_{nm} \end{pmatrix} \quad (2.7.11)$$

$$\begin{pmatrix} C_{nm}^{(j)} \\ D_{nm}^{(j)} \end{pmatrix} \approx \frac{1}{v_s} \left\{ \frac{\sqrt{\pi} k_s^n}{2^{n+1} (n-1) \Gamma(n+1/2)} \right\} \begin{pmatrix} c_{nm}^{(j)} \\ d_{nm}^{(j)} \end{pmatrix}$$

The solutions (2.7.2) satisfy homogeneous wave equations in

the region $r > 0$.⁽¹⁾ Hence, in view of the definitions of the 'physical potentials' $\tilde{\Theta}^{(1)}$ and $\tilde{\Omega}_j^{(1)}$ given by (2.2.7), these potentials are associated with a vector displacement field satisfying the homogeneous equation of motion if $r > 0$, given by

$$(\lambda + 2\mu)\nabla(\nabla \cdot \underline{u}^{(1)}) - \mu\nabla \times \nabla \times \underline{u}^{(1)} = \rho \frac{\partial^2}{\partial t^2} \underline{u}^{(1)}$$

Or, transforming this equation to the frequency domain and using the definitions of $\tilde{\Theta}^{(1)}$ and $\tilde{\Omega}_j^{(1)}$, one has

$$(\lambda + 2\mu)\nabla\tilde{\Theta}^{(1)} - 2\mu\nabla \times \tilde{\Omega}^{(1)} = -\rho\omega^2 \underline{u}^{(1)}$$

Therefore, the displacement field associated with these potentials is

$$\underline{u}^{(1)}(\underline{r}, \omega) = -\frac{1}{k_p^2} \nabla \tilde{\Theta}^{(1)} + \frac{2}{k_s^2} \nabla \times \tilde{\Omega}^{(1)} \quad (2.7.12)$$

The importance of this relationship is that it allows the stress field associated with the source radiation to be calculated by the use of the dilatation and rotation vector. Since the boundary conditions require continuity of stress, then it is clearly necessary that the stresses be calculated for the solution of any boundary value problem.

The displacement field is, in terms of the potentials $\tilde{\Psi}_j^{(1)}$

$$\tilde{\Psi}_j^{(1)}$$

⁽¹⁾Direct substitution of the potentials $\tilde{\Theta}^{(1)}$ and $\tilde{\Omega}_j^{(1)}$ in (2.7.2) into the equations $(\nabla^2 + k_p^2)\tilde{\Theta}^{(1)} = 0$ and $(\nabla^2 + k_s^2)\tilde{\Omega}_j^{(1)} = 0$ shows this to be the case.

$$\underline{u}^{(1)}(\underline{r}, \omega) = \nabla \tilde{\delta}^{(1)} + \nabla \times \tilde{\psi}^{(1)}$$

and the similarity of this relationship with that in (2.7.12) is the basis for the designation of Θ and $\underline{\Omega}$ as potentials.

2.8. Transformations of the Primary Field for the Initial Value Source

The power of the representation given by (2.7.2) arises from the existence of methods of transforming these solutions into expansions in terms of the eigenfunctions of the wave equation in other coordinate systems. Thus, if the translation (without relative rotations) of the spherical coordinates from the source origin to the center of a spherical earth is considered, as in Figure 15, with r_0 , θ_0 and ϕ_0 the coordinates of the new origin with respect to the source origin, then Friedman and Russek (1954) have shown⁽¹⁾

(1) Ben-Menahem (1962) has given operational forms to certain additional theorems of this type which are analytically useful.

$$\begin{aligned}
 & \left[\sum_{\nu=0}^{\infty} \sum_{\mu=-\nu}^{\nu} i^{\nu-n} (2\nu+1) \frac{(\nu-|\mu|)!}{(\nu+|\mu|)!} j_{\nu}(kr') \right. \\
 & \quad \times P_{\nu}^{\mu}(\cos \theta') e^{-i\mu\phi'} \\
 & \quad \times e^{i(m+\mu)\phi_0} \sum_P i^P a(|m|, |\mu|; p, n, \nu) \\
 & \quad \times h_p^{(2)}(kr_0) P_p^{m+\mu}(\cos \theta_0) \\
 & \quad \quad \quad r' < r_0 \\
 & \left. h_n^{(2)}(kr) P_n^m(\cos \theta) e^{im\phi} = \right. \\
 & \quad \left[\sum_{\nu=0}^{\infty} \sum_{\mu=-\nu}^{\nu} i^{\nu-n} (2\nu+1) \frac{(\nu-|\mu|)!}{(\nu+|\mu|)!} j_{\nu}(kr_0) \right. \\
 & \quad \times P_{\nu}^{\mu}(\cos \theta') e^{-i\mu\phi'} \\
 & \quad \times e^{i(m+\mu)\phi_0} \sum_P i^P a(|m|, |\mu|; p, n, \nu) \\
 & \quad \times h_p^{(2)}(kr') P_p^{m+\mu}(\cos \theta_0) \\
 & \quad \quad \quad r' > r_0
 \end{aligned} \tag{2.8.1}$$

where

$$\begin{aligned}
 a(|m|, |\mu|; p, n, \nu) &= \frac{(2p+1)(n+\nu-p-1)!!}{(n+p-\nu)!!(\nu+p-n)!!(p+\nu+n+1)!!} \\
 & \times \sum_{j=0}^a \binom{a}{j} \frac{(n+j+|m|)!}{(n-j-|m|)!} \frac{(\nu-|m|-j+p)!}{(\nu+|m|+j-p)!} e^{i\pi(\frac{1}{2}(n+p-\nu)+|m|+j)} \\
 & \tag{2.8.2}
 \end{aligned}$$

$$a = p - |m| - |\mu| \quad ; \quad (s)!! = s(s-2)\dots 2 \text{ or } 1; \quad (0)!! = (-1)!! = 1$$

and p runs over the set $\nu + n, \nu + n - 2 \dots \nu - n$.

The general translation of potentials like those in (2.7.2) is easily obtained through use of this addition theorem. The solutions of the form

$$\tilde{\Phi}(\underline{r}, \omega) = \sum_{n=1}^{\infty} \sum_{m=1}^n \{ A_{nm} \cos m\phi + B_{nm} \sin m\phi \} h_n^{(2)}(k_p r) P_n^m(\cos \theta)$$

may also be written as

$$\tilde{\Phi}(\underline{r}, \omega) = \sum_{n=1}^{\infty} h_n^{(2)}(k_p r) \sum_{m=-n}^n a'_{nm} P_n^m(\cos \theta) e^{im\phi} \quad (2.8.3)$$

with

$$a'_{nm} = \begin{cases} \frac{1}{2} (A_{nm} - iB_{nm}) & m > 0 \\ A_{nm} & m = 0 \\ \frac{1}{2} (A_{nm} + iB_{nm}) \frac{(n+|m|)!}{(n-|m|)!} & m < 0 \end{cases}$$

a form to which the addition theorem is easily applied. Thus, requiring the translated potential to have the form

$$\tilde{\Phi}(\underline{r}', \omega) = \sum_{\ell=0}^{\infty} \sum_{k=-\ell}^{\ell} G_{\ell k}(r', \omega) P_{\ell}^k(\cos \theta') e^{-ik\phi'} \quad (2.8.4)$$

then, after substitution of (2.8.1) into (2.8.3) and equating the result to the above desired expansion, one has immediately

$$\begin{aligned}
 G_{\ell k}(r', \omega) &= (2\ell + 1) \frac{(\ell - |k|)!}{(\ell + |k|)!} \begin{pmatrix} j_{\ell}(k_p r') \\ j_{\ell}(k_p r_o) \end{pmatrix} \sum_{n=1} i^{\ell-n} \sum_{m=-n}^n a'_{nm} \\
 \times \sum_{P=\ell-n}^{\ell+n} i^P a(|m|, |k|; p, n, \ell) &\begin{pmatrix} h_p^{(2)}(k_p r_o) \\ h_p^{(2)}(k_p r') \end{pmatrix} P_p^{k+m}(\cos \theta_o) e^{i(k+m)\phi_o}
 \end{aligned} \tag{2.8.5}$$

where the upper pair of Bessel functions are used when $r' < r_o$, and lower when $r' > r_o$.

If the translation is constrained so that $\theta_o = \pi$, $\phi_o = 0$, corresponding to a translation along the z axis, as is often adequate, then this addition theorem reduces to a simpler form in the primed coordinates due to the conditions

$$P_p^{m+\mu}(1) = \delta_{\mu, -m} = \begin{cases} 0, & \mu \neq -m \\ 1, & \mu = -m \end{cases}$$

$$P_p^{m+\mu}(-1) = (-1)^{p-m-\mu} P_p^{m+\mu}(1)$$

Thus, in this case

$$\begin{aligned}
 G_{\ell k}(r', \omega) &= (2\ell + 1) \frac{(\ell - |k|)!}{(\ell + |k|)!} \begin{pmatrix} j_{\ell}(k_p r') \\ j_{\ell}(k_p r_o) \end{pmatrix} \sum_{n=|k|} i^{\ell-n} a'_{n, -k} \\
 \times \sum_P (-1)^P a(|k|, |k|; p, n, \ell) &\begin{pmatrix} h_p^{(2)}(k_p r_o) \\ h_p^{(2)}(k_p r') \end{pmatrix}
 \end{aligned} \tag{2.8.6}$$

These expansions are of a form compatible with the solutions (2.2.17) for the homogeneous equations of motion in a layered spherical body,

since both solutions, of the form (2.8.4), have the same angular dependence. These results are therefore useful for the explicit computation of the excitation of the modes of vibration for a layered spherical earth.

In addition to the transformation of the representation from one spherical coordinate system to another, it is also possible to transform the solution into representations in terms of the eigenfunctions for the wave equation in both the rectangular and cylindrical coordinate system.

Thus, Sato (1950a) has shown

$$\begin{aligned}
 h_n^{(2)}(kr)P_n^m(\cos \theta) &= i^{n-2m}k^{-1} \int_0^\infty J_m(k\rho) \overline{P}_n^m \left\{ (k^2 - k^2)^{1/2} / k \right\} \\
 &\quad \times \frac{e^{-i \left\{ k^2 - k^2 \right\}^{1/2} z}}{(k^2 - k^2)^{1/2}} k dk \\
 & \\
 h_n^{(2)}(kr)P_n^m(\cos \theta)e^{\pm im\phi} &= \left(\frac{i^{n-2m}}{2\pi} \right) k^{-1} \int_{-\infty}^{+\infty} \int_{-\infty}^{+\infty} \left\{ \frac{k_1 \pm ik_2}{K} \right\}^m \\
 &\quad \times P_n^{(m)} \left\{ (k^2 - k_3^2)^{1/2} / k \right\} \exp \left\{ ik_1 x + ik_2 y - i(k^2 - k_3^2)^{1/2} z \right\} \\
 &\quad \times (k^2 - k_3^2)^{-1/2} dk_1 dk_2
 \end{aligned} \tag{2.8.7}$$

where $\overline{P}_n^m(\xi)$ denotes Hobson's definition of the associated Legendre function and $P_n^m(\xi)$ is the usual definition of Ferrers, that is

$$P_n^m(\xi) = (1-\xi^2)^{m/2} \frac{d^m}{d\xi^m} P_n(\xi) = (1-\xi^2)^{m/2} P_n^{(m)}(\xi)$$

$$\overline{P}_n^m(\xi) = (\xi^2-1)^{m/2} \frac{d^m}{d\xi^m} P_n(\xi) = (\xi^2-1)^{m/2} P_n^{(m)}(\xi)$$

and finally, where k_1, k_2, k_3 , and k are wave numbers, with

$$k = k_3 = [k_1^2 + k_2^2]^{1/2}$$

$$K = (k_p, k_s); \quad k_p = \omega/v_p, \quad k_s = \omega/v_s$$

Therefore, the source radiation field in cylindrical coordinates is given by

$$\begin{aligned} \tilde{\Phi}(\rho, z, \phi; \omega) &= \sum_{n=1}^{\infty} \sum_{m=0}^n \left\{ A'_{nm} \cos m\phi + B'_{nm} \sin m\phi \right\} \\ &\times \int_0^{\infty} J_m(k) \overline{P}_n^m \left\{ \frac{(k_p^2 - k^2)^{1/2}}{k_p} \right\} \frac{e^{-i(k_p^2 - k^2)^{1/2} z}}{(k_p^2 - k^2)^{1/2}} k dk \end{aligned} \quad (2.8.8a)$$

$$\begin{aligned} \tilde{\chi}_j(\rho, z, \phi; \omega) &= \sum_{n=1}^{\infty} \sum_{m=0}^n \left\{ C^{(j)'}_{nm} \cos m\phi + D^{(j)'}_{nm} \sin m\phi \right\} \int_0^{\infty} J_m(k\rho) \\ &\times \overline{P}_n^m \left\{ \frac{(k_s^2 - k^2)^{1/2}}{k_s} \right\} \frac{e^{-i(k_s^2 - k^2)^{1/2} z}}{(k_s^2 - k^2)^{1/2}} k dk \end{aligned} \quad (2.8.8b)$$

where

$$\begin{pmatrix} A'_{nm} \\ B'_{nm} \end{pmatrix} = e^{i(n-2m)\pi/2} \left(\frac{1}{k_p} \right) \begin{pmatrix} A_{nm} \\ B_{nm} \end{pmatrix} \quad (2.8.9)$$

$$\begin{pmatrix} C^{(j)'}_{nm} \\ D^{(j)'}_{nm} \end{pmatrix} = e^{i(n-2m)\pi/2} \left(\frac{1}{k_s} \right) \begin{pmatrix} C^{(j)}_{nm} \\ D^{(j)}_{nm} \end{pmatrix}$$

with $A_{nm}, \dots, D^{(j)}_{nm}$ given by expressions such as those in section 2.7.

Likewise, in Cartesian coordinates

$$\begin{aligned} \tilde{\Phi}(x, y, z; \omega) = & \frac{1}{2\pi} \sum_{n=1}^{\infty} \sum_{m=0}^n \int_{-\infty}^{+\infty} \int_{-\infty}^{+\infty} \left(A'_{nm} \left[\left\{ \frac{k_1 + ik_2}{k_p} \right\}^m + \left\{ \frac{k_1 - ik_2}{k_p} \right\}^m \right] \right. \\ & \left. + iB'_{nm} \left[\left\{ \frac{k_1 + ik_2}{k_p} \right\}^m - \left\{ \frac{k_1 - ik_2}{k_p} \right\}^m \right] \right) P_n^{(m)} \left\{ (k_p^2 - k_3^2)^{1/2} / k_p \right\} \\ & \times \frac{\exp \left\{ ik_1 x + ik_2 y - i(k_p^2 - k_3^2)^{1/2} z \right\}}{(k_p^2 - k_3^2)^{1/2}} dk_1 dk_2 \quad (2.8.10a) \end{aligned}$$

$$\begin{aligned} \tilde{\chi}_j(x, y, z; \omega) = & \frac{1}{2\pi} \sum_{n=1}^{\infty} \sum_{m=0}^n \int_{-\infty}^{+\infty} \int_{-\infty}^{+\infty} \left(C^{(j)'}_{nm} \left[\left\{ \frac{k_1 + ik_2}{k_s} \right\}^m + \left\{ \frac{k_1 - ik_2}{k_s} \right\}^m \right] \right. \\ & \left. + iD^{(j)'}_{nm} \left[\left\{ \frac{k_1 + ik_2}{k_s} \right\}^m - \left\{ \frac{k_1 - ik_2}{k_s} \right\}^m \right] \right) P_n^{(m)} \left\{ (k_s^2 - k_3^2)^{1/2} / k_s \right\} \\ & \times \frac{\exp \left\{ ik_1 x + ik_2 y - i(k_s^2 - k_3^2)^{1/2} z \right\}}{(k_s^2 - k_3^2)^{1/2}} dk_1 dk_2 \quad (2.8.10b) \end{aligned}$$

with $A_{nm}^i, \dots, D_{nm}^{(j) i}$ defined as in (2.8.9) above.

The representation of (2.8.8) and (2.8.10) are appropriate expansions for the study of surface wave excitation in a layered half space. Thus, a layered half space earth model, which is a reasonable model for the higher frequency surface waves, may be used along with these solutions to predict surface waves for different sources in terms of their physical properties or, conversely, the source properties may be deduced from the observed surface wave radiation. Such investigations may also be carried out (somewhat more accurately) using the spherical earth model and the source solutions (2.8.4). The details will be taken up in the following chapters.

2.9. General Representations for Finite Volume Sources

More generally, if the source terms in (2.7.1) are not restricted to initial values and are not, therefore, necessarily harmonic functions, then it is necessary to resort either to the multipole theory developed earlier or to performing the integrations in (2.7.1) directly. If, however, the source terms in question are not initial values, then, ruling out general body forces such as gravity, they will be limited to some finite volume within the medium. Thus, a direct integration is formally possible, since one may use the expansions of $\exp(-ikr^*)/r^*$ introduced previously and the addition theorem

$$P_n(\cos \gamma) = \sum_{m=0}^n (2 - \delta_{m0}) \frac{(n-m)!}{(n+m)!} P_n^m(\cos \theta) P_n^m(\cos \theta')$$

$$\times \left[\cos m\phi \cos m\phi' + \sin m\phi \sin m\phi' \right]$$

to write (2.7.1) in the form

$$\tilde{\Theta}'(\underline{r}, \omega) = \frac{-ik_p}{4\pi(\lambda+2\mu)} \sum_{n=0}^{\infty} \sum_{m=0}^n \left\{ \mathfrak{L}_{nm} \cos m\phi + \mathfrak{M}_{nm} \sin m\phi \right\}$$

$$\times P_n^m(\cos \theta) h_n^{(2)}(k_p r)$$
(2.9.1)

$$\tilde{\Omega}_j(\underline{r}, \omega) = \frac{-ik_s}{8\pi\mu} \sum_{n=0}^{\infty} \sum_{m=0}^n \left\{ \rho_{nm}^{(j)} \cos m\phi + \mathfrak{Q}_{nm}^{(j)} \sin m\phi \right\}$$

$$\times P_n^m(\cos \theta) h_n^{(2)}(k_s r)$$

where

$$\begin{pmatrix} \mathfrak{L}_{nm} \\ \mathfrak{M}_{nm} \end{pmatrix} = (2 - \delta_{m0}) \frac{(n-m)!}{(n+m)!} (2n+1) \int_0^{2\pi} \int_0^{\pi} \left[\int_a^b (\nabla \cdot \tilde{f}') j_n(k_p r') r'^2 dr' \right]$$

$$\times P_n^m(\cos \theta') \begin{pmatrix} \cos m\phi \\ \sin m\phi \end{pmatrix} \sin \theta' d\theta' d\phi'$$
(2.10.2)

$$\begin{pmatrix} \rho_{nm}^{(j)} \\ \mathfrak{Q}_{nm}^{(j)} \end{pmatrix} = (2 - \delta_{m0}) \frac{(n-m)!}{(n+m)!} (2n+1) \int_0^{2\pi} \int_0^{\pi} \left[\int_a^b (\nabla \times \tilde{f}') j_n(k_s r') r'^2 dr' \right]$$

$$\times P_n^m(\cos \theta) \begin{pmatrix} \cos m\phi \\ \sin m\phi \end{pmatrix} \sin \theta' d\theta' d\phi'$$

The limits of the integral over r' are finite and, therefore, the

integration presents no fundamental difficulties. In this regard, an integral theorem due to Hobson is useful (Hobson, p. 161, (1931)). Thus, by a minor rearrangement and condensation of Hobson's result, one has the general integral relation

$$\int_0^{2\pi} \int_0^\pi f(x, y, z) S_n^a(\theta, \phi) \sin \theta \, d\theta \, d\phi = 4\pi r^n \frac{2^n n!}{(2n)!!} \sum_{k=0}^{\infty} \frac{r^{2k}}{(2k)!!(2n+2k+1)!!}$$

$$\times \left[Y_n^a \left(\frac{\partial}{\partial x}, \frac{\partial}{\partial y}, \frac{\partial}{\partial z} \right) \nabla^{2k} f(x, y, z) \right]_{x=y=z=0} \quad (2.9.3)$$

where $f(x, y, z)$ is any function representable by an absolutely and uniformly convergent power series within the region bounded by a sphere of radius $R > r$ and centered at $(0, 0, 0)$. Also

$$S_n^a(\theta, \phi) \equiv P_n^m(\cos \theta) \begin{cases} \cos m\phi & ; \quad a = 0 \\ \sin m\phi & ; \quad a = 1 \end{cases}$$

$$Y_n^a(\theta, \phi) = r^n S_n^a(\theta, \phi) \equiv Y_n^a(x, y, z)$$

where the solid harmonic Y_n^a may be expressed as a multinomial in x, y and z . Thus, the operator $Y_n^a \left(\frac{\partial}{\partial x}, \frac{\partial}{\partial y}, \frac{\partial}{\partial z} \right)$ is obtained from the multinomial form by replacing x_i by $\frac{\partial}{\partial x_i}$, $i = 1, 2, 3$, so

$$Y_n^a \left(\frac{\partial}{\partial x}, \frac{\partial}{\partial y}, \frac{\partial}{\partial z} \right) = \sum_{P_1, P_2, P_3} A_{P_1, P_2, P_3}^a \left(\frac{\partial}{\partial x} \right)^{P_1} \left(\frac{\partial}{\partial y} \right)^{P_2} \left(\frac{\partial}{\partial z} \right)^{P_3}$$

Therefore, if the limits of the integral over r^1 in (2.9.2) are independent of θ^1 and ϕ^1 , then the integration over θ^1 and ϕ^1 may

be performed first, and so using (2.9.3), one has, for example

$$\mathfrak{L}_{nm} = 4\pi(2-g_{mo}) \frac{(n-m)!}{(n+m)!} (2n+1) \frac{2^n n!}{(2n)!!} \sum_{k=0}^{\infty} \frac{\Lambda_{nk}^{(0)}}{(2k)!!(2n+2k+1)!!}$$

$$\times \int_a^b r^{2k+n+2} j_n(k_p r') dr'$$

with

$$\Lambda_{nk}^{(0)} = \left\{ Y_n^0 \left(\frac{\partial}{\partial x}, \frac{\partial}{\partial y}, \frac{\partial}{\partial z} \right) \nabla^{2k} \left[\nabla \cdot \underline{\tilde{f}} \right] \right\}_{x=y=z=0}$$

The integral over the radial coordinate may be evaluated as a Hankel transform, since

$$\int_a^b r^{2k+n+2} j_n(k_p r') dr' = \left(\frac{\pi}{2} \right)^{1/2} \left(\frac{1}{k_p} \right)$$

$$\times \left[\int_0^{\infty} g_1^{(k)}(r') J_{n+(1/2)}(k_p r') (k_p r')^{1/2} dr' \right.$$

$$\left. - \int_0^{\infty} g_2^{(k)}(r') J_{n+(1/2)}(k_p r') (k_p r')^{1/2} dr' \right]$$

with

$$g_i^{(k)}(r') = \begin{cases} r'^{2k+n+1} & , \quad 0 < r' < a_i \\ 0 & , \quad a_i < r' < \infty \end{cases}$$

$$a_i = \begin{cases} b, & i = 1 \\ a, & i = 2 \end{cases}$$

Therefore (Erdelyi et al, 1954),

$$\int_a^b r'^{2k+n+2} j_n(k_p r') dr' = \left(\frac{\pi}{2}\right)^{\frac{1}{2}} \left(\frac{1}{k_p}\right)^{2k+n+3} \left\{ (2k+2n+1) \left[(k_p b) J_{n+\frac{1}{2}}(k_p b) \right. \right. \\ \times S_{2k+n+\frac{1}{2}, n-\frac{1}{2}}(k_p b) - (k_p a) J_{n+\frac{1}{2}}(k_p a) S_{2k+n+\frac{1}{2}, n-\frac{1}{2}}(k_p a) \\ \left. \left. - \left[(k_p b) J_{n-\frac{1}{2}}(k_p b) S_{2k+n+(3/2), n+\frac{1}{2}}(k_p b) \right. \right. \right. \\ \left. \left. \left. - (k_p a) J_{n-\frac{1}{2}}(k_p a) S_{2k+n+(3/2), n+\frac{1}{2}}(k_p a) \right] \right] \right\} \quad (2.9.4)$$

where $S_{\mu, \nu}(z)$ is Lommel's function, defined in terms of more elementary functions by

$$S_{\mu, \nu}(z) = \frac{z^{\mu+1}}{(\mu-\nu+1)(\mu+\nu+1)} {}_1F_2 \left(1; \frac{\mu-\nu+3}{2}, \frac{\mu+\nu+3}{2}; -\frac{z^2}{4} \right) \\ + 2^{\mu-1} \Gamma\left(\frac{\mu-\nu+1}{2}\right) \Gamma\left(\frac{\mu+\nu+1}{2}\right) \left[\sin\left(\frac{\mu-\nu}{2} \pi\right) J_{\nu}(z) \right. \\ \left. - \cos\left(\frac{\mu-\nu}{2} \pi\right) N_{\nu}(z) \right]$$

where ${}_1F_2$ is a generalized hypergeometric function and $N_{\nu}(z)$ is the Bessel function of the second kind.

If $a = 0$ in the integral, then (2.9.4) becomes

$$\int_0^b r'^{2k+n+2} j_n(k_p r') dr' = \left(\frac{\pi}{2}\right)^{\frac{1}{2}} \left(\frac{1}{k_p}\right)^{2k+n+3} \\ \times \left\{ (2k+2n+1) (k_p b) J_{n+\frac{1}{2}}(k_p b) S_{2n+n+\frac{1}{2}, n-\frac{1}{2}}(k_p b) \right. \\ \left. - (k_p b) J_{n-\frac{1}{2}}(k_p b) S_{2k+n+(3/2), n+\frac{1}{2}}(k_p b) + 2^{n+(3/2)} \Gamma(n+(3/2)) S_{k0} \right\} \\ (2.9.5)$$

Denoting the value of the integral over the radial variable in (2.9.4) or (2.9.5) by $\mathfrak{R}_{nk}(a, b; k_p)$, then, when a and b are independent of θ and ϕ in (2.9.2),

$$\begin{aligned} \left(\begin{array}{c} \mathfrak{L} \\ \mathfrak{M} \\ \mathfrak{N} \end{array} \right)_{nm} &= 4\pi(2-\mathfrak{S}_{mo}) \frac{(n-m)!}{(n+m)!} (2n+1) \frac{2^n n!}{(2n)!!} \\ &\times \sum_{k=0}^{\infty} \frac{\mathfrak{R}_{nk}(a, b; k_p)}{(2k)!!(2n+2k+1)!!} \left(\begin{array}{c} \Lambda_{nk}^{(0)} \\ \Lambda_{nk}^{(1)} \end{array} \right) \end{aligned} \quad (2.9.6)$$

$$\begin{aligned} \left(\begin{array}{c} \mathfrak{P} \\ \mathfrak{Q} \end{array} \right)_{nm} &= 4\pi(2-\mathfrak{S}_{mo}) \frac{(n-m)!}{(n+m)!} (2n+1) \frac{2^n n!}{(2n)!!} \\ &\times \sum_{k=0}^{\infty} \frac{\mathfrak{R}_{nk}(a, b; k_s)}{(2k)!!(2n+2k+1)!!} \left(\begin{array}{c} j\Gamma_{nk}^{(0)} \\ j\Gamma_{nk}^{(1)} \end{array} \right) \end{aligned}$$

where

$$\begin{aligned} \Lambda_{nk}^{(a)} &= \left\{ Y_n^{(a)} \left(\frac{\partial}{\partial x}, \frac{\partial}{\partial y}, \frac{\partial}{\partial z} \right) \nabla^{2k} \left[\nabla \cdot \underline{\tilde{f}} \right] \right\}_{r=0} \\ j\Gamma_{nk}^{(a)} &= \left\{ Y_n^{(a)} \left(\frac{\partial}{\partial x}, \frac{\partial}{\partial y}, \frac{\partial}{\partial z} \right) \nabla^{2k} \left[\nabla \times \underline{\tilde{f}} \right]_j \right\}_{r=0} \end{aligned}$$

Thus, under the conditions stated for a and b , the evaluation of the integrals in (2.9.2) can be accomplished, the results being a rapidly converging series. If a and b depend on θ and ϕ , then the integration over the radial variable must be performed first. In any case, the integration is a Hankel transform. Once the transform is evaluated in terms of θ and ϕ as parameters, then Hobson's result (2.9.3) may be applied as in the case just computed.

In any case, the potentials of (2.9.1) are of the form of (2.7.8), and, therefore, the transformations to the various coordinate systems previously considered may be applied to this solution as well; the results are therefore as given in the equations (2.8.2) through (2.8.7).

The displacement field in the region outside the source volume may be obtained from the equations of motion. Unlike the case for an initial value source, the equations of motion contain an explicit source term, in particular

$$\rho \frac{\partial^2}{\partial t^2} \underline{u}^{(1)} = (\lambda + 2\mu) \nabla \Theta^{(1)} - 2\mu \nabla \times \underline{\Omega}^{(1)} + \underline{f} ; \text{ for all } \underline{r}$$

However, for the region outside the finite source zone, $\underline{f} \equiv 0$ by definition and therefore, when $\tilde{\Theta}^{(1)}$ and $\tilde{\underline{\Omega}}^{(1)}$ have been determined, then $\tilde{\underline{u}}^{(1)}$ is given by

$$\tilde{\underline{u}}^{(1)}(\underline{r}, \omega) = - \frac{1}{k_p^2} \nabla \tilde{\Theta}^{(1)} + \frac{2}{k_s^2} \nabla \times \tilde{\underline{\Omega}}^{(1)} \quad (2.9.7)$$

Applications of the appropriate representation to source problems of geophysical interest will be considered in subsequent chapters. Of the various source types of general interest, special consideration will be given to the tectonic source, and consequently the potentials given by the equations (2.7.2) will be the most useful.

2.10. Summary of Theoretical Results

The theoretical developements of the previous sections have provided a number of results of a relatively general nature. They can be summarized as follows:

- (1) The primary source field has been expressed in three different forms, appropriate for the investigation and prediction of the source field under somewhat different initial conditions and from alternate points of view. In particular:
 - (a) Multipole field expansions, useful for the investigation of certain general field properties. ⁽¹⁾
 - (b) Spherical wave expansions, more practically useful general representations of the field in terms of spherical waves. ⁽¹⁾
 - (c) A spherical wave expansion for the initial value elastic field, wherein the series coefficients are algebraically related to the initial field, and the source time variation is automatically specified.
- (2) The dynamic source field approaches the static source field in the limit, $\omega \rightarrow 0$.
- (3) A general volume source may always be expressed as a

⁽¹⁾ In both cases, the appropriate solution coefficients for any given body force distribution are given in terms of multipole integrals and differential formulas, respectively.

multipole field. For separable source functions, $\underline{f}(\underline{r}, t)$, appearing in the equations of motion, it has been shown that a special relationship exists between the static and dynamic fields, in that the transformed dynamic field is given by the simple product of the static field and a propagation function. For non-separable source functions, the dynamic field is given by the product of the propagation function and a multipole field with frequency dependent multipole coefficients. The latter field is identical with the static field in the limit as $\omega \rightarrow 0$, and the frequency dependent coefficients are in general linearly independent functions of frequency.

Physical interpretations and applications of these rather formal mathematical results will be made in subsequent sections.

One cannot fail to note, however, from the preceding considerations, that the appealing purity and power of a purely mathematical approach is considerably diluted by the physical sterility of the results.

Chapter 3

TECTONIC SOURCE THEORY

3.1. Introduction

The intent of the present chapter is to incorporate within the basic structure of the mathematical theory of elastic sources the salient features of tectonic (or natural) sources. It seems hardly necessary to point out that such sources are basically non-linear in nature and, from a physical as well as mathematical standpoint, extremely complex, so that an attempt to describe the radiation field in precise terms will require some idealization of the physical processes involved. In the following developments an attempt will be made to clearly set forth the idealizations required in the theory. It is not, however, always possible to clearly and precisely estimate the degree of approximation associated with such a theory or even with one single aspect of the theory since our experimental knowledge is so limited. Therefore in the formulation of the field theory, the most generally accepted principles and phenomenon associated with material rupture will be adopted as a basis for the theory. On such a basis the general mathematical theory will be developed, the precepts of the theory then being largely associated with observational facts of a macroscopic nature.

Thus the elastic rebound theory (Reid, 1933) is used as an initial model of rupture and is generalized to include modes of rupture other than simple fracture. In addition the mechanism of release of elastic energy is generalized to include volume radiation due to

stress relaxation in the vicinity of a rupture zone.

In addition to a macroscopic rupture theory, which serves as an appropriate dynamical model, the microscopic mechanisms associated with rupture, in particular the observations of physical dislocations⁽¹⁾ and related phenomena (creep), are reviewed. The microscopic theories of rupture consistent with the experimental evidence of deformation and rupture in metals and earth materials at normal and elevated pressures and temperatures are discussed and related to rupture in the earth. This physical theory is shown to be consistent with the less detailed elastic relaxation model.

The mathematical description of the radiation field associated with the tectonic source will constitute an extension of the mathematical theory in Chapter 2, incorporating additional physical properties associated with rupture and stress relaxation.

3. 2. Macroscopic Mechanisms of Seismic Rupture

Reid's elastic rebound theory may be summarized as follows (e. g. Teisseyre, 1960)

- (1) A fracture occurs as a result of the elastic strain exceeding the strength of the material, whereby mutual displacement of the surrounding masses takes place.
- (2) Displacements do not originate suddenly and the

⁽¹⁾ In the present context the term physical dislocation refers to the microscopic imperfections of the crystalline lattice as opposed to the purely mathematical concept of a dislocation or discontinuity in the displacement field within an elastic continuum.

velocities of the material points reach a maximum only after a finite time.

- (3) The movement is a rapid elastic rebound of the sides of the fracture towards a position of no elastic strain.
- (4) The dynamic processes start on a small area, which subsequently are rapidly enlarged. Radiation of elastic energy occurs from the surface of the fracture.
- (5) The source of the elastic energy is the elastic strain energy of the medium.

Of these concepts, all except the last will be altered in order that they conform more closely with the concept of stress relaxation and the ensuing radiation from the volume surrounding the rupture. Thus since the source of elastic energy in the radiation field is in the initial strain field of the medium, it follows that once the rupture is initiated, then the stress field must readjust toward a state of equilibrium determined by boundary conditions on the rupture surface. This readjustment or relaxation must be accomplished by radiation of seismic energy whenever the medium is ideally elastic, since there is no other mechanism. However the behavior of the medium undoubtedly departs appreciably from that of a perfect elastic solid in the region immediately surrounding the rupture. Therefore in this region the stress relaxation is considered to be accomplished primarily by flow or microscopic fracture phenomenon rather than by radiation. In this zone however, the essential feature introduced, is an inability of at least some of the material to sustain tectonic

shear stress. As a first model, the whole non-linear region will be considered a shear free region. As an idealization of the process then, the whole rupture zone will be considered to be enclosed within a surface over which the shear tractions vanish, so that the equilibrium state of the medium is determined by this boundary condition. The width of the rupture zone is in all likelihood small, however, in the theory to follow, this dimension is treated as finite and is represented parametrically in the formulation. In the limit it may, of course, be considered very small or zero in which case the rupture volume reduces to the rupture plane itself.

The tacit assumption that the whole rupture volume remains essentially fluid throughout the time interval of rupturing is rather a tenuous proposition, at least at depths where the temperature is rather far from the melting point. While phase change, particularly melting, is a highly plausible rupture mechanism at all depths, except possibly within a few kilometers of the earth's surface, it is quite possible that recrystallization and an accompanying increase in viscosity of the melt will follow rapidly in the wake of the melting or rupture front. Hence a growing rupture boundary of zero traction might not be the most realistic model for all depths in the earth. In such circumstances, or in instances of brittle rupture, a more plausible model can be used. Thus as a second model of natural rupture, a region of zero rigidity will be assumed to propagate over the total zone of rupture. In this case the boundary condition on this propagating volume is taken as the vanishing of the tractions, as in

the previous model, but the boundary itself is defined over only a relatively small region at the front of the rupture zone. The material which had previously been within this moving rupture zone is assumed to have at least partially recrystallized, so that this old rupture will be considered as healed and necessarily in a manner such that the equilibrium field in the region surrounding the rupture boundary is, at any time, that which is appropriate to the rupture in the presence of the initial tectonic stress field.

The two models of rupture are represented schematically in Figure 3. In general the first of these spontaneous rupture models will be referred to in terms of rupture growth, while the second in terms of rupture propagation.

Thus the dynamical properties of a tectonic source will be described in terms of a readjustment or relaxation of pre-existing stress by elastic radiation from the vicinity of a region in which the physical properties, principally the rigidity modulus, are changed abruptly. The tectonic source is therefore viewed in terms of the release of potential strain energy from within the elastic zone of the medium itself. Within the non-elastic rupture zone the stress release is accomplished by flow, fracture phenomenon or phase change, and the original strain energy stored within this volume is assumed to be taken up in the work of non-elastic deformation. The energy would appear, in part, as heat rather than as (seismic) elastic radiation and so further reduce the effective rigidity of the material during the initial rupturing.

As a consequence of the emphasis placed on the stress relaxation concept in the development of the tectonic source in the present study, it is convenient to describe the theory, which will be developed more fully, as an elastic relaxation theory in order to distinguish it from other theories, principally the elastic rebound theory and various mathematical dislocation models. Although these approaches to a description and explanation of the tectonic source are certainly not without common features, there are at least some fundamental differences which will result in different predicted characteristics for the source.

The relaxation theory incorporates the main features of the elastic rebound theory as a possible special case. However the theory is generalized so as to include the specific role of the initial strain field, the associated effect of the volume radiation and further the effects of a rupture volume, and its boundary surface which expand or propagate as the case may be, with a finite rupture velocity.

The essential features of the relaxation theory to be utilized in the following developments may be summarized as follows:

- (1) A rupture zone occurs as a result of the accumulated strain exceeding the "strength" of the material and represents a region of large relative displacement and deformation beyond the elastic limits. The rupture volume is characterized as a region of vanishing shear strength.
- (2) All processes, including elastic relaxation, require finite and physically realizable time intervals for their

accomplishment. The rupture volume and its boundary surface are functions of time and their growth or propagation may be characterized by a definite and finite velocity function.

- (3) After a proper time delay, the material points exterior to the rupture volume move toward new positions of elastic equilibrium, determined by the vanishing of shear traction on the boundary surface of the rupture volume and by the dimensions of the boundary surface.
- (4) The dynamic relaxation processes start at the position of initial rupture and subsequently expand throughout the volume of the prestressed medium with the appropriate compressional or shear wave velocity. Radiation of elastic energy occurs from throughout the prestressed volume exterior to the rupture zone.
- (5) The source of the elastic energy is the elastic strain energy of the medium.

It is evident that the relaxation process is complicated by the propagation of the rupture boundary and the fact that the medium is characterized by two velocities of wave propagation. The dynamical effects of an elementary rupture in a prestressed material have been described as a generalized initial value problem in Chapter 2. The introduction of potentials has served to separate effects occurring with the two characteristic wave velocities of the medium. The synthesis of the elementary source solution to yield a solution for a

time dependent rupture or growth propagation is a matter of some complexity in detail but in essence the method is one of superposition. The problem will be simplified in the present chapter by the explicit introduction of a source time variable τ , in analogy with the usual Green's function technique. By superposing the elementary solutions over a source time interval corresponding to an appropriate expansion of the rupture, it will be possible to approximate the rupture growth or propagation and the accompanying stress relaxation.

The source model and representation theory of the present study therefore includes as physical parameters, the rupture velocity, initial stress field (assumed homogeneous to first order) and source dimensions.

An additional and important feature of the elastic relaxation theory is the specification of the time variation of the radiation field from the tectonic source. Thus, since the time variation of the relaxation mechanism is automatically determined from a formulation of the process as the "initial value" problem described previously, then as a necessary consequence the radiation field will be seen to follow a prescribed time variation. In addition the total energy radiated from the source may be computed from the difference between the initial or prestress field and the final equilibrium stress field in the medium. To a good approximation the strain energy reduction so obtained may be interpreted as the energy radiated from the effective source volume.

Knopoff (1958) originally computed the energy release

associated with the introduction of a two-dimensional rupture surface (infinite sheet) into an infinite, prestressed medium. Later Keylis-Borok (1959) extended this approach to a three-dimensional spheroidal model of a fault where the major dimensions were circular. Press and Archambeau (1962) applied the concept to an explosive induced tectonic source and computed the strain energy release to be expected from the vicinity of a spherical shock zone in prestressed media. Knopoff's original model implies a dynamical model at least similar to that introduced in this study and can be considered the static predecessor of the present detailed dynamical theory.

The present relaxation model of tectonic sources has been framed in terms of natural or earthquake sources, however essentially the same mechanism would apply to any process in which the properties of the material are changed abruptly. As a consequence one may conclude that stress relaxation in a prestrained medium may also be induced artificially by an explosive source producing a strong shock wave in the material. In this case a rupture zone is created by the shock wave (e. g., Haskell, 1961), interior to which the medium is assumed to be altered so as not to be able to sustain tectonic shear stress. Quite clearly this shock induced rupture zone is equivalent to that previously postulated for the general tectonic source, so that the general theory is applicable. Press and Archambeau used these same physical arguments for their computation of tectonic energy radiated from such a source. This source

will be treated in the fullest detail in the following sections.

3.3. A Comparative Review of Tectonic Source Theory

A great many tectonic source models have been suggested and used with varied success in the past. In general a particular model is suitable for the explanation of some particular aspect of the observed radiation field. Until quite recently the tectonic source was most successfully described in terms of an equivalent point source or in terms of an equivalent volume source. Balakina, Savarensky, and Vvedenskaya (1961) have reviewed the tectonic source theory up to 1960, Honda (1962 and 1957) gives a similar and somewhat more extensive review. In all cases extensive bibliographies are compiled. The source models may be considered equivalent multipole sources and for the purposes of this study may be conveniently summarized as follows:⁽¹⁾

- (1) Byerly-Hodgson point source model: On the basis of an early theoretical study by Nakano (1923), Byerly and later Hodgson assumed a double force with moment (single couple) tectonic source model and compared the predicted polarity⁽²⁾ of the radiated P waves as a function of the

⁽¹⁾ Since only a very superficial survey of the methods and theory of the equivalent point and volume sources commonly used is given here, reference can be made to Balakina, Savarensky and Vvedenskaya (1961) or Honda (1957) and (1962) for a more complete discussion and listing of the contributions from the numerous researchers involved in the establishment and application of these representations.

⁽²⁾ In the present context the term polarity is used to imply directionality of the first motion. Thus for example an outwardly directed P first motion is considered positive, and inward, toward the source, as negative.

angular coordinates with that observed for numerous earthquakes. Using only the polarity of first motions of P waves, these investigators followed by many others obtain a simple and reasonable, although not unambiguous, interpretation of the source mechanism.

- (2) Keylis-Borok point source models: Numerous point sources based on the strain nuclei introduced by Love (1944) are considered as possible source representations. Using the theoretically predicted amplitudes and polarities as functions of the angular coordinates for P, SH and SV waves, Keylis-Borok and others conclude that, of the point sources considered, the single couple generally gives the best overall agreement with the observed polarity of P and S waves.
- (3) Honda volume source models: Earthquake foci are represented by a small spherical distribution of forces arranged in a particular manner. That is, the spherical volume is divided into four parts by two mutually perpendicular planes and in two opposite parts, forces of compression are assumed while in the remaining two quadrants tensional forces are assumed. This system is clearly equivalent to a point multipole source and may in fact be seen to be equivalent to a double couple. Using this model Honda and others have obtained agreement with the polarity of the radiated first motions of P and occasionally S

waves and to some degree, statical agreement with the displacements at the surface for shallow tectonic sources.

An equivalent multipole system has long been considered a valid representation scheme for the usual type of volume source. This contention has in fact been shown to be valid in general for bounded force distributions by the theory of Chapter 2. Since the models summarized above are equivalent to multipole field solutions, although of a very select type, the representations do therefore have a clear logical basis. In addition the Byerly-Hodgson and Keylis-Borok representations, which are equivalent, are also, loosely speaking, in apparent first order agreement with elastic rebound theory if the single couple is envisioned as the force pair giving a sudden relative shearing movement to opposite sides of a rupture. However, even in terms of the rather severely idealized elastic rebound theory, both the single couple and double couple sources represent highly restricted representations which either arbitrarily assume or completely ignore the effects of the actual physical dimensions of the sources, the complicated time dependence of the rupturing and resulting radiation and the relationship of the initial stress field to the radiation field. Therefore these multipole sources are usually considered as valid representations of only the initial "movement" at the source, that is at the focus of the tectonic source. The initial motion may, possibly, be indicative of the fault mechanism. However, the precise relationship of the first motions from a tectonic source to the total motion and source mechanism has never been

clearly established.

If the additional source properties were included, an objective analysis of the observed radiation in terms of a multipole theory would require a representation involving a superposition of multipoles. This follows from the theory of Chapter 2 in which a distributed force system of arbitrary time dependence, that is, where the time and spatial dependence of the force system need not be separable, will in general give rise to a superposed multipole radiation field. It was shown that in general the multipole coefficients for the transformed field were independent functions of frequency, so that the source may have quite a different radiation pattern for any two different frequency ranges. Further, the equilibrium requirements on the stress field during rupturing require readjustment in all stresses, including compressional stresses as well as all the shear stress components, regardless of the orientation of the rupture with respect to the initial shear field, so that the simple physical interpretations commonly given to the couple sources are unrealistic. Thus for these reasons, one would expect greater complications in the first motion radiation and in its interpretation than is afforded by the single couple and double couple sources.

It would therefore be expected that the initial features of the motion associated with the radiation field would normally be described by a superposition of multipole fields with particular multipoles or combinations of multipoles being dominant at certain frequencies and within certain distances and azimuths from the source. In addition,

the conditions for the dominance of a particular multipole are clearly critically dependent on the initial shear field and the geometrical nature of the rupturing taking place over a time interval comparable to the periods of the displacements associated with the initial P and S wave motion. In view of these considerations, it seems likely that the agreement between a single or a double couple source model with the observed first motion of P and S waves for many earthquakes represents a determination of the dominant multipole contributions from the initial motion at the beginning of the rupturing. (See also Knopoff and Gilbert (1960) in this regard.) Aki's (1964) experimental studies tend to confirm this line of reasoning. Thus Aki argues, on the basis of his own and other experimental evidence obtained largely from surface wave studies, that in most cases a single couple source model does not explain the observed long period surface wave radiation from strike slip faulting and that a double couple model is better. He notes however that single couple models give better agreement for dip slip faults. Consequently the author adopts a modified source consisting of a particular superposition of single and double couples weighted so as to give reasonable agreement with surface wave observations from a number of earthquakes. In terms of the present point of view, to be theoretically substantiated in the following sections, this procedure amounts to the adoption of the dominant part of the multipole solution previously discussed. Thus the multipole coefficients correspond to the weighting of the couples and are chosen (experimentally) so as to be approximately valid for

the long period radiation observed. In a different frequency range and also for different initial stress fields and rupture orientations, these weighting factors should be different, so that the modified couple model would have to be superimposed in a different manner. Thus it is not unlikely that shorter period radiation would indicate an entirely different model or that the model would change somewhat from earthquake to earthquake indicating a difference in the basic rupture parameters.

Recently, some relatively sophisticated theoretical source models have been advanced. Honda (1962) includes a brief description of some of the models in his review of tectonic source theory. The models may be conveniently grouped and summarized as follows:

1. Elastic Dislocation (E. T. D.) Models: Two possible mechanisms for earthquakes have been advanced, based on analogies with the physical dislocation theory appropriate to plastic deformations in crystals. Some basic dislocation types are shown in Figure 4. These dislocations are described generally by Volterra's theory of dislocations (e. g. Love, 1944, § 146A). The static elastic field associated with such an infinitesimal dislocation was computed by Burgers (1939) and the results were extended by Nabarro (1951) to give the instantaneous displacements produced by a moving dislocation of the edge type. The dislocation movement is effected by a synthesis of dislocations in a stress field, the instantaneous displacements produced by the sudden creation of an infinitesimal dislocation loop are also, therefore, obtained in conjunction with the synthesis.

Vvedenskaya (Balakina, Savarensky and Vvedenskaya, 1960) considers an earthquake to be equivalent to the creation of a dislocation and uses Nabarro's results to model the source. The author considers the formation of a rupture to be equivalent to the instantaneous removal of stresses from the fault surface which is taken, in turn, to be equivalent to a sudden application of stresses in an unstressed medium. This procedure gives an equivalent source which corresponds to the double couple point source, as was pointed out by Honda (1962).

Droste and Teisseyre (1959, 1960), Teisseyre (1961) consider the basic earthquake mechanism to consist of a mutual annihilation of a pair of dislocations or in the release of potential energy in a dislocation as it moves to or across a boundary with rigidity contrast. These authors compute the energy associated with the dislocation annihilation and boundary release at the free surface of the earth. Using Nabarro's results they obtain expressions for the static field to be expected from an earthquake of either type and approximate expressions for the radiation field due to the rapid movement and annihilation of a single dislocation at the surface or a pair of dislocations at depth (Teisseyre, 1961). The authors compare their results with the observed energies of earthquakes and the static displacements measured geodetically near surface faults (Byerly and DeNoyer, 1958). The dynamical predictions of the model were not utilized by the authors, however their roughly computed radiation field appears to correspond to the double couple point source. By

choice of suitable dislocation parameters and elastic constants, the authors achieve approximate agreement between predicted energy release and the surface static field and the empirical values observed for these quantities. This model provides a rather detailed model of the earthquake mechanism wherein the time variation at the source is also predicted and constitutes an important feature.

Steketee (1958) and Chinnery (1960, 1961) have considered energy and equilibrium properties of a dislocation and applications of the general theory to geophysical problems associated with faulting are discussed in general terms. Steketee (1958) has shown that creation of a dislocation in either a stressed or unstressed medium will increase the strain energy of the medium so that external forces would be necessary to create a dislocation. Various types of dislocations are considered and Steketee shows that the dislocation equivalent to the double couple point source is in equilibrium, while that equivalent to a single couple is not. That is, static equilibrium of the medium is maintained only by the application of a moment at the medium boundary in the case of a single couple source. Chinnery (1960) takes up this argument in the dynamic case and making use of some of the results stated by Knopoff and Gilbert (1960), concludes that for first motion at least, the medium must continuously adjust to equilibrium as the rupture breaks. That is, 'that the impulse delivered by the source to the medium must be in equilibrium'. Coupled with the static equilibrium argument of Steketee, the author suggests that a double couple source is most tenable with these

equilibrium arguments. Extending the hypothesis of the double couple source, Chinnery (1961) uses the static field from a dislocation equivalent to a double couple to interpret the observed surface displacements near several faults. The author achieves reasonable good agreement with the observed field and further concludes that non-elastic effects are confined to a small zone in the immediate neighborhood of the fault.

Housner (1955) considered a distribution of "shear dislocations" as a model of a fault plane and assumed that faulting was equivalent to the relaxation of the accumulated shear stresses on the individual dislocations. He assumed that the relaxation of each individual dislocation was dynamically equivalent to a single couple and that the total field was a superposition of the fields from these couples. No detailed predictions concerning the radiation field were made but statistical considerations were advanced to show that such a model could be put into general statistical agreement with observations of the strong motion in the neighborhood of earthquakes. This type of source corresponds to the adoption of an equivalent volume distribution of sources and the concept of a dislocation distribution, which is treated loosely, was introduced as a basis for the choice of the elemental equivalent source.

In this context, a more rigorous treatment of the concept of a dislocation distribution has been given by Weertman (1964). In this case an initial two-dimensional distribution is assumed corresponding to a pre-existing fault plane and this distribution is fixed

by the frictional forces and the stress field due to tectonic forces. When the applied tectonic stress exceeds the frictional forces, the continuum of dislocations is free to move and redistribute so as to relieve the stress. The treatment is limited to equilibrium considerations where certain initial and final distributions are considered but the dynamical implications suggest radiation from the propagating dislocations (Nabarro, 1951), so that the total radiation field would be due to the superposition of fields from a "swarm" of propagating dislocations.

Weertman shows that on the basis of this approach, an anomalously low value of the coefficient of friction is required within the earth's crust in order to explain the observed surface rupturing and the simultaneously observed, rather deep epicenters of some earthquakes.

While there are some basic difficulties associated with the use of dislocation models involving the creation, propagation or annihilation of a single large dislocation (see section 3.4), these same problems are avoided or at least are not evident, when a continuum distribution of infinitesimal dislocations is used to describe the rupture process. Indeed the results of the present study, wherein the radiation and static fields associated with rupture are predicted, can be described equivalently as resulting from the propagation or expansion of a volume distribution of dislocations. While Weertman treats the equilibrium of a two-dimensional array of dislocations and considers the process to be essentially one of

fracture on a pre-existing fault plane, the consensus reached in the present study favors a volume distribution of dislocations and associated unstable creep phenomenon at even modest depths (Orowan, 1960) or shear melting (Griggs and Handin, 1960).

Fracture is considered likely at only shallow depths, less than approximately 10 km. Thus the mechanism of rupture is considered to be basically the disordering phenomenon associated with infinitesimal dislocations resulting in a loss of cohesion due to the resulting unstable creep, phase change, or fracture at the shallow depths.

It seems possible that near surface fracture could occur with, or as a result of, unstable creep or phase change at greater depth so that deep epicenters and observed surface fracture corresponding to a very shallow dislocation distribution could correspond to two different but associated phenomenon. Thus as an alternate to Weertmans conclusion of a low coefficient of friction, one might describe the observations by saying that the distribution of dislocations behaves in different ways and induces a different failure mode under different pressure and temperature conditions and that these modes of behavior may occur together or be influenced by one another.

2. Knopoff-Gilbert dislocation models: Knopoff and Gilbert (1959, 1960) consider the rupture to be equivalent to a discontinuity in both strain and displacement along a two-dimensional surface. The authors restrict their investigations to first motions and approximate the physical model accordingly. In general they consider a propagating rupture wherein the particles adjacent to the fault are

initially assumed quiet until the passage of the fault front, at which time the particles on opposite sides of the fault plane are suddenly displaced in opposite directions parallel to the fault plane. The displacements are taken to conform in magnitude to the static values of displacement along an infinite two-dimensional crack in a homogeneously strained infinite medium (Knopoff, 1958), the time variation is taken to be in the form of a unit step function. When the effect of the second, depth, dimension is ignored, so that the source model is reduced to a line source, then the radiation field may be computed exactly. These results are further approximated to facilitate the computations, and first motion radiation equivalent to a double couple is obtained, (Knopoff and Gilbert, 1959). Alternately, taking the first motions of the P and S wave radiation to depend exclusively on the initial breaking at the focus of the earthquake, the authors consider all possible initial dislocations corresponding to this initial motion model. Neglecting the radiation from all points on the fault plane except that from the focus, the authors conclude that two of the possible dislocations are physically significant, namely a sudden displacement dislocation parallel to the fault and a sudden shear-strain dislocation. The displacement dislocation corresponds to a double couple and the strain dislocation to an isolated force. A third model is also considered possible on the basis of the fault-plane solutions obtained from the previously described Byerly-Hodgson source model. In this case a sudden release of shear strain in a laminar region ("laminar strain dislocation") is shown to correspond

to the single couple source. In all cases the time dependence of the first motion at the focus is taken to be a step function and it is argued that should the time dependence be otherwise, a simple convolution would provide the correct radiation field and in any event cannot affect the spatial dependence of the first motion radiation field.

3. Ben Menahem's propagating source models: Ben Menahem, (1961, 1962) adopts a clever device to represent the propagation of the rupture and associated stress release during an earthquake. Taking a directed point force as an elemental source, the author, following Yanovskaya (1958), obtains the surface wave excitation in a half space. Next assuming a finite line distribution of such sources, the author integrates the surface wave solution previously obtained with respect to this (depth) variable. Finally assuming that this line segment of sources moves with the rupture velocity over a finite distance, thereby defining the fault plane, the previous line source solutions are integrated over the fault length assuming a finite speed of movement for the line source. Thus by superposition of an elementary source solution, Ben Menahem achieves an effect at least similar to that to be expected from an actual propagating rupture. In the course of synthesizing the source, several approximations are introduced in order that the various integrations may be performed, in particular that the distance of the point of observation from the focus be much larger than both the wave length of the radiation field and the greatest rupture dimension. For the intended application of the model to surface waves these restrictions are not considered to seriously

impair the generality of the theory. Press, Ben Menahem and Toksöz (1961) verified the mathematical validity of the theory by model studies and its physical relationship to actual faulting through the verification of the predicted surface wave radiation from the Chilean earthquake of 1960. In particular the theory predicts a directional modulation of the surface wave radiation associated with the movement of the line source distribution ("directivity function"), the parameters of this factor depending on the fault length, rupture velocity and direction of the rupturing. Proper choice of these parameters give general agreement with the observed radiation spectra in this respect, and the parameters so chosen are in first order agreement with the same parameters estimated by other means. A similar directivity factor is obtained for the body wave radiation (Ben Menahem, 1962). Predictions for the body waves have not been verified however. Ben Menahem points out that the model is capable of further generalization in that other, higher order elemental sources such as couples etc., may be obtained by differentiation and combination of the results for the vector source. Haskell (1963) has recently undertaken this generalization.

The theory has been used by Ben Menahem and Toksöz (1962, 1963), to estimate fault length and rupture velocity of earthquakes. Quite reasonable values are obtained which are in general agreement with values estimated by other observations.

3.4. The Physics of Dislocation Rupture in the Earth

In view of Steketee's result regarding the energetics of dislocations, sudden creation of a very large dislocation per se, is considered unlikely, if not an impossible physical process in the earth, since such an event would require a large sudden increase in the tectonic forces. The theoretical source models explicitly based on such a mechanism are therefore physically implausible and as a consequence quite arbitrary. Symptomatic of this condition is the arbitrary time dependence of the source models used by Vvedenskaya and Knopoff and Gilbert.

The dislocation processes which are relevant to rupture in the earth appear to be associated with the same or similar mechanisms leading to creep in crystalline solids. In this context then, the term dislocation refers to the microscopic disordering of the ideal crystal lattice rather than to any single, large macroscopic discontinuity of the displacement field within an elastic continuum. Confusion of the two concepts, the first being essentially a physical concept, the second mathematical, arises from the recent use of the microscopic dislocation theory (e. g. Droste and Teisseyre, 1959, 1960, and Vvedenskaya, 1960) and particularly the physical concepts associated with it, as models for macroscopic seismic rupture. Therefore, while a microscopic description of rupture in terms of dislocation theory is appropriate, use of these concepts in a macroscopic sense seems inappropriate.

Thus creation and synthesis of physical dislocations on a

microscopic level is quite certainly an active process in a tectonically strained region and is probably manifested in the observed creep phenomenon near tectonically active regions. However, contrary to the viewpoint of Droste and Teisseyre, a slow synthesis of the infinitesimal dislocations treated in Nabarro's theory to give very large dislocations is highly unlikely in a heterogeneous, crystalline medium like the earth. The unlikelihood of such a phenomenon is due to: (1) the presence of impurity atoms in the crystal lattice which tend to pin the dislocations and impede their movement and synthesis, (2) grain boundaries or crystal boundaries presenting effective barriers to the growth or movement of dislocations within the medium, and (3) the existence of stable node points for a network of dislocations in a stress field (Mason, Chap. IX, 1958). The role of these inhomogeneities in the dynamics of dislocation growth and movement has been extensively studied (e. g. , Mason, 1958; Cottrell, 1953; Read, 1953) in conjunction with detailed studies of the non-elastic properties of polycrystalline solids.

The actual behavior of dislocations in the presence of a stress field and their interaction with other inhomogeneities within a crystalline solid is extremely complex and varied. Certainly not all the possibilities of interaction have been thoroughly investigated nor are all of their manifestations in terms of bulk properties of the solid completely understood. However, the gross behavior of dislocations in polycrystalline material as a function of shear stress

is fairly well understood (e. g. Mason, Chap. IX, 1958).⁽¹⁾

In particular, moderately high stresses are required to unpin a dislocation from an impurity atom and at moderate stress, the process is not unstable. That is, once unpinned from the impurity atoms, the dislocation loop is still attached at the node points or intersection points with other dislocations so that it is not free to move nor combine.

Creation of additional dislocation loops at higher stress occurs, and the mechanism is described by the Frank-Read dislocation source. This process is activated when the stresses are large enough to unpin a dislocation. For a sufficiently large applied stress, the unpinned loop bulges out until it reaches a semicircular form. Any further stress causes the loop to become unstable and it begins to increase in area. If the loop does not strike any obstructions, it will follow the steps shown in Figure 5 until it doubles back on itself and forms a free loop and a new pinned dislocation. For high stresses the process will be repeated and a large number of loops are formed. Basically then, high stress fields will cause an unstable generation of dislocations rather than a synthesis of free dislocations to form a small number of very large dislocations, as envisioned by Dtroste and Teisseyre in their theory of dislocation annihilation. In addition, the physical possibility of the creation of the

⁽¹⁾ There is in fact, little doubt that dislocations and dislocation interaction phenomenon constitute the mechanisms responsible for ductile rupture and creep under moderate stress.

very large dislocation hypothesized by Vvedenskaya is seen to be at variance with the actual mechanisms of dislocation growth and generation. That is, the process is essentially that of creep.

The probability that seismic rupture at depth in the earth is associated with unstable creep phenomenon seems relatively great. Such a mechanism has in fact been suggested by Orowan (1960). Thus if a creep mechanism is relevant, and arguments will be presented in its favor, then a microscopic description of the phenomenon will be provided by dislocation theory. The likelihood of the creep mechanism arises in part from the experimental facts relating to the behavior of dislocations at relatively low shear stresses. In addition to unstable creep or ductile processes of rupture, brittle fracture and uncontrolled phase change may be initiated, and thereby controlled, by the presence of dislocations within the crystalline matrix. Thus certain aspects of the microscopic theory of lattice defects in a crystalline solid, in particular those related to dislocations, are likely to be pertinent to an understanding of the origins of seismic rupture. The mechanisms of importance will be described in a qualitative manner in this section.

The dislocation mechanism leading to ductile rupture at relatively high stresses seems to be connected with the Frank-Read dislocation mechanism. The process has been observed to consist of two stages, dependent on the magnitude of the applied stress. For stresses somewhat below that required for rupture, unstable Frank-Read dislocation loops are produced, but are prevented from going

through the reproduction process indicated in Figure 5 by the presence of dislocations in other slip planes. In particular when the loop becomes unstable and strikes an obstructing dislocation, it may cut through several such dislocations but is eventually held by so many cross-dislocations that the stress on the free dislocation is not sufficient to cut them, and the generation of multiple loops is prevented. However an important side effect of a dislocation cutting a screw dislocation is the production of a jog on each dislocation, or a dislocation of a dislocation.

At this level of stress the process is anelastic, that is, if the stress is reduced the dislocations return to their former state and the process can be reproduced. However, a plastic strain is introduced in addition to elastic strain, and so the shear modulus, which is just the ratio of the stress to the total strain, is reduced.

If the applied stress is increased further, the jogs produced in the cross-dislocations due to cutting by the unpinned Frank-Read dislocations will create vacancies as they move through the material under the action of the stress field (Friedel, 1956; Seegar, 1955; and Mason, 1958). At this level of stress the material develops fatigue cracks and then fractures. It is believed that the rupture phase is due to the dislocation loops cutting through the pinning dislocations and producing jogs, vacancies and an uncontrolled number of Frank-Read loops. (A large number of vacancies in the lattice are produced by a jog, and actual pictures of vacancy production have been obtained by Dash (1958).) According to Mott (1956), the vacancies

can accumulate to initiate fatigue cracks. The "cracks" may occur when the vacancy-filled material recrystallizes on the distorted material on either side of the slip band.

Once such cracks are produced, rupture can follow if the stress is large enough to cause separation of the crystal planes between cracks, that is, by a Griffith crack propagation mechanism (e. g. Griffith, 1920; Sneddon, 1951) or if the recrystallization or melting is uncontrolled along planes of vacancies. These mechanisms require considerably less energy than does rupture due to actual separation of undistorted crystal planes (Seitz, 1940, p. 98).

Numerous other mechanisms involving dislocation imperfections, in addition to vacancy production and recrystallization or melting, may also result in the production of cracks and cavities of microscopic dimensions within crystals or along grain boundaries. The presence of such flaws, defining a "weak zone," can then lead to brittle fracture at low confining pressure and temperature. A few of these mechanisms are considered by Orowan (1954). Thus Orowan suggests the formation of cracks due to high tensile stresses generated by the accumulation of a large number of edge dislocations at a lattice inhomogeneity, such as a hard precipitate, a grain boundary or crossed dislocations due to preceding plastic deformation. In this case the dislocations accumulate in a common slip plane and superposition of their associated stress fields can locally exceed the tensile strength of the material, thereby producing a

fracture with its long axis normal to the slip plane. A similar phenomenon arises from a row of edge dislocations in parallel slip planes. In this case the superposed dislocation fields give rise to a large tensile stress at the end of the row which would lead to cracking along a slip plane.

The effect of accumulated dislocations and resulting high stress fields could also lead to localized phase change under high temperature and pressure conditions. This may occur when the dislocations accumulate at lattice inhomogeneities and increase the strain energy of the lattice and its surroundings to a level at which a change of state is possible.

The mechanisms described in the preceding paragraphs are considered, in the present study at least, to be the most likely microscopic process leading to seismic rupture. While most of the detailed observations concerning the dislocation mechanisms considered above have been made on laboratory samples of metals at relatively high frequencies of applied stress, it has been shown, (Mason, 1958; Cottrell, 1953) that these mechanisms are essentially independent of frequency at high stress and apply to other crystalline materials as well. In particular dislocations and dislocation induced vacancies have been shown to be responsible for a number of non-elastic processes observed in quartz and other non-metallic crystals (Mason, Chap. X, 1958). In addition numerous high pressure and temperature deformation experiments with rocks have demonstrated the plastic or ductile properties of the constituents of the earth at

moderate depths (Griggs et al., 1960). Therefore it is concluded that the ductile processes described apply at least down to a depth above which the rock is yet crystalline.

This conclusion is also supported by Orowan's (1960) theoretical inferences and by the deductions of Griggs and Handin (1960) based on their experimental work in rock rupture and deformation under high pressures. Thus Orowan has concluded that effects of temperature and especially pressure below 5 - 10 km. in the earth precludes all the classical mechanisms of earthquakes (e. g. fracture and release of static friction followed by sliding) and that plastic deformation (creep) is the only plausible alternate presently available. Although not mentioning the precise microscopic mechanisms involved, Orowan arrives at the same conclusions reached in the present survey; namely a mechanism associated with creep instability. Griggs and Handin also conclude that ordinary coulomb fracture, even at a few tens of kilometers, is clearly impossible in view of the high pressure and the finite coefficient of friction, and that the most reasonable mechanism of energy release at great depth is a phase change and that the most probable phase change is melting. In particular the authors state that calculations suggest that, once a crack or flaw exists, there is ample elastic energy to propagate the 'crack' by shear melting even if the stress difference is only a few tens of bars. The dislocation induced "flaws" and melt zones are just the processes required by Griggs and Handin to initiate shear melting. Thus in addition to the possibility of

rupture by separation of crystal planes between cracks (friction rupturing of weakened material), shear melting or uncontrolled recrystallization due to stress concentration at moderate and great depth constitutes an additional mechanism of 'rupture' requiring only small shear stresses.

On a microscopic level, a description of the seismic rupture mechanism in terms of dislocation theory can hardly be avoided if the material is crystalline, inasmuch as a dislocation theory is nothing more than a means of describing the departures of the crystalline material from an ideal crystal. Thus, the grain boundaries in a polycrystalline solid are described in terms of locked-in dislocations. Even a single crystal, formed under ideal conditions, will contain a large number of dislocations. Further, the deformation of a crystalline solid under non-hydrostatic stress is necessarily described on a microscopic level by dislocation movement and interaction.

Thus since the material of the earth's crust and upper mantle is almost certainly crystalline, then the existence of dislocation imperfections in this region is quite certain. The presence of non-hydrostatic stress fields within the crust and upper mantle is suggested by numerous lines of evidence, the most recent and direct evidence in this regard arising from observations of large scale perturbations in the earth's gravity field (e. g. Kaula, 1963). These observations imply a strength of the order of 300 bars for the crust and 100 bars (10^8 dynes/cm²) for the upper mantle. The presence of

a non-hydrostatic stress field of the order of 10^8 dynes/cm² must therefore initiate movement and interaction among the existing dislocations and the eventual generation of additional dislocations (unstable creep).

The question seems to be then, which of the rupture mechanisms described by dislocation phenomenon is pertinent to the earth? Clearly the temperature and pressure conditions will, at least in part, control the mode of rupture.

At shallow depths stress concentration due to an accumulation of dislocations would initiate tension cracks which could grow by a Griffith crack propagation mechanism. The material at such depths would then be considered brittle. At greater depths the high pressure would preclude the possibility of brittle rupture mechanisms dependent on the existence of initial voids or cracks. At such depths unstable creep associated with Frank-Read dislocation sources can result in creep rupture described macroscopically as shear melting or uncontrolled recrystallization.

Thus, dislocations exist, the non-hydrostatic stress field required for interaction and movement of these dislocations is present and there are a number of microscopic mechanisms associated with dislocations which would lead to stress concentration and either brittle or creep rupture, dependent upon the temperature and stress condition.

Dislocation theory should provide a description of other observed macroscopic phenomenon arising from further departure

of the material from the ideal crystalline state under applied stress. Most of this phenomenon is associated with rupture. Thus the existence of unconsolidated weak zones among a fault would result in a concentration of stress with a subsequent generation of dislocations on creep in the surrounding material. Hence, the observed creep along lateral faults can be viewed in terms of plastic deformation described by microscopic dislocation movement. The density of dislocations would however be higher at the ends of the unconsolidated portions of the fault in view of the tendency for elastic stress concentration, as at the extremities of a crack, leading to possible additional rupture. The shear strain observed at the earth's surface along an active fault trace would correspond in part to plastic strain under this interpretation. The effective rigidity of the region would depend on the dislocation mechanisms activated, that is on the level of the applied stress. In any case the effective rigidity corresponding to the tectonic stresses would be reduced due to plastic strain produced in addition to the elastic strain.

Orowan (1960) has discussed fore-shock and after-shock sequences as phenomenon related to creep instability rupture. Benioff (1951) previously proposed a visco-elastic mechanism involving an "anelastic" strain relaxation within the material surrounding a friction fault, allowing recurring stress accumulation on the fault and a sequence of seismic events. Orowan has compared the two hypotheses and shown that either could account for the observed effects. Orowan's discussion shows that a creep mechanism would

normally result in a series of seismic events since any initial rupturing due to creep would result in a high stress concentration along the margins of the rupture resulting in further creep instability as was suggested in the preceding paragraph. Microscopically the creep instability is associated with the generation of dislocations which will tend to concentrate in a narrow band of slip planes, and clearly the time required for a concentration sufficient to initiate a phase change will depend on the stress and temperature levels, and the nature of the material. Thus an initial rupture would naturally be followed by further creep rupturing until the regional stress was reduced to a low level. The seismic sequences associated with what is probably brittle fracture at shallower depths could be explained by stress concentration and a similar generation of dislocations in parallel slip planes near the ends of the rupture. In this case the thermodynamic environment, particularly the temperature, would not favor easy movement of the dislocations in the polycrystalline matrix but rather an accumulation of dislocations at grain boundaries and at impurities resulting eventually in tension cracks and further large scale rupture. Thus the basic mechanism for near surface rupture is probably the same as for creep instability at greater depths and a sequence of seismic events would be expected in view of the time required for the generation and movement of dislocations in the stress field.

3.5. Compatibility of the Macroscopic and Microscopic Mechanisms of Seismic Rupture

It seems reasonably clear that the macroscopic description of seismic faulting provided by the elastic relaxation process described earlier is in accord with the microscopic mechanisms just outlined. A consistent theory encompassing both the non-linear mechanisms associated with dislocations and the linear relaxation processes resulting in the radiation of stored elastic energy is achieved by postulating the existence of a well defined uniformly propagating or growing rupture surface surrounding a zone of zero shear strength. In this manner the necessity of explicitly delineating the detailed nature of the rupturing is in reality avoided in the macroscopic theory, except in so far as it is necessary to show that a propagating or growing rupture volume, as the case may be, has physical significance. On the other hand, the conclusion that the radiation field is an elastic volume radiation effect can be proved whenever such a surface is introduced into a strained medium.

The existence of such an idealized surface follows from the previous discussion of the rupture mechanism. It will be considered the boundary between the narrow melt or fracture zone and the stressed, essentially elastic, surrounding material. The important assumption that the frictional coupling across the boundary is negligible seems justified in view of the likelihood of a rupture mechanism involving phase change, particularly melting. Indeed

the plausibility of such a mechanism arises from the fact that frictional effects are very small.

Even in the case of brittle fracture at shallow depths, as described in the preceding section, dislocation mechanisms and resulting plastic deformation are fundamentally involved in the process of stress concentration. When such brittle rupture is appropriate, it is reasonable to assume that a loss of cohesion, plastic flow and melting would be associated with the large and rapid stress changes in the immediate vicinity of the fracture. Frictional coupling between the elastic zone and the rupture volume would undoubtedly be larger than for "creep rupture," yet still probably small compared to the changes in the traction at the boundary. This assumption would clearly fail very near the surface however, since while the frictional forces would tend to decrease somewhat, the comparative shear stress changes would tend to decrease much faster.

Thus a boundary enclosing a region of vanishing effective rigidity appears to be a reasonable first order description in all cases except very near the free surface. In cases when the rupture zone intersects the free surface it is likely then that the present model may not accurately predict the radiation from the near surface zone. There are also other difficulties associated with "surface rupturing" which reduce the clear applicability of the source theory developed in this study to occurrences of rupture at depth (i. e., not intersecting the surface).

On the basis of the microscopic processes involved in rupture, there is little to choose from between the growth model of rupture and the propagating rupture. However the assumptions involving frictional coupling across the rupture boundary are less severe for the propagating rupture model and for this reason this model is preferred at shallow depths, and certainly for brittle rupture.

Due to melting and probably large deformations within the rupture zone, it is further concluded that the previously stored strain energy goes into heat rather than into elastic radiation. This too is entirely plausible in view of the deformation mechanisms involved in faulting. Further one might suppose that the heat generated within the rupture zone will further reduce the possibility of friction at the boundary.

In view of the detachment of the radiation theory from the details of the mechanisms leading to faulting, the method is applicable to tectonic sources in general. Thus the theory is applied to the calculation of the tectonic radiation from explosions in pre-strained material.

While it is possible, in theory at least, to predict the nature of the 'rupture' volume growth from the physics of the mechanisms leading to rupture, such an undertaking, while undoubtedly ultimately desirable, is considered outside our present grasp due to a general lack of knowledge concerning the detailed physical state of the material at depth in the earth.

The following list of generally measurable quantities,

associated at least indirectly with the source mechanism, may be predicted in terms of the source parameters and provides an indication of the generality of the present source theory and a means of checking the validity of the models and theory.

- (1) Prediction of body on direct wave spectra.
- (2) Prediction of surface wave radiation, directional properties, mode excitation, etc.
- (3) Prediction of the total energy radiated.
- (4) Prediction of the oscillations in an inhomogeneous spherical earth.
- (5) Prediction of the static displacements at the earths surface.
- (6) Prediction of initial phases "at the source."

On the other hand, if the source parameters can be chosen so as to give good agreement with the observable variables enumerated above, then such a "fit" will provide a determination of the source parameters, although not necessarily a unique one. These parameters are:

- (1) The rupture velocity function and final fault dimensions in terms of the semi-axes of an ellipsoid.
- (2) Initial stress state of the medium.
- (3) Location and orientation of the rupture.

It is clear that a general lack of uniqueness exists. That is, although a reasonable fit to the observed field properties may be achieved by choice of the source parameters, this in itself does not

insure that the set of parameters is the only set capable of providing a fit. In addition, the effect of errors in both the observations and the fit would be unknown. The uncertainty may be reduced by comparing the source parameters obtained with direct, independent observations of some of the parameters, when possible.

More basic uncertainties are also involved. In particular, the macroscopic source model does not explicitly specify the nature of the rupture mechanism. Thus any deductions concerning the physics of the source, based on estimates of the source parameters, must be predicated on additional hypotheses. If a plausible microscopic mechanism of rupture is assumed, then the parameters estimated from the radiation field could well be useful in assessing the validity of such a mechanism.

3.6. Approximations for Dynamical Models of the Tectonic Source

The models of Knopoff and Gilbert are first motion models, by contrast the present theory represents an extension of the mathematical theory to encompass the total motion and in addition proposes a physical theory of rupture. The dislocation and first motion models are essentially arbitrary, inasmuch as both the time variation and the displacement or strain discontinuities across the rupture or at the focus are chosen on a subjective basis. Thus while Knopoff and Gilbert observe that the true time variation may be obtained by simple convolution, this is only true if the source function $\underline{f}(\underline{r}, t)$, as considered in Chapter 2, is a separable function in \underline{r} and t . If the function cannot be so separated then, as was shown in

Chapter 2, each multipole coefficient giving the radiation field is, in general, a different function of frequency. In the present chapter it will be shown that this condition prevails for fault sources and consequently that it is therefore not always possible to achieve generality by convolution. Further the volume properties of the source are in effect represented by a discontinuity in displacement which is propagated down the fault surface and the equivalence of this representation and the properties of volume radiation is not obvious. If there is an equivalence, it is likely to be found by first solving the initial value problem associated with an elastic relaxation theory, as will be shown in Section 3.9.

Ben Menahem's source model is similarly arbitrary in both the choice of time variation and the fundamental source nuclei. Thus the model avoids consideration of the properties of volume radiation and the dependence of the radiation on the initial stress field. The model may be viewed as a moving equivalent source, and is consequently similar to the Knopoff and Gilbert model. Ben Menahem's successful evaluation of the far field radiation from the model and the first order agreement achieved with the observed spectrum of surface waves tends to support the contention that a moving source is, at least with respect to the amplitude dependence of surface waves within a restricted frequency and distance range, an adequate first order model. In physical terms this agreement appears to result from the relatively large and rapid stress changes occurring at the propagating "front" of the rupture, which for large

distances from the fault will approximate a moving point or line source. The detailed nature of the moving line source, that is the appropriate time and spatial dependence of the force system of this equivalent source, can in principle be obtained from the present elastic relaxation theory and would be expressed in terms of the fundamental parameters of the initial stress field and rupture surface.

Mathematically, the crux of the difference between a relaxation theory and the previous theories reviewed lies in the difference between an initial value problem and a boundary value problem. Thus Chinnery (1960) may only speculate on the nature of the relaxation of the stress, while in the present theory the process is analytically prescribed. In this connection, the stress relaxation is a manifestation of dynamical equilibrium wherein an equilibrium value of the stressfield is defined at every instant, in the static sense, and the stress changes in a manner determined by the dynamical equations toward a stress state consistent with this equilibrium state. This does not, however, imply that the stressfield is continuously in static equilibrium with the propagating rupture but only that the field continuously adjusts in a manner determined by the equilibrium field. Since this adjustment requires finite time, one may conclude that the field is never in equilibrium with the rupture surface at any given time during rupture. The precise relationship is analytically described in a following section. Thus while Steketee's and Chinnery's arguments concerning equilibrium in the static case are applicable, the extension of these arguments

to the dynamic problem is not so clear.

The present model should yield more meaningful estimates of tectonic source parameters and a more complete description of the source and its radiation field in layered media than has been possible before. This contention is based primarily on the reasonable physical basis for the relaxation model of the source. Nevertheless it is worthwhile to note the limitations and approximate nature of the theoretical predictions arising from the necessarily idealized physical models and their approximate mathematical representation. Among the more important physical effects not explicitly accounted for in the models are:

1. The effects of perturbations of the density within the rupture volume arising from phase change or recrystallization.
2. Departures from ideal elastic behavior and variations in the elastic constants and density in the exterior "elastic" zone due to large changes in the equilibrium stress field.
3. Interaction of the rupture boundary with the radiation field, giving rise to possible interface waves.
4. Frictional coupling between the material within the rupture zone and the elastic zone.

In addition, some compromises in the generality of the mathematical representation will be made in order to simplify both the analysis and the theoretical results. The approximations are equivalent to the following assumptions.

1. The growing rupture zone is, at any time, ellipsoidal and the "width" of the zone is small compared to any of the other dimensions.
2. The propagating rupture sweeps out an ellipsoidal region during the course of its movement, at any time the traction free rupture surface is a small fraction of the total rupture surface.
3. The diffracted and reflected field from the rupture is negligible outside the immediate vicinity of the rupture volume and does not influence the stress relaxation phenomenon.
4. The elastic tectonic stress field is locally homogeneous outside a narrow zone of stress concentration (i. e. the relaxation field is assumed to be derived from a homogeneous initial elastic field).
5. The rupture growth and/or propagation is with a rupture velocity V_R which is constant.
6. Stress relaxation is a local effect in the strict sense. That is, changes in the equilibrium field are induced at a point primarily by changes in the form of the rupture boundary nearest the point in question.

If the neglected physical effects are not of second order or if the assumptions required for mathematical tractability are not fulfilled, then special modifications or additions to the theory will be required in those exceptional cases. It is, however, difficult to

see how any of the approximations in the theory could have any large or critical effect on the predicted radiation field with the possible exceptions of an inhomogeneous initial stress field or a density perturbation. In regard to the latter, Benioff (1963) has speculated that this phenomenon might well explain the observed radiation from several deep focus earthquakes. The effect, when not of second order compared to stress relaxation effects, is probably confined to deep focus sources in a very restricted depth range.

A secondary effect, arising from the omission of density variations, is that the body forces such as gravity play only a very indirect part in determining the radiation field. In the following section, the constant body forces will in fact be shown to vanish identically from the equations determining the change in the equilibrium field during rupture. The initial stress field would in theory however contain the stress due to the gravitational forces. Since the change in the equilibrium field depends on the value of the initial field, then the gravitational stresses would implicitly be accounted for. However the initial field in the present theory is assumed to be homogeneous and pure shear which will result in a good approximation if the tectonic stress is locally quite uniform and if changes in the shear stresses are larger than the dynamical fluctuations in the hydrostatic pressure during rupture. Nevertheless part of the initial stress field can in general be considered to be associated with gravitational forces.

Love (1944), p. 109-111, considers the general case in which

the density is allowed to change. It is clear that the gravitation forces at least, would in such cases give rise to an energy release corresponding to a liberation of a relatively small amount of potential energy if a localized density change occurs. Thus the effect of the body forces can only be indirect in terms of the present theory, in that the initial stress field and the rupture parameters, such as the velocity of boundary propagation, may be affected.

3.7. Basic Equilibrium Relationships

Clearly the essential problem in the representation of a tectonic source is a dynamical description of stress relaxation. A basis for a mathematical description is provided by an elementary consideration of equilibrium.⁽¹⁾ In order to simplify the discussion and to temporarily eliminate the effects of rupture propagation or growth from the problem, consider the instantaneous creation of a traction free surface in a prestrained medium as in Chapter 2. The boundary of the surface, once inserted into the medium, is then considered fixed. Prior to the creation of the boundary, each material point of the continuum is in a state of equilibrium with a tectonic force field \underline{f} . Thus the pre-stressed state of the medium is given by equations of the form

$$\frac{\partial \sigma_{ij}^{(0)}(\underline{r})}{\partial x_i} + \rho f_i = 0 \quad (3.7.1)$$

⁽¹⁾Love (1944), §§ 128, considers equilibrium aspects associated with a suddenly applied or reversed load which is a similar problem to that considered here.

where $\sigma_{ij}^{(0)}$ is the initial stress field and f_i is the tectonic force density. After creation of the boundary, however, the new equilibrium state is given by a stress field $\sigma_{ij}^{(1)}$ determined by⁽¹⁾

$$\frac{\partial \sigma_{ij}^{(1)}(\underline{r})}{\partial x_i} + \rho f_i = 0 \quad (3.7.2a)$$

with the added boundary condition

$$\sigma_{ij}^{(1)} n_j = 0 ; \underline{r} \in B \quad (3.7.2b)$$

where B denotes the traction free surface with normal \underline{n} .

Thus, it is intuitively clear at least, that each element of the medium acts as a source of seismic energy. The total energy, w_s , released as radiation at a given point \underline{r}_0 is determined by the net change in the equilibrium stress at the point, that is by

$$w_s(\underline{r}_0) = \frac{1}{2\mu} (\sigma_{ij}^{(0)} - \sigma_{ij}^{(1)})^2 \quad (3.7.3)$$

where μ is the rigidity. This contention will in fact be proved in the following section.

The change in the equilibrium value of the field may be deduced from a solution of the static equations (3.7.1) and (3.7.2). In order to provide for later generalizations, it is convenient to define a (source) time parameter τ . The dimensions of the boundary

⁽¹⁾ As was previously noted, the theory is concerned with first order effects and the second order phenomenon associated with changes in the elastic constants and density are neglected.

will be considered as specified by the value of τ given. Therefore the boundary B is a function of the parameter τ , as was previously indicated in Figure 3, and consequently so are the field variables, such as dilatation. This dependence on τ will be displayed explicitly throughout the formulation.

The change in the equilibrium value of stress is

$$\sigma_{ij}^*(\underline{x}, \tau) = \sigma_{ij}^{(0)}(\underline{x}) - \sigma_{ij}^{(1)}(\underline{x}, \tau) \quad (3.7.4)$$

and therefore the equations of equilibrium (3.7.1) and (3.7.2) show that σ_{ij}^* is given by

$$\begin{aligned} \frac{d\sigma_{ij}^*}{dx_j} &= 0 \\ (\sigma_{ij}^{(0)} - \sigma_{ij}^*)n_j &= 0 ; \underline{x} \in B(\tau) \end{aligned} \quad (3.7.5)$$

where τ is considered a fixed parameter. In addition to the boundary condition at $B(\tau)$, a condition on the field σ_{ij}^* at large distances from the boundary will be imposed, namely that

$$\underline{u}^*(\underline{x}, \tau) = O\left(\frac{1}{r^a}\right) \quad a \geq 2$$

This will insure that the field at large distances approaches $\sigma_{ij}^{(0)}$.

The boundary value problem for the changes in the equilibrium values of the stresses or displacements is therefore given by ,

$$(\sigma = \lambda/2(\lambda + \mu)) ,$$

$$(1-2\sigma)\nabla^2 \underline{u}^* + \nabla(\nabla \cdot \underline{u}^*) = 0$$

$$\underline{u}^* = O\left(\frac{1}{r^a}\right) \quad ; \quad a \geq 2 \quad (3.7.6)$$

$$\sigma_{ij}^* n_j = \sigma_{ij}^{(0)} n_j \quad ; \quad r \in B(\tau)$$

The solution of (3.7.6) may be obtained by a number of well known methods, in particular (Landau and Lifshitz, 1959) \underline{u}^* may be taken as an arbitrary biharmonic vector function

$$\nabla^4 \underline{u}^* = 0 \quad (3.7.7)$$

and by adjustment of the undetermined coefficients, the equations in (3.7.6) may be satisfied. Love, (1944, p. 265) gives general integrals of the equilibrium equations in terms of spherical harmonics, and if, as in Chapter 2,

$$\underline{g}_n(\theta, \phi) = g_n^{(j)}(\theta, \phi) \hat{e}_j = \sum_{m=0}^n \left[a_{nm}^{(j)} \cos m\phi + b_{nm}^{(j)} \sin m\phi \right] P_n^m(\cos \theta) \hat{e}_j$$

then

$$\underline{u}^*(\underline{r}, \tau) = \left(\frac{1}{r}\right)^{n+1} \underline{g}_n(\theta, \phi) + \frac{\lambda + \mu}{2[(n+2)\lambda + (3n+5)\mu]} \nabla \left(\nabla \cdot \left\{ \left(\frac{1}{r}\right)^{n+1} \underline{g}_n(\theta, \phi) \right\} \right) r^2 \quad (3.7.8)$$

Thus the coefficients $a_{nm}^{(j)}$, $b_{nm}^{(j)}$ and order n of (3.7.8) may be adjusted to satisfy the boundary conditions of (3.7.6). Further, solutions of different orders may be superposed for additional generality. Examples of solutions using these two approaches are

used in a later section for the computation of radiation fields.

More generally, the biharmonic "Galerkin vector" \underline{G} provides general integrals of the equilibrium equations (Landau and Lifschitz, 1959) given by

$$\underline{u}^* = \nabla^2 \underline{G} - \frac{1}{2(1-\sigma)} \nabla(\nabla \cdot \underline{G}) \quad (3.7.9)$$

where

$$\nabla^4 \underline{G} = 0 \quad (3.7.10)$$

Thus, the first of the equations (3.7.6) is satisfied and the arbitrary coefficients of \underline{G} may be determined so as to satisfy the boundary conditions in (3.7.6).

Solutions of the biharmonic equations (3.7.7) and (3.7.10) may be obtained by the methods of Chapter 2. Thus taking the Cartesian component equations of (3.7.10), for example, gives

$$\nabla^2(\nabla^2 G_i) = 0$$

Thus, if F_i is harmonic then $\nabla^2 F_i = 0$, and therefore if

$$\nabla^2 G_i = -F_i \quad (3.7.11)$$

then G_i is biharmonic. But solutions of (3.7.11) are

$$G_i(\underline{r}) = \frac{1}{4\pi} \iiint_V F_i(\underline{r}') \left(\frac{1}{r^*} \right) d\underline{r}' \quad (3.7.12)$$

$$|r^*| = |\underline{r} - \underline{r}'|$$

However, if \underline{u}^* is to be of the order r^{-2} for large r , then from the first term of (3.7.9) one sees that F_i must be a harmonic function of at least the order r^{-2} , hence an appropriate F_i function for an application to the boundary value problem (3.7.6) is

$$F_i = \sum_{n=1} \left(\frac{1}{r}\right)^{n+1} \sum_{m=0}^n \left\{ a_{nm}^{(i)} \cos m\phi + \beta_{nm}^{(i)} \sin m\phi \right\} P_n^m(\cos \theta)$$

with F_i of this form ($n \geq 1$), the evaluation of (3.7.12) as given in Chapter 2 gives for $G_i(\underline{r})$

$$G_i(\underline{r}) = \frac{1}{2} \sum_{n=1} \left(\frac{1}{r}\right)^{n-1} \sum_{m=0}^n \left\{ a_{nm}^{(i)} \cos m\phi + \beta_{nm}^{(i)} \sin m\phi \right\} P_n^m \cos \theta \quad (3.7.13)$$

This particular solution is therefore appropriate to the description of the equilibrium field in a pre-stressed medium with a cavity. The general solution is clearly obtained by adding to (3.7.13) harmonic functions corresponding to $\nabla^2 G_i = 0$.

Finally, the dilatation $\Theta^* = \nabla \cdot \underline{u}^*$ and rotation $\Omega^* = \frac{1}{2} \nabla \times \underline{u}^*$ are, from (3.7.9)

$$\Theta^* = \frac{1 - 2\sigma}{2(1 - \sigma)} \nabla \cdot (\nabla^2 \underline{G}) \quad (3.7.14)$$

$$\Omega^* = \frac{1}{2} \nabla \times (\nabla^2 \underline{G})$$

And operating on these equations with the Laplacian ∇^2 , and using (3.7.10), gives

$$\nabla^2 \Theta^* = 0 \tag{3.7.15}$$

$$\nabla^2 \underline{\Omega}^* = 0$$

Thus both the dilatation and rotation are harmonic functions. This fact will prove to be very useful in the evaluation of the associated radiation field, as was previously indicated in Chapter 2.

Sternberg and Eubanks (1957) have shown that solutions of the inhomogeneous equation

$$\nabla^2 \underline{u}^* + \frac{1}{1-2\sigma} \nabla(\nabla \cdot \underline{u}^*) = \alpha \nabla f$$

are

$$\underline{u}^* = \nabla(\phi + \underline{r} \cdot \underline{\omega}) - 4(1-\sigma)\underline{\omega} \tag{3.7.16}$$

with ϕ and $\underline{\omega}$ given by

$$\nabla^2 \underline{\omega} = 0 \quad \text{and} \quad \nabla^2 \phi = \alpha \left(\frac{1-2\sigma}{2(1-\sigma)} \right) f \tag{3.7.17}$$

Therefore in the present case $f \equiv 0$, so that both ϕ and $\underline{\omega}$ are harmonic. Thus general solutions are given by (3.7.16) to the boundary value problem posed in (3.7.6) in terms of harmonic functions ϕ and $\underline{\omega}$.

The alternate methods of solution given above will be used in solving several static problems in the following sections. The method used in a given case will depend on the geometry of the boundaries within the medium.

Finally, since it is always possible to introduce displacement potentials \mathfrak{D}^* and $\underline{\psi}^*$ such that

$$\underline{u}^* = \nabla \delta^* + \nabla \times \underline{\psi}^*$$

then, from (3.7.7) it may be seen that δ^* and $\underline{\psi}^*$ may be taken to be biharmonic, so

$$\nabla^4 \delta^* = 0, \quad \nabla^4 \underline{\psi}^* = 0 \quad (3.7.18)$$

and the equations (3.7.6) may be satisfied by adjustment of the undetermined coefficients of these biharmonic functions. Thus these potentials are analogous to the potentials δ and $\underline{\psi}$ for the dynamic case, but are biharmonic.

3.8. Radiation Energy from Elastic Relaxation Sources

As was previously noted, Knopoff (1958) has computed the energy release due to the insertion of an infinite two-dimensional traction free boundary in a prestrained medium. It was argued therein that the difference between the elastic strain field before and after insertion of the boundary must necessarily account for the elastic energy radiated when the result indicated a net reduction of strain energy and so long as the medium behaved elastically.

This basic argument will be extended and generalized to a form applicable to the present dynamical model of the source. Thus regardless of the microscopic details of rupture formation, if the initial and final equilibrium states of stress in the medium are such that a net reduction of strain potential energy results from the creation of a rupture, then the macroscopic rupture mechanism will be viewed as a reasonable spontaneous process which is possible,

even under the stringent conditions of ideal elastic behavior, without the sudden application of external forces. A reduction of elastic strain energy is then interpreted as the energy radiated seismically. Such a result would be in contrast to that obtained for the macroscopic dislocation models of rupture in prestrained media, where the formation of the dislocation would increase the potential energy of the medium rather than lower it (Steketee, 1958).

Explicit consideration will be given to the growing rupture model wherein the whole rupture zone is maintained in a shear free state for a period of time long compared to the time interval of rupturing. In this case a final shear free rupture volume is defined, so that a calculation of the total energy change in the region outside this final volume can easily be made by utilizing the boundary condition of zero traction. On the other hand, while the propagating rupture model will define a region in which rupture has taken place, the region is also essentially healed by the time this final zone is defined. Hence, no boundary condition, except that of continuity, is applicable to this region. Nevertheless, the energy of the radiation field is derived from the change in the equilibrium field outside this volume and may be obtained by integrating or adding up the energy change at every external point just as with the previous model. In either case it will be shown that insertion of a shear free volume element reduces the potential energy of the medium, so that on the basis of potential energy considerations, both models are reasonable. In view of the fact that relaxation is a local effect and that most of the

energy is released at the "front" of the rupture zone, whether it is represented by a growing or propagating shear free volume, then it is reasonable to assume that both models will release essentially the same total energy. Thus for the sake of convenience, the calculation of total energy released as radiation by either model will be made on the basis of a growing rupture model with a well defined final boundary condition of vanishing traction, and the energy value obtained will be used as an order of magnitude estimate for spontaneous rupture in general.

The generalization of the two-dimensional theory of energy release to a three-dimensional form suitable both for computation and interpretation requires a somewhat different mathematical approach than was employed by Knopoff. The method is essentially that used by Press and Archambeau (1962).

In terms of the field variables and relations expressed in equations (3.7.1) through (3.7.6), the change in the potential energy of the medium after complete formation of the rupture volume is defined by⁽¹⁾

$$\delta W^* = W^{(0)} - W^{(1)} = \frac{1}{2} \int \int \int_{V_0 + V_1} [\sigma_{ij}^{(0)} e_{ij}^{(0)} - \sigma_{ij}^{(1)} e_{ij}^{(1)}] d\tau \quad (3.8.1)$$

where V_0 is the rupture region and V_1 the region outside the rupture volume as is indicated in Figure 6. From the previous formulation of the equilibrium problem, it is seen that the region V_1 is bounded

⁽¹⁾ The usual modified tensor notation will be used, that is, the summation convention and the notation for differentiation, e. g. $u_{i,j} \equiv \partial u_i / \partial x_j$ etc.

internally by the rupture surface B, and that

$$\begin{aligned}
 \text{(i)} \quad & \sigma_{ij}^{(1)} n_j = 0, \quad r \in B \\
 \text{(ii)} \quad & u_j^* = u_j^{(0)} - u_j^{(1)} = O\left(\frac{1}{r^\alpha}\right); \quad \alpha \geq 2
 \end{aligned}
 \tag{3.8.2}$$

On the other hand, an alternate pair of conditions may be utilized in the present context. Thus the medium may be assumed to be externally bounded by a free surface, S, so that

$$\begin{aligned}
 \text{(i)} \quad & \sigma_{ij}^{(1)} n_j = 0; \quad r \in B \\
 \text{(ii)} \quad & \sigma_{ij}^{(1)} n_j = 0; \quad r \in S
 \end{aligned}
 \tag{3.8.3}$$

Quite clearly this case corresponds to the problems of interest in the present study at least as well as does the previous set.

The reciprocity theorem of Betti and Rayleigh (Sokolnikoff, 1956, p. 390) states that

$$\frac{1}{2} \iiint_V \sigma_{ij}^{(0)} e_{ij}^{(1)} d\tau = \frac{1}{2} \iiint_V \sigma_{ij}^{(1)} e_{ij}^{(0)} d\tau$$

Therefore, with $\sigma_{ij}^* = \sigma_{ij}^{(0)} - \sigma_{ij}^{(1)}$, etc.

$$\begin{aligned}
 \frac{1}{2} \iiint_{V_0 + V_1} [\sigma_{ij}^{(0)} e_{ij}^{(0)} - \sigma_{ij}^{(1)} e_{ij}^{(1)}] d\tau &= \frac{1}{2} \iiint_{V_0 + V_1} \sigma_{ij}^* e_{ij}^* d\tau \\
 &+ \iiint_{V_0 + V_1} \sigma_{ij}^{(1)} e_{ij}^* d\tau
 \end{aligned}$$

and the change in strain energy can be expressed as

$$\begin{aligned} \delta W^* = & \frac{1}{2} \iiint_{V_0} \sigma_{ij}^* e_{ij}^* d\tau + \frac{1}{2} \iiint_{V_1} \sigma_{ij}^* e_{ij}^* d\tau + \iiint_{V_1} \sigma_{ij}^{(1)} e_{ij}^* d\tau \\ & + \iiint_{V_0} \sigma_{ij}^{(1)} e_{ij}^* d\tau \end{aligned} \quad (3.8.4)$$

The final two integrals may be transformed by noting that

$$\begin{aligned} e_{ij}^* &\equiv u_{i,j}^* - \omega_{ij}^* & \text{with} & \quad \omega_{ij}^* \equiv \frac{1}{2} (u_{i,j}^* - u_{j,i}^*) \\ \sigma_{ij}^{(1)} \omega_{ij}^* &\equiv 0 \end{aligned}$$

Thus, coupled with the identity

$$\sigma_{ij}^{(1)} u_{i,j} = (\sigma_{ij}^{(1)} u_i^*)_{,j} - u_i^* \sigma_{ij,j}^{(1)}$$

and the equations of equilibrium

$$\sigma_{ij,j}^{(1)} = -F_i$$

then the final integrals become, after also applying the divergence theorem

$$\begin{aligned} \iiint_{V_1} \sigma_{ij}^{(1)} e_{ij}^* d\tau &= \iint_S u_i^* \sigma_{ij}^{(1)} n_j da + \iint_B u_i^* \sigma_{ij}^{(1)} n_j da \\ &+ \iiint_{V_1} F_i u_i^* d\tau \\ \iiint_{V_0} \sigma_{ij}^{(1)} e_{ij}^* d\tau &= \iint_B u_i^* \sigma_{ij}^{(1)} n_j da + \iiint_{V_0} F_i u_i^* d\tau \end{aligned}$$

Now since the surface tractions $\sigma_{ij}^{(1)} n_j$ vanish on the rupture

boundary B, then the surface integrals over B vanish. In addition the surface integral over S, in the case of an infinite medium approximation, where the conditions (3.8.2) hold, vanishes in the limit as S recedes to infinity provided

$$\sigma_{ij}^{(1)} = O\left(\frac{1}{r^\beta}\right); \quad \beta > 0 \quad (3.8.5)$$

or if the angular dependence of the integrand is such that the contributions over the surface cancel for the terms of $\sigma_{ij}^{(1)}$ which are not of the order $r^{-\beta}$. If the medium is bounded by a free surface, then the vanishing of the surface integral over S is immediate, owing to the second of the conditions in (3.8.3). Thus one has

$$\begin{aligned} \iiint_{V_1} \sigma_{ij}^{(1)} e_{ij}^* d\tau &= \iiint_{V_1} F_i u_i^* d\tau \\ \iiint_{V_0} \sigma_{ij}^{(1)} e_{ij}^* d\tau &= \iiint_{V_0} F_i u_i^* d\tau \end{aligned}$$

and collecting results,

$$\delta W^* = \frac{1}{2} \iiint_{V_0} \sigma_{ij}^* e_{ij}^* d\tau + \frac{1}{2} \iiint_{V_1} \sigma_{ij}^* e_{ij}^* d\tau + \iiint_{V_0+V_1} F_i u_i^* d\tau \quad (3.8.6)$$

The interpretation of this formal result is straightforward, the first term is merely the change in the elastic strain energy within the rupture zone and is positive definite, so that the energy is available for the formation of the rupture zone. However, this term cannot be considered a realistic estimate of the energy change within

a rupture zone, since by definition the energy change in V_0 is accomplished by nonlinear processes. Certainly then elastic stresses $\sigma_{ij}^{(1)}$ and strains $e_{ij}^{(1)}$ are not appropriate representations of the residual deformed state of the material in this region. In the present context, the elastic stresses and strains following rupture, should be replaced by the corresponding plastic strains etc. within V_0 . Under these conditions, carrying out the transformation of (3.8.1) only with respect to the elastic field in V_1 , an alternate expression for δW^* is obtained

$$\begin{aligned} \delta W^* = & \left[\frac{1}{2} \iiint_{V_0} \sigma_{ij}^{(0)} e_{ij}^{(0)} d\tau - \frac{1}{2} \iiint_{V_0} (\tau_{ij} \epsilon_{ij} + 2\mathcal{E}) d\tau \right] \\ & + \frac{1}{2} \iiint_{V_1} \sigma_{ij}^* e_{ij}^* d\tau + \iiint_{V_1} F_i u_i^* d\tau \end{aligned} \quad (3.8.7)$$

with τ_{ij} and ϵ_{ij} representing the non-elastic deformation within V_0 and the term \mathcal{E} denoting the energy required for recrystallization, phase change or fraction, etc., accompanying the formation of a rupture zone. Under the assumptions of the present rupture model, the shear stresses associated with τ_{ij} are small compared to $p = \frac{1}{3} (\tau_{11} + \tau_{22} + \tau_{33})$, the hydrostatic pressure in V_0 . In view of the fact that the initial elastic stress and strain are equilibrium values, then the diagonal terms of the tensor $\sigma_{ij}^{(0)}$ must be such that $p = \frac{1}{3} (\sigma_{11}^{(0)} + \sigma_{22}^{(0)} + \sigma_{33}^{(0)})$. To first order then, the energy derived from the diagonal terms of the initial elastic energy density

tensor $\frac{1}{2} \sigma_{ij}^{(0)} e_{ij}^{(0)}$ compensate the energy required for the plastic deformation. Thus, when the shear stress energy of the initial field is of the order of the energy \mathcal{E} , the energy required for the non-linear processes (including work done against the gravitational forces), then rupture can occur. A necessary condition for rupture is therefore that

$$\frac{1}{2} \sigma_{ij}^{(0)} e_{ij}^{(0)} > \frac{1}{2} \tau_{ij} \epsilon_{ij} + \mathcal{E}$$

or approximately

$$\frac{1}{2\mu} (\gamma_{ij}^*)^2 \geq \mathcal{E} ; \quad i \neq j \quad (3.8.8)$$

where $\frac{1}{2\mu} (\gamma_{ij}^*)^2$ represents the shear stress energy released at and within the rupture zone for a unit volume of increase in the rupture, while \mathcal{E} is the energy required for a unit volume increase of the rupture zone, and is associated with the mechanisms of the type previously noted. Further, for propagation or growth of the rupture, it is also necessary that (Sneddon, 1951; Griggs and Handin, 1960)

$$\frac{\partial}{\partial \tau} \left\{ \frac{1}{2\mu} (\gamma_{ij}^*)^2 - \mathcal{E} \right\} \geq 0 \quad (3.8.9)$$

with τ denoting the rupture volume. In view of the discussion culminating in equation (3.8.8), it is concluded that most of the radiation field arises from the shear stresses. In later applications then the initial prestress will be taken as pure shear.

The second energy integral in (3.8.6) or (3.8.7), involving

the elastic field in V_1 , is necessarily positive definite and represents the strain energy reduction in the elastic zone. In the present context, the integrand of this energy term is interpreted as the energy density, w^* , for the elastic stress relaxation mechanism appropriate to the material points in the medium outside the rupture zone. Thus one may take

$$w^* = \frac{1}{2} (\sigma_{ij}^{(0)} - \sigma_{ij}^{(1)}) (e_{ij}^{(0)} - e_{ij}^{(1)}) \quad (3.8.10)$$

as the total energy radiated via elastic stress relaxation at a point.

The final integral in (3.8.7) involves the body forces, including gravity and the tectonic forces. The term represents either the total work done by these forces during rupture, in which case the term is positive, or else it is the work done against the forces and is negative. In either case its magnitude is likely to be much smaller than either of the other terms, since the displacement field u_i^* is very localized (i. e., $u_i^* = O(\frac{1}{r^*})$ with $\alpha \geq 2$), and the tectonic force field is probably non-zero only in a very restricted region reglatively far removed from the rupture zone. The effect of gravity can be shown to be small in the elastic region.

Thus the term of significance for dynamical considerations is the relaxation energy term and as an estimated lower bound on the energy radiated during rupture, E_r , one has

$$E_r = \iiint_{V_1} w^* d\tau = \frac{1}{2} \iiint_{V_1} \sigma_{ij}^* e_{ij}^* d\tau \quad (3.8.11)$$

This value of the energy will be a lower bound since the volume integration is taken over only the volume outside the final rupture zone. Hence contributions arising from those points outside the rupture zone during its growth, yet eventually within the final rupture volume V_0 , are excluded. These contributions may not be negligible if the final rupture volume is large. As an upper bound on the total energy radiated, one may use the first term in (3.8.7) for an estimate of the contributions to the field from this source. Thus taking only the initial shear energy density terms $2\mu e_{ij}^{(0)} e_{ij}^{(0)}$ as an upper limit on the radiation energy available, assuming \mathcal{E} in (3.8.7) to be relatively small, then

$$\frac{1}{2} \iiint_{V_1} \sigma_{ij}^* e_{ij}^* d\tau \leq E_r \leq \frac{1}{2} \iiint_{V_1} \sigma_{ij}^* e_{ij}^* d\tau + \iiint_{V_0} \mu e_{ij}^{(0)} e_{ij}^{(0)} d\tau \quad (3.8.12)$$

This relation provides an order of magnitude estimate of the energy radiation of a tectonic source and will be applied to give theoretical estimates.

The processes associated with anelastic creep phenomenon resulting in delayed radiation effects are assumed to have characteristic relaxation times at least in excess of the time interval of rupturing. If, as was previously suggested, this known effect manifests itself only in the observed aftershock phenomenon corresponding to a long relaxation time, then no serious error in the estimate of the radiated energy by purely elastic relaxation should occur.

3.9. Dynamical Elastic Relaxation

Having demonstrated the nature and existence of the solutions for the equilibrium field, consider the dynamical equations for the medium

$$\frac{\partial \sigma_{ij}}{\partial x_j} - \rho f_i = \rho \frac{\partial^2 u_i}{\partial t^2}$$

The static force term may be eliminated by defining a relative dynamic stress and displacement

$$\begin{aligned} \tau_{ij}(\underline{x}, t/\tau) &= \sigma_{ij}(\underline{x}, t/\tau) - \sigma_{ij}^{(0)}(\underline{x}) \\ y_i(\underline{x}, t/\tau) &= u_i(\underline{x}, t/\tau) - u_i^{(0)}(\underline{x}) \end{aligned} \tag{3.9.1}$$

And in terms of these functions, the dynamical equations are simply

$$\frac{\partial \tau_{ij}}{\partial x_j} = \rho \frac{\partial^2 y_i}{\partial t^2} \tag{3.9.2}$$

In vector form (3.9.2) becomes

$$(\lambda + 2\mu)\nabla(\nabla \cdot \underline{y}) - \mu \nabla \times \nabla \times \underline{y} = \rho \frac{\partial^2}{\partial t^2} \underline{y} \tag{3.9.3}$$

Operating on this equation successively with the divergence and curl, one obtains the two familiar wave equations

$$\begin{aligned} \nabla^2 \Theta - \frac{1}{v_p^2} \frac{\partial^2 \Theta}{\partial t^2} &= 0 \\ \nabla^2 \underline{\Omega} - \frac{1}{v_s^2} \frac{\partial^2 \underline{\Omega}}{\partial t^2} &= 0 \end{aligned} \tag{3.9.4}$$

where Θ and $\underline{\Omega}$ are the dynamic dilatation and rotation. In addition the equilibrium values of these field variables satisfy Laplace's equation and are therefore harmonic as was previously remarked in Chapter 2. The acceleration field $\frac{\partial^2}{\partial t^2} \underline{y}$ can be obtained in terms of Θ and $\underline{\Omega}$ from the equations of motion (as in Chapter 2), since from (3.9.3)

$$\frac{\partial^2}{\partial t^2} \underline{y} = v_p^2 \nabla \Theta - 2v_s^2 \nabla \times \underline{\Omega}$$

Thus the Fourier transforms of \underline{y} and these physical potentials are related by

$$\tilde{\underline{y}} = - \frac{1}{k_p^2} \nabla \Theta + \frac{2}{k_s^2} \nabla \times \tilde{\underline{\Omega}} \quad (3.9.5)$$

The radiation field may also be described in terms of the usual dynamic potentials, so that

$$\underline{y}(\underline{r}, t/\tau) = \nabla \mathfrak{s}(\underline{r}, t/\tau) + \nabla \times \underline{\psi}(\underline{r}, t/\tau)$$

provided \mathfrak{s} and $\underline{\psi}$ are solutions of the wave equations

$$\begin{aligned} \nabla^2 \mathfrak{s} - \frac{1}{v_p^2} \frac{\partial^2}{\partial t^2} \mathfrak{s} &= 0 \\ \nabla^2 \underline{\psi} - \frac{1}{v_s^2} \frac{\partial^2}{\partial t^2} \underline{\psi} &= 0 \end{aligned} \quad (3.9.6)$$

The equilibrium values of these potentials have been shown to satisfy the biharmonic equations (3.7.18). Thus the radiation field due to

the growth of a traction free boundary $B(\tau)$ within the pre-strained medium may be obtained in terms of either the dilatation or rotation, in which case $\Theta^*(\underline{r}, \tau)$ and $\underline{\Omega}^*(\underline{r}, \tau)$ are harmonic functions specifying the initial values, or in terms of the displacement potentials, in which case the biharmonic functions $\mathcal{S}^*(\underline{r}, \tau)$ and $\underline{\Psi}^*(\underline{r}, \tau)$ are the initial values.

Due to the mathematical similarity of the two approaches to the problem, generalized potentials $\Phi(\underline{r}, t/\tau)$ and $\chi(\underline{r}, t/\tau)$ will be used, where

$$\Phi(\underline{r}, t/\tau) = \begin{Bmatrix} \Theta(\underline{r}, t/\tau) \\ \mathcal{S}(\underline{r}, t/\tau) \end{Bmatrix} \quad \Phi^*(\underline{r}, \tau) = \begin{Bmatrix} \Theta^*(\underline{r}, \tau) \\ \mathcal{S}^*(\underline{r}, \tau) \end{Bmatrix}$$

$$\chi(\underline{r}, t/\tau) = \begin{Bmatrix} \underline{\Omega}(\underline{r}, t/\tau) \\ \underline{\Psi}(\underline{r}, t/\tau) \end{Bmatrix} \quad \chi^*(\underline{r}, \tau) = \begin{Bmatrix} \underline{\Omega}^*(\underline{r}, \tau) \\ \underline{\Psi}^*(\underline{r}, \tau) \end{Bmatrix}$$

with Φ , Φ^* etc. representing either dilatation or scalar displacement potentials etc. Wherever these symbolic potentials are used, the formulas will be valid for either set of field variables.

In Chapter 2 the radiation associated with the relaxation of the elastic stresses due to the insertion of a traction free boundary was computed. In view of the actual growth of propagation of a rupture boundary at some finite velocity, it is necessary to interpret that result as the radiation due to the growth of an infinitesimal rupture with a speed larger than the compressional wave velocity in the medium. In such a case the rupture volume is effectively created

instantaneously, since when the rupture velocity V_R is larger than the compressional velocity, the existence of the rupture is not manifested until it has reached its final dimensions. Thereafter relaxation at a given point in the medium will begin after a time appropriate to the propagation of signal from the rupture surface to the point in question. Taking the rupture element to be roughly spherical, of radius δR , and outside of the constant factors

$$\frac{\delta R}{v_R} - \frac{\delta R}{v_p} \quad \text{and} \quad \frac{\delta R}{v_R} - \frac{\delta R}{v_s}$$

then the delay in the initiation of the relaxation at a point is r/v_p , for the dilatation or scalar potential and r/v_s for the rotation or vector potential, as was asserted in Chapter 2. Thus the arrival of signal from the boundary, the signal itself being the result of relaxation along the boundary and at intermediate surrounding points, is taken to define a change in the potential field, an "initial value," which would reduce the field to a value in equilibrium with the entire rupture. The actual dynamical relaxation of the potential will begin at this time in a manner determined by this "initial value" and the dynamical equations of motion. While this view of the process of relaxation will be adopted throughout, only in the case in which the rupture boundary is controlled by propagating shock front can the instantaneous rupture model be directly utilized. Thus the results previously obtained are applicable to tectonic energy release associated with shock induced rupture.

On the other hand spontaneous rupture proceeds with a velocity which is less than the shear wave velocity, so that the actual growth or propagation of a rupture will affect the relaxation and therefore the radiation field. In order to provide for this anticipated complication it is only necessary to generalize, but slightly, the previous formulation of the dynamical effects of elastic relaxation. This is easily accomplished through use of the source time parameter τ .

Thus let the total variation of the equilibrium potentials and rupture boundary over the complete time interval of rupturing be subdivided at source times $\tau_1, \tau_2, \dots, \tau_k, \dots, \tau_{N-1}, \tau_N$ into equal, infinitesimal time intervals $\delta\tau$. Further let the change in the rupture surface and the equilibrium potentials in these intervals be represented by discrete jumps or steps, the total variation of the potential or rupture dimension over any particular interval $\delta\tau = \tau_{k+1} - \tau_k$, being accomplished in a single jump within the interval. By consideration of an arbitrary source time τ_k and time interval $\delta\tau$, the radiation field resulting from a single discrete (infinitesimal) change in the rupture boundary may be computed and then superposition with proper time delays will give the effect of the boundary growth. In addition, a continuous rupture growth can be effected by a suitable limit of the superposition procedure.

Hence take the rupture boundary to be of finite size appropriate to the rupture surface at some arbitrary time, τ_k , during its propagation or growth. Then the radiation field associated with a discrete change in the rupture boundary (and equilibrium potential

fields) in a source time interval $\delta\tau$ is given in terms of the following initial value problem

$$\begin{aligned} \nabla^2 \Phi(\underline{r}, t/\tau'_k) - \frac{1}{v_p^2} \frac{\partial^2}{\partial t^2} \Phi(\underline{r}, t/\tau'_k) &= 0 \\ \nabla^2 \chi_j(\underline{r}, t/\tau'_k) - \frac{1}{v_s^2} \frac{\partial^2}{\partial t^2} \chi_j(\underline{r}, t/\tau'_k) &= 0 \end{aligned} \quad (3.9.7)$$

$$\lim_{\epsilon \rightarrow 0} \left[\Phi(\underline{r}, \tau'_k - \epsilon/\tau'_k) - \Phi(\underline{r}, \tau'_k + \epsilon/\tau'_k) \right] = \Phi^*(\underline{r}, \tau_k) - \Phi^*(\underline{r}, \tau_k + \delta\tau)$$

$$\lim_{\epsilon \rightarrow 0} \left[\chi_j(\underline{r}, \tau''_k - \epsilon/\tau'_k) - \chi_j(\underline{r}, \tau''_k + \epsilon/\tau'_k) \right] = \chi_j^*(\underline{r}, \tau_k) - \chi_j^*(\underline{r}, \tau_k + \delta\tau)$$

$$\tau_{ij}(\underline{r}, t/\tau'_k) n_j = 0 \quad ; \quad r \in B(\tau), \quad \tau_k < \tau'_k < \tau_k + \delta\tau = \tau_{k+1}$$

where the source time is restricted to the value τ'_k and the initial values for the dynamic potentials are given in terms of limits for generality, The "jumps" occur at

$$t = \tau' = \tau'_k + \tau_1^* = \tau'_k + \zeta/v_p \quad (3.9.8)$$

for $\Phi(\underline{r}, t/\tau'_k)$, with $\zeta(\underline{r}, t)$ denoting the minimum distance from the rupture surface to the point at which relaxation occurs, Figure 7, and at

$$t = \tau'' = \tau'_k + \tau_2^* = \tau'_k + \frac{\zeta}{v_s} \quad (3.9.9)$$

for $\chi_j(\underline{r}, t/\tau'_k)$. Here again the causality relationship between the rupture and the relaxation of the elastic field is accounted for by

delay times τ_1^* and τ_2^* . The minimal distance ζ will depend on the rupture dimensions as well as on \underline{r} , the coordinates of the point. An essential difference between the growing or expanding rupture model and a propagating rupture will be in the evaluation of this minimal distance, to be taken up in the following section.

The solution of the problem posed in (3.9.7) may be obtained through use of the Fourier transform with respect to the real time variable t . Thus, applying the transform

$$\mathcal{F}\{\Phi\} = \frac{1}{\sqrt{2\pi}} \int_{-\infty}^{+\infty} \Phi e^{-i\omega t} dt = \tilde{\Phi}(\underline{r}, \omega/\tau) \quad (3.9.10)$$

to the equations of (3.9.7) and taking into account the discontinuities of Φ and χ_j , yields

$$\begin{aligned} \nabla^2 \tilde{\Phi}(\underline{r}, \omega/\tau_k') + k_p^2 \tilde{\Phi}(\underline{r}, \omega/\tau_k') - \frac{i\omega}{\sqrt{2\pi}} \left(\frac{1}{v_p}\right) \delta\Phi^*(\underline{r}, \tau_k') e^{-i\omega\tau_k'} &= 0 \\ \nabla^2 \tilde{\chi}_j(\underline{r}, \omega/\tau_k') + k_s^2 \tilde{\chi}_j(\underline{r}, \omega/\tau_k') - \frac{i\omega}{\sqrt{2\pi}} \left(\frac{1}{v_s}\right) \delta\chi_j^*(\underline{r}, \tau_k') e^{-i\omega\tau_k'} &= 0 \end{aligned} \quad (3.9.11)$$

$$\tilde{\tau}_{ij}(\underline{r}, \omega/\tau_k') n_j = 0 \quad ; \quad \underline{r} \in B(\tau)$$

with

$$k_p = \omega/v_p \quad , \quad k_s = \omega/v_s$$

and where the discontinuities in the equilibrium fields are denoted by

$$\delta\Phi^*(\underline{r}, \tau_k') = \Phi^*(\underline{r}, \tau_k) - \Phi^*(\underline{r}, \tau_k + \delta\tau) \quad (3.9.12)$$

$$\delta\chi_j^*(\underline{r}, \tau_k') = \chi_j^*(\underline{r}, \tau_k) - \chi_j^*(\underline{r}, \tau_k + \delta\tau)$$

Particular solutions of (3.9.11) corresponding to the source radiation, or "primary field," are obtained from the Kirchoff solution of the inhomogeneous Helmholtz equation (e.g. Chapter 2, eqs. (2.2.22) and (2.2.28)). Thus, with $\mathcal{R}(\tau)$ denoting the region outside the boundary $B(\tau)$, as indicated in Figure 7, one has for $\tilde{\Phi}$, and analogously for $\tilde{\chi}_j$, $j = 1, 2, 3$,

$$\tilde{\Phi}(\underline{r}, \omega/\tau'_k) = - \frac{i\omega}{4\pi v_p^2} \left(\frac{1}{\sqrt{2\pi}} \right) \iiint_{\mathcal{R}(\tau)} \frac{\delta\Phi^*(\underline{r}', \tau'_k)}{r^*} e^{-ik_p(r^* + v_p \tau')} d\underline{r}'$$

with $r^* = \underline{r} - \underline{r}'$. This may be regarded as a formal solution of the hypothetical problem previously posed. By summing the contributions from a succession of such problems, each with a different value for the parameter τ'_k corresponding to different boundary dimensions, it is clearly possible to generalize to the case of either a propagating or an expanding rupture. The superposition may be best accomplished by first transforming (3.9.13) back to the real time domain. First defining a generalized delta function, $\delta_n(t)$, in terms of its Fourier transform by

$$(2\pi)^{1/2} \int_{-\infty}^{+\infty} \delta_n(t) e^{-i\omega t} dt = (i\omega)^n \quad (3.9.14)$$

where it may also be observed that, formally

$$\delta_n(t) = \frac{d^{(n)}}{dt^{(n)}} \{ \delta(t) \}$$

and then applying the inverse transform \mathcal{F}^{-1} to (3.9.13), yields

$$\Phi(\underline{r}, t/\tau_k^1) = -\frac{1}{4\pi v_p^2} \iiint_{\mathcal{R}(\tau)} \frac{\delta\Phi^*(\underline{r}', \tau_k^1)}{r^*} \delta_1(t - \frac{r^*}{v_p} - \tau^1) dr' \quad (3.9.15)$$

and analogously

$$\chi_j(\underline{r}, t/\tau_k^1) = -\frac{1}{4\pi v_s^2} \iiint_{\mathcal{R}(\tau)} \frac{\delta\chi_j^*(\underline{r}', \tau_k^1)}{r^*} \delta_1(t - \frac{r^*}{v_s} - \tau^1) dr' \quad (3.9.16)$$

Comparing these integral solutions to those for a medium with external sources of energy, it is seen that a source term $-(1/v_p^2)\delta\Phi^*(\underline{r}, \tau_k^1)\delta_1(t-\tau^1)$ in an unstrained medium gives a result equivalent to (3.9.15) and a source term $-(1/v_s^2)\delta\chi_j^*(\underline{r}, \tau_k^1)\delta_1(t-\tau^1)$ a result equivalent to (3.9.16). If the potentials Φ and χ_j are taken to represent the dilatation and rotation, for example, then the equivalent inhomogeneous equations are, for $\underline{r} \in \mathcal{R}$,

$$\nabla^2 \Theta(\underline{r}, t/\tau_k^1) - \frac{1}{v_p^2} \frac{\partial^2}{\partial t^2} \Theta(\underline{r}, t/\tau_k^1) = \frac{1}{v_p^2} \delta\Theta^*(\underline{r}, \tau_k^1) \delta_1(t-\tau^1)$$

$$\nabla^2 \Omega_j(\underline{r}, t/\tau_k^1) - \frac{1}{v_s^2} \frac{\partial^2}{\partial t^2} \Omega_j(\underline{r}, t/\tau_k^1) = \frac{1}{v_s^2} \delta\Omega_j^*(\underline{r}, \tau_k^1) \delta_1(t-\tau^1)$$

The source term for the dilatation, for example, can be interpreted as delivering an impulse at a time $t = \tau_k^1 + \frac{\zeta}{v_p}$ which develops for a short time until the required initial displacement is achieved. At this time a second impulse is applied to reduce the velocity to zero but leave the displacement unchanged. The source term has the explicit form described if it is written as

$$\frac{1}{v_p} \delta \Theta^* (\underline{r}, \tau_k') \delta_1(t-\tau') = \frac{1}{v_p} \lim_{\epsilon \rightarrow 0} \left[\delta \Theta^* \left\{ \frac{\delta(t-\tau'+\epsilon) - \delta(t-\tau'-\epsilon)}{2\epsilon} \right\} \right]$$

The foregoing therefore describes a means of simulating the relaxation effect in the medium surrounding a rupture by means of a volume distribution of equivalent sources. The time dependence is seen to be a doublet impulse for both the dilatation and rotation, but that the action of these two distortional processes begins at different times, determined by the shear and compressional velocities of the medium. Furthermore both the magnitude and time at which the source is activated depends on the distance and angular location of the point relative to the rupture.

It is instructive to consider the nature of the distribution of equivalent sources on the rupture surface that would give a radiation field at least similar to that of the relaxation field. A reduction to surface sources can be made by direct modification of the results (3.9.15) and (3.9.16). Thus taking the potentials Φ^* and χ_j^* to be the dilatation Θ^* and rotation Ω_j^* , noting that

$$\delta \Theta^* = \nabla \cdot \delta u^*, \quad \delta \Omega_j^* = \frac{1}{2} \nabla \times \delta u^*$$

then the integrands of (3.9.15) and (3.9.16) may be written as

$$\frac{\delta\Theta}{r^*} \delta_1(t - \frac{r^*}{v_p} - \tau') = \nabla \cdot \left\{ \delta \underline{u}^* \left(\frac{\delta_1(t - \frac{r^*}{v_p} - \tau')}{r^*} \right) \right\} - \nabla \left(\frac{\delta_1(t - \frac{r^*}{v_p} - \tau')}{r^*} \right) \cdot \delta \underline{u}^*$$

$$\frac{\delta\Omega_j}{r^*} \delta_1(t - \frac{r^*}{v_s} - \tau'') = \nabla \times \left\{ \delta \underline{u}^* \left(\frac{\delta_1(t - \frac{r^*}{v_s} - \tau'')}{r^*} \right) \right\} - \nabla \left(\frac{\delta_1(t - \frac{r^*}{v_s} - \tau'')}{r^*} \right) \times \delta \underline{u}^*$$

Thus the solutions for this elementary relaxation source may be put in the form

$$\begin{aligned} \Theta(\underline{r}, t/\tau'_k) &= -\frac{1}{4\pi v_p^2} \iint_{B(\tau)} \frac{\delta_1(t - \frac{r^*}{v_p} - \tau'_k)}{r^*} \delta \underline{u}^* \cdot \underline{n} \, ds' \\ &\quad + \frac{1}{4\pi v_p^2} \iiint_{\mathcal{R}(\tau)} \nabla \left(\frac{\delta_1(t - \frac{r^*}{v_p} - \tau')}{r^*} \right) \cdot \delta \underline{u}^* \, d\underline{r}' \\ \underline{\Omega}(\underline{r}, t/\tau'_k) &= -\frac{1}{8\pi v_s^2} \iint_{B(\tau)} \frac{\delta_1(t - \frac{r^*}{v_s} - \tau'_k)}{r^*} \delta \underline{u}^* \times \underline{n} \, ds \\ &\quad + \frac{1}{8\pi v_s^2} \iiint_{\mathcal{R}(t)} \nabla \left(\frac{\delta_1(t - \frac{r^*}{v_s} - \tau'')}{r^*} \right) \times \delta \underline{u}^* \, d\underline{r}' \end{aligned}$$

The final volume integrals in these expressions are of the same order as the surface integrals and therefore they cannot be neglected. They may be reduced to surface integrals through use of the mean value theorem. In particular the region may be divided into sectors such that in each, the functions $\nabla \left\{ \delta_1(t - (r^*/v_p) - \tau') / r^* \right\}$ and $\nabla \left\{ \delta_1(t - (r^*/v_s) - \tau'') / r^* \right\}$ are of constant sign. Applying the mean value theorem to each separate integral so formed, one has for example

$$\begin{aligned}
 & \iiint_{\mathcal{R}(\tau)} \nabla \left(\frac{\delta_1(t - \frac{r^*}{v_p} - \tau')}{r^*} \right) \cdot \delta \underline{u}^* \, d\underline{r}' = \\
 & = \sum_j \delta \underline{u}^*(\tilde{\underline{r}}_j, \tau'_k) \cdot \iiint_{\mathcal{R}_j(\tau)} \nabla \left(\frac{\delta_1(t - \frac{r^*}{v_p} - \tau')}{r^*} \right) \, d\underline{r}' \\
 & = \sum_j \iiint_{B_j(\tau)} \left(\frac{\delta_1(t - \frac{r^*}{v_p} - \tau'_k)}{r^*} \right) \delta \underline{u}_j \cdot \underline{n} \, ds
 \end{aligned}$$

where $\delta \underline{u}_j = \delta \underline{u}^*(\tilde{\underline{r}}_j, \tau'_k)$ is a value of the increment in the equilibrium field within the volume sector $\mathcal{R}_j(\tau)$, evaluated at a point $\tilde{\underline{r}}$, such that, with R the radial coordinate of the rupture surface,

$$|\tilde{\underline{r}}_j| \geq R$$

A similar evaluation applies to the volume integral for the rotation, where however the partitioning of the volume $\mathcal{R}(\tau)$ is different and so is the increment in the equilibrium field, $\delta \bar{\underline{u}}_j$, corresponding to $\delta \underline{u}_j$. The solutions in terms of surface integrals are therefore

$$\begin{aligned}
 \Theta(\underline{r}, t/\tau'_k) &= -\frac{1}{4\pi v_p^2} \sum_j \iiint_{B_j(\tau)} \frac{\delta_1(t - \frac{r^*}{v_p} - \tau'_k)}{r^*} (\delta \underline{u}^* - \delta \underline{u}_j) \cdot \underline{n} \, ds \\
 \underline{\Omega}(\underline{r}, t/\tau'_k) &= -\frac{1}{8\pi v_s^2} \sum_i \iiint_{B_i(\tau)} \frac{\delta_1(t - \frac{r^*}{v_s} - \tau'_k)}{r^*} (\delta \underline{u}^* - \delta \bar{\underline{u}}_i) \times \underline{n} \, dx
 \end{aligned}$$

These representations show that sources $(\delta \underline{u}^* - \delta \underline{u}_j) \cdot \underline{n} \delta_1(t - \tau'_k)$ and

$(\delta \underline{u}^* - \delta \underline{u}_i) \times \underline{n} \delta(t - \tau_k')$ for the two potentials, distributed along the rupture surface, will give rise to a radiation field equivalent to the volume relaxation field, the dilatational field being generated by a displacement in the direction of the normal to the rupture and rotation by a displacement along the rupture surface. Due to the presence of the factors $\delta \underline{u}_j$ and $\delta \underline{u}_i$, it is clear that the radiation field is not determined solely by the actual physical displacements on the rupture surface, as is implied by dislocation theory. Further, the displacements $\delta \underline{u}_j$ and $\delta \underline{u}_i$ are functions of the source time so that as the rupture propagates or grows, these factors will also change, and values of the equilibrium displacement field throughout the volume surrounding the rupture will be involved in the equivalent surface source. Thus the equivalent displacements on the rupture surface will bear little relationship to the actual physical displacements on this surface and are in fact intimately connected with the details of the relaxation field surrounding the rupture.

Returning to the fundamental solutions (3.9.15) and (3.9.16), some minor amplifications of the form of these solutions are desirable. Treating only the scalar potential Φ explicitly, the same comments being equally valid for each of the components of the vector potential, equation (3.9.15) may be written as

$$\Phi(\underline{r}, t/\tau_k') = - \frac{1}{4\pi v_p^2} \iint d\Omega \int_{R(\Omega, t)}^{\infty} \frac{\delta \Phi^*(\underline{r}', \tau_k')}{r^*} \delta_1(t - \tau' - \frac{r^*}{v_p}) r'^2 dr' \quad (3.9.19)$$

where $R(\Omega, \tau)$ is the radial coordinate from the origin of the coordinates to $B(\tau)$, while $d\Omega$ denotes the solid angle subtended by an element of a spherical surface of radius r' . Figure 7 shows the relationships of these variables to the rupture surface and to each other. If the rupture surface $B(\tau)$ is not spherical for all τ , then R is a function of both τ and Ω as indicated.

3.10. Rupture Propagation and Growth Effects

First consider a growing rupture model and take the rupture surface to be, in general, ellipsoidal, for any source time τ , with axes a, b, c . Let the time when the rupture reaches its final dimensions be denoted by τ_0 . The effect of the growth of the rupture at an arbitrary point of observation is a superposition of the contributions to the radiation from each increment of growth in the boundary, that is a superposition of elementary solutions of the form obtained in section 3.9. These increments were taken to be finite, but arbitrarily small, so that if the time interval of rupturing, $\tau = 0$ to $\tau = \tau_0$, is divided into N intervals $\delta\tau$ and if $\Phi(\underline{r}, t)$ and $\chi_j(\underline{r}, t)$ are the composite fields due to the rupture at any time t , then the indicated superposition is given by

$$\Phi(\underline{r}, t) = \lim_{\substack{N \rightarrow \infty \\ \delta\tau \rightarrow 0}} \sum_{k=1}^N \Phi(\underline{r}, t/\tau'_k) ; \quad \chi_j(\underline{r}, t) = \lim_{\substack{N \rightarrow \infty \\ \delta\tau \rightarrow 0}} \sum_{k=1}^N \chi_j(\underline{r}, t/\tau'_k)$$

Here the summations are implicitly limited to a source time interval τ_0 . This dependence can be made explicit. That is, using the

results of the form given by (3.9.20), one has for example

$$\Phi(\underline{r}, t) = - \left(\frac{1}{4\pi v_p^2} \right) \lim_{\substack{N \rightarrow \infty \\ \delta\tau \rightarrow 0}} \sum_{k=1}^N \times \left[\iint d\Omega \int_{R(\Omega, \tau)}^{\infty} \left(\frac{\delta\Phi^*(\underline{r}', \tau'_k)}{\delta\tau} \right) \frac{\delta_1(t - \tau' - \frac{r}{v_p^*})}{r^*} r'^2 dr' \right] \delta\tau$$

and in the limit the summation can be written as an integral over the source time, which gives

$$\Phi(\underline{r}, t) = - \left(\frac{1}{4\pi v_p^2} \right) \int_0^t S(\tau - \tau_0) \times \iint d\Omega \int_{R(\Omega, \tau)}^{\infty} \left(\frac{\partial\Phi^*(\underline{r}', \tau'_k)}{\partial\tau} \right) \frac{\delta_1(t - \tau' - \frac{r}{v_p^*})}{r^*} r'^2 dr' d\tau \quad (3.10.2)$$

where $S(\tau - \tau_0)$ is a step function defining the duration of rupturing,

$$S(\tau - \tau_0) = \begin{cases} 1, & 0 \leq \tau \leq \tau_0 \\ 0, & \text{otherwise} \end{cases}$$

and

$$\tau' = \tau + \frac{r}{v_p}$$

Here $\partial\Phi^*/\partial\tau$ denotes the partial derivative of Φ^* with respect to the source time. The solution (3.10.2) represents a complete formal solution for the growing rupture, and in fact applies to the propagating rupture model as well. The evaluation of this integral, and those of

similar form for $\chi_j(\underline{r}, t)$, may be effected after taking advantage of the special properties of spontaneous rupturing, that is, after introducing simplifications based on the particular models of rupture adopted in this study.

In particular, the radial factor $R(\Omega, \tau)$ was originally introduced into the integrations for the primary radiation field in order to exclude the non-linear rupture zone. Considering a growing rupture, taking the ellipsoidal parameters to be of the form

$$\begin{aligned} a(\tau) &= v_R \tau \\ b(\tau) &= (b_o/a_o)v_R \tau \\ c(\tau) &= (c_o/a_o)v_R \tau \end{aligned} \tag{3.10.3}$$

where $a_o > b_o > c_o$ are the final dimensions of the rupture, then it is reasonable to assume, on physical grounds, that the "width" c_o of this region will be much smaller than the "length" a_o . That is, in view of the likelihood of high stress concentration in a long narrow zone by the mechanisms of creep, resulting in phase change or melting within the zone, then it follows that for such a mechanism

$$c_o \ll a_o \tag{3.10.4}$$

$$b_o < a_o$$

and that the volume of melting and plastic deformation is very small compared to the total volume contributing to the radiation field.

Thus if the radial factor $\mathcal{R}(\Omega, \tau)$ appearing in (3.10.2) is neglected, that is set equal to zero, then this is clearly equivalent to assuming $c_0 \simeq 0$. While there is little doubt that a non-linear zone of some thickness will appear during rupture, it could be argued that recrystallization of the melt along the contact with the crystalline surrounding material would rapidly reduce the thickness to a rather thin zone, much as is assumed for the propagating rupture, yet not with the same complete and rapid solidification as is proposed in this latter case.

Thus simplifying the formal solution by setting $\mathcal{R}(\Omega, \tau)$ to zero and thereby adopting the physical assumptions stated above, one can rewrite (3.10.2) in the form

$$\Phi(\underline{r}, t) = -\left(\frac{1}{4\pi v_p^2}\right) \iiint \left(\frac{1}{r^*}\right) d\underline{r}' \int_0^t S(\tau-\tau_0) \left(\frac{\partial \Phi^*}{\partial \tau}\right) \delta_1\left(t-\tau - \frac{\zeta+r^*}{v_p}\right) d\tau$$

Observing that

$$\delta_1\left(t-\tau - \frac{\zeta+r^*}{v_p}\right) \equiv \frac{d}{dt} \delta\left(t-\tau - \frac{\zeta+r^*}{v_p}\right)$$

then the integral over the surface time parameter τ becomes

$$\begin{aligned} \int_0^t S(\tau-\tau_0) \left(\frac{\partial \Phi^*}{\partial \tau}\right) \frac{d}{dt} \delta\left(t-\tau - \frac{\zeta+r^*}{v_p}\right) d\tau &= \frac{d}{dt} \int_0^t S(\tau-\tau_0) \left(\frac{\partial \Phi^*}{\partial \tau}\right) \delta\left(t-\tau - \frac{\zeta+r^*}{v_p}\right) d\tau \\ &- S(t-\tau_0) \left(\frac{\partial \Phi^*}{\partial \tau}\right)_{\tau=t} \delta\left(\frac{\zeta(t)+r^*}{v_p}\right) \end{aligned}$$

If the point of observation at \underline{r} is never on the rupture boundary,

then the last term of this expression will vanish due to the delta function. Therefore

$$\Phi(\underline{r}, t) = -\left(\frac{1}{4\pi v_p^2}\right) \iiint \left(\frac{1}{r^*}\right) dr' \times \left\{ \frac{d}{dt} \int_0^t S(\tau - \tau_0) \left(\frac{\partial \Phi^*}{\partial \tau}\right) \delta\left(t - \tau - \frac{\zeta + r^*}{v_p}\right) d\tau \right\} \quad (3.10.5)$$

and likewise

$$\chi_j(\underline{r}, t) = -\left(\frac{1}{4\pi v_s^2}\right) \iiint \left(\frac{1}{r^*}\right) dr' \times \left\{ \frac{d}{dt} \int_0^t S(\tau - \tau_0) \left(\frac{\partial \chi_j^*}{\partial \tau}\right) \delta\left(t - \tau - \frac{\zeta + r^*}{v_s}\right) d\tau \right\} \quad (3.10.6)$$

provided, in both cases that

$$\underline{r} \notin B(\tau)$$

An important common characteristic of both the propagating and expanding ruptures is that the elemental field solution is applicable to both models. Therefore the field potential (3.10.2) is appropriate for either model. If the propagating rupture is taken to be represented geometrically by an ellipsoidal region which both grows, that is changes dimension with time, and translates in some direction with time as in Figure 10b, then, under the same conditions on the dimensions of this ellipsoid as were assumed for the growing ellipsoid, the radial factor $\mathcal{R}(\Omega, \tau)$ may be neglected in the integrations. The results given by (3.10.5) and (3.10.6) will then follow.

On the other hand, suppose the propagating rupture zone is represented by a translating and dimensionally time variable sphere as in Figure 10a. In view of the relative simplicity of the calculations of the equilibrium fields, Φ^* , χ_j^* , for a spherical rupture, such a model has merit if only because of this simplicity and since it would be expected that the changes in the stress field surrounding such a spherical rupture at any time would not differ appreciably from those in the vicinity of a comparable propagating ellipsoidal rupture. Aside from these considerations, it is conceivable that a melt zone, for example, might well be roughly spherical.

In any event, adoption of such a model in itself prevents the use of the previous arguments for the simplification of (3.10.2). That is, it is not possible nor logically consistent to consider the thickness of the rupture zone to be small compared to the other dimensions in view of the very nature of the model. While such a contention has a reasonable physical basis for a description of natural rupture, it is by no means a certainty. Thus, by considering a propagating spherical rupture, it is possible to relax the condition that the rupture zone be narrow, as well as to drop the condition that the boundary condition be well defined over the total interval of rupturing and at all points on the rupture envelope.

At the moment however it is difficult to delete the contributions to the field from within the spherical rupture zone except in the very formal manner indicated by the results (3.10.2). Nevertheless the

expression of the field indicated by (3.10.2) must be simplified and made more explicit if the integrals in this expression are to be evaluated and the results used to compute the excitation of the medium. The issue may be sidestepped momentarily by including the contributions to the field from within the spherical rupture region $|\underline{r}'| \leq R(\Omega, \tau)$. If this is done the procedures leading to the results (3.10.5) and (3.10.6) are valid and the simplification of the expressions for the field is thereby accomplished. In order to then recover the contributions from within the propagating rupture zone and exclude them from the final field representation, the integral solutions in (3.10.5) and (3.10.6) must be separated into terms which represent the field contributions from specific regions within and without the rupture zone. This procedure will be adopted and eventually carried out in final detail in section 3.12 for this model. For the moment the results (3.10.5) and (3.10.6) will be taken to represent the field from this model with the provision of later modification along the lines indicated.

In addition to the effects of rupture expansion or propagation on the delay factor ζ , the equilibrium fields Φ^* and χ_j^* will clearly depend upon the nature of the rupture formation. Indeed the effects of rupture growth or propagation will manifest themselves primarily in the variation of the equilibrium fields with respect to the source time. Thus, proceeding with this most direct effect first, let the generalized potentials Φ^* and χ_j^* be taken to be the dilatation Θ^* and rotation Ω_j^* respectively. Let O'' be the origin of a coordi-

nate system centered at the point of intersection of the rupture ellipsoid axes or at the center of a spherical rupture at any source time τ , with the coordinate axis x_3'' taken in the direction of the major axis, or in the direction of rupture propagation, as shown in Figure 8. Such a coordinate system therefore will move or translate with the rupture. At any source time τ the equilibrium potentials, when expressed in this translating system, are

$$\Theta^*(\underline{r}'', \tau) = \sum_{n=1}^{\infty} \left(\frac{1}{r''}\right)^{n+1} \sum_{m=0}^n \left\{ \alpha_{nm}(\tau) \cos m\phi'' + \beta_{nm}(\tau) \sin m\phi \right\} P_n^m(\cos \theta)$$

(3.10.7)

$$\Omega_j^*(\underline{r}'', \tau) = \sum_{n=1}^{\infty} \left(\frac{1}{r''}\right)^{n+1} \sum_{m=0}^n \left\{ \gamma_{nm}^{(j)}(\tau) \cos m\phi'' + \delta_{nm}^{(j)}(\tau) \sin m\phi \right\} P_n^m(\cos \theta)$$

in view of the results given by (3.7.15). That is, both Θ^* and Ω_j^* are harmonic and are taken to be of order $(r'')^{-\alpha}$ with $\alpha \geq 2$, so that the displacement field u^* is at least $O(r''^{-2})$, as is required by the boundary conditions on the equilibrium field, (equations (3.7.6)). Here the dependence of the coefficients $\alpha_{nm}(\tau)$... etc. on the source time τ is through the dependence of the rupture dimensions on the source time and not through the dependence of the rupture position on τ .

This latter effect is obtained by expressing the potentials in terms of a fixed coordinate system. Thus choosing a fixed system with origin at O' , the point of initial rupture, taking the coordinate axis x_3^1 coincident with the axis x_3'' of the translating system and *letting*

$d(\tau)$ represent the physical separation of the origins, as in Figure 8, one has immediately from Appendix 3

$$\Theta^* = \left\{ \begin{array}{l} \sum_{n=1}^{\infty} \left(\frac{1}{r'}\right)^{n+1} \sum_{m=0}^n \left\{ \alpha_{nm}(\tau) \cos m\phi' + \beta_{nm}(\tau) \sin m\phi' \right\} \sum_{s=0}^{\infty} (-1)^s \frac{(n-m+s)!}{s! (n-m)!} \\ \quad \times \left(\frac{d(\tau)}{r'}\right)^s P_{n+s}^m(\cos\theta') ; d(\tau) < r' \\ \sum_{n=1}^{\infty} (-1)^{n+1} \left(\frac{1}{d(\tau)}\right)^{n+1} \sum_{m=0}^n \left\{ \alpha_{nm}(\tau) \cos m\phi' + \beta_{nm}(\tau) \sin m\phi' \right\} \\ \quad \times \sum_{s=0}^{\infty} (-1)^{m+s} \frac{(n+m+s)!}{(2m+s)! (n-m)!} \left(\frac{r'}{d(\tau)}\right)^{m+s} P_{m+s}^m(\cos\theta') ; d(\tau) > r' \end{array} \right. \quad (3.10.8)$$

$$\Omega_j^* = \left\{ \begin{array}{l} \sum_{n=1}^{\infty} \left(\frac{1}{r'}\right)^{n+1} \sum_{m=0}^n \left\{ \gamma_{nm}^{(j)}(\tau) \cos m\phi' + \delta_{nm}^{(j)}(\tau) \sin m\phi' \right\} \sum_{s=0}^{\infty} (-1)^s \\ \quad \times \frac{(n-m+s)!}{s! (n-m)!} \left(\frac{d(\tau)}{r'}\right)^s P_{n+s}^m(\cos\theta') ; d(\tau) < r' \\ \sum_{n=1}^{\infty} (-1)^{n+1} \left(\frac{1}{d(\tau)}\right)^{n+1} \sum_{m=0}^n \left\{ \gamma_{nm}^{(j)}(\tau) \cos m\phi' + \delta_{nm}^{(j)}(\tau) \sin m\phi' \right\} \\ \quad \times \sum_{s=0}^{\infty} (-1)^{m+s} \frac{(n+m+s)!}{(2m+s)! (n-m)!} \left(\frac{r'}{d(\tau)}\right)^{m+s} P_{m+s}^m(\cos\theta') ; d(\tau) > r' \end{array} \right. \quad (3.10.9)$$

These solutions for the equilibrium "potentials" are now in the form appropriate for the description of the equilibrium field in the vicinity of any kind of growing or propagating rupture. The only unspecified factors are the "multipole coefficients" $\alpha_{nm}(\tau) \dots$ etc. and the rupture translation factor $d(\tau)$. This latter function depends on the model of rupture used, that is, it is determined by the choice of model. The rupture models indicated in Figures 9 and 10 provide values for the various models of interest.

In practice the "multipole coefficients" are obtained by

solving for the equilibrium field at an arbitrary, fixed, source time τ in the translating coordinates by the methods outlined in section 3. In this situation the solutions will be parametric functions of the ellipsoidal axes a, b, c , which are appropriate to a rupture of arbitrary dimensions with a geometrical shape determined by their relative magnitudes. Thus replacement of these dimension parameters by appropriate functions of the source time τ , determined by the model, will give the equilibrium field potentials appropriate to an expanding rupture at any instant, in the form (3.10.7). This procedure is carried out for several models in later sections.

Finally, in order to proceed with the evaluation of the potentials given by (3.10.5) and (3.10.6), it is necessary to devote some attention to the explicit form of the delay factor, $\zeta(\tau)$, for particular models of rupture. After a little consideration of the geometrical relationships indicated in Figures 9 and 10 it is clear that the precise value of ζ is a rather complicated function of the source time τ , through the geometrical dependence on the rupture dimensions and position, and the coordinates of the source point at \underline{r} . An approximation for the expanding rupture models represented in Figure 9 can however be obtained without much difficulty. Thus referring to the diagram in Figure 9, it is seen that

$$(RQ)^2 = (OQ)^2 + (OR)^2 - 2(OQ)(OR) \cos \theta'$$

To a good approximation, for the minor axis $c \ll b < a$,

$$RQ \simeq \zeta(\tau) + (b \sin \theta' \sin \phi') \sin \theta' \sin \phi'$$

$$OR \simeq (d + a \cos \theta')$$

and by definition

$$OQ = r'$$

Thus, for rather small values of θ' , utilizing the fact that most of the energy is released from the region near the rupture, particularly near either end, then

$$(RQ)^2 \simeq (OQ - OR \cos \theta')^2$$

Therefore

$$\zeta(\tau) \simeq |r' - d \cos \theta' - a \cos^2 \theta'| - b \sin^2 \theta' \sin^2 \phi' \quad (3.10.10)$$

For the bilateral and unilateral ruptures of Figure 9, uniform growth or expansion is assumed and consequently

$$d = \left(\frac{d_o}{a_o + d_o} \right) v_R \tau, \quad a = \left(\frac{a_o}{a_o + d_o} \right) v_R \tau, \quad b = \left(\frac{b_o}{a_o} \right) v_R \tau \quad (3.10.11)$$

where a_o , b_o are the final rupture axes, again the minor axis c_o is assumed to be small, and d_o is the final value of the translation parameter. When $d_o = a_o$ these equations represent unilateral rupture, as is illustrated in Figure 3a. If $d_o = 0$, then the rupture is equilateral and the equations (3.10.8) and (3.10.9) reduce to those of (3.10.7), while the delay factor $\zeta(\tau)$ likewise simplifies somewhat.

To a further approximation (3.10.10) will be modified so as to give a representation compatible with those for Θ^* and Ω_j^* in the equations (3.10.8) and (3.10.9), that is

$$\zeta(\tau) \simeq r' - v_R \left\{ \left(\frac{a_o}{a_o + d_o} \right) \cos^2 \theta' + \left(\frac{d_o}{a_o + d_o} \right) \cos \theta' + \left(\frac{b_o}{a_o} \right) \sin^2 \theta' \sin^2 \phi' \right\} \tau$$

and with

$$\Gamma_1(\theta', \phi') = \left(\frac{a_o}{a_o + d_o} \right) \cos^2 \theta' + \left(\frac{d_o}{a_o + d_o} \right) \cos \theta' + \left(\frac{b_o}{a_o} \right) \sin^2 \theta' \sin^2 \phi' \quad (3.10.12a)$$

then

$$\zeta(\tau) \simeq r' - v_R \Gamma_1(\theta', \phi') \tau \quad (3.10.12b)$$

This expression most accurately approximates the minimum distance to the rupture in the regions near either end of the rupture. That is near the points $(0, 0, a+d)$ and $(0, 0, d-a)$ in Figure 9. Since most of the energy is released near these points during the course of rupture, it is desirable that such agreement be achieved. At those points where the approximation is not very accurate, the energy release is, fortunately, relatively small.

The choice of rupture dimension parameters is such that the front of the rupture is extended with a rupture velocity V_R , which is constant. This condition is used for all the rupture models. The expanding ellipsoidal rupture models will be denoted by the model index $M = 1$, while the propagating ruptures of Figure 10 are denoted

by $M = 2$, for the spherical rupture, and $M = 3$ for the ellipsoidal case.

Precisely the same procedures leading to (3.10.10) may be applied to the propagating rupture models. Subsequent approximations are, however, best deduced by first choosing the general form of the (approximate) result desired. In view of the previous result, it is natural to require

$$\zeta(\tau) \cong r' - v_R \Gamma_m(\theta', \phi')\tau \quad (3.10.13)$$

in all cases, with Γ_m ($m = 1, 2, 3$) appropriate to the particular model in question. The value of this approach arises from the fact that it is possible to deduce the effect of Γ_m , the only "free parameter" in (3.10.13), on the radiation field. With this additional knowledge, the approximations for the propagating rupture can be made under criteria which are known to improve the validity and simplicity of the final result for the radiation field.

Thus adopting this approximation for the delay factor the potentials (3.10.5) and (3.10.6) are of the form

$$\Phi(\underline{r}, t) = -\frac{1}{4\pi v_p^2} \iiint \left(\frac{1}{r^*} \right) d\underline{r}' \left\{ \frac{d}{dt} \int_0^t S(\tau - \tau_0) \frac{\partial \Phi^*}{\partial \tau} \delta\left(\tau - \left(1 - \frac{v_R}{v_p} \Gamma_m\right)\tau - \frac{r' + r^*}{v_p}\right) d\tau \right\}$$

Setting

$$\begin{aligned} r^{**} &= r^* + r' & t_p^* &= \frac{1}{\eta_m} \left[t - \frac{r^{**}}{v_p} \right] \\ \eta_m(\theta', \phi') &= 1 - (v_R/v_p)\Gamma_m \end{aligned} \quad (3.10.14)$$

and making use of the delta function, gives

$$\Phi(\underline{r}, t) = -\frac{1}{4\pi v_p^2} \iiint \left(\frac{1}{r^*} \right) \left\{ \frac{d}{dt} \left[S(t_p^* - \tau_0) \left(\frac{\partial \bar{\Phi}}{\partial \tau} \right)_{\tau=t_p^*} \right] \right\} d\underline{r}' \quad (3.10.15)$$

From this expression it is clear that if $t_p^* > \tau_0$, or if $t_p^* < 0$, then the contribution to the field, given by Φ , will at such times, be zero. Thus, from (3.10.14), when $t < r^{**}/v_p$, then the field is zero, in that the effect has not yet reached the point of observation. It is worth noting that the radiation from an arbitrary source point \underline{r}' , does not contribute to the radiation field observed at any point \underline{r} until after a time appropriate to the propagation of a disturbance from the origin, or point of initial rupture, to \underline{r}' . Then, in addition to this delay there is the usual delay in the propagation from \underline{r}' to the point of observation at \underline{r} . The extra delay factor is clearly due to the causality relationship between the relaxation at the source point \underline{r}' and the rupture surface.

In addition to this rather obvious causality effect, it is apparent that the growth and/or propagation of the rupture surface affects the field through the presence of the angular factor $\eta_m(\theta', \phi')$ in the definition for t_p^* . In particular, if η_m is negative for some values of θ' and ϕ' , then such points will contribute to the observed field when $t < r^{**}/v_p$, which is of course physically impossible in view of the preceding interpretation of the time r^{**}/v_p . It is clear then, that in the approximation of ζ by (3.10.13), that $\Gamma_m(\theta', \phi')$ must be such that

$$\eta_m(\theta', \phi') = 1 - \left(\frac{v_R}{v_p} \right) \Gamma_m(\theta', \phi') \geq 0, \text{ for all } \theta', \phi' \quad (3.10.16)$$

If $\eta_m = 0$, for some values of θ', ϕ' , then $t_p^* > \tau_o$ or $t_p^* < 0$ at any time $t \neq r^{**}/v_p$, and all such source points will not contribute to the field, except (possibly) at the time $t = r^{**}/v_p$. Ordinarily then, it would be expected that

$$\eta_m(\theta', \phi') = 1 - \left(\frac{v_R}{v_p} \right) \Gamma_m(\theta', \phi') > 0 \text{ for all } \theta', \phi'$$

Indeed from the previous considerations of the growing or expanding ellipsoidal rupture model, it may be verified that

$$\Gamma_1(\theta', \phi') = \left(\frac{a_o}{a_o + d_o} \right) \cos^2 \theta' + \left(\frac{d_o}{a_o + d_o} \right) \cos \theta' + \left(\frac{b_o}{a_o} \right) \sin^2 \theta' \sin^2 \phi'$$

is such that

$$\eta_1(\theta', \phi') = 1 - \frac{v_R}{v_p} \Gamma_1(\theta', \phi') > 1 - \frac{v_R}{v_p} > 0$$

so long as $b_o < a_o$ and under the assumption that $v_R < v_s < v_p$. Consequently, for this model, it may be shown that every point contributes to the radiation field over the total time interval of rupturing.

Consider then the model described as a propagating spherical rupture, schematically represented in Figure 10a. Proceeding with the evaluation of ζ along the same lines as for the growing rupture models

$$(RQ)^2 = (OQ)^2 + (OR)^2 - 2(OQ)(OR)\cos \theta' \simeq (OQ - OR \cos \theta')^2$$

where

$$RQ = \zeta(\tau) + R(\tau)$$

$$OR = d(\tau)$$

$$OQ = r'$$

so that

$$\zeta(\tau) \simeq |r' - d(\tau) \cos \theta'| - R(\tau) \quad (3.10.17)$$

In the case illustrated, the rupture parameters $R(\tau)$ and $d(\tau)$ are chosen so that the envelope of the propagating rupture is an ellipsoid. Therefore $R(\tau)$ is chosen so that it is zero at $\tau = 0$ and $\tau = \tau_0$ and has a maximum value at $\tau_0/2$ of b_0 . Since

$$\tau_0 = \frac{2a_0}{v_R}$$

then

$$R(\tau) = \frac{b_0}{a_0} \left(2 - \frac{v_R \tau}{a_0} \right) v_R \tau \quad (3.10.18)$$

with a_0 and b_0 being the major and minor axes of the final ellipsoid envelope. If the rupture "front" is constrained to propagate with a constant velocity v_R then $d(\tau)$ turns out to be given by

$$d(\tau) = \left[1 - \frac{b_0}{a_0} \left(2 - \frac{v_R \tau}{a_0} \right) \right] v_R \tau \quad (3.10.19)$$

As with the ellipsoidal model, the absolute value in (3.10.18) will be ignored, so that when $r' < d(\tau) \cos \theta'$, then the value of $\zeta(\tau)$ will

be in error. However within this region the contributions to the radiation field would normally be expected to be small compared to those from $r' > d(\tau) \cos \theta'$. In addition such a modification of (3.10.18) tends to delay these contributions more than normal and therefore to enhance the possibility of excluding the contributions from within that part of this region which corresponds to the rupture zone. Figure 11 shows the region $r' < d(\tau) \cos \theta'$ for the spherical rupture and the equivalent region $r' < a(\tau) \cos^2 \theta' + d(\tau) \cos \theta'$ for the ellipsoidal ruptures, relative to the rupture zones appropriate to the models.

Thus dropping the absolute value in (3.10.17) and substituting (3.10.18) and (3.10.19) into the resulting representation of $\zeta(\tau)$ gives

$$\zeta(\tau) \simeq r' - v_R \left\{ \cos \theta' + \left(2 - \frac{v_R \tau}{a_0} \right) \frac{b_0}{a_0} (1 - \cos \theta') \right\} \tau$$

If the average value of $(2 - v_R \tau / a_0)$ is used, which is adequate for the present approximation since the formula need only be highly accurate when $(b_0/a_0)(1 - \cos \theta')$ is small, then

$$\zeta(\tau) \simeq r' - v_R \left\{ \cos \theta' + \frac{3}{2} \left(\frac{b_0}{a_0} \right) (1 - \cos \theta') \right\} \tau \quad (3.10.20)$$

Thus η_2 is given by

$$\eta_2(\theta', \phi') = 1 - \left(\frac{v_R}{v_p} \right) \Gamma_2(\theta', \phi') \quad (3.10.21a)$$

with

$$\Gamma_2(\theta', \phi') = \left\{ \cos \theta' + \frac{3}{2} \left(\frac{b_0}{a_0} \right) (1 - \cos \theta') \right\} \quad (3.10.21b)$$

Figure 12a shows the numerical value of the factor η_2 as a function of θ' for a representative choice of b_o , a_o , v_p and v_R . In all cases it may be shown that $\eta_2(\theta', \phi') > 0$.

Finally, for the propagating ellipsoidal rupture, one has by the approach leading to (3.10.10), that same result, which is, after dropping the absolute value as before

$$\zeta(\tau) \simeq r' - \left\{ d \cos \theta' + a \cos^2 \theta' + b \sin^2 \theta' \sin^2 \phi \right\}$$

By the same reasoning which led to the expressions for the spherical rupture parameters

$$\begin{aligned} a(\tau) &= a_o \left(2 - \frac{v_R \tau}{a_o} \right) v_R \tau \\ b(\tau) &= \frac{b_o}{a_o} \left(2 - \frac{v_R \tau}{a_o} \right) v_R \tau \\ d(\tau) &= \left[1 - a_o \left(2 - \frac{v_R \tau}{a_o} \right) \right] v_R \tau \end{aligned} \quad (3.10.22)$$

Again a_o and b_o represent the final rupture envelope axes. The constant a_o determines the maximum length of the major axis of the propagating rupture during the period of rupturing, $\tau_o = 2a_o/v_R$. Since this is chosen to occur at $\tau = \tau_o/2$ for the model of Figure 10b, then

$$a(\tau_o/2) = a_o a_o \quad (3.10.23)$$

Following the approximation procedures leading to (3.10.20) for the propagating spherical rupture, one has

$$\eta_3(\theta', \phi') = 1 - \left(\frac{v_R}{v_p} \right) \Gamma_3(\theta', \phi') \quad (3.10.24)$$

$$\Gamma_3(\theta', \phi') = \left\{ \left(1 - \frac{3}{2} a_o \right) \cos \theta' + \frac{3}{2} \left[a_o \cos^2 \theta' + \frac{b_o}{a_o} \sin^2 \theta' \sin^2 \phi' \right] \right\}$$

Numerical values of the angular delay factors η_1 and η_3 for special representative ranges of the angular variables and rupture parameters are shown in Figures 12b to 12d.

Solutions of the form given by equation (3.10.15) are therefore appropriate to all the source models introduced. A treatment of the potentials in the frequency domain however, considerably simplifies the evaluation of the spatial integrals, as well as the interpretation and application of the results. Thus taking the Fourier transform of (3.10.15) gives

$$\tilde{\Phi}(\underline{r}, \omega) = \frac{i\omega}{4\pi v_p^2} \iiint \left(\frac{1}{r^*} \right) d\underline{r}' \left[\int_{-\infty}^{+\infty} \left(\frac{\partial \Phi^*}{\partial \tau} \right)_{r=t_p^*} S(t_p^* - \tau_0) e^{-i\omega t} dt \right]$$

The Fourier integral may be transformed to an integral over t_p^* , since from (3.10.14)

$$t = \eta_m t_p^* + \frac{r}{v_p}$$

Thus, introducing this relationship gives

$$\tilde{\Phi}(\underline{r}, \omega) = \frac{i\omega}{4\pi v_p^2} \iiint \left(\frac{e^{-i k_p r}}{r^*} \right) d\underline{r}' \left[\int_0^{\tau_0} \left(\frac{\partial \Phi^*}{\partial t_p^*} \right) e^{-i\omega \eta_m t_p^*} \eta_m dt_p^* \right]$$

Since t_p^* now appears only as a dummy variable, there is no longer any need to retain any special notation for this symbol and it may be replaced by a time factor τ . Finally, then

$$\tilde{\Phi}(\underline{r}, \omega) = \frac{i\omega}{4\pi v_p^2} \iiint \left(\frac{e^{-i k_p r^{**}}}{r^{**}} \right) d\underline{r}' \left\{ \eta_m \int_0^{\tau_0} \frac{\partial \Phi^*}{\partial \tau} e^{-i\omega \eta_m \tau} d\tau \right\} \quad (3.10.25)$$

If $\chi_j(\underline{r}, t)$ is considered, the same procedures as were used in deriving (3.10.25) from (3.10.5) are valid throughout and one need only replace v_p wherever it appears by v_s . Introducing an angular delay factor $\xi_m(\theta', \phi')$ corresponding to $\eta_m(\theta', \phi')$ and obtained by replacing v_p by v_s in η_m , one has then, the results

$$\chi_j(\underline{r}, \omega) = \frac{i\omega}{4\pi v_s^2} \iiint \left(\frac{e^{-i k_s r^{**}}}{r^{**}} \right) d\underline{r}' \left\{ \xi_m \int_0^{\tau_0} \frac{\partial \chi_j^*}{\partial \tau} e^{-i\omega \xi_m \tau} d\tau \right\} \quad (3.10.26)$$

$$\xi_m = \lim_{v_p \rightarrow v_s} \eta_m; \quad m = 1, 2, 3$$

3.11. Primary Field Potentials for Natural Tectonic Sources: Expanding Ellipsoidal Rupture

As was previously asserted, two physically distinct types of tectonic source are of interest in the present study. They are those due to naturally induced rupture, or faulting, and those associated with explosive sources in a pre-strained medium. Of these two processes resulting in the release of tectonic energy, that associated

with natural rupture is the more difficult to describe analytically since the process involves growth or propagation of the rupture surface in a nonsymmetrical manner with a velocity which is less than either of the two velocities of wave propagation in the medium. Nevertheless an analytical formulation appropriate to the description of the radiation field from such a source was obtained in the previous section and can be used to give explicit expression to the radiation properties of a natural tectonic source. As an extension of the results of the previous section, the expression of the radiation field from fault sources will be considered. In a following section the expressions for the tectonic radiation associated with an explosion in prestrained media will be obtained.

In order to describe the direct or "primary" field from a fault source by means of any one of the specific models introduced, it is simplest to take for the potentials in (3.10.26) and (3.10.27), the dilatation $\tilde{\Theta}^{(1)}(\underline{r}, \omega)$ and rotation $\tilde{\Omega}_j^{(1)}(\underline{r}, \omega)$.⁽¹⁾ Thus

$$\tilde{\Theta}^{(1)}(\underline{r}, \omega) = \frac{i\omega}{4\pi V_p^2} \iiint \left(\frac{e^{-i k_p r}}{r^*} \right) d\underline{r}' \left\{ \eta_m \int_0^{r_0} \frac{\partial \Theta^*}{\partial \tau} e^{-i\omega \eta_m \tau} d\tau \right\} \quad (3.11.1)$$

$$\tilde{\Omega}_j^{(1)}(\underline{r}, \omega) = \frac{i\omega}{4\pi V_s^2} \iiint \left(\frac{e^{-i k_s r}}{r^*} \right) d\underline{r}' \left\{ \xi_m \int_0^{r_0} \frac{\partial \Omega_j^*}{\partial \tau} e^{-i\omega \xi_m \tau} d\tau \right\}$$

In this case the "initial value" functions Θ^* and Ω_j^* are given by (3.10.8) and (3.10.9).

⁽¹⁾ Alternately, the scalar and vector potentials, φ and $\underline{\psi}$ could be used, as was pointed out in section 3.7.

Consider first the expanding ellipsoidal rupture models. Propagating ruptures will be considered in the next section. In the case of an expanding rupture, $M = 1$, so

$$d(\tau) = \left(\frac{d_0}{a_0 + d_0} \right) v_R \tau, \quad \tau_0 = \frac{a_0 + d_0}{v_R}$$

and the equilibrium field is given by

$$\Theta^*(\underline{r}', \tau) = \begin{cases} \Theta_1^*(\underline{r}', \tau) ; & r' > \left(\frac{d_0}{a_0 + d_0} \right) v_R \tau \text{ or } \tau < \frac{a_0 + d_0}{v_R} \left(\frac{r'}{d_0} \right) \\ \Theta_2^*(\underline{r}', \tau) ; & r' < \left(\frac{d_0}{a_0 + d_0} \right) v_R \tau \text{ or } \tau > \frac{a_0 + d_0}{v_R} \left(\frac{r'}{d_0} \right) \end{cases} \quad (3.11.2a)$$

where

$$\begin{aligned} \Theta_1^*(\underline{r}', \tau) = & \sum_{n=1}^{\infty} \left(\frac{1}{r'} \right)^{n+1} \sum_{m=0}^n \left\{ \alpha_{nm}(\tau) \cos m\phi' + \beta_{nm}(\tau) \sin m\phi' \right\} \\ & \times \sum_{s=0}^{\infty} (-1)^s \frac{(n-m+s)!}{s! (n-m)!} \left(\frac{d_0}{a_0 + d_0} \right)^s (v_R \tau)^s \left(\frac{1}{r'} \right)^s P_{n+s}^m(\cos \theta') \end{aligned} \quad (3.11.2b)$$

$$\begin{aligned} \Theta_2^*(\underline{r}', \tau) = & \sum_{n=1}^{\infty} (-1)^{n+1} \sum_{m=0}^n \left\{ \alpha_{nm}(\tau) \cos m\phi' + \beta_{nm}(\tau) \sin m\phi' \right\} \\ & \times \sum_{s=0}^{\infty} (-1)^{m+s} \frac{(n+m+s)!}{(2m+s)! (n-m)!} \left(\frac{a_0 + d_0}{d_0} \right)^{n+m+s+1} \left(\frac{1}{v_R \tau} \right)^{n+m+s+1} (r')^{m+s} P_{m+s}^m(\cos \theta) \end{aligned}$$

and similarly for the rotation components Ω_j^* . Again treating only $\tilde{\Theta}^{(1)}(\underline{r}, \omega)$ explicitly, the solution becomes, after taking careful note

of the discontinuous nature of Θ^* ,

$$\begin{aligned} \tilde{\Theta}^{(1)}(\underline{r}, \omega) = & \frac{i\omega}{4\pi v_p^2} \left\{ \iint d\Omega \int_0^{d_0} \left(\frac{e^{-ik_p r'^*}}{r'^*} \right) r'^2 dr' \left[\eta_1 \int_0^{\frac{a_0+d_0}{v_R} \left(\frac{r'}{d_0} \right)} \left(\frac{\partial \Theta_1^*}{\partial \tau} \right) e^{-i\omega \eta_1 \tau} d\tau \right. \right. \\ & + \eta_1 \int_{\frac{a_0+d_0}{v_R} \left(\frac{r'}{d_0} \right)}^{\frac{a_0+d_0}{v_R}} \left(\frac{\partial \Theta_2^*}{\partial \tau} \right) e^{-i\omega \eta_1 \tau} d\tau \left. \right] + \iint d\Omega \int_{d_0}^{\infty} \left(\frac{e^{-ik_p r'^*}}{r'^*} \right) r'^2 dr' \\ & \times \left[\eta_1 \int_0^{\frac{a_0+d_0}{v_R}} \left(\frac{\partial \Theta_1^*}{\partial \tau} \right) e^{-i\omega \eta_1 \tau} d\tau \right] \left. \right\} \end{aligned} \quad (3.11.13)$$

Here the integration over the radial coordinate r' has been broken into two parts, $(0, d_0)$ and (d_0, ∞) , so that the transforms with respect to τ can be written explicitly in terms of Θ_1^* and Θ_2^* . The time interval for the first of the transforms in (3.11.3) is such that $r' > d(\tau)$, yet with $r' < d_0$. This contribution is important, especially when $|a(\tau) \pm d(\tau)| < d_0$. The second τ integral represents a time interval such that $r' < d(\tau) < d_0$. It represents the contribution to the field from the region near the rupture origin and usually⁽¹⁾ from the region well behind the rupture "fronts" at $a(\tau) + d(\tau)$ and $d(\tau) - a(\tau)$. The region is indicated in Figures 11 and 13, for all the rupture models, by the spherical region of radius $d(\tau)$. During the time interval represented by the limits of integration

$$\frac{a_0+d_0}{v_R} \left(\frac{r'}{d_0} \right) \text{ to } \frac{a_0+d_0}{v_R}$$

the relaxation and consequently the radiation from this region will be

⁽¹⁾ Exceptions occur for certain bilateral rupture geometrics, these exceptions are considered later.

small in view of the nearly constant dimensions of the rupture surface in this zone. Thus, once again making use of the fact that most of the radiation will be derived from the region near the rupture front where the boundary changes are most rapid and large, this integral will be neglected in the evaluation of the field since it will be relatively small. In addition it can be argued that neglecting this particular term should actually improve the validity of the model, since it is equivalent to relaxing the condition of a well defined rupture surface in this region.

The final time transform corresponds to a time interval such that $r' > d_0 > d(\tau)$ and this term will be small compared to the first, until $|a(\tau) \pm d(\tau)| > d_0$, thereafter it will be larger. The term must certainly be retained, but clearly for first motion studies the first time transform is all that need be considered. In the present study however, the total field is desired while the first motions are of but secondary interest.

The appropriate modified form of the solution is therefore

$$\begin{aligned} \tilde{\Theta}^{(1)}(\underline{r}, \omega) = & \frac{i\omega}{4\pi v_p^2} \left\{ \iint d\Omega \int_0^{d_0} \left(\frac{e^{-ik_p r^{**}}}{r^*} \right) r'^2 dr' \left(\eta_1 \int_0^{\frac{a_0+d_0}{v_R} \left(\frac{r'}{d_0} \right)} \left(\frac{\partial \Theta_1^*}{\partial \tau} \right) e^{-i\omega \eta_1 \tau} d\tau \right) \right. \\ & \left. + \iint d\Omega \int_{d_0}^{\infty} \left(\frac{e^{-ik_s r^{**}}}{r^*} \right) r'^2 dr' \left(\eta_1 \int_0^{\frac{a_0+d_0}{v_R}} \left(\frac{\partial \Theta_1^*}{\partial \tau} \right) e^{-i\omega \eta_1 \tau} d\tau \right) \right\} \end{aligned}$$

(3.11.4)

with an equivalent form for $\tilde{\Omega}_j^{(1)}(\underline{r}, \omega)$.

It should be mentioned, if not emphasized at this point, that the integral neglected in (3.11.4) is not especially difficult to treat and may be evaluated without difficulty. Furthermore all the spatial integrations arising from this term can likewise be evaluated, although in a somewhat approximate fashion. The fact that the neglected term may be evaluated is not especially significant except in cases of bilateral rupture for which $d_0 < a_0/2$. In such cases the rupture "front" at $d(\tau) - a(\tau)$ (Figure 11) is always within the region $r' \leq d(\tau)$ and hence would be neglected by (3.11.4). It would seem then that, in such instances, (3.11.3) should be used in its entirety. However the application of (3.11.4) is actually not so restricted as is implied by these remarks and the converse condition $d_0 \leq a_0/2$. In particular, when $d_0 = a_0$, the condition for unilateral rupture, only one end of the ellipsoidal rupture changes its position with time so that the region near the fixed end of the rupture at the origin is excluded by (3.11.4). This is clearly justified in terms of the argument that the energy release from this zone will be small at times such that the rupture "front" is well away from this region. More precisely then, the applicability of (3.11.4) is limited to ruptures for which

$$d_0 \approx a_0 \quad \text{or} \quad d_0 \leq a_0/2$$

Essentially, the representation afforded by (3.11.4) is restricted to ruptures which are nearly unilateral or equilateral. In the present study, detailed consideration of general bilateral rupturing will be

omitted, so that the subsequent development of the theory will utilize (3.11.4) exclusively. The more complicated analysis of the bilateral rupture will be deferred until some verification of the simpler related models and theory has been obtained.

Some further approximations of the field representations are warranted in the cases of near unilateral or equilateral rupture. Reference to Figures 12b and 12d shows that, for representative cases of equilateral and unilateral rupture, the angular delay factor $\eta_1(\theta', \phi')$ is a very slowly varying function of the angular variables, especially in the regions of greatest energy release. For equilateral rupture the regions of maximum energy release will certainly be within the ranges $0 \leq \theta' \leq \tan^{-1}(2b_o/a_o)$ and $\pi \leq \theta' \leq \pi - \tan^{-1}(2b_o/a_o)$ while for unilateral rupture only the region in which $0 \leq \theta' \leq \tan^{-1}(2b_o/a_o)$ is of importance. In any case η_1 (and ξ_1) is nearly constant within such ranges for the two types of rupture and consequently can be approximated by a constant in (3.11.4), provided the range of d_o is suitably restricted to the unilateral and equilateral cases. The restrictions on d_o must be somewhat more severe than have been indicated previously. In the bilateral rupture case shown in Figure 12c it is clear that, while $d_o < a_o/2$ and η_1 is nearly constant in the regions of maximum energy release, nevertheless η_1 assumes different constant values near $\theta' = 0$ and $\theta' = \pi$. Thus, this delay factor has a spatial asymmetry which cannot be approximated by the same constant value in the two regions of importance. As the rupture becomes nearly equilateral the limiting values of the

two "constants" approach the same value. Thus in (3.11.4),
restricting d_o to be such that

$$d_o \simeq a_o \text{ or } d_o \simeq 0 \quad (3.11.5)$$

then η_1 is, to a good approximation, given by

$$\eta_1 = 1 - \frac{v_R}{v_p} \left\{ 1 - \left(\frac{\frac{3}{2} a_o + d_o}{a_o + d_o} \right) \left(\frac{b_o}{2a_o} \right)^2 \right\} \quad (3.11.6)$$

where the appropriate mean value of θ' has been chosen to be

$$\theta'_{\text{mean}} = \tan^{-1} \left(\frac{b_o}{2a_o} \right)$$

likewise

$$\xi_1 = 1 - \frac{v_R}{v_s} \left\{ 1 - \left(\frac{\frac{3}{2} a_o + d_o}{a_o + d_o} \right) \left(\frac{b_o}{2a_o} \right)^2 \right\} \quad (3.11.7)$$

This approximation will result in a considerable simplification
in the evaluation of (3.11.4). In particular consider the simplest case,
namely equilateral rupture. In this case $d_o \simeq 0$ and (3.11.4)
reduces to

$$\Theta^{(1)}(\underline{r}, \omega) = \frac{i\omega}{4\pi v_p^2} \iint d\Omega \int_0^\infty \left(\frac{e^{-i k_r r^{**}}}{r^{**}} \right) r'^2 dr' \left(\eta_1 \int_0^{a_o/v_R} \frac{\partial \Theta_i^*}{\partial \tau} e^{-i\omega \eta_1 \tau} d\tau \right) \quad (3.11.8)$$

with

$$\Theta_1^*(r', \tau) = \sum_{n=1}^{\infty} \left(\frac{1}{r'}\right)^{n+1} \sum \left\{ \alpha_{nm}(\tau) \cos m\phi' + \beta_{nm}(\tau) \sin m\phi' \right\} P_n^m(\cos \theta')$$

(3.11.9)

$$\eta_1 = 1 - \frac{v_R}{v_p} \left\{ 1 - \frac{3}{2} (b_o/2a_o)^2 \right\}$$

Integrals of the type (3.11.8) have been treated in section 2.8. Thus by arguing that, at large distances from the rupture, the "initial values" Θ^* and Ω_j^* are negligible, so that within this region bounded by a sphere of radius R_s ,

$$\frac{e^{-ik_p r}}{r} = -i k_p \sum_{l=0}^{\infty} (2l+1) P_l(\cos \psi) j_l(k_p r') h_l^{(2)}(k_p r) ; r > R_s \geq r'$$

then proceeding as in Section 2.7

$$\tilde{\Theta}^{(1)}(\underline{r}, \omega) = \sum_{n=1}^{\infty} h_n^{(2)}(k_p r) \sum_{m=0}^n \left[A_{nm}(\omega) \cos m\phi + B_{nm}(\omega) \sin m\phi \right] P_n^m(\cos \theta)$$

(3.11.10)

$$\tilde{\Omega}_j^{(1)}(\underline{r}, \omega) = \sum_{n=1}^{\infty} h_n^{(2)}(k_s r) \sum_{m=0}^n \left[C_{nm}^{(j)}(\omega) \cos m\phi + D_{nm}^{(j)}(\omega) \sin m\phi \right] P_n^m(\cos \theta)$$

where, ⁽¹⁾

⁽¹⁾ Alternate expressions for the coefficients $A_{nm}(\omega)$, etc. may also be obtained as suggested in Section 2.7, the long and short period limits may be obtained from (2.7.6) and (2.7.11) respectively.

$$\begin{pmatrix} A_{nm}(\omega) \\ B_{nm}(\omega) \end{pmatrix} = \frac{1}{4V_p} (z k_p)^n \begin{pmatrix} \tilde{\alpha}_{nm}(\omega) \\ \tilde{\beta}_{nm}(\omega) \end{pmatrix} \sum_{s=0}^{\infty} \frac{\Gamma(n+s+1)}{\Gamma(2n+s+2)} \left(\frac{1}{s+2}\right) \frac{(-z i k_p R_s)^{s+2}}{\Gamma(s+1)}$$

(3.11.11)

$$\begin{pmatrix} C_{nm}^{(j)}(\omega) \\ D_{nm}^{(j)}(\omega) \end{pmatrix} = \frac{1}{4V_s} (z k_s)^n \begin{pmatrix} \tilde{\gamma}_{nm}^{(j)}(\omega) \\ \tilde{\delta}_{nm}^{(j)}(\omega) \end{pmatrix} \sum_{s=0}^{\infty} \frac{\Gamma(n+s+1)}{\Gamma(2n+s+2)} \left(\frac{1}{s+2}\right) \frac{(-z i k_s R_s)^{s+2}}{\Gamma(s+1)}$$

with

$$\begin{pmatrix} \tilde{\alpha}_{nm}(\omega) \\ \tilde{\beta}_{nm}(\omega) \end{pmatrix} = \eta_1 \int_0^{a_0/V_R} \begin{pmatrix} \frac{d\alpha_{nm}(\tau)}{d\tau} \\ \frac{d\beta_{nm}(\tau)}{d\tau} \end{pmatrix} e^{-i\omega\eta_1\tau} d\tau$$

(3.11.12)

$$\begin{pmatrix} \tilde{\gamma}_{nm}^{(j)}(\omega) \\ \tilde{\delta}_{nm}^{(j)}(\omega) \end{pmatrix} = \xi_1 \int_0^{a_0/V_R} \begin{pmatrix} \frac{d\gamma_{nm}^{(j)}(\tau)}{d\tau} \\ \frac{d\delta_{nm}^{(j)}(\tau)}{d\tau} \end{pmatrix} e^{-i\omega\xi_1\tau} d\tau$$

The contention that Θ^* and Ω_j^* are negligible at large distances from the rupture is basic to the development of the fundamental representations (3.11.1), as well as to the particular results given by (3.11.10) - (3.11.12). That is, implicit in every approximation leading to the final formulas for the radiation from naturally induced rupture, has been a condition implying that a change in the equilibrium field can be associated, almost completely, with a change in the local rupture boundary shape or position while changes in the boundary at greater distances have a rapidly diminishing influence (with dis-

tance). This is merely an assertion that stress relaxation is a very local effect and clearly implies that Θ^* and Ω_j^* rapidly diminish with distance from the rupture boundary. Indeed Θ^* and Ω_j^* will be shown to be of the order $1/r^3$, which is a rapid fall off compared to the usual $1/r$ dependence of a radiation field.

This entire line of reasoning is further enforced by physical arguments based on the observation that the strain released after earthquakes near active faults has been found to be relatively localized (e. g. Byerly and De Noyer, 1958). These measurements can be taken as direct evidence of the localized nature of stress relaxation associated with the tectonic source.

Finally it should be mentioned that while the equilibrium stresses giving the relaxation field Θ^* and Ω_j^* , are obtained from solutions in an infinite space, this only means in practice that boundaries and various other strong inhomogeneities within the medium are assumed to be sufficiently far removed as to be negligible in their effect on stress relaxation. Thus the basis upon which the equilibrium field computation is made, is seen to involve the condition that the changes in the equilibrium field itself be strongly local to the rupture region. In view of the observations of strain release, this approach seems entirely reasonable.

Turning again to the evaluation of the integral solutions for the radiation field from a rupture source, consider the more complicated case of unilateral rupture expansion. From (3.11.4) - (3.11.7), setting $d_0 = a_0$,

$$\begin{aligned} \tilde{\Theta}^{(1)}(\underline{r}, \omega) = & \frac{i\omega}{4\pi v_p z} \left\{ \iint d\Omega \int_0^{a_0} \frac{e^{-ik_p(\pi^* + \pi')}}{\pi^*} r'^2 dr' \left(\eta_1 \int_0^{z(\frac{r'}{v_R})} \frac{\partial \Theta_1^*}{\partial \tau} e^{-i\omega \eta_1 \tau} d\tau \right) \right. \\ & \left. + \iint d\Omega \int_{a_0}^{\infty} \frac{e^{-ik_p(\pi^* + \pi')}}{\pi^*} r'^2 dr' \left(\eta_1 \int_0^{2a_0/v_R} \frac{\partial \Theta_1^*}{\partial \tau} e^{-i\omega \eta_1 \tau} d\tau \right) \right\} \end{aligned}$$

(3.11.13)

with

$$\begin{aligned} \Theta_1^*(\tau) = & \sum_{n=1}^{\infty} \left(\frac{1}{r'}\right)^{n+1} \sum_{m=0}^n \left\{ \alpha_{nm}(\tau) \cos m\phi' + \beta_{nm}(\tau) \sin m\phi' \right\} \\ & \times \sum_{s=0}^{\infty} (-1)^s \frac{(n-m+s)!}{s!(n-m)!} \left(\frac{v_R}{z}\right)^s \left(\frac{z}{r'}\right)^s P_{n+s}^m(\cos\theta') \end{aligned} \quad (3.11.14)$$

$$\eta_1 = 1 - \frac{v_R}{v_p} \left\{ 1 - \frac{5}{4} \left(\frac{b_0}{2a_0} \right)^2 \right\}$$

Similar expressions may be written for $\tilde{\Omega}_j^{(1)}$ by using v_s in place of v_p in (3.11.13), while ${}^{(1)}\Omega_j^*$ replaces $\Theta_1^*(\tau)$. The coefficients α_{nm}, β_{nm} replaced by $\gamma_{nm}^{(j)}$ and $\delta_{nm}^{(j)}$ will transform $\Theta_1^*(\tau)$ in (3.11.14) to ${}^{(1)}\Omega_j^*(\tau)$.

In order to evaluate the first of the volume integrals in (3.11.13) it is necessary to be more explicit. In particular the dependence of $\Theta_1^*(\tau)$ on the source time variable τ must be specified if the evaluation is to proceed further. For this purpose it is sufficient to assume that the τ dependent coefficients, α_{nm} and β_{nm} , are analytic and may be expanded as series in τ . The assumption is only a temporary expedient since it will be shown that the coefficients are,

for all models, simple low order polynomials in τ . Thus the coefficients will be taken as

$$a_{nm}(\tau) = \sum_{P \geq 0} A_{nm}^{(P)} \tau^P, \quad \beta_{nm}(\tau) = \sum_{P \geq 0} B_{nm}^{(P)} \tau^P \quad (3.11.15)$$

so as to provide the explicit τ dependence required. The coefficients $A_{nm}^{(P)}$ and $B_{nm}^{(P)}$ will be obtained later as functions of the source model parameters.

Using these expansions in (3.11.14) along with the expansions

$$\frac{e^{-ik_p r}}{r^*} = -ik_p \sum_{\ell=0}^{\infty} (2\ell+1) P_{\ell}(\cos \gamma) j_{\ell}(k_p r') h_{\ell}^{(2)}(k_p r); \quad r > R_s \geq r'$$

$$P_{\ell}(\cos \gamma) = P_{\ell}(\cos \theta \cos \theta' + \sin \theta \sin \theta' \cos(\phi - \phi'))$$

$$= P_{\ell}(\cos \theta) P_{\ell}(\cos \theta') + 2 \sum_{k=1}^{\ell} \frac{(\ell-k)!}{(\ell+k)!} P_{\ell}^k(\cos \theta) P_{\ell}^k(\cos \theta') \cos m(\phi - \phi')$$

In (3.11.13), then after substitution and rearrangement⁽¹⁾

⁽¹⁾ Some special matrix notations will be introduced in order to shorten some of the expressions to follow. In particular

$\begin{pmatrix} x_1 \\ x_2 \end{pmatrix}$ denotes the usual column matrix, but $\begin{Bmatrix} x_1 \\ x_2 \end{Bmatrix}$ will be used to

denote the new matrix $(x_1 x_2)$. Thus, for example, as in (3.11.16)

$$\begin{Bmatrix} x_1 \\ x_2 \end{Bmatrix} \begin{pmatrix} y_1 \\ y_2 \end{pmatrix} = (x_1 x_2) \begin{pmatrix} y_1 \\ y_2 \end{pmatrix} = x_1 y_1 + x_2 y_2$$

$$\begin{aligned}
 \tilde{\Theta}_1(\underline{r}, \omega) &= \frac{k_p^z}{4\pi V_p} \sum_{\ell=0}^{\infty} (2\ell+1) \sum_{n=1}^{\infty} \sum_{m=0}^n \sum_{s=0}^{\infty} (-1)^s \frac{(n-m+s)!}{s! (n-m)!} h_{\ell}^{(z)}(k_p r) \\
 &\times \left\{ \int_0^{2\pi} \int_0^{\pi} P_{\ell}(\cos \gamma) P_{n+s}^m(\cos \theta') \begin{Bmatrix} \cos m\phi' \\ \sin m\phi' \end{Bmatrix} \sin \theta' d\theta' d\phi' \left(\eta_1 \int_0^{a_0} \begin{pmatrix} n I_{\alpha}^{(s)}(r') \\ n I_{\beta}^{(s)}(r') \end{pmatrix} \right. \right. \\
 &\times \left. \left. \frac{e^{-i k_p r'}}{(r')^{n-1}} j_{\ell}(k_p r') dr' + \eta_1 \begin{pmatrix} n J_{\alpha}^{(s)}(a_0) \\ n J_{\beta}^{(s)}(a_0) \end{pmatrix} \int_{a_0}^{R_s} \left(\frac{1}{r'}\right)^{n+s-1} e^{-i k_p r'} j_{\ell}(k_p r') dr' \right\}
 \end{aligned}
 \tag{3.11.16}$$

where

$$\begin{pmatrix} n I_{\alpha}^{(s)}(r') \\ n I_{\beta}^{(s)}(r') \end{pmatrix} = \left(\frac{V_R}{z}\right)^s \left(\frac{1}{r'}\right)^s \int_0^{zr'/V_R} \frac{\partial}{\partial \tau} \left[\tau^s \begin{pmatrix} \alpha_{nm}(\tau) \\ \beta_{nm}(\tau) \end{pmatrix} \right] e^{-i\omega\eta_1\tau} d\tau
 \tag{3.11.17}$$

$$\begin{pmatrix} n J_{\alpha}^{(s)}(a_0) \\ n J_{\beta}^{(s)}(a_0) \end{pmatrix} = \left(\frac{V_R}{z}\right)^s \int_0^{za_0/V_R} \frac{\partial}{\partial \tau} \left[\tau^s \begin{pmatrix} \alpha_{nm}(\tau) \\ \beta_{nm}(\tau) \end{pmatrix} \right] e^{-i\omega\eta_1\tau} d\tau$$

or, using the relations (3.11.15), and from Erdelyi et al. (1954, Vol. 1)

$$\begin{pmatrix} n I_{\alpha}^{(s)}(r') \\ n I_{\beta}^{(s)}(r') \end{pmatrix} = \sum_{p \geq 0} \begin{pmatrix} A_{nm}^{(p)} \\ B_{nm}^{(p)} \end{pmatrix} \left\{ \left(\frac{zr'}{V_R}\right)^p {}_1F_1(s+p; s+p+1; \frac{-zi\omega\eta_1 r'}{V_R}) \right\}
 \tag{3.11.18}$$

with ${}_1F_1$ denoting a confluent hypergeometric function, so that

$${}_1F_1(s+p; s+p+1; -2i\eta_1 k_R r') = \sum_{q=0}^{\infty} \frac{s+p}{s+p+q} \frac{(-2i\eta_1 k_R r')^q}{\Gamma(q+1)}$$

Likewise

$$\begin{pmatrix} n \\ \alpha \end{pmatrix} J_a^{(s)}(a_0) = \sum_{p \geq 0} \begin{pmatrix} H_{nm}^{(p)} \\ B_{nm}^{(p)} \end{pmatrix} \left\{ \left(\frac{za_0}{v_R} \right)^p \alpha_0^s {}_1F_1(s+p; s+p+1; -2i\eta, k_R a_0) \right\} \quad (3.11.19)$$

In both expressions $k_R \equiv \omega/v_R$. Thus, using the orthogonal properties of the trigonometric and Legendre functions to evaluate the angular integrals in (3.11.16), in particular the results

$$\begin{aligned} & \int_0^{2\pi} \int_0^\pi P_\ell(\cos \gamma) P_{n+s}^m(\cos \theta') \begin{pmatrix} \cos m\phi' \\ \sin m\phi' \end{pmatrix} \sin \theta' d\theta' d\phi' \\ &= \frac{4\pi}{2\ell+1} P_\ell^m(\cos \theta) \begin{pmatrix} \cos m\phi \\ \sin m\phi \end{pmatrix} \delta_{n+s, \ell} \end{aligned}$$

with

$$\delta_{n+s, \ell} = \begin{cases} 0, & n+s \neq \ell \\ 1, & n+s = \ell \end{cases}$$

then (3.11.16) can be written in the convenient form

$$\tilde{\Theta}^{(1)}(\underline{r}, \omega) = \sum_{\ell=1}^n \sum_{k=0}^{\ell} h_\ell^{(2)}(k, p, r) \left\{ G_{\ell k}(\omega) \cos m\phi + \beta_{\ell k}(\omega) \sin m\phi \right\} P_\ell^k(\cos \theta) \quad (3.11.20)$$

where, with $s \equiv \ell - n$

$$\begin{aligned} \begin{pmatrix} G_{\ell k}(\omega) \\ \beta_{\ell k}(\omega) \end{pmatrix} &= \frac{k_p^2 \eta_i}{v_p} \sum_{p \geq 0} \left(\frac{z}{v_R} \right)^p \sum_{n=1}^{\ell} (-1)^{\ell-n} \begin{pmatrix} H_{nk}^{(p)} \\ B_{nk}^{(p)} \end{pmatrix} \frac{\Gamma(\ell-k+1)}{\Gamma(\ell-n+1)\Gamma(n-k+1)} \\ & \times \left[\int_0^{a_0} \left(\frac{1}{r'} \right)^{n-p-1} {}_1F_1(s+p; s+p+1; -2i\eta, k_R r') e^{-ik_p r'} j_\ell(k_p r') dr' \right. \\ & \left. + \alpha_0^{s+p} {}_1F_1(s+p; s+p+1; -2i\eta, k_R a_0) \int_{a_0}^{R_s} \left(\frac{1}{r'} \right)^{\ell-1} e^{-ik_p r'} j_\ell(k_p r') dr' \right] \end{aligned} \quad (3.11.21)$$

The integrals appearing in (3.11.21) are of the same general type treated before. Their evaluation and the subsequent algebraic simplification of (3.11.21) is given in Appendix 5.

The expressions for the rotation vector components are obtained in precisely the same manner as is the dilatation. The complete description of the direct field from the unilaterally expanding rupture is therefore given by

$$\tilde{\Theta}^{(1)}(\underline{r}, \omega) = \sum_{\ell=1}^{\infty} h_{\ell}^{(2)}(k_p r) \sum_{k=0}^{\ell} \left\{ A_{\ell k}(\omega) \cos k\phi + B_{\ell k}(\omega) \sin k\phi \right\} P_{\ell}^k(\cos\theta) \quad (3.11.22)$$

$$\tilde{\Omega}_j^{(1)}(\underline{r}, \omega) = \sum_{\ell=1}^{\infty} h_{\ell}^{(2)}(k_s r) \sum_{k=0}^{\ell} \left\{ C_{\ell k}^{(j)}(\omega) \cos k\phi + D_{\ell k}^{(j)}(\omega) \sin k\phi \right\} P_{\ell}^k(\cos\theta)$$

where all the coefficients in (3.11.22) are given by the results of Appendix 5, as

$$\begin{aligned} \begin{pmatrix} A_{\ell k}(\omega) \\ B_{\ell k}(\omega) \end{pmatrix} &= -\frac{\eta_i}{4V_p} (2k_p a_0)^{\ell} \sum_{p=0}^{\ell} \left(\frac{2a_0}{V_R} \right)^p \sum_{n=1}^{\ell} (-1)^{\ell-n} \begin{pmatrix} A_{nk}^{(p)} \\ B_{nk}^{(p)} \end{pmatrix} \frac{\Gamma(\ell-k+1)}{\Gamma(\ell-n+1)\Gamma(n-k+1)} \\ &\times \left(\frac{1}{a_0} \right)^n \sum_{q=0}^{\ell-n+p} \frac{(\ell-n+p)}{(\ell-n+p+q)} \left[E_{\ell}^{(i)}(\eta_i, \delta; 0; k_p a_0) + E_{\ell}^{(i)}(\eta_i, 0; a_0; k_p R_s) \right] \\ &\times \frac{(-2i\eta_i k_R a_0)^q}{\Gamma(q+1)} \end{aligned} \quad (3.11.23)$$

$$\begin{aligned} \begin{pmatrix} C_{\ell k}^{(j)}(\omega) \\ D_{\ell k}^{(j)}(\omega) \end{pmatrix} &= -\frac{\xi_i}{4V_s} (2k_s a_0)^{\ell} \sum_{p=0}^{\ell} \left(\frac{2a_0}{V_R} \right)^p \sum_{n=1}^{\ell} (-1)^{\ell-n} \begin{pmatrix} C_{nk}^{(p)} \\ D_{nk}^{(p)} \end{pmatrix} \frac{\Gamma(\ell-k+1)}{\Gamma(\ell-n+1)\Gamma(n-k+1)} \\ &\times \left(\frac{1}{a_0} \right)^n \sum_{q=0}^{\ell-n+p} \frac{(\ell-n+p)}{(\ell-n+p+q)} \left[E_{\ell}^{(i)}(\xi_i, \delta; 0; k_s a_0) + E_{\ell}^{(i)}(\xi_i, 0; a_0; k_s R_s) \right] \\ &\times \frac{(-2i\xi_i k_R a_0)^q}{\Gamma(q+1)} \end{aligned} \quad (3.11.24)$$

with

$$\gamma \equiv \ell - n + p + q$$

The functions of the form $E_{\ell}^{(1)}(\mu, \gamma; x; by)$ are defined by the series representation

$$E_{\ell}^{(1)}(\mu, \gamma; x; by) = \sum_{n=0}^{\infty} \frac{\Gamma(\ell+n+1)}{\Gamma(2\ell+n+2)} \left(\frac{1}{y+n+2} \right) \left[1 - \left(\frac{x}{y} \right)^{n+\gamma+2} \right] \frac{(-2iby)^{n+2}}{\Gamma(n+1)} \quad (3.11.25)$$

They may also be expressed in terms of hypergeometric functions.

The coefficients $A_{nk}^{(p)}$... etc. are given by

$$\begin{pmatrix} a_{nk}(\tau) \\ \beta_{nk}(\tau) \end{pmatrix} = \sum_{P \geq 0} \begin{pmatrix} A_{nk}^{(p)} \\ B_{nk}^{(p)} \end{pmatrix} \tau^p ; \quad \begin{pmatrix} \gamma_{nk}^{(j)}(\tau) \\ \delta_{nk}^{(j)}(\tau) \end{pmatrix} = \sum_{P \geq 0} \begin{pmatrix} j C_{nk}^{(p)} \\ j D_{nk}^{(p)} \end{pmatrix} \tau^p \quad (3.11.26)$$

with $a_{nk}(\tau)$... etc., being the coefficients in the multipole solution for the equilibrium field at an arbitrary source time τ . Calculation of these factors, using the methods of section 3.7, will provide then, the complete solution for the direct or primary field for the expanding rupture models treated in this section. These equilibrium calculations will be considered in section 3.14.

3.12. Primary Field Potentials for Natural Tectonic Sources: Propagating Ruptures

The development of the field representations for the propagating ruptures will proceed along the same lines as for the unilateral rupture of the previous section. Thus, from the potentials of (3.11.1),

one has for either of the propagating rupture models

$$\tilde{\Theta}^{(1)}(\underline{r}, \omega) = \frac{i\omega}{4\pi V_p^2} \iiint \left(\frac{e^{-ik_p R^{**}}}{R^{**}} \right) d\underline{R}' \left\{ \eta_m \int_0^{\tau_0} \frac{\partial \Theta^*}{\partial \tau} e^{-i\omega \eta_m \tau} d\tau \right\} \quad (3.12.1)$$

$$\tilde{\Omega}_j^{(1)}(\underline{r}, \omega) = \frac{i\omega}{4\pi V_s^2} \iiint \left(\frac{e^{-ik_s R^{**}}}{R^{**}} \right) d\underline{R}' \left\{ \xi_m \int_0^{\tau_0} \frac{\partial \Omega_j^*}{\partial \tau} e^{-i\omega \xi_m \tau} d\tau \right\}$$

It is possible to treat both ellipsoidal and spherical rupture propagation simultaneously. In particular the translation parameter, $d(\tau)$, for either model can be written in the form

$$d(\tau) = \left[1 - \alpha_0^m (2 - v_R \tau / a_0) \right] v_R \tau \quad (3.12.2)$$

where the parameter α_0^m , $m = 2, 3$ depends on the model and is defined by equation (3.10.19) for spherical rupture and equations (3.10.22) and (3.10.23) for the ellipsoidal case. That is,

$$\alpha_0^{(2)} = b_0 / a_0 \quad (\text{spherical case}) \quad (3.12.3)$$

$$\alpha_0^{(3)} \equiv \alpha_0 = a(\tau_0/2) / a_0 \quad (\text{ellipsoidal case})$$

Here, τ_0 is the time interval of rupturing and is, for either model

$$\tau_0 = \frac{2a_0}{v_R}$$

Thus, α_0^m is a measure of the shape and size of the propagating rupture and will be termed the "form factor." In the ellipsoidal case $\alpha_0^{(3)}$ is treated as a "free" parameter, that is, it is independent

of the other rupture parameters a_o , b_o , c_o , etc.

The rupture parameter a_o^m plays a rather crucial role in the development of the solutions (3.12.1). In particular two classes will be distinguished, first those ruptures for which

$$1/10 \leq a_o^m < 1/2 \quad (3.12.4)$$

and secondly the remaining ruptures for which

$$a_o^m < 1/10 \quad (3.12.5)$$

In the first case the propagating rupture zone can be rather large and roughly comparable in its maximum dimensions to the final rupture envelope. The second case, (3.12.5), will be used to describe a smaller propagating rupture zone and while $d(\tau)$, as given by (3.12.2), will be used with the larger values of a_o^m given by (3.12.4), an approximate form of $d(\tau)$ will be used, when convenient, when a_o^m is small, as in (3.12.5). Thus, as an approximation

$$d(\tau) \simeq (1 - a_o^m) v_R \tau \quad \text{when } a_o^m < 1/10 \quad (3.12.6)$$

In addition to the features of the propagating ruptures previously pointed out, these models have other useful and interesting geometrical properties which engender considerable representational flexibility. For example if $a_o^{(3)} < b_o/a_o$, in the case of a propagating ellipsoidal rupture, then the ellipsoid is elongated in a direction normal to the direction of rupture propagation, while if $a_o^{(3)} > b_o/a_o$ the elongation is in the direction of propagation. In the limit $a_o^{(3)} \rightarrow 0$,

the ellipsoid degenerates to a propagating "line" source of variable length. When $a_0^{(2)} \rightarrow 0$, in the spherical case, the source reduces to a propagating "point" source. In either case the time dependence of the rupture parameters has been chosen so that the actual rupture has zero volume initially but grows as it propagates, reaching a maximum volume at a source time $\tau_0/2$, thereafter decreasing to zero again at τ_0 .

The equilibrium fields Θ^* and Ω_j^* in (3.12.1) are given by (3.10.8) and (3.10.9). Thus when

$$1/10 \leq a_0^m < 1/2$$

then $d(\tau)$ is given by (3.12.2) and for either model

$$\Theta^*(\underline{r}', \tau) = \begin{cases} \Theta_1^*(\underline{r}', \tau) ; & r' > d(\tau) \\ \Theta_2^*(\underline{r}', \tau) ; & r' < d(\tau) \end{cases}$$

where

$$\begin{aligned} \Theta_1^*(\underline{r}', \tau) &= \sum_{n=1}^{\infty} \left(\frac{1}{r'}\right)^{n+1} \sum_{k=0}^m \left\{ \alpha_{nk} \cos k\phi' + \beta_{nk} \sin k\phi' \right\} \sum_{s=0}^{\infty} (-1)^s \frac{(n-k+s)!}{s!(n-k)!} \left(\frac{1}{r'}\right)^s \\ &\quad \times \sum_{j=0}^s \left(\frac{\alpha_0^m}{a_0}\right)^j \frac{s!}{(s-j)!j!} (1-2\alpha_0^m)^{s-j} (V_R \tau)^{j+s} P_{n+s}^k(\cos \theta') \\ \Theta_2^*(\underline{r}', \tau) &= \sum_{n=1}^{\infty} (-1)^{n+1} \sum_{k=0}^n \left\{ \alpha_{nk}(\tau) \cos k\phi' + \beta_{nk}(\tau) \sin k\phi' \right\} \\ &\quad \times \sum_{s=0}^{\infty} (-1)^{k+s} \frac{(n+k+s)!}{(2k+s)!(n-k)!} \left(\frac{1}{V_R \tau}\right)^{n+k+s+1} \left\{ 1 - \alpha_0^m \left(\frac{r-V_R \tau}{a_0}\right)^{-(n+k+s+1)} \right\} \\ &\quad \times (r')^{k+s} P_{k+s}^k(\cos \theta') \end{aligned}$$

(3.12.8)

with similar expressions for $\Omega_j^*(r', \tau)$.

As was the case with the expanding ellipsoidal ruptures it is advantageous to stipulate the source time intervals corresponding to the inequalities $r' \lesssim d(\tau)$ in (3.12.7). Thus inverting these expressions gives

$$\tau \geq \frac{a_o}{v_R} \left[\left(\frac{1-2a_o^m}{2a_o^m} \right)^2 + \frac{1}{a_o^m} \left(\frac{r'}{a_o} \right) \right]^{1/2} - \left(\frac{1-2a_o^m}{2a_o^m} \right) \frac{a_o}{v_R} \quad (3.12.9)$$

This expression will be approximated over appropriate ranges of the variable r' . Thus for

$$0 \leq r' < \frac{(1-2a_o^m)^2}{4a_o^m} a_o \quad (3.12.10)$$

the quadratic may be expanded, to yield

$$\begin{aligned} \tau \geq & \left(\frac{1-2a_o^m}{2a_o^m} \right) \left[1 + \frac{1}{2a_o^m} \left(\frac{2a_o^m}{1-2a_o^m} \right)^2 \left(\frac{r'}{a_o} \right) - \frac{1}{8a_o^m} \left(\frac{2a_o^m}{1-2a_o^m} \right)^4 \left(\frac{r'}{a_o} \right)^2 + \dots \right] \\ & \times \left(\frac{a_o}{v_R} \right) - \left(\frac{1-2a_o^m}{2a_o^m} \right) \frac{a_o}{v_R} \end{aligned}$$

Approximating the series as a first order term in (r'/a_o) gives, after estimating the higher order terms,

$$\tau \geq \left(\frac{1-a_o^m}{1-2a_o^m} \right) \left(\frac{r'}{v_R} \right) \quad (3.12.11)$$

appropriate to the region given by (3.12.10).

Next (3.12.9) will be approximated over the range

$$\frac{(1-2\alpha_o^m)^2}{4\alpha_o^m} a_o \leq r' < (\beta_m + 1)\alpha_o^m a_o \quad (3.12.12)$$

where β_m will be chosen so that $\tau = 2a_o/v_R = \tau_o$ when $r' = (\beta_m + 1)\alpha_o^m a_o$. However, regardless of the value of β_m , (3.12.12) gives

$$\frac{1}{\alpha_o^m} \left(\frac{r'}{a_o} \right) - \beta_m < 1$$

so that (3.12.9) may be written as

$$\tau \geq \frac{a_o}{v_R} \left[\left\{ \left(\frac{1-2\alpha_o^m}{2\alpha_o^m} \right)^2 + \beta_m \right\} + \left\{ \frac{1}{\alpha_o^m} \left(\frac{r'}{a_o} \right) - \beta_m \right\} \right]^{1/2} - \left(\frac{1-2\alpha_o^m}{2\alpha_o^m} \right) \frac{a_o}{v_R}$$

and expansion of the quadratic in powers of $\left\{ \frac{1}{\alpha_o^m} \left(\frac{r'}{a_o} \right) - \beta_m \right\}$ is convergent. In particular, to first order

$$\begin{aligned} \tau \geq & \frac{a_o}{v_R} \left[\left(\frac{1-2\alpha_o^m}{2\alpha_o^m} \right)^2 + \beta_m \right]^{1/2} \left\{ 1 - \frac{\beta_m}{2} \left[\left(\frac{1-2\alpha_o^m}{2\alpha_o^m} \right)^2 + \beta_m \right]^{-1} \right\} \\ & - \left(\frac{1-2\alpha_o^m}{2\alpha_o^m} \right) \frac{a_o}{v_R} + \frac{1}{2\alpha_o^m} \left[\left(\frac{1-2\alpha_o^m}{2\alpha_o^m} \right)^2 + \beta_m \right]^{-1/2} \left(\frac{r'}{v_R} \right) \end{aligned}$$

For convenience let

$$\begin{aligned} f_m &= \left(\frac{1-2\alpha_o^m}{2\alpha_o^m} \right) \\ g_m &= \left[f_m^2 + \beta_m \right]^{1/2} \left\{ 1 - \frac{\beta_m}{2} \left[f_m^2 + \beta_m \right]^{-1} \right\} - f_m \\ h_m &= \frac{1}{2\alpha_o^m} \left[f_m^2 + \beta_m \right]^{-1/2} \end{aligned} \quad (3.12.13)$$

so that

$$\tau \geq g_m \left(\frac{a_o}{v_R} \right) + h_m \left(\frac{r'}{v_R} \right) \quad (3.12.14)$$

Now, if it is required that β_m be such that the right side of (3.12.14) approach $2a_o/v_R$ as r' approaches $(\beta_m + 1)a_o^m$, then this is equivalent to the condition

$$g_m + (\beta_m + 1)a_o^m h_m = 2 \quad (3.12.15)$$

or, that

$$f_m^2 + \beta_m + \frac{1}{2} = (f_m + 2) \left[f_m^2 + \beta_m \right]^{1/2}$$

Solving for β_m , the required value is given by

$$\beta_m = \frac{3 + 4f_m - f_m^2}{2} + \frac{1}{2} \left[f_m^4 + 8f_m^3 + 26f_m^2 + 24f_m + 8 \right]^{1/2} \approx \frac{2}{a_o^m} - 1$$

Thus, the partitioning $0 \leq r' < \infty$, $0 \leq \tau \leq \frac{2a_o}{v_e}$ has been made:

If

$$0 \leq r' < \frac{(1 - 2a_o^m)^2}{4a_o^m} a_o$$

then

$$\Theta^* = \Theta_1^* \quad \text{when} \quad \tau < \left(\frac{1 - a_o^m}{1 - 2a_o^m} \right) \left(\frac{r'}{v_R} \right) \quad (3.12.16)$$

or

$$\Theta^* = \Theta_2^* \quad \text{when} \quad \tau > \left(\frac{1 - a_o^m}{1 - 2a_o^m} \right) \left(\frac{r'}{v_R} \right)$$

If

$$\frac{(1-2a_o^m)^2}{4a_o^m} a_o \leq r' < (\beta_m + 1)a_o^m a_o$$

then

$$\Theta^* = \Theta_1^* \quad \text{when} \quad \tau < g_m \left(\frac{a_o}{v_R} \right) + h_m \left(\frac{r'}{v_R} \right) \quad (3.12.17)$$

or

$$\Theta^* = \Theta_2^* \quad \text{when} \quad \tau > g_m \left(\frac{a_o}{v_R} \right) + h_m \left(\frac{r'}{v_R} \right)$$

The functions β_m , g_m and h_m are shown in Figure 13. Figure 14a shows the spatial partitioning chosen for various values of the form factor a_o^m , while Figure 14b indicates the resulting approximate time partitioning appropriate to the spatial division for the representative case, $a_o^m = 1/8$. The exact time partitioning appropriate to (3.12.7), as given by equation (3.12.9), is indicated as well and it is seen that the approximations given by (3.12.16) and (3.12.17) are quite accurate. It is also clear that when $r' \geq 2a_o$, then the case $r' > d(\tau)$ in (3.12.7) prevails. In fact, β_m has been so chosen that when $r' \geq (\beta_m + 1)a_o^m a_o$, then $r' > d(\tau)$. This is indicated in Figure 14 as well. Thus:

If

$$r' \geq (\beta_m + 1)a_o^m a_o \quad (3.12.18)$$

then

$$\Theta^* = \Theta_1^* \quad \text{when} \quad 0 \leq \tau \leq 2a_o/v_R$$

Translating this manipulation of the source variable domain into a subdivision of the integration range for the radiation field in

(3.12.1) gives, for example

$$\begin{aligned}
 \tilde{\Theta}^{(1)}(\underline{r}, \omega) = & \frac{i\omega}{4\pi V_p^2} \iint d\Omega \left\{ \int_0^{\frac{(1-2\alpha_0^m)^2}{4\alpha_0^m} a_0} \left(\frac{e^{-ik_p R^{**}}}{R^*} \right) R'^2 dR' \left[\eta_m \int_0^{\frac{(1-\alpha_0^m)R'}{1-2\alpha_0^m} V_R} \frac{\partial \Theta_1^*}{\partial T} e^{-i\omega \eta_m T} dT \right. \right. \\
 & + \eta_m \int_{\frac{2a_0}{V_R}}^{\frac{(1-\alpha_0^m)R'}{1-2\alpha_0^m} V_R} \frac{\partial \Theta_2^*}{\partial T} e^{-i\omega \eta_m T} dT \left. \right] + \int_{\frac{(1-2\alpha_0^m)^2}{4\alpha_0^m} a_0}^{(\rho_{m+1})\alpha_0^m a_0} \left(\frac{e^{-ik_p R^{**}}}{R^*} \right) R'^2 dR' \\
 & \times \left[\eta_m \int_0^{g_m \left(\frac{a_0}{V_R} \right) + h_m \left(\frac{R'}{V_R} \right)} \frac{\partial \Theta_2^*}{\partial T} e^{-i\omega \eta_m T} dT + \eta_m \int_{\frac{2a_0}{V_R}}^{g_m \left(\frac{a_0}{V_R} \right) + h_m \left(\frac{R'}{V_R} \right)} \frac{\partial \Theta_1^*}{\partial T} e^{-i\omega \eta_m T} dT \right] \\
 & + \left. \int_{(\rho_{m+1})\alpha_0^m a_0}^{\infty} \eta_m \left(\frac{e^{-ik_p R^{**}}}{R^*} \right) R'^2 dR' \int_0^{\frac{2a_0}{V_R}} \frac{\partial \Theta_1^*}{\partial T} e^{-i\omega \eta_m T} dT \right\} \quad (3.12.19)
 \end{aligned}$$

The practical result of the previous (approximate) partitioning of the space-time domain for the source is that it allows the solution to be written out explicitly in terms of Θ_1^* and Θ_2^* , and in terms of integrals whose limits are linear functions of r' . This procedure will, in fact, make possible the evaluation of the integrals in question through use of the results of the previous section. In addition the break-up of the domain of integration makes it possible to reject, at least in part, that part of the field arising from within the actual rupture zone. Thus the opportunity of correcting the field representation for the propagating spherical rupture model is at hand.

In particular, the time integrals involving Θ_2^* in (3.12.19) all arise from the region within or behind the propagating rupture. This follows from the same interpretation as was placed on similar integrals appearing in the integral solution for the expanding ruptures of the previous section. In the present circumstances the elimination

of these contributions is of more crucial importance, in view of the nature of the spherical rupture model. This, excluding these contributions to the field, which corresponds to omission of the energy radiated from the spherical region $r' \leq d(\tau)$ indicated in Figure 11, gives

$$\begin{aligned} \tilde{\Theta}^{(1)}(\underline{r}, \omega) = & \frac{i\omega}{4\pi V_p^2} \iint d\Omega \left\{ \int_0^{\frac{(1-2\alpha_0^m)^2 a_0}{4\alpha_0^m}} \left(\frac{e^{-ik_p R^{**}}}{R^*} \right) R'^2 dR' \left(\gamma_m \int_0^{\frac{(1-\alpha_0^m) R'}{(1-2\alpha_0^m) V_e}} \frac{\partial \Theta_i^*}{\partial \tau} e^{-i\omega \eta_m \tau} d\tau \right) \right. \\ & + \int \frac{(\beta_m+1)\alpha_0^m a_0}{4\alpha_0^m} \left(\frac{e^{-ik_p R^{**}}}{R^*} \right) R'^2 dR' \left(\gamma_m \int_0^{g_m\left(\frac{a_0}{V_e}\right) + h_m\left(\frac{R'}{V_e}\right)} \frac{\partial \Theta_i^*}{\partial \tau} e^{-i\omega \eta_m \tau} d\tau \right) \\ & \left. + \int_{(\beta_m+1)\alpha_0^m a_0}^{\infty} \left(\frac{e^{-ik_p R^{**}}}{R^*} \right) R'^2 dR' \left(\gamma_m \int_0^{\frac{2a_0}{V_e}} \frac{\partial \Theta_i^*}{\partial \tau} e^{-i\omega \eta_m \tau} d\tau \right) \right\} \quad (3.12.20) \end{aligned}$$

$$\begin{aligned} \tilde{\Omega}_j^{(1)}(\underline{r}, \omega) = & \frac{i\omega}{4\pi V_s^2} \iint d\Omega \left\{ \int_0^{\frac{(1-2\alpha_0^m)^2 a_0}{4\alpha_0^m}} \left(\frac{e^{-ik_s R^{**}}}{R^*} \right) R'^2 dR' \right. \\ & \times \left(\xi_m \int_0^{\frac{(1-\alpha_0^m) R'}{(1-2\alpha_0^m) V_e}} \frac{\partial \Omega_j^*}{\partial \tau} e^{-i\omega \xi_m \tau} d\tau \right) \\ & + \int \frac{(\beta_m+1)\alpha_0^m a_0}{4\alpha_0^m} \left(\frac{e^{-ik_s R^{**}}}{R^*} \right) R'^2 dR' \left(\xi_m \int_0^{g_m\left(\frac{a_0}{V_e}\right) + h_m\left(\frac{R'}{V_e}\right)} \frac{\partial \Omega_j^*}{\partial \tau} e^{-i\omega \xi_m \tau} d\tau \right) \\ & \left. + \int_{(\beta_m+1)\alpha_0^m a_0}^{\infty} \left(\frac{e^{-ik_s R^{**}}}{R^*} \right) R'^2 dR' \left(\xi_m \int_0^{\frac{2a_0}{V_e}} \frac{\partial \Omega_j^*}{\partial \tau} e^{-i\omega \xi_m \tau} d\tau \right) \right\} \quad (3.12.21) \end{aligned}$$

where the rotation is obtained in the same way as in $\tilde{\Theta}^{(1)}(r, \omega)$, and $\Omega_j^{(1)*}$ is given by (3.12.8) with the coefficients a_{nk} and β_{nk} replaced by $\gamma_{nk}^{(j)}$ and $\delta_{nk}^{(j)}$, respectively. These then are the appropriate integral solutions for propagating ruptures, in the range

$$1/10 \leq \alpha_0^m < 1/2$$

Consider the case in which

$$a_o^m < 1/10$$

In this circumstance (3.12.6) will be applied to (3.12.7) to give, as an approximate relationship

$$\Theta^* = \begin{cases} \Theta_1^* ; r' > (1-a_o^m)v_R\tau, \text{ or when } \tau < \frac{1}{1-a_o^m} \left(\frac{r'}{v_R} \right) \\ \Theta_2^* ; r' > (1-a_o^m)v_R\tau, \text{ or when } \tau > \frac{1}{1-a_o^m} \left(\frac{r'}{v_R} \right) \end{cases} \quad (3.12.22)$$

where Θ_1^* and Θ_2^* are as given in equation (3.12.8). Again partitioning the space-time domain, the solutions may be put into the form

$$\begin{aligned} \tilde{\Theta}^{(1)}(\underline{r}, \omega) = & \frac{i\omega}{4\pi v_p^2} \iint d\Omega \left\{ \int_0^{2(1-a_o^m)a_o} \left(\frac{e^{-ik_p R^{**}}}{R^*} \right) R'^2 dR' \left(\eta_m \int_0^{\frac{1}{1-a_o^m} \left(\frac{R'}{v_R} \right)} \frac{\partial \Theta_1^*}{\partial \tau} e^{-i\omega \eta_m \tau} d\tau \right. \right. \\ & + \left. \eta_m \int_{\frac{1}{1-a_o^m} \left(\frac{R'}{v_R} \right)}^{\frac{2a_o}{v_R}} \frac{\partial \Theta_2^*}{\partial \tau} e^{-i\omega \eta_m \tau} d\tau \right) + \int_{2(1-a_o^m)a_o}^{\infty} \left(\frac{e^{-ik_p R^{**}}}{R^*} \right) R'^2 dR' \\ & \left. \times \left(\eta_m \int_0^{\frac{2a_o}{v_R}} \frac{\partial \Theta_1^*}{\partial \tau} e^{-i\omega \eta_m \tau} d\tau \right) \right\} \end{aligned}$$

Excluding the integral involving Θ_2^* , for the reasons previously cited, one has for the solution in this case

$$\begin{aligned} \tilde{\Theta}^{(1)}(\underline{r}, \omega) = & \frac{i\omega}{4\pi v_p^2} \iint d\Omega \left\{ \int_0^{2(1-a_o^m)a_o} \left(\frac{e^{-ik_p R^{**}}}{R^*} \right) R'^2 dR' \right. \\ & \left. \times \left(\eta_m \int_0^{\frac{1}{1-a_o^m} \left(\frac{R'}{v_R} \right)} \frac{\partial \Theta_1^*}{\partial \tau} e^{-i\omega \eta_m \tau} d\tau \right) + \int_{2(1-a_o^m)a_o}^{\infty} \left(\frac{e^{-ik_p R^{**}}}{R^*} \right) R'^2 dR' \left(\eta_m \int_0^{\frac{2a_o}{v_R}} \frac{\partial \Theta_1^*}{\partial \tau} e^{-i\omega \eta_m \tau} d\tau \right) \right\} \end{aligned}$$

(3.12.23)

$$\tilde{\Omega}_j^{(1)}(\underline{r}, \omega) = \frac{i\omega}{4\pi V_s^2} \iint d\Omega \left\{ \int_0^{2(1-\alpha_0^m)a_0} \left(\frac{e^{-ik_s r^{**}}}{r^*} \right) r'^2 dr' \left(\xi_m \int_0^{\frac{1}{1-\alpha_0^m} \left(\frac{r'}{V_R} \right)} \frac{d\Omega_j^*}{2T} e^{-i\omega \xi_m \tau} d\tau \right) \right. \\ \left. + \int_{2(1-\alpha_0^m)a_0}^{\infty} \left(\frac{e^{-ik_s r^{**}}}{r^*} \right) r'^2 dr' \left(\xi_m \int_0^{\frac{2a_0}{V_R} \left(\frac{r'}{V_R} \right)} \frac{d\Omega_j^*}{2T} e^{-i\omega \xi_m \tau} d\tau \right) \right\} \quad (3.12.24)$$

Now, for any of the solutions (3.12.20) - (3.12.21) or (3.12.23) - (3.12.24), the angular delay factors η_m and ξ_m are to first order constant. This follows from the fact that the energy release is local to the rupture surface and since the delay factors are very slowly varying functions of θ' and ϕ' , as is illustrated in Figures 12a and 12d for the cases $m = 2$ and 3. The delay factors are, for the two cases in question

$$\eta_2 = 1 - \frac{v_R}{v_p} \left[\cos \theta' + \frac{3}{2} \left(\frac{b_0}{a_0} \right) (1 - \cos \theta') \right] \quad (3.12.25)$$

$$\xi_2 = 1 - \frac{v_R}{v_s} \left[\cos \theta' + \frac{3}{2} \left(\frac{b_0}{a_0} \right) (1 - \cos \theta') \right]$$

$$\eta_3 = 1 - \frac{v_R}{v_p} \left[\left(1 - \frac{3}{2} \alpha_0 \right) \cos \theta' + \frac{3}{2} \left(\alpha_0 \cos^2 \theta' + \frac{b_0}{a_0} \sin^2 \theta' \sin^2 \phi' \right) \right] \quad (3.12.26)$$

$$\xi_3 = 1 - \frac{v_R}{v_s} \left[\left(1 - \frac{3}{2} \alpha_0 \right) \cos \theta' + \frac{3}{2} \left(\alpha_0 \cos^2 \theta' + \frac{b_0}{a_0} \sin^2 \theta' \sin^2 \phi' \right) \right]$$

Therefore, taking an appropriate mean value for θ' , in particular

$$\theta'_{\text{mean}} \simeq \tan^{-1} \frac{b_0}{2a_0}$$

as was done in the previous section, and setting $\phi' = \pi/2$, then

$$\eta_2 \approx 1 - \frac{v_R}{v_p} \left[1 - \frac{3}{2} \left(\frac{b_o}{2a_o} \right)^3 \right] \quad (3.12.27)$$

$$\xi_2 \approx 1 - \frac{v_R}{v_s} \left[1 - \frac{3}{2} \left(\frac{b_o}{2a_o} \right)^3 \right]$$

$$\eta_3 \approx 1 - \frac{v_R}{v_p} \left[1 - \frac{1}{2} \left(1 - \frac{9}{2} a_o \right) \left(\frac{b_o}{2a_o} \right)^2 \right] \quad (3.12.28)$$

$$\xi_3 \approx 1 - \frac{v_R}{v_s} \left[1 - \frac{1}{2} \left(1 - \frac{9}{2} a_o \right) \left(\frac{b_o}{2a_o} \right)^2 \right]$$

Under these conditions it is clear that the solutions may be evaluated in precisely the same way as in the preceding section.

Thus consider first the representation of (3.12.20) and (3.12.21). The procedures of the previous section (e.g. equations 3.11.17) through (3.11.25)) result in the following expansion

$$\tilde{\Theta}^{(1)}(\underline{r}, \omega) = \frac{k_p^2}{4\pi v_p} \sum_{l=0}^{\infty} (2l+1) \sum_{n=1}^{\infty} \sum_{k=0}^n \sum_{s=0}^{\infty} \frac{(-1)^s (n-k+s)!}{s! (n-k)!} h_l^{(2)}(k_p r)$$

$$\times \left\{ \left[\int_0^{2\pi} \int_0^{\pi} P_l(\cos \theta) P_{n+s}^k(\cos \theta') \left\{ \begin{matrix} \cos m\phi' \\ \sin m\phi' \end{matrix} \right\} \sin \theta' d\theta' d\phi' \right] \right.$$

$$\times \left(\eta_m \int_0^{R_o^{(m)}} \begin{pmatrix} n I_{\alpha}^{(s)}(r') \\ n I_{\beta}^{(s)}(r') \end{pmatrix} \frac{e^{-ik_p r'}}{(r')^{n-1}} j_l(k_p r') dr' + \eta_m \int_{R_o^{(m)}}^{R_s^{(m)}} \begin{pmatrix} n K_{\alpha}^{(s)}(r') \\ n K_{\beta}^{(s)}(r') \end{pmatrix} \right.$$

$$\left. \times \frac{e^{-ik_p r'}}{(r')^{n-1}} j_l(k_p r') dr' + \eta_m \begin{pmatrix} n J_{\alpha}^{(s)}(a_o) \\ n J_{\beta}^{(s)}(a_o) \end{pmatrix} \int_{R_o^{(m)}}^{R_s} \left(\frac{1}{r'} \right)^{n+s-1} e^{-ik_p r'} j_l(k_p r') dr' \right\}$$

(3.12.29)

as was done in the previous section, and setting $\phi' = \pi/2$, then

$$\begin{aligned} \eta_2 &\approx 1 - \frac{v_R}{v_p} \left[1 - \frac{3}{2} \left(\frac{b_o}{2a_o} \right)^3 \right] \\ \xi_2 &\approx 1 - \frac{v_R}{v_s} \left[1 - \frac{3}{2} \left(\frac{b_o}{2a_o} \right)^3 \right] \end{aligned} \quad (3.12.27)$$

$$\begin{aligned} \eta_3 &\approx 1 - \frac{v_R}{v_p} \left[1 - \frac{1}{2} \left(1 - \frac{9}{2} a_o \right) \left(\frac{b_o}{2a_o} \right)^2 \right] \\ \xi_3 &\approx 1 - \frac{v_R}{v_s} \left[1 - \frac{1}{2} \left(1 - \frac{9}{2} a_o \right) \left(\frac{b_o}{2a_o} \right)^2 \right] \end{aligned} \quad (3.12.28)$$

Under these conditions it is clear that the solutions may be evaluated in precisely the same way as in the preceding section.

Thus consider first the representation of (3.12.20) and (3.12.21). The procedures of the previous section (e. g. equations 3.11.17) through (3.11.25)) result in the following expansion

$$\begin{aligned} \tilde{\Theta}^{(1)}(\underline{r}, \omega) &= \frac{k_p^2}{4\pi v_p} \sum_{l=0}^{\infty} (2l+1) \sum_{n=1}^{\infty} \sum_{k=0}^n \sum_{s=0}^{\infty} \frac{(-1)^s (n-k+s)!}{s! (n-k)!} h_l^{(2)}(k_p r) \\ &\times \left\{ \left[\int_0^{2\pi} \int_0^{\pi} P_l(\cos r) P_{n+s}^k(\cos \theta') \left\{ \begin{matrix} \cos m\phi' \\ \sin m\phi' \end{matrix} \right\} \sin \theta' d\theta' d\phi' \right] \right. \\ &\times \left(\eta_m \int_0^{r_o^{(m)}} \begin{pmatrix} n I_{\alpha}^{(s)}(r') \\ n I_{\beta}^{(s)}(r') \end{pmatrix} \frac{e^{-ik_p r'}}{(r')^{n-1}} j_s(k_p r') dr' + \eta_m \int_{r_o^{(m)}}^{r_s^{(m)}} \begin{pmatrix} n K_{\alpha}^{(s)}(r') \\ n K_{\beta}^{(s)}(r') \end{pmatrix} \right. \\ &\left. \left. \times \frac{e^{-ik_p r'}}{(r')^{n-1}} j_s(k_p r') dr' + \eta_m \begin{pmatrix} n J_{\alpha}^{(s)}(a_o) \\ n J_{\beta}^{(s)}(a_o) \end{pmatrix} \int_{r_o^{(m)}}^{R_s} \left(\frac{1}{r'} \right)^{n+s-1} e^{-ik_p r'} j_s(k_p r') dr' \right) \right\} \end{aligned} \quad (3.12.29)$$

with

$$r_0^{(m)} \equiv \frac{(1-2\alpha_0^m)^2}{4\alpha_0^m} a_0 \quad (3.12.30)$$

$$r_1^{(m)} \equiv (\beta_m + 1) \alpha_0^m a_0$$

and η_m given by (3.12.27) or (3.12.28). The functions $n_a^{(s)}(r')$... etc. are

$$\begin{pmatrix} n_a^{(s)} \\ n_\beta^{(s)} \end{pmatrix} = \left(\frac{1}{r'}\right)^s \sum_{j=0}^s \left(\frac{\alpha_0^m}{a_0}\right)^j \frac{s!}{(s-j)!j!} (1-2\alpha_0^m)^{s-j} (V_R)^{s+j} \int_0^{\frac{(1-\alpha_0^m)r'}{1-2\alpha_0^m} V_R} \frac{\partial}{\partial \tau} \left[\begin{pmatrix} \alpha_{nk}(\tau) \\ \beta_{nk}(\tau) \end{pmatrix} \tau^{s+j} \right] e^{-i\omega\eta_m \tau} d\tau \quad (3.12.31)$$

$$\begin{pmatrix} n_a^{(s)} \\ n_\beta^{(s)} \end{pmatrix} = \left(\frac{1}{r'}\right)^s \sum_{j=0}^s \left(\frac{\alpha_0^m}{a_0}\right)^j \frac{s!}{(s-j)!j!} (1-2\alpha_0^m)^{s-j} (V_R)^{s+j} \int_0^{g_m \frac{a_0}{V_R} + h_m \frac{r'}{V_R}} \frac{\partial}{\partial \tau} \left[\begin{pmatrix} \alpha_{nk}(\tau) \\ \beta_{nk}(\tau) \end{pmatrix} \tau^{s+j} \right] e^{-i\omega\eta_m \tau} d\tau \quad (3.12.32)$$

$$\begin{pmatrix} n_a^{(s)} \\ n_\beta^{(s)} \end{pmatrix} = \sum_{j=0}^s \left(\frac{\alpha_0^m}{a_0}\right)^j \frac{s!}{(s-j)!j!} (1-2\alpha_0^m)^{s-j} (V_R)^{s+j} \int_0^{2a_0/V_R} \frac{\partial}{\partial \tau} \left[\begin{pmatrix} \alpha_{nk}(\tau) \\ \beta_{nk}(\tau) \end{pmatrix} \tau^{s+j} \right] e^{-i\omega\eta_m \tau} d\tau \quad (3.12.33)$$

Introducing the expansions for the coefficients $\alpha_{nk}(\tau)$ and $\beta_{nk}(\tau)$ of equation (3.11.15), with the same provisions previously stated, so

$$\alpha_{nk}(\tau) = \sum_{P \geq 0} A_{nk}^{(P)} \tau^P, \quad \beta_{nk}(\tau) = \sum_{P \geq 0} B_{nk}^{(P)} \tau^P$$

then (3.12.31) - (3.12.33) may be integrated to yield

$$\begin{pmatrix} n I_a^{(s)} \\ n I_\beta^{(s)} \end{pmatrix} = \sum_{p \geq 0} \left(\frac{1}{\sqrt{r}}\right)^p \begin{pmatrix} A_{nm}^{(p)} \\ B_{nm}^{(p)} \end{pmatrix} \sum_{j=0}^s \left(\frac{\alpha_0^m}{a_0}\right)^j \frac{s!}{(s-j)! j!} (1-2\alpha_0^m)^{s-j} \left(\frac{1-\alpha_0^m}{1-2\alpha_0^m}\right)^{s+p+j} \\ \times (r')^{p+j} {}_1F_1(s+p+j; s+p+j+1; -i\eta_m \left(\frac{1-\alpha_0^m}{1-2\alpha_0^m}\right) k_R r') \quad (3.12.34)$$

$$\begin{pmatrix} n K_a^{(s)} \\ n K_\beta^{(s)} \end{pmatrix} = \sum_{p \geq 0} \left(\frac{1}{\sqrt{r}}\right)^p \begin{pmatrix} A_{nm}^{(p)} \\ B_{nm}^{(p)} \end{pmatrix} \sum_{j=0}^s \left(\frac{\alpha_0^m}{a_0}\right)^j \frac{s!}{(s-j)! j!} (1-2\alpha_0^m)^{s-j} (g_m a_0)^{s+p+j} \\ \times \left(\frac{1}{r'}\right)^s \left(1 + \frac{h_m r'}{j_m a_0}\right)^{s+p+j} {}_1F_1(s+p+j; s+p+j+1; -i\eta_m (g_m a_0 + h_m r') k_R) \quad (3.12.35)$$

$$\begin{pmatrix} n J_a^{(s)} \\ n J_\beta^{(s)} \end{pmatrix} = \sum_{p \geq 0} \left(\frac{2a_0}{\sqrt{r}}\right)^p \begin{pmatrix} A_{nm}^{(p)} \\ B_{nm}^{(p)} \end{pmatrix} \sum_{j=0}^s \left(\frac{\alpha_0^m}{a_0}\right)^j \frac{s!}{(s-j)! j!} (1-2\alpha_0^m)^{s-j} (2a_0)^{s+p+j} \\ \times {}_1F_1(s+p+j; s+p+j+1; -2i\eta_m k_R a_0) \quad (3.12.36)$$

with

$${}_1F_1(s+p+j; s+p+j+1; -ix) = \sum_{q=0}^{\infty} \frac{(s+p+j)_q}{(s+p+j+q)_q} \frac{(-ix)^q}{\Gamma(q+1)}$$

Finally, utilizing the orthogonal properties of the angular functions in (3.12.29) gives, upon integration over θ' and ϕ'

$$\tilde{\Theta}^{(1)}(\underline{r}, \omega) = \sum_{l=1}^n \sum_{k=0}^l h_l^{(2)}(k_p r) \left\{ a_{lk}(\omega) \cos k\phi + \beta_{lk}(\omega) \sin k\phi \right\} P_l^k(\cos\theta) \quad (3.12.37)$$

where, with $s = l - n$

$$\begin{aligned} \begin{pmatrix} a_{lk}(\omega) \\ \beta_{lk}(\omega) \end{pmatrix} &= \frac{k_p^2 \eta_m}{\nu_p} \sum_{p \geq 0} \left(\frac{1}{V_R}\right)^p \sum_{n=1}^l (-1)^{l-n} \frac{(l-k)!}{(n-k)!} \begin{pmatrix} A_{nk}^{(p)} \\ B_{nk}^{(p)} \end{pmatrix} \sum_{j=0}^{l-n} \left(\frac{\alpha_0^m}{a_0}\right)^j \\ &\times \frac{(1-2\alpha_0^m)^{l-n-j}}{(l-n-j)! j!} \left\{ \left(\frac{1-\alpha_0^m}{1-2\alpha_0^m}\right)^{s+p+j} \int_0^{R_0^{(m)}} \left(\frac{1}{R'}\right)^{n-p-j-1} {}_1F_1(s+p+j; s+p+j+1; \right. \\ &\quad \left. -i\eta_m d_m k_p R') e^{-ik_p R'} j_l(k_p R') dr' + (g_m a_0)^{s+p+j} \right. \\ &\times \int_{R_0^{(m)}}^{R_1^{(m)}} \left(\frac{1}{R'}\right)^{l-1} \left(1 + \frac{h_m R'}{g_m a_0}\right)^{s+p+j} {}_1F_1(s+p+j; s+p+j+1; -i\eta_m k_p (g_m a_0 + h_m R')) e^{-ik_p R'} \\ &\quad \left. j_l(k_p R') dr' + (a_0)^{s+p+j} {}_1F_1(s+p+j; s+p+j+1; -2i\eta_m k_p a_0) \right. \\ &\times \left. \int_{R_1^{(m)}}^{R_s} \left(\frac{1}{R'}\right)^{l-1} e^{-ik_p R'} j_l(k_p R') dr' \right\} \end{aligned} \quad (3.12.38)$$

Entirely equivalent results apply to the rotation, $\tilde{\Omega}_j^{(1)}$.

The integrals appearing in this rather complicated and lengthy expression are of precisely the form already treated in Appendix 5. These results are utilized in Appendix 6 to reduce (3.12.38) to a convenient algebraic form. One has from Appendix 6, the final results for both $\tilde{\Theta}^{(1)}$ and $\tilde{\Omega}_j^{(1)}$

$$\Theta^{(1)}(\underline{x}, \omega) = \sum_{l=1}^n \sum_{k=0}^l h_l^{(2)}(k_p \pi) \{ \alpha_{lk}(\omega) \cos k\varphi + \beta_{lk}(\omega) \sin k\varphi \} P_l^k(\cos \theta) \quad (3.12.39)$$

$$\tilde{\Omega}_j^{(1)}(\underline{x}, \omega) = \sum_{l=1}^n \sum_{k=0}^l h_l^{(2)}(k_s \pi) \{ C_{lk}^{(1)}(\omega) \cos k\varphi + D_{lk}^{(1)}(\omega) \sin k\varphi \} P_l^k(\cos \theta)$$

$$\begin{aligned} \begin{pmatrix} \alpha_{lk}(\omega) \\ \beta_{lk}(\omega) \end{pmatrix} &= \frac{-\eta_m (4k_p a_0)^l}{4V_p} \sum_{p \geq 0} \left(\frac{2a_0}{\sqrt{R}} \right)^p \sum_{n=1}^l (-1)^{l-n} \frac{\Gamma(l-k+1)}{\Gamma(n-k+1)} \left(\frac{1}{2a_0} \right)^n \\ &\quad \begin{pmatrix} A_{nk}^{(p)} \\ B_{nk}^{(p)} \end{pmatrix} \sum_{L=0}^{l-n} \frac{(\alpha_0^m/2)^L}{\Gamma(L+1)} \times \frac{(1-2\alpha_0^m)^{l-n-L}}{\Gamma(l-n-L+1)} \sum_{q=0}^{l-n+L} \frac{(l-n+L)}{(l-n+L+q)} \times \\ &\quad \left\{ \left(\frac{d_m \pi_0^m}{2a_0} \right)^\alpha E_l^{(1)}(\eta_m, \alpha; 0; k_p \pi_0^m) + \left(\frac{q_m}{2} \right)^\alpha \sum_{N=0}^{\alpha} \frac{\Gamma(\alpha+1)}{\Gamma(\alpha-N+1)} \times \right. \\ &\quad \left. \frac{(2/q_m - 1)^N}{\Gamma(N+1)} E_l^{(1)}(\eta_m, N; \pi_0^m; k_p \pi_0^m) + E_l^{(1)}(\eta_m, 0; \pi_0^m; k_p R_s) \right\} \end{aligned} \quad (3.12.40)$$

$$\begin{aligned} \begin{pmatrix} C_{lk}^{(j)}(\omega) \\ D_{lk}^{(j)}(\omega) \end{pmatrix} &= \frac{(-2i\eta_m k_p a_0)^q}{\Gamma(q+1)} \\ &= \frac{-\xi_m (4k_s a_0)^l}{4V_s} \sum_{p \geq 0} \left(\frac{2a_0}{\sqrt{R}} \right)^p \sum_{n=1}^l (-1)^{l-n} \frac{\Gamma(l-k+1)}{\Gamma(n-k+1)} \left(\frac{1}{2a_0} \right)^n \\ &\quad \begin{pmatrix} {}_j C_{nk}^{(p)} \\ {}_j D_{nk}^{(p)} \end{pmatrix} \sum_{L=0}^{l-n} \frac{(\alpha_0^m/2)^L}{\Gamma(L+1)} \frac{(1-2\alpha_0^m)^{l-n-L}}{\Gamma(l-n-L+1)} \sum_{q=0}^{l-n+L} \frac{(l-n+L)}{(l-n+L+q)} \times \\ &\quad \left\{ \left(\frac{d_m \pi_0^m}{2a_0} \right)^\alpha E_l^{(1)}(\xi_m, \alpha; 0; k_s \pi_0^m) + \left(\frac{q_m}{2} \right)^\alpha \sum_{N=0}^{\alpha} \frac{\Gamma(\alpha+1)}{\Gamma(\alpha-N+1)} \times \right. \\ &\quad \left. \frac{(2/q_m - 1)^N}{\Gamma(N+1)} E_l^{(1)}(\xi_m, N; \pi_0^m; k_s \pi_0^m) + E_l^{(1)}(\xi_m, 0; \pi_0^m; k_s R_s) \right\} \\ &\quad \frac{(-2i\xi_m k_s a_0)^q}{\Gamma(q+1)} \end{aligned} \quad (3.12.41)$$

with

$$\alpha \equiv l - n + p + L + q, \quad d_m \equiv \frac{1 - a_0^m}{1 - 2a_0^m}$$

$$E_l^{(1)}(\mu, \alpha; R_0; \kappa R) = \sum_{r=0}^{\infty} \frac{\Gamma(l+r+1)}{\Gamma(2l+r+2)} \left(\frac{1}{\alpha+r+2} \right) \left[1 - \left(\frac{R_0}{R} \right)^{n+\alpha+2} \right] \times \frac{(-2i\kappa R)^{r+2}}{\Gamma(r+1)} \quad (3.12.42)$$

As for the case of rupture expansion in the previous section, the results are expressed in a form which is appropriate for the computation of the solution coefficients.

Finally in the case

$$a_0^m < 1/10$$

the appropriate solutions are given by (3.12.23), and after introducing the expansion (3.12.8) for Θ_1^* , gives for example,

$$\begin{aligned} \tilde{\Theta}^{(1)}(\underline{r}, \omega) &= \frac{k_p^2}{4\pi V_p} \sum_{l=0}^{\infty} (2l+1) \sum_{n=1}^{\infty} \sum_{k=0}^n \sum_{s=0}^{\infty} (-1)^s \frac{(n-k+s)!}{s!(n-k)!} h_l^{(2)}(k_p R) \\ &\times \left\{ \int_0^{2\pi} \int_0^{\pi} P_l(\cos \vartheta) P_{n+s}^k(\cos \theta') \left\{ \begin{matrix} \cos m\varphi' \\ \sin m\varphi' \end{matrix} \right\} \sin \theta' d\theta' d\varphi' \right. \\ &\times \left(\eta_m \int_0^{R_2^{(m)}} \left(\begin{matrix} n I_{\alpha}^{(s)}(r') \\ n I_{\beta}^{(s)}(r') \end{matrix} \right) \frac{e^{-ik_p r'}}{(r')^{n-1}} j_l(k_p r') dr' \right. \\ &\left. \left. + \eta_m \left(\begin{matrix} n J_{\alpha}^{(s)}(a_0) \\ n J_{\beta}^{(s)}(a_0) \end{matrix} \right) \int_{R_2^{(m)}}^{R_1} \left(\frac{1}{r'} \right)^{n+s-1} e^{-ik_p r'} j_l(k_p r') dr' \right) \right\} \end{aligned} \quad (3.12.43)$$

with

$$r_2^{(m)} = 2(1 - \alpha_0^m) a_0 \quad (3.12.44)$$

and where η_m is given by (3.12.27) or (3.12.28). The functions

$n_a^{I(s)}(r')$... etc. are

$$\begin{pmatrix} n_a^{I(s)}(r') \\ n_\beta^{I(s)}(r') \end{pmatrix} = \left(\frac{1}{r'}\right)^s \sum_{j=0}^s \left(\frac{\alpha_0^m}{a_0}\right)^j \frac{5!}{(5-j)!j!} (1-2\alpha_0^m)^{s-j} (V_R)^{s+j} \int_0^{\frac{1}{1-\alpha_0^m} \left(\frac{r'}{V_R}\right)} \frac{2}{\partial \tau} \left[\begin{pmatrix} \alpha_{nk}(\tau) \\ \beta_{nk}(\tau) \end{pmatrix} \tau^{s+j} \right] e^{-i\omega \eta_m \tau} d\tau$$

$$\begin{pmatrix} n_a^{J(s)}(a_0) \\ n_\beta^{J(s)}(a_0) \end{pmatrix} = \sum_{j=0}^s \left(\frac{\alpha_0^m}{a_0}\right)^j \frac{5!}{(5-j)!j!} (1-2\alpha_0^m)^{s-j} (V_R)^{s+j} \int_0^{\frac{2a_0}{V_R}} \frac{2}{\partial \tau} \left[\begin{pmatrix} \alpha_{nk}(\tau) \\ \beta_{nk}(\tau) \end{pmatrix} \tau^{s+j} \right] e^{-i\omega \eta_m \tau} d\tau$$

After introducing the expansions for $\alpha_{nk}(\tau)$ and $\beta_{nk}(\tau)$ given previously, integration of these expressions gives, where

$$b_m = \frac{1}{1 - \alpha_0^m}$$

$$\begin{pmatrix} n_a^{I(s)}(r') \\ n_\beta^{I(s)}(r') \end{pmatrix} = \sum_{p \geq 0} \left(\frac{1}{V_R}\right)^R \begin{pmatrix} A_{nm}^{(p)} \\ B_{nm}^{(p)} \end{pmatrix} \sum_{j=0}^s \left(\frac{\alpha_0^m}{a_0}\right)^j \frac{5!}{(5-j)!j!} (1-2\alpha_0^m)^{s-j} b_m^{s+p+j}$$

$$\times (r')^{p+j} {}_1F_1(s+p+j; s+p+j+1; -i\eta_m b_m k_R r')$$

(3.12.45)

$$\begin{pmatrix} n \\ \alpha \end{pmatrix}^{J(s)}(a_0) = \sum_{p \geq 0} \left(\frac{2a_0}{V_R}\right)^p \begin{pmatrix} A_{nm}^{(p)} \\ B_{nm}^{(p)} \end{pmatrix} \sum_{j=0}^s \left(\frac{\alpha_0^m}{a_0}\right)^j \frac{j!}{(s-j)!j!} (1-2\alpha_0^m)^{s-j} (2a_0)^{s+j} \\ \times {}_1F_1(s+p+j; s+p+j+1; -2i\eta_m k_R a_0) \quad (3.12.46)$$

Thus, as before, using the orthogonal properties of the angular functions in (3.12.43), gives upon integration

$$\tilde{\Theta}^{(1)}(\underline{r}, \omega) = \sum_{l=1}^n \sum_{k=0}^n h_l^{(2)}(k_p R) \{A_{lk}(\omega) \cos k\varphi + B_{lk}(\omega) \sin k\varphi\} P_l^k(\cos \theta) \quad (3.12.47)$$

$$\begin{pmatrix} C_{lk}(\omega) \\ B_{lk}(\omega) \end{pmatrix} = \frac{k_p^2 \eta_m}{V_p} \sum_{p \geq 0} \left(\frac{1}{V_R}\right)^p \sum_{n=1}^l (-1)^{l-n} \frac{(l-k)!}{(n-k)!} \begin{pmatrix} A_{nk}^{(p)} \\ B_{nk}^{(p)} \end{pmatrix} \sum_{j=0}^{l-n} \left(\frac{\alpha_0^m}{a_0}\right)^j \\ \frac{(1-2\alpha_0^m)^{l-n-j}}{(l-n-j)!j!} \left\{ b_m \int_0^{r_2^{(m)}} \left(\frac{1}{r'}\right)^{n-p+j-1} {}_1F_1(s+p+j; s+p+j+1; -i\eta_m b_m k_R r') e^{-ik_p r'} j_x(k_p r') dr' + (2a_0)^{l-n+p+j} \right. \\ \left. \times {}_1F_1(s+p+j; s+p+j+1; -2i\eta_m k_R a_0) \int_{r_2^{(m)}}^{r_s} \left(\frac{1}{r'}\right)^{l-1} e^{-ik_p r'} j_x(k_p r') dr' \right\} \quad (3.12.48)$$

with $s = l - n$. The radial integrals appearing in this result are those treated in Appendix 6. In fact, comparing (3.12.48) with the coefficients previously computed and expressed in (3.12.38), it is seen that if $r_0^{(m)}$ and $r_1^{(m)}$ are both set equal to $r_2^{(m)}$ and $d_m = (1-\alpha_0^m)/(1-2\alpha_0^m)$ replaced by b_m , then (3.12.38) reduces to

(3.12.48). Using these replacements then, gives

$$\begin{aligned} \begin{pmatrix} C_{lk}(\omega) \\ B_{lk}(\omega) \end{pmatrix} &= -\frac{\eta_m}{4V_p} (4k_p a_0)^l \sum_{p \geq 0} \left(\frac{2a_0}{V_R}\right)^p \sum_{n=1}^l (-1)^{l-n} \frac{\Gamma(l-k+1)}{\Gamma(n-k+1)} \left(\frac{1}{2a_0}\right)^n \\ &\quad \begin{pmatrix} A_{nk}^{(p)} \\ B_{nk}^{(p)} \end{pmatrix} \sum_{L=0}^{l-n} \frac{(\alpha_0^m/2)^L}{\Gamma(L+1)} \frac{(1-2\alpha_0^m)^{l-n-L}}{\Gamma(l-n-L+1)} \sum_{q=0}^{l-n+L} \frac{(l-n+p+L)}{(l-n+p+L+q)} \\ &\quad \left\{ E_1^{(1)}(\eta_m, \alpha; 0; k_p R_2^{(m)}) + E_2^{(1)}(\eta_m, 0; R_2^{(m)}; k_p R_s) \right\} \frac{(-2i\eta_m k_p a_0)^q}{\Gamma(q+1)} \quad (3.12.49) \end{aligned}$$

$$\begin{aligned} \begin{pmatrix} C_{lk}(\omega) \\ D_{lk}(\omega) \end{pmatrix} &= -\frac{\xi_m}{4V_s} (4k_s a_0)^l \sum_{p \geq 0} \left(\frac{2a_0}{V_R}\right)^p \sum_{n=1}^l (-1)^{l-n} \frac{\Gamma(l-k+1)}{\Gamma(n-k+1)} \left(\frac{1}{2a_0}\right)^n \\ &\quad \begin{pmatrix} jC_{nk}^{(p)} \\ jD_{nk}^{(p)} \end{pmatrix} \sum_{L=0}^{l-n} \frac{(\alpha_0^m/2)^L}{\Gamma(L+1)} \frac{(1-2\alpha_0^m)^{l-n-L}}{\Gamma(l-n-L+1)} \sum_{q=0}^{l-n+L} \frac{(l-n+p+L)}{(l-n+p+L+q)} \\ &\quad \left\{ E_1^{(1)}(\xi_m, \alpha; 0; k_s R_2^{(m)}) + E_2^{(1)}(\xi_m, 0; R_2^{(m)}; k_s R_s) \right\} \\ &\quad \times \frac{(-2i\xi_m k_s a_0)^q}{\Gamma(q+1)} \quad (3.12.50) \end{aligned}$$

with

$$a = l-n+L+p+q, \quad b_m = \frac{1}{1-\alpha_0^m}, \quad r_2^{(m)} = 2(1-\alpha_0^m)a_0$$

The application of these results, as in the case of the expanding rupture models, awaits only the calculation of the source field coefficients $A_{nk}^{(p)}$, $B_{nk}^{(p)}$, $jC_{nk}^{(p)}$, and $jD_{nk}^{(p)}$ appropriate to the model. These calculations are considered in section 3.14.

3.13. Shock Induced Tectonic Radiation from a Homogeneously Prestrained Medium

The representation of the radiation field from the prestrained region around an explosive source can be developed directly from the theory and results of section 2.7. It is only necessary to observe that the rupture zone is created by a shock wave propagating through the medium with a velocity which is larger than the compressional velocity (Duvall, 1962). In this case a spherical or nearly spherical rupture volume⁽¹⁾ would be created with a rupture velocity v_R equal to the shock velocity and such that

$$v_R > v_p > v_s \quad (3.13.1)$$

For tectonic stress relaxation, this is equivalent to instantaneous creation of the rupture, in view of the causality relationships appropriate to stress relaxation and by virtue of the symmetry of the rupture. The prestress energy of the material within the rupture zone is assumed to be taken up in the non-elastic processes of rupture and flow, so that the radiation field is derived from the stress relaxation in the elastic region exterior to the rupture zone and from the conversion of the shock wave to a compressional elastic wave. In this section the tectonic radiation will be considered, the detailed treatment of shock transition being outside the scope of the present study.

(1) It is assumed that the material is nearly isotropic and homogeneous in the region affected by the shock wave and the ensuing stress relaxation. Only a large departure from this condition could seriously affect the results of this section.

Thus it seems clear that this tectonic source may be treated as an initial value problem, where the initial values of the dilatation and rotation are determined from the boundary condition of zero traction on the final spherical rupture surface. Therefore from section 2.7

$$\tilde{\Theta}^{(1)}(\underline{r}, \omega) = \frac{-ik_p}{4\pi V_p} \iiint_V \theta^*(\underline{r}') e^{-i\omega\tau_1^*} \left(\frac{e^{-ik_p r^*}}{r^*} \right) d\underline{r}' \quad (3.13.2)$$

$$\tilde{\Omega}_j^{(1)}(\underline{r}, \omega) = \frac{-ik_s}{4\pi V_s} \iiint_V \Omega_j^*(\underline{r}') e^{-i\omega\tau_2^*} \left(\frac{e^{-ik_s r^*}}{r^*} \right) d\underline{r}'$$

where, in the present application, the rupture volume is to be excluded as a source of radiation. Therefore, taking the origin time to be the instant at which the explosion occurs, then with R_0 the rupture radius

$$\tau_1^* = \frac{R_0}{v_R} + \frac{r - R_0}{v_p}, \quad \tau_2^* = \frac{R_0}{v_R} + \frac{r - R_0}{v_s} \quad (3.13.3)$$

The difference or change in the equilibrium field due to the creation of the rupture zone will be of the form

$$\Theta^* = \sum_{n=1} \left(\frac{1}{r} \right)^{n+1} \sum_{m=0}^n \{ \alpha_{nm} \cos m\phi + \beta_{nm} \sin m\phi \} P_n^m(\cos\theta) \quad (3.13.4)$$

$$\Omega_j^* = \sum_{n=1} \left(\frac{1}{r} \right)^{n+1} \sum_{m=0}^n \{ \gamma_{nm}^{(j)} \cos m\phi + \delta_{nm}^{(j)} \sin m\phi \} P_n^m(\cos\theta)$$

Under these conditions the expressions for the radiation field have the form

$$\tilde{\Theta}^{(1)}(\underline{r}, \omega) = \frac{-ik_p}{4\pi V_p} e^{ik_p(1-V_p/V_R)R_0} \sum_{n=1}^{\infty} \int_0^{2\pi} \int_0^{\pi} S_n(\theta', \varphi') \sin\theta' d\theta' d\varphi' \int_{R_0}^{\infty} \left(\frac{1}{r'}\right)^{n-1} \times e^{-ik_p r'} \left[\frac{e^{-ik_p r'^*}}{r'^*} \right] dr'$$

Thus introducing the expression

$$\frac{e^{-ik_p r'^*}}{r'^*} = -ik_p \sum_{l=0}^{\infty} (2l+1) P_l(\cos \gamma) j_l(k_p r') h_l^{(2)}(k_p r) ; r > R_s > r'$$

and integrating over the angular variables, using the orthogonality properties of the Legendre functions, gives

$$\tilde{\Theta}^{(1)}(\underline{r}, \omega) = -\frac{k_p^2}{V_p} e^{ik_p(1-V_p/V_R)R_0} \sum_{l=1}^{\infty} h_l^{(2)}(k_p r) \sum_{k=0}^l \{ \alpha_{lk} \cos k\varphi + \beta_{lk} \sin k\varphi \} \times P_l^k(\cos\theta) \int_{R_0}^{R_s} \left(\frac{1}{r'}\right)^{l-1} e^{-ik_p r'} j_l(k_p r') dr'$$

Or, rearranging terms

$$\tilde{\Theta}^{(1)}(\underline{r}, \omega) = \sum_{l=1}^{\infty} h_l^{(2)}(k_p r) \sum_{k=0}^l [A_{lk}(\omega) \cos k\varphi + B_{lk}(\omega) \sin k\varphi] P_l^k(\cos\theta) \quad (3.13.5)$$

where

$$\begin{pmatrix} A_{lk}(\omega) \\ B_{lk}(\omega) \end{pmatrix} = \frac{-k_p^2}{V_p} e^{ik_p(1-V_p/V_R)R_0} \begin{pmatrix} \alpha_{lk} \\ \beta_{lk} \end{pmatrix} \left[\int_0^{R_s} \left(\frac{1}{r'}\right)^{l-1} e^{-ik_p r'} j_l(k_p r') dr' - \int_0^{R_0} \left(\frac{1}{r'}\right)^{l-1} e^{-ik_p r'} j_l(k_p r') dr' \right] \quad (3.13.6)$$

The integrals in (3.13.6) have been evaluated in Appendices 5 and 6.

Thus

$$\int_0^{R_s} \left(\frac{1}{r'}\right)^{l-1} e^{-ik_p r'} j_l(k_p r') dr' = \sqrt{\pi/2} R_s^2 \frac{k_p^l}{2^{l+3/2} \Gamma(l+3/2)}$$

$$\times {}_2F_2(l+1, 2; 3, 2l+2; -2ik_p R_s)$$

$$\int_0^{R_0} \left(\frac{1}{r'}\right)^{l-1} e^{-ik_p r'} j_l(k_p r') dr' = \sqrt{\pi/2} R_0^2 \frac{k_p^l}{2^{l+3/2} \Gamma(l+3/2)}$$

$$\times {}_2F_2(l+1, 2; 3, 2l+2; -2ik_p R_0)$$

These results may be substituted back into (3.13.6) and after rearrangement, the final solutions are, with R_s the radius of the volume in which stress relaxation occurs,

$$\tilde{\sigma}^{(1)}(\underline{r}, \omega) = \sum_{l=2}^{\infty} h_l^{(2)}(k_p r) \sum_{k=0}^l [A_{lk}^{(1)}(\omega) \cos k\varphi + B_{lk}^{(1)}(\omega) \sin k\varphi] P_l^k(\cos\theta)$$

(3.13.7)

$$\tilde{\sigma}_j^{(1)}(\underline{r}, \omega) = \sum_{l=2}^{\infty} h_l^{(2)}(k_p r) \sum_{k=0}^l [C_{lk}^{(j)}(\omega) \cos k\varphi + D_{lk}^{(j)}(\omega) \sin k\varphi] P_l^k(\cos\theta)$$

where

$$\begin{pmatrix} A_{lk}(\omega) \\ B_{lk}(\omega) \end{pmatrix} = \left(\frac{1}{4v_p}\right) e^{ik_p(1-v_p/v_e)R_0} (2k_p)^l \begin{pmatrix} \alpha_{2k} \\ \beta_{2k} \end{pmatrix} \\ \times \sum_{n=0}^{\infty} \frac{\Gamma(l+n+1)}{\Gamma(2l+n+2)} \left(\frac{1}{2+n}\right) \left\{1 - \left(\frac{R_0}{R_s}\right)^{n+2}\right\} \frac{(-2ik_p R_s)^{n+2}}{\Gamma(n+1)} \quad (3.13.8)$$

$$\begin{pmatrix} C_{lk}^{(j)}(\omega) \\ D_{lk}^{(j)}(\omega) \end{pmatrix} = \left(\frac{1}{4v_s}\right) e^{ik_s(1-v_s/v_e)R_0} (2k_s)^l \begin{pmatrix} \gamma_{2k}^{(j)} \\ \delta_{2k}^{(j)} \end{pmatrix} \\ \times \sum_{n=0}^{\infty} \frac{\Gamma(l+n+1)}{\Gamma(2l+n+2)} \left(\frac{1}{2+n}\right) \left\{1 - \left(\frac{R_0}{R_s}\right)^{n+2}\right\} \frac{(-2ik_s R_s)^{n+2}}{\Gamma(n+1)}$$

Clearly the series in (l) converge rapidly. In some cases of interest $k_p R_s$ and $k_s R_s$ will be small and in this case the coefficients for $l = 2$ and $k = 0, 1, 2$ are the ones of greatest importance and are, to a first approximation

$$\begin{pmatrix} A_{2k}(\omega) \\ B_{2k}(\omega) \end{pmatrix} \approx -\frac{1}{30v_p} (R_s^2 - R_0^2) k_p^4 \begin{pmatrix} \alpha_{2k} \\ \beta_{2k} \end{pmatrix}$$

$$\begin{pmatrix} C_{2k}^{(j)}(\omega) \\ D_{2k}^{(j)}(\omega) \end{pmatrix} \approx -\frac{1}{30v_s} (R_s^2 - R_0^2) k_s^4 \begin{pmatrix} \gamma_{2k}^{(j)} \\ \delta_{2k}^{(j)} \end{pmatrix}$$

when

$$1 \gg 2k_s R_s > 2k_p R_s$$

In any event the radiation field is given by the equations

(3.13.7) and (3.13.8). Consider now the evaluation of the coefficients α_{nm} , β_{nm} , etc. for the initial value field. The procedures for this computation have been outlined in section 3.7, the present computation will serve as an application of these methods.

Thus, let the initial stress field be homogeneous and pure shear. In this case the initial stress $\sigma_{ij}^{(0)}$ is given by

$$\sigma_{ij}^{(0)} = \begin{pmatrix} 0 & \sigma_{12}^{(0)} & \sigma_{13}^{(0)} \\ \sigma_{12}^{(0)} & 0 & \sigma_{23}^{(0)} \\ \sigma_{13}^{(0)} & \sigma_{23}^{(0)} & 0 \end{pmatrix} \quad (3.13.9)$$

with the matrix elements all constants.

In this case, following Landau and Lifshitz (1959) p. 24, consider solutions of the equation (3.7.7)

$$\nabla^4 \underline{u}^* = 0 \quad (3.13.10)$$

which satisfy the boundary value problem posed in equation (3.7.6) as

$$(1-2\sigma)\nabla^2 \underline{u}^* + \nabla(\nabla \cdot \underline{u}^*) = 0$$

$$\underline{u}^* = O(1/r^a), \quad a \geq 2 \quad (3.13.11)$$

$$\sigma_{ij}^* \eta_j = \sigma_{ij}^{(0)} \eta_j; \quad \text{when } |\underline{r}| = R_0$$

Since any solution of the biharmonic equation can be written as a linear combination of centrally symmetric solutions and their spatial derivatives of various orders, Landau and Lifshitz consider the

symmetric functions r and r^{-1} and obtain the solution⁽¹⁾

$$u_i^* = \frac{5R_0^3(1-\sigma)}{\mu(7-5\sigma)} \sigma_{ik}^{(0)} \frac{\partial}{\partial \chi_k} \left(\frac{1}{r} \right) - \frac{R_0^5}{4\mu(7-5\sigma)} \sigma_{kl}^{(0)} \frac{\partial^3}{\partial \chi_i \partial \chi_k \partial \chi_l} \left(\frac{1}{r} \right) - \frac{5R_0^3}{4\mu(7-5\sigma)} \sigma_{kl}^{(0)} \frac{\partial^3}{\partial \chi_i \partial \chi_k \partial \chi_l} (r) \quad (3.13.12)$$

satisfying all the equations above. From this result one finds for the dilatation, rotation and stress fields:

$$\Theta^*(\underline{r}) = \frac{5R_0^3(1-2\sigma)}{\mu(7-5\sigma)} \left[\sigma_{12}^{(0)} \frac{\partial^2 r^{-1}}{\partial \chi_1 \partial \chi_2} + \sigma_{13}^{(0)} \frac{\partial^2 r^{-1}}{\partial \chi_1 \partial \chi_3} + \sigma_{23}^{(0)} \frac{\partial^2 r^{-1}}{\partial \chi_2 \partial \chi_3} \right] \quad (3.13.13)$$

$$\Omega_1^*(\underline{r}) = \frac{5R_0^3(1-\sigma)}{\mu(7-5\sigma)} \left[\sigma_{12}^{(0)} \frac{\partial^2 r^{-1}}{\partial \chi_3 \partial \chi_1} + \sigma_{23}^{(0)} \frac{\partial^2 r^{-1}}{\partial \chi_3^2} - \sigma_{13}^{(0)} \frac{\partial^2 r^{-1}}{\partial \chi_2 \partial \chi_1} - \sigma_{23}^{(0)} \frac{\partial^2 r^{-1}}{\partial \chi_2^2} \right]$$

$$\Omega_2^*(\underline{r}) = \frac{5R_0^3(1-\sigma)}{\mu(7-5\sigma)} \left[\sigma_{13}^{(0)} \frac{\partial^2 r^{-1}}{\partial \chi_1^2} + \sigma_{23}^{(0)} \frac{\partial^2 r^{-1}}{\partial \chi_2 \partial \chi_1} - \sigma_{12}^{(0)} \frac{\partial^2 r^{-1}}{\partial \chi_2 \partial \chi_3} - \sigma_{13}^{(0)} \frac{\partial^2 r^{-1}}{\partial \chi_3^2} \right]$$

$$\Omega_3^*(\underline{r}) = \frac{5R_0^3(1-\sigma)}{\mu(7-5\sigma)} \left[\sigma_{12}^{(0)} \frac{\partial^2 r^{-1}}{\partial \chi_2^2} + \sigma_{13}^{(0)} \frac{\partial^2 r^{-1}}{\partial \chi_3 \partial \chi_2} - \sigma_{12}^{(0)} \frac{\partial^2 r^{-1}}{\partial \chi_1^2} - \sigma_{23}^{(0)} \frac{\partial^2 r^{-1}}{\partial \chi_3 \partial \chi_1} \right] \quad (3.13.14)$$

⁽¹⁾ The notation of the present study differs slightly from that used by Landau and Lifshitz, for equivalence: $\sigma_{ij}^{(1)} \equiv \sigma_{ij}^{(0)}$, $\sigma_{ij}^* \equiv -\sigma_{ij}^{(1)}$, $u_i^* \equiv -u_i^{(1)}$, where $\sigma_{ij}^{(0)}$ is the initial field and $\sigma_{ij}^{(1)}$ is the change in the equilibrium stress field in the notation of the authors.

$$\begin{aligned} \sigma_{ik}^*(\underline{r}) = & -\frac{1}{(7-5\sigma)} \left(\frac{R_0}{r}\right)^3 \sigma_{ik}^{(0)} \left\{ 5(1-2\sigma) + 3\left(\frac{R_0}{r}\right)^2 \right\} + \frac{15}{(7-5\sigma)} \left(\frac{R_0}{r}\right)^3 \left\{ \left(\frac{R_0}{r}\right)^2 - \sigma \right\} \times \\ & \times (\sigma_{il}^{(0)} n_k n_l + \sigma_{kl}^{(0)} n_l n_i) + \frac{15}{2(7-5\sigma)} \left(\frac{R_0}{r}\right)^3 \left\{ 5 - 7\left(\frac{R_0}{r}\right)^2 \right\} \sigma_{lm}^{(0)} n_l n_m n_k \\ & + \frac{15}{2(7-5\sigma)} \left(\frac{R_0}{r}\right)^3 \left\{ 2\sigma + \left(\frac{R_0}{r}\right)^2 - 1 \right\} \delta_{ik} \sigma_{lm}^{(0)} n_l n_m \end{aligned} \quad (3.13.15)$$

where

$$(n_k) = (n_1, n_2, n_3) = (\sin \theta \cos \phi, \sin \theta \sin \phi, \cos \theta) = \mathbf{x}_k / r$$

The dilatation and rotation are clearly harmonic functions and may be put in the form of equation (3.13.4), thus

$$\Theta^*(\underline{r}) = \frac{1}{r^3} \sum_{m=0}^2 \left\{ \alpha_{2m} \cos m\phi + \beta_{2m} \sin m\phi \right\} P_2^m(\cos \theta) \quad (3.13.16)$$

$$\Omega_j^*(\underline{r}) = \frac{1}{r^3} \sum_{m=0}^2 \left\{ \gamma_{2m}^{(j)} \cos m\phi + \delta_{2m}^{(j)} \sin m\phi \right\} P_2^m(\cos \theta)$$

where, from Appendix 1, one has immediately ($m = 0, 1, 2$)

$$(\alpha_{2m}) = \frac{5(1-2\sigma)}{\mu(7-5\sigma)} R_0^3 \begin{pmatrix} 0 & \sigma_{13}^{(0)} & 0 \end{pmatrix} \quad (3.13.17)$$

$$(\beta_{2m}) = \frac{5(1-2\sigma)}{\mu(7-5\sigma)} R_0^3 \begin{pmatrix} 0 & \sigma_{23}^{(0)} & \sigma_{12}^{(0)}/2 \end{pmatrix}$$

$$(\gamma_{2m}^{(j)}) = \begin{pmatrix} \gamma_{20}^{(1)} & \gamma_{21}^{(1)} & \gamma_{22}^{(1)} \\ \gamma_{20}^{(2)} & \gamma_{21}^{(2)} & \gamma_{22}^{(2)} \\ \gamma_{20}^{(3)} & \gamma_{21}^{(3)} & \gamma_{22}^{(3)} \end{pmatrix} = \begin{pmatrix} 3\sigma_{23}^{(0)} & \sigma_{12}^{(0)} & \sigma_{23}^{(0)}/2 \\ -3\sigma_{13}^{(0)} & 0 & \sigma_{13}^{(0)}/2 \\ 0 & -\sigma_{23}^{(0)} & -\sigma_{12}^{(0)} \end{pmatrix} \frac{5(1-\sigma)R_0^3}{\mu(7-5\sigma)} \quad (3.13.18)$$

$$(\delta_{2m}^{(j)}) = \begin{pmatrix} \delta_{20}^{(1)} & \delta_{21}^{(1)} & \delta_{22}^{(1)} \\ \delta_{20}^{(2)} & \delta_{21}^{(2)} & \delta_{22}^{(2)} \\ \delta_{20}^{(3)} & \delta_{21}^{(3)} & \delta_{22}^{(3)} \end{pmatrix} = \begin{pmatrix} 0 & 0 & -\sigma_{13}^{(0)}/2 \\ 0 & -\sigma_{12}^{(0)} & \sigma_{23}^{(0)}/2 \\ 0 & \sigma_{13}^{(0)} & 0 \end{pmatrix} \frac{5(1-\sigma) R_0^3}{\mu(7-5\sigma)} \quad (3.13.19)$$

It is seen from these results that the initial value field is such that $l > 1$, as was previously inferred. Indeed only the quadrupole field ($l = 2$) is present.

Therefore, the dynamic dilatation and rotation fields associated with the relaxation of stress in the region surrounding the shock induced "crushed zone" of radius R_0 is, from equations (3.13.7), (3.13.8) and (3.13.17) through (3.13.19)

$$\tilde{\Theta}^{(1)}(\underline{x}, \omega) = \sum_{m=0}^2 \{ A_{2m}(\omega) \cos m\varphi + B_{2m}(\omega) \sin m\varphi \} h_2^{(2)}(k_p R) P_2^m(\cos \theta) \quad (3.13.20)$$

$$\tilde{\Omega}_j^{(1)}(\underline{x}, \omega) = \sum_{m=0}^2 \{ C_{2m}^{(j)}(\omega) \cos m\varphi + D_{2m}^{(j)}(\omega) \sin m\varphi \} h_2^{(2)}(k_s R) P_2^m(\cos \theta)$$

with ($m = 0, 1, 2$)

$$\begin{pmatrix} A_{2m} \\ B_{2m} \end{pmatrix} = \frac{5(1-2\sigma)}{\mu(7-5\sigma)} \left(\frac{R_0}{V_p} \right) (k_p R_0)^2 e^{ik_p(1-V_p/V_e)R_0} \begin{pmatrix} 0 & \sigma_{13}^{(0)} & 0 \\ 0 & \sigma_{23}^{(0)} & \sigma_{12}^{(0)}/2 \end{pmatrix} \\ \times \sum_{s=0}^{\infty} (s+1) \left[1 - \left(\frac{R_0}{R_s} \right)^{s+2} \right] \frac{(-2ik_p R_0)^{s+2}}{\Gamma(s+6)} \quad (3.13.21)$$

$$(C_{2m}^{(j)}) = \frac{5(1-\sigma)}{\mu(7-5\sigma)} \left(\frac{R_0}{V_s}\right) (k_s R_0)^2 e^{ik_s(1-V_s/V_k)R_0} \begin{pmatrix} 3\sigma_{23}^{(0)} & \sigma_{12}^{(0)} & \sigma_{23}^{(0)}/2 \\ -3\sigma_{13}^{(0)} & 0 & \sigma_{13}^{(0)}/2 \\ 0 & -\sigma_{23}^{(0)} & -\sigma_{12}^{(0)} \end{pmatrix} \\ \times \sum_{s=0}^{\infty} (s+1) \left[1 - \left(\frac{R_0}{R_s}\right)^{s+2}\right] \frac{(-2ik_s R_0)^{s+2}}{\Gamma(s+6)} \quad (3.13.22)$$

$$(D_{2m}^{(j)}) = \frac{5(1-\sigma)}{\mu(7-5\sigma)} \left(\frac{R_0}{V_s}\right) (k_s R_0)^2 e^{ik_s(1-V_s/V_k)R_0} \begin{pmatrix} 0 & 0 & -\sigma_{13}^{(0)}/2 \\ 0 & -\sigma_{12}^{(0)} & \sigma_{23}^{(0)}/2 \\ 0 & \sigma_{13}^{(0)} & 0 \end{pmatrix} \\ \times \sum_{s=0}^{\infty} (s+1) \left[1 - \left(\frac{R_0}{R_s}\right)^{s+2}\right] \frac{(-2ik_s R_0)^{s+2}}{\Gamma(s+6)} \quad (3.13.23)$$

Here $m = 0, 1, 2$, and $j = 1, 2, 3$ for the components of the rotation.

The coefficients have been condensed to matrix form where the index m is used as a column index. Thus for example

$$(C_{2m}^{(j)}) = \begin{pmatrix} C_{20}^{(1)} & C_{21}^{(1)} & C_{22}^{(1)} \\ C_{20}^{(2)} & C_{21}^{(2)} & C_{22}^{(2)} \\ C_{20}^{(3)} & C_{21}^{(3)} & C_{22}^{(3)} \end{pmatrix}$$

The displacement field is, from the transformed equations of motion

$$\tilde{y}_j(\underline{r}, \omega) = -\frac{1}{k_p^2} \frac{\partial \theta}{\partial x_j} + \frac{2}{k_s^2} \epsilon_{jkl} \frac{\partial \tilde{\Omega}_l}{\partial x_k} \quad (3.13.24)$$

and using the formulas expressed in Appendix 4, the spherical components of the displacement \tilde{y}_r , \tilde{y}_θ and \tilde{y}_ϕ may be obtained. In general, and specifically in the present case, the nature of the radiation field is much more apparent from an inspection of the solutions for the dilatation and rotation than from a similar consideration of

the displacement components. For the present it is sufficient to note that the solutions show that the dilatation and rotation components of the field exhibit a quadrupole radiation pattern around the source. A more detailed investigation of this radiation field will be made in the following chapter.

Perhaps the most important property of these solutions is the ease with which they may be transformed to other coordinate systems and into other types of curvilinear coordinates. As has been indicated in section 2.8, the transformation to a system of spherical coordinates with origin at the center of a spherical earth is possible. In the present case it is only necessary to translate the origin of coordinates along the z axis with no rotations, so that with r' , θ' and ϕ' the coordinates of an arbitrary point with respect to the new system of coordinates and r_0 the separation of the new and old origins, then

$$\tilde{\Theta}^{(1)}(\underline{r}', \omega) = \sum_{l=0}^{\infty} \sum_{k=-l}^l a_{lk}(r', \omega) P_l^k(\cos \theta') e^{-ik\phi'} \quad (3.13.25)$$

$$\tilde{\Omega}_j^{(1)}(\underline{r}', \omega) = \sum_{l=0}^{\infty} \sum_{k=-l}^l C_{lk}^{(j)}(r', \omega) P_l^k(\cos \theta') e^{-ik\phi'}$$

with

$$C_{lk}(r', \omega) = \begin{cases} (2l+1) \frac{(l-|k|)!}{(l+|k|)!} j_l(k_p r') \left\{ i^{l-2} \alpha_{2,-k} \sum_{p=l-2}^{l+2} a_p h_p^{(2)}(k_p r_0) \right\} \\ \text{for } r' < r_0 \\ (2l+1) \frac{(l-|k|)!}{(l+|k|)!} j_l(k_p r_0) \left\{ i^{l-2} \alpha_{2,-k} \sum_{p=l-2}^{l+2} a_p h_p^{(2)}(k_p r') \right\} \\ \text{for } r' > r_0 \end{cases} \quad (3.13.26)$$

$$c_{lk}^{(j)}(r', \omega) = \begin{cases} \frac{(2l+1)(l-|k|)!}{(l+|k|)!} j_l(k_s r') \left\{ i^{l-2} \beta_{2,-k}^{(j)} \sum_{p=l-2}^{l+2} a_p h_p^{(2)}(k_s r_0) \right\} \\ \text{for } r' < r_0 \\ \frac{(2l+1)(l-|k|)!}{(l+|k|)!} j_l(k_s r_0) \left\{ i^{l-2} \beta_{2,-k}^{(j)} \sum_{p=l-2}^{l+2} a_p h_p^{(2)}(k_s r') \right\} \\ \text{for } r' > r_0 \end{cases} \quad (3.13.27)$$

with

$$a_{2k} = \begin{cases} \frac{1}{2} (A_{2k} - iB_{2k}); & \text{for } k > 0 \\ A_{20}; & \text{for } k = 0 \\ \frac{1}{2} \frac{(2+|k|)!}{(2-|k|)!} (A_{2k} + iB_{2k}); & \text{for } k < 0 \end{cases}$$

$$\beta_{2k}^{(j)} = \begin{cases} \frac{1}{2} (C_{2k}^{(j)} - iD_{2k}^{(j)}) ; & \text{for } k > 0 \\ C_{20}^{(j)} ; & \text{for } k = 0 \\ \frac{1}{2} \frac{(2+|k|)!}{(2-|k|)!} (C_{2k}^{(j)} + iD_{2k}^{(j)}) ; & \text{for } k < 0 \end{cases}$$

and where, from section 2.8 the constants a_p are, in the present case, given by

$$a_p \equiv a(|k|, |k|; p, 2, l) = \frac{(2p+1)(l-p+1)!!}{(2+p-l)!!(l+p-2)!!(p+l+3)!!}$$

$$\times \sum_{j=0}^{p-2/|k|} \binom{p-2/|k|}{j} \frac{(j+|k|+2)!(l-|k|-j+p)!}{(2-j-|k|)!(l+|k|+j-p)!} e^{i\pi(|k|+j+\frac{p-l}{2}+1)}$$

The index p ranges through the set $l+2, l, l-2,$

Likewise, one has the results given by the equations (2.8.5)

through (2.8.7) for the transformation of the solution to cylindrical or rectangular coordinates. Thus the solutions for induced tectonic radiation are in these systems

$$\begin{aligned} \tilde{\Theta}(\rho, z, \phi; \omega) = \sum_{m=0}^{\infty} \left\{ A'_{2m} \cos m\phi + B'_{2m} \sin m\phi \right\} \int_0^{\infty} J_m(k\rho) P_2^{(m)} \left\{ \frac{(k_p^2 - k^2)^{1/2}}{k_p} \right\} \\ \times \frac{e^{-i(k_p^2 - k^2)^{1/2} z}}{(k_p^2 - k^2)^{1/2}} k dk \end{aligned} \quad (3.13.28)$$

$$\begin{aligned} \tilde{\Omega}_j(\rho, z, \phi; \omega) = \sum_{m=0}^{\infty} \left\{ C_{2m}^{(j)'} \cos m\phi + D_{2m}^{(j)'} \sin m\phi \right\} \int_0^{\infty} J_m(k\rho) P_2^{(m)} \left\{ \frac{(k_s^2 - k^2)^{1/2}}{k_s} \right\} \\ \times \frac{e^{-i(k_s^2 - k^2)^{1/2} z}}{(k_s^2 - k^2)^{1/2}} k dk \end{aligned} \quad (3.13.29)$$

for the cylindrical coordinates and

$$\begin{aligned} \tilde{\Theta}(x, y, z; \omega) = \frac{1}{2\pi} \sum_{m=0}^{\infty} \int_{-\infty}^{\infty} \int_{-\infty}^{\infty} \left(A'_{2m} \left[\left\{ \frac{k_1 + ik_2}{k_p} \right\}^m + \left\{ \frac{k_1 - ik_2}{k_p} \right\}^m \right] \right. \\ \left. + i B'_{2m} \left[\left\{ \frac{k_1 + ik_2}{k_p} \right\}^m - \left\{ \frac{k_1 - ik_2}{k_p} \right\}^m \right] \right) P_2^{(m)} \left\{ \frac{(k_p^2 - k_3^2)^{1/2}}{k_p} \right\} \\ \times \frac{\exp \{ ik_1 x + ik_2 y - i(k_p^2 - k_3^2)^{1/2} z \}}{(k_p^2 - k_3^2)^{1/2}} dk_1 dk_2 \end{aligned} \quad (3.13.30)$$

$$\begin{aligned} \tilde{\Omega}_j(x, y, z; \omega) = \frac{1}{2\pi} \sum_{m=0}^{\infty} \int_{-\infty}^{\infty} \int_{-\infty}^{\infty} \left(C_{2m}^{(j)'} \left[\left\{ \frac{k_1 + ik_2}{k_s} \right\}^m + \left\{ \frac{k_1 - ik_2}{k_s} \right\}^m \right] \right. \\ \left. + i D_{2m}^{(j)'} \left[\left\{ \frac{k_1 + ik_2}{k_s} \right\}^m - \left\{ \frac{k_1 - ik_2}{k_s} \right\}^m \right] \right) P_2^{(m)} \left\{ \frac{(k_s^2 - k_3^2)^{1/2}}{k_s} \right\} \\ \times \frac{\exp \{ ik_1 x + ik_2 y - i(k_s^2 - k_3^2)^{1/2} z \}}{(k_s^2 - k_3^2)^{1/2}} dk_1 dk_2 \end{aligned} \quad (3.13.31)$$

in rectangular coordinates. ⁽¹⁾ In these expressions the coefficients A_{2m}' etc. are related to those in (3.13.21) through (3.13.23), by

$$\begin{pmatrix} A_{2m}' \\ B_{2m}' \end{pmatrix} = (-1)^{m-1} (k_p)^{-1} \begin{pmatrix} A_{2m} \\ B_{2m} \end{pmatrix}; \quad \begin{pmatrix} C_{2m}^{(j)'} \\ D_{2m}^{(j)'} \end{pmatrix} = (-1)^{m-1} (k_s)^{-1} \begin{pmatrix} C_{2m}^{(j)} \\ D_{2m}^{(j)} \end{pmatrix}$$

In the application of these results to wave propagation in a layered model of the earth it is usually convenient to use (3.13.25) for the long period radiation where the curvature will be an important consideration and (3.13.30) or (3.13.31) for shorter periods and for distances reasonably close to the source where the effects of curvature are unimportant. In this latter case a plane layered model of the earth is adequate. The application of these results to spherical or plane layered earth models is quite straightforward, inasmuch as the solutions have been put in the form of the solutions for the homogeneous equations of motion (equations (2.2.15) through (2.2.17) and the discussion relevant to them).

(1) Here

$$P_n^{(m)}(z) \equiv \left(\frac{d}{dz} \right)^m P_n(z)$$

$$\overline{P}_n^m(z) = (z^2 - 1)^{m/2} \frac{d^m}{dz^m} P_n(z)$$

3.14. Tectonic Radiation Due to Spontaneous Rupture in a Homogeneously Prestrained Medium

Formal expansions for the radiation field associated with several models of spontaneous rupture have been obtained in sections 3.11 and 3.12. These representations are valid for the growth or propagation of a rupture zone within an arbitrarily stressed medium. As in the previous section however, the initial stress field will be taken to be homogeneous and pure shear. More general cases can be investigated in the future should this assumption prove too strong.

In the derivations of all these field representations, it has been assumed that the multipole coefficients for the equilibrium field could be expanded in the forms

$$\begin{pmatrix} a_{nm}(\tau) \\ \beta_{nm}(\tau) \end{pmatrix} = \sum_{P \geq 0} \begin{pmatrix} A_{nm}^{(p)} \\ B_{nm}^{(p)} \end{pmatrix} \tau^P \quad (3.14.1)$$

$$\begin{pmatrix} \gamma_{nm}^{(j)}(\tau) \\ \delta_{nm}^{(j)}(\tau) \end{pmatrix} = \sum_{P \geq 0} \begin{pmatrix} j C_{nm}^{(p)} \\ j D_{nm}^{(p)} \end{pmatrix} \tau^P$$

In the course of calculating the equilibrium fields for the various rupture models in this section, this unfinished business will be concluded and the assertion will be shown to be valid.

In view of the availability of the results for the change in the equilibrium field in the vicinity of a spherical rupture, the propagating spherical rupture model will be treated first. In particular, from

section 3.13, the change in the equilibrium field at a source time τ is

$$\Theta^*(\underline{r}, \tau) = \frac{1}{R^3} \sum_{m=0}^2 \left\{ \alpha_{2m}(\tau) \cos m\varphi + \beta_{2m}(\tau) \sin m\varphi \right\} P_2^m(\cos\theta) \quad (3.14.2)$$

$$\Omega_j^*(\underline{r}, \tau) = \frac{1}{R^3} \sum_{m=0}^2 \left\{ \gamma_{2m}^{(j)}(\tau) \cos m\varphi + \delta_{2m}^{(j)}(\tau) \sin m\varphi \right\} P_2^m(\cos\theta)$$

where

$$(\alpha_{2m}(\tau)) = \frac{5(1-2\sigma)}{\mu(7-5\sigma)} [R(\tau)]^3 (0 \quad \sigma_{13}^{(0)} \quad 0)$$

$$(\beta_{2m}(\tau)) = \frac{5(1-2\sigma)}{\mu(7-5\sigma)} [R(\tau)]^3 (0 \quad \sigma_{23}^{(0)} \quad \sigma_{12}^{(0)}/2)$$

$$(\gamma_{2m}^{(j)}(\tau)) = \frac{5(1-2\sigma)}{\mu(7-5\sigma)} [R(\tau)]^3 \begin{pmatrix} 3\sigma_{23}^{(0)} & \sigma_{12}^{(0)} & \sigma_{23}^{(0)}/2 \\ -3\sigma_{13}^{(0)} & 0 & \sigma_{13}^{(0)}/2 \\ 0 & -\sigma_{23}^{(0)} & -\sigma_{12}^{(0)} \end{pmatrix} \quad (3.14.3)$$

$$(\delta_{2m}^{(j)}(\tau)) = \frac{5(1-\sigma)}{\mu(7-5\sigma)} [R(\tau)]^3 \begin{pmatrix} 0 & 0 & -\sigma_{13}^{(0)}/2 \\ 0 & -\sigma_{12}^{(0)} & \sigma_{23}^{(0)}/2 \\ 0 & \sigma_{13}^{(0)} & 0 \end{pmatrix}$$

The rupture radius as a function of the source time is, from equation (3.10.18)

$$R(\tau) = \frac{b_0}{a_0} \left(2 - \frac{v_R \tau}{a_0} \right) v_R \tau \quad (3.14.4)$$

Incorporating this definition in the results (3.14.3) and recasting the expressions into the form of (3.14.1) gives

$$\begin{pmatrix} \alpha_{2m}(\tau) \\ \beta_{2m}(\tau) \end{pmatrix} = \sum_{P \geq 3}^6 \begin{pmatrix} A_{2m}^{(P)} \\ B_{2m}^{(P)} \end{pmatrix} \tau^P \quad (3.14.5)$$

$$\begin{aligned} A_{2m}^{(P)} &= \left(A_{2m}^{(3)}, -\frac{3}{2} \left(\frac{V_R}{a_0} \right) A_{2m}^{(3)}, \frac{3}{4} \left(\frac{V_R}{a_0} \right)^2 A_{2m}^{(3)}, -\frac{1}{8} \left(\frac{V_R}{a_0} \right)^3 A_{2m}^{(3)} \right) \\ B_{2m}^{(P)} &= \left(B_{2m}^{(3)}, -\frac{3}{2} \left(\frac{V_R}{a_0} \right) B_{2m}^{(3)}, \frac{3}{4} \left(\frac{V_R}{a_0} \right)^2 B_{2m}^{(3)}, -\frac{1}{8} \left(\frac{V_R}{a_0} \right)^3 B_{2m}^{(3)} \right) \\ A_{2m}^{(3)} &= \frac{5(1-2\sigma)}{\mu(7-5\sigma)} (2\alpha_0^{(2)} V_R)^3 \begin{pmatrix} 0 & \sigma_{13}^{(0)} & 0 \end{pmatrix} \\ B_{2m}^{(3)} &= \frac{5(1-2\sigma)}{\mu(7-5\sigma)} (2\alpha_0^{(2)} V_R)^3 \begin{pmatrix} 0 & \sigma_{23}^{(0)} & \sigma_{12}^{(0)}/2 \end{pmatrix} \end{aligned} \quad (3.14.6)$$

$$\begin{pmatrix} \gamma_{2m}^{(j)}(\tau) \\ \delta_{2m}^{(j)}(\tau) \end{pmatrix} = \sum_{P \geq 3}^6 \begin{pmatrix} j C_{2m}^{(P)} \\ j D_{2m}^{(P)} \end{pmatrix} \tau^P \quad (3.14.6)$$

$$\begin{aligned} j C_{2m}^{(P)} &= \left(j C_{2m}^{(3)}, -\frac{3}{2} \left(\frac{V_R}{a_0} \right) j C_{2m}^{(3)}, \frac{3}{4} \left(\frac{V_R}{a_0} \right)^2 j C_{2m}^{(3)}, -\frac{1}{8} \left(\frac{V_R}{a_0} \right)^3 j C_{2m}^{(3)} \right) \\ j D_{2m}^{(P)} &= \left(j D_{2m}^{(3)}, -\frac{3}{2} \left(\frac{V_R}{a_0} \right) j D_{2m}^{(3)}, \frac{3}{4} \left(\frac{V_R}{a_0} \right)^2 j D_{2m}^{(3)}, -\frac{1}{8} \left(\frac{V_R}{a_0} \right)^3 j D_{2m}^{(3)} \right) \end{aligned}$$

$$j C_{2m}^{(3)} = \frac{5(1-\sigma)}{\mu(7-5\sigma)} (2\alpha_0^{(2)} V_R)^3 \begin{pmatrix} 3 \sigma_{23}^{(0)} & \sigma_{12}^{(0)} & \sigma_{23}^{(0)}/2 \\ -3 \sigma_{13}^{(0)} & 0 & \sigma_{13}^{(0)}/2 \\ 0 & -\sigma_{23}^{(0)} & -\sigma_{12}^{(0)} \end{pmatrix} \quad (3.14.7)$$

$$j D_{2m}^{(3)} = \frac{5(1-\sigma)}{\mu(7-5\sigma)} (2\alpha_0^{(2)} V_R)^3 \begin{pmatrix} 0 & 0 & -\sigma_{13}^{(0)}/2 \\ 0 & -\sigma_{12}^{(0)} & \sigma_{23}^{(0)}/2 \\ 0 & \sigma_{13}^{(0)} & 0 \end{pmatrix}$$

These results show that the change in the equilibrium field is dependent on r^{-3} and that the expansion (3.14.1) is also valid. Therefore the results of section 3.12 are appropriate and so for the case

$$1/10 \leq \alpha_0^{(2)} < 1/2$$

the radiation field is given by

$$\tilde{\Theta}^{(1)}(\underline{r}, \omega) = \sum_{l=2}^{\infty} \sum_{k=0}^l h_l^{(2)}(k_p R) \left[a_{lk}^{(1)}(\omega) \cos k\varphi + B_{lk}^{(1)}(\omega) \sin k\varphi \right] P_l^k(\cos \theta) \quad (3.14.8)$$

$$\tilde{\Theta}_j^{(1)}(\underline{r}, \omega) = \sum_{l=2}^{\infty} \sum_{k=0}^l h_l^{(2)}(k_s R) \left[C_{lk}^{(1)}(\omega) \cos k\varphi + D_{lk}^{(1)}(\omega) \sin k\varphi \right] P_l^k(\cos \theta)$$

with

$$\begin{aligned} \begin{pmatrix} A_{lk}^{(p)}(\omega) \\ B_{lk}^{(p)}(\omega) \end{pmatrix} &= (-1)^{l-1} \frac{\eta_2}{4V\rho} (4k_p a_0)^l \frac{\Gamma(l-k+1)}{\Gamma(3-k)} \sum_{p=3}^6 \left(\frac{2a_0}{\sqrt{R}} \right)^p \left(\frac{1}{2a_0} \right)^2 \begin{pmatrix} A_{2k}^{(p)} \\ B_{2k}^{(p)} \end{pmatrix} \\ &\times \sum_{l=0}^{l-2} \frac{(\alpha_0^{(2)}/2)^L}{\Gamma(L+1)} \times \frac{(1-2\alpha_0^{(2)})^{l-L-2}}{\Gamma(l-L-1)} \sum_{q=0}^{l-L-2} \frac{(l+p+L-2)}{(l+p+L+q-2)} \left\{ \left(\frac{d_2 R_0}{2a_0} \right)^\alpha \right. \\ &\times E_l^{(1)}(\eta_2, \alpha; 0; k_p R_0^{(2)}) + \left(\frac{q_2}{2} \right)^\alpha \sum_{N=0}^{\alpha} \frac{\Gamma(\alpha+1)}{\Gamma(\alpha-N+1)} \frac{(2/q-1)^N}{\Gamma(N+1)} \\ &\times E_l^{(1)}(\eta_2, N; R_0^{(2)}; k_p R_1^{(2)}) + E_l^{(1)}(\eta_2, 0; R_1^{(2)}; k_p R_5) \left. \right\} \quad (3.14.9) \\ &\times \frac{(-2i\eta_2 k_p a_0)^q}{\Gamma(q+1)} \end{aligned}$$

$$\begin{aligned}
 \begin{pmatrix} C_{lk}^{(j)}(\omega) \\ D_{lk}^{(j)}(\omega) \end{pmatrix} &= (-1)^{l-1} \frac{\xi_2}{4V_5} (4k_5 a_0)^l \frac{\Gamma(l-k+1)}{\Gamma(3-k)} \sum_{p=3}^l \left(\frac{2a_0}{V_k}\right)^p \left(\frac{1}{2a_0}\right)^2 \begin{pmatrix} j \\ i \end{pmatrix} \begin{pmatrix} C_{2k}^{(p)} \\ D_{2k}^{(p)} \end{pmatrix} \\
 &\times \sum_{L=0}^{l-2} \frac{(\alpha_0/2)^L}{\Gamma(L+1)} \frac{(1-2\alpha_0^{(2)})^{l-L-2}}{\Gamma(l-L-1)} \sum_{q=0}^{\infty} \frac{(l+p+L-2)}{(l+p+L+q-2)} \left\{ \left(\frac{d_2 b_0^{(2)}}{2a_0}\right)^\alpha \right. \\
 &\times E_l^{(1)}(\xi_2, \alpha; 0; k_5 R_0^{(2)}) + \left(\frac{q_2}{2}\right)^\alpha \sum_{N=0}^{\infty} \frac{\Gamma(\alpha+1)}{\Gamma(\alpha-N+1)} \frac{(2/q_2-1)^N}{\Gamma(N+1)} E_l^{(1)}(\xi_2, N; R_0^{(2)}; k_5 R_1^{(2)}) \\
 &\left. + E_l^{(1)}(\xi_2, 0; R_1^{(2)}; k_5 R_3) \right\} \frac{(-2i \xi_2 k_R a_0)^q}{\Gamma(q+1)} \tag{3.14.10}
 \end{aligned}$$

where

$$\alpha = l + p + q + k - 2$$

and

$$E_l^{(1)}(\mu, \alpha; R_0; KR) = \sum_{R=0}^{\infty} \frac{\Gamma(l+R+1)}{\Gamma(2l+R+2)} \left(\frac{1}{\alpha+R+2}\right) \left[1 - \left(\frac{R_0}{R}\right)^{R+\alpha+2}\right] \frac{(-2iKR)^{R+2}}{\Gamma(R+1)}$$

The parameters appearing in these results have the following definitions in terms of a_0 and b_0 , the final rupture dimensions of length and depth or width respectively:

$$\alpha_0^{(2)} = \frac{b_0}{a_0} \quad (\text{"form factor"})$$

$$f_2 = \left(\frac{1 - 2\alpha_0^{(2)}}{2\alpha_0^{(2)}} \right)$$

$$\beta_2 = \frac{3+4f_2-f_2^2}{2} + \frac{1}{2} [f_2^4+8f_2^3+26f_2^2+24f_2+8]^{1/2} \approx \frac{2}{\alpha_0^{(2)}} - 1$$

$$g_2 = [f_2^2+\beta_2]^{1/2} \left\{ 1 - \frac{\beta_2}{2} [f_2^2+\beta_2]^{-1} \right\} - f_2$$

$$\begin{aligned}
 h_2 &= \frac{1}{2a_o^{(2)}} [f_2^2 + \beta_2]^{-1/2} \\
 d_2 &= \left(\frac{1 - a_o^{(2)}}{1 - 2a_o^{(2)}} \right) & \eta_2 &= 1 - \frac{v_R}{v_p} \left[1 - \frac{3}{2} \left(\frac{b_o}{2a_o} \right)^3 \right] \\
 r_o^{(2)} &= \frac{(1 - 2a_o^{(2)})^2}{4a_o^{(2)}} a_o & \xi_2 &= 1 - \frac{v_R}{v_s} \left[1 - \frac{3}{2} \left(\frac{b_o}{2a_o} \right)^3 \right] \\
 r_1^{(2)} &= (\beta_2 + 1) a_o^{(2)} a_o & k_p &= \omega/v_p, \quad k_R = \omega/v_R
 \end{aligned}$$

The radial parameter R_s again denotes the volume within which essentially all the stress relaxation occurs. That is, it is the radius of the effective source volume. It is clear that in an application of this theory to the description of a near surface earthquake, an error will arise from the implicit assumption that stress relaxation takes place throughout a spherical volume surrounding the rupture. In actual fact this obviously cannot be the case since the medium does not extend beyond the bounding free surface. However, if the actual rupture zone is not too near the free surface, this error will be negligible since the contributions to the theoretically predicted field from the effective source region actually lying beyond the true boundary of the medium will arise from changes in the theoretical equilibrium field which are small compared to those near the rupture, so that the radiation contribution from this fictitious zone also be small.

The radiation field for this propagating spherical rupture is seen to correspond to a superposition of multipoles, the lowest being

a quadrupole term. The coefficients for the multipole terms are proportional to $[\Gamma(\ell+1)]^{-1}$ and so the multipole contributions fall off with increasing ℓ . Thus the quadrupole field is, on this simple minded basis, weighted more heavily than the higher multipoles. Clearly however, the dominant multipole contribution to the field at a given distance from the rupture will depend on the frequency range of the radiation observed, particularly in view of the factors $(k_p a_o)^\ell$ and $(k_s a_o)^\ell$ in these results. Thus, for frequencies at which these factors are appreciably greater than one, other higher multipoles may be dominant or at least comparable to the quadrupole term. In addition, the results show a rather complicated dependence on the source parameters. In view of this complexity, a numerical investigation of the coefficients as functions of ω and the source parameters is carried out in the following chapter.

The field for the case

$$a_o^{(2)} < 1/10$$

is obtained in exactly the same manner. The results are given by the equations (3.14.6) - (3.14.8) without modification, while the coefficients $G_{\ell k}$, etc., in the multipole or spherical wave expansions have the approximate values given by (3.12.49) and (3.12.50). Thus, with $n = 2$ in these latter relations

$$\begin{aligned}
 \begin{pmatrix} C_{\ell k}^{(p)}(\omega) \\ B_{\ell k}^{(p)}(\omega) \end{pmatrix} &= (-1)^{\ell-1} \frac{\eta_2}{4V_p} (4k_p a_0)^\ell \frac{\Gamma(\ell-k+1)}{\Gamma(3-k)} \sum_{p=3}^{\ell} \left(\frac{2a_0}{V_R}\right)^p \left(\frac{1}{2a_0}\right)^2 \begin{pmatrix} A_{2k}^{(p)} \\ B_{2k}^{(p)} \end{pmatrix} \\
 &\times \sum_{L=0}^{\ell-2} \frac{(\alpha_0^{(2)}/2)^L}{\Gamma(L+1)} \frac{(1-2\alpha_0^{(2)})^{\ell-L-2}}{\Gamma(\ell-L-1)} \sum_{q=0}^{\ell+L-2} \frac{(\ell+p+L-2)}{(\ell+p+L+q-2)} \\
 &\left\{ E_\ell^{(1)}(\eta_2, \alpha; 0; k_p R_2^{(2)}) + E_\ell^{(1)}(\eta_2, 0; R_2^{(2)}; k_p R_5) \right\} \frac{(-2i\eta_2 k_p a_0)^{q+2}}{\Gamma(q+1)} \quad (3.14.11)
 \end{aligned}$$

$$\begin{aligned}
 \begin{pmatrix} C_{\ell k}^{(j)}(\omega) \\ D_{\ell k}^{(j)}(\omega) \end{pmatrix} &= (-1)^{\ell-1} \frac{\xi_2}{4V_s} (4k_s a_0)^\ell \frac{\Gamma(\ell-k+1)}{\Gamma(3-k)} \sum_{p=3}^{\ell} \left(\frac{2a_0}{V_R}\right)^p \left(\frac{1}{2a_0}\right)^2 \begin{pmatrix} i C_{2k}^{(p)} \\ j D_{2k}^{(p)} \end{pmatrix} \\
 &\times \sum_{L=0}^{\ell-2} \frac{(\alpha_0^{(2)}/2)^L}{\Gamma(L+1)} \frac{(1-2\alpha_0^{(2)})^{\ell-L-2}}{\Gamma(\ell-L-1)} \sum_{q=0}^{\ell+L-2} \frac{(\ell+p+L-2)}{(\ell+p+L+q-2)} \\
 &\left\{ E_\ell^{(1)}(\xi_2, \alpha; 0; k_s R_2^{(2)}) + E_\ell^{(1)}(\xi_2, 0; R_2^{(2)}; k_s R_5) \right\} \frac{(-2i\xi_2 k_s a_0)^{q+2}}{\Gamma(q+1)} \\
 &\quad (3.14.12)
 \end{aligned}$$

with $\alpha = \ell + p + q + L - 2$. The parameters previously listed define most of the symbols appearing in these results and the additional parameters are defined by

$$b_2 = \frac{1}{1 - \alpha_0^{(2)}}, \quad r_2^{(2)} = 2(1 - \alpha_0^{(2)})a_0$$

The radiation field associated with an ellipsoidal rupture, whether of the propagating or expanding rupture variety, is dependent upon the multipole coefficients appropriate to the equilibrium field in the region surrounding an ellipsoidal, traction free boundary within

the prestressed medium. Therefore consider the formulation of this latter problem in the form given by the equations (3.7.10) - (3.7.17), that is for

$$\nabla^2 \underline{u}^* + \frac{1}{1-2\sigma} \nabla(\nabla \cdot \underline{u}^*) = 0 \quad (3.14.13)$$

$$\underline{u}^* = O(1/r^a), \quad a \leq 2$$

where, on the ellipsoidal boundary

$$(\sigma_{ij}^{(0)} - \sigma_{ij}^*) n_j = 0 \quad (3.14.14)$$

then solutions of (3.14.13) are

$$\underline{u}^* = \nabla(\phi + \underline{r} \cdot \underline{\omega}) - 4(1-\sigma)\omega \quad (3.14.15)$$

with the potentials ϕ and $\underline{\omega}$ given by

$$\nabla^2 \phi = 0, \quad \nabla^2 \underline{\omega} = 0 \quad (3.14.16)$$

Thus ϕ and the Cartesian components of $\underline{\omega}$ are harmonic functions. In view of the geometry of the boundary value problem, it is obviously best to treat the problem in ellipsoidal coordinates from the beginning. This system is described in Appendix 7. If the prestress field $\sigma_{ij}^{(0)}$ is prescribed as a homogeneous field in Cartesian coordinates, then it will be necessary to transform this representation to the ellipsoidal system. Thus adopting this initial description of the prestress field, the required transformed stress field is given in Appendix 7. Furthermore, it is of considerable advantage to use the Cartesian components

of the vector potential $\underline{\omega}$, expressed however in the ellipsoidal variables. In this case ϕ and the components ω_k , $k = 1, 2, 3$, may be treated together as harmonic functions. The expression of the stress σ_{ij}^* in terms of ϕ and the ω_k is also given in Appendix 7, so that the boundary conditions (3.14.14) take the form

$$\begin{aligned} \sigma_{\rho\mu}^* &= \sigma_{\rho\mu}^{(0)} \\ \sigma_{\rho\nu}^* &= \sigma_{\rho\nu}^{(0)} \\ \sigma_{\rho\rho}^* &= \sigma_{\rho\rho}^{(0)} \end{aligned} \quad (3.14.17)$$

on the ellipsoid surface $\rho = \text{constant}$, and these expressions provide the necessary conditions on the potentials to determine all arbitrary coefficients.

The potentials ϕ and ω_k are ellipsoidal harmonics, a description of the properties of these functions and a list of the first few are given in Appendix 8. The theory and notation employed is that given by Hobson (1931). Thus, in terms of the Lamé functions defined in Appendix 8

$$\begin{aligned} \phi(\rho, \mu, \nu) &= \sum_{n=0}^{\infty} \sum_{\sigma=0}^{2n+1} a_{n\sigma} F_n^\sigma(\rho) E_n^\sigma(\mu) E_n^\sigma(\nu) \\ \omega_k(\rho, \mu, \nu) &= \sum_{n=0}^{\infty} \sum_{\sigma=0}^{2n+1} C_{n\sigma}^{(k)} F_n^\sigma(\rho) E_n^\sigma(\mu) E_n^\sigma(\nu) \end{aligned} \quad (3.14.18)$$

Substitution of these solutions into the boundary conditions (3.14.17) gives a set of equations which determine the coefficients $a_{n\sigma}$ and

$c_{n\sigma}^{(k)}$. These equations are extremely cumbersome as is evident from the expressions given for the stresses and strains in Appendix 7, but it may be seen by inspection that the boundary conditions may be satisfied if the potentials are chosen to have the forms (expressed explicitly in terms of the functions and parameters given in Appendix 8)

$$\begin{aligned} \phi(\rho, \mu, \nu) = & a_{21} F_2'(\rho) \left\{ \mu^2 + \frac{1}{6}(\rho-4)\alpha \right\} \left\{ \nu^2 + \frac{1}{6}(\rho-4)\alpha \right\} \\ & + a_{22} F_2^2(\rho) \left\{ \mu^2 + \frac{1}{6}(\rho-4)\alpha \right\} \left\{ \nu^2 + \frac{1}{6}(\rho-4)\alpha \right\} \\ & + a_{23} F_2^3(\rho) \mu \nu \sqrt{k^2 - \mu^2} \sqrt{k^2 - \nu^2} + a_{24} F_2^4(\rho) \mu \nu \sqrt{\mu^2 - h^2} \sqrt{h^2 - \nu^2} \\ & + a_{25} F_2^5(\rho) \sqrt{\mu^2 - h^2} \sqrt{k^2 - \mu^2} \sqrt{h^2 - \nu^2} \sqrt{k^2 - \nu^2} \end{aligned} \quad (3.14.19)$$

$$\begin{aligned} \omega_1 = & C_{12}^{(1)} F_1^2(\rho) \sqrt{k^2 - \mu^2} \sqrt{k^2 - \nu^2} + C_{13}^{(1)} F_1^3(\rho) \sqrt{\mu^2 - h^2} \sqrt{h^2 - \nu^2} \\ \omega_2 = & C_{11}^{(2)} F_1'(\rho) \mu \nu + C_{12}^{(2)} F_1^2(\rho) \sqrt{k^2 - \mu^2} \sqrt{k^2 - \nu^2} \\ \omega_3 = & C_{11}^{(3)} F_1'(\rho) \mu \nu + C_{13}^{(3)} F_1^3(\rho) \sqrt{\mu^2 - h^2} \sqrt{h^2 - \nu^2} \end{aligned} \quad (3.14.20)$$

As a practical matter the coefficients in these solutions are obtained by substitution of these potentials into the stated boundary conditions and by then equating the coefficients of the independent functions of μ and ν to zero. The procedure is extremely arduous, but nevertheless poses no basic difficulties. Inasmuch as an acceptable rupture model has been obtained in the form of the propagating spherical rupture, the determination of these coefficients in terms of the ellipsoidal rupture dimensions, is not a pressing requirement for

the preliminary applications to be considered in the present study. Therefore the results as expressed in (3.14.19) - (3.14.20) are considered adequate for the purposes of the present study, and represent a starting point for future applications.

While it is deemed reasonable to postpone the explicit determination of the coefficients, it is however necessary to show that the dilatation and rotation derived from these potentials can be put in the form of a series of spherical harmonics as in (3.10.7), since this is required in the dynamical theory previously formulated. In particular it is necessary to compute the coefficients in a spherical harmonic expansion of the equilibrium field. This can be accomplished by transforming the ellipsoidal harmonics to spherical harmonics. This is done in Appendix 9, employing the operation relations given by Hobson (Chap. XI). Since the dilatation and rotation are related to the vector potential $\underline{\omega}$ by (Appendix 7, equation (7-13))

$$\Theta = -2(1 - 2\sigma) \frac{\partial \omega_k}{\partial x_k} \tag{3.14.2}$$

$$\Omega_i = -2(1 - \sigma) \epsilon_{ijk} \frac{\partial \omega_j}{\partial x_k}$$

then it is only necessary to consider the expansion of the potentials ω_k of (3.14.20). The required expansion is given by the results (9-7) through (9-9) in Appendix 9 and when incorporated in (3.14.21), gives the necessary spherical harmonic expansion for Θ and the components of $\underline{\Omega}$.

Therefore, in principle the proper expansions for the equili-

brium field have been obtained and the results of section 3.11 and 3.12 are directly applicable. Practical application of the results yet requires some rather tedious algebraic manipulation however and will be taken up in future studies.

As was the case in the previous section, it is possible to express the solutions for either the propagating or expanding rupture models in other coordinate systems by applying the results of section 2.8. Here the solutions for all the rupture models have the form of (3.14.2), which is, as required, also the same form as for the case of induced rupture. However in the present case the transformation is not quite as straightforward, since the source coordinates are fixed by the long (a) axis of the rupture ellipsoid. For the induced spherical rupture it was clearly possible to choose the source coordinates so that the z axis was either parallel to the earth's polar axis or normal to the earth's surface directly above the source, since the initial stress field could always be adjusted to conform to the system desired. For spontaneous rupture however, the rupture surface itself has been used to fix the coordinates so that a rotation of the source coordinates to a suitable fixed reference frame is eventually necessary for applications. In this way the remaining source parameters specifying the orientation of the rupture relative to the earth's surface (strike and dip) and its location relative to the polar and equatorial axes (hypo-center) will be incorporated in the solutions.

The solutions are best transformed by first expressing them

in a translated spherical system at the center of the earth, by the formulas (2.8.3) - (2.8.5) of section 2.8. The coordinate relationships involved are indicated in Figure 15. These results are obtained by mere substitution of (3.14.9) - (3.14.10), for example, in the indicated relations and need not be reproduced here. As a second step the boundary conditions fixing the coefficients in the homogeneous solutions would be applied to yield the complete solution in a layered spherical earth model. Such a solution would be expressed in terms of spherical coordinates relative to a system whose polar axis did not necessarily coincide with the rotational axis of the earth as in Figure 15. These solutions could however be expressed in a system coinciding with the rotational axis by utilizing the relationships between the surface harmonics in two relatively rotated systems. In particular Sato (1950b) has given explicit relationships suitable for computational purposes. These relations need not be given here since it seems sufficient, for the present study at least, only to make note of their existence in order to outline the general approach for future applications of the source solutions.

Thus, it seems clearly established that the general solutions obtained for spontaneous rupture can be transformed in a manner which allows the oscillations within a spherically layered earth model to be calculated. The solution will contain as parameters, the coordinates of the hypocenter of the source as well as the rupture orientation and dimensions, the initial stress field and the speed of rupture growth or propagation.

Chapter 4

PRELIMINARY APPLICATIONS OF THE THEORY

4.1. Introduction

The applications of the present chapter will be those which, while making use of the previous general theory, are the simplest and most straightforward. There will be no special attempt to follow the rather systematic development of the preceding chapters, but rather a few problems will be selected and treated in a rather preliminary and loosely connected fashion. Most of the applications considered are indicative and generally connected to some of the more ambitious applications that are envisioned for the future. Some of these programs are mentioned below. The following practical considerations will serve as an illustration of the potentialities of the theoretical solutions in the analysis of the many aspects of rupture phenomenon in the earth.

The most directly related applications of the theory are comparative studies designed to show the degree of accuracy with which the radiation field is predicted by one or the other of the models proposed in this study. Next, the inverse problem involving the prediction of the source parameters would be of even greater interest and importance. Unfortunately crucial uncertainties usually exist in the independent estimates of the source parameters. Therefore a rather wide range of source parameters could reasonably be used in a comparative study with a measured field and the results of such a study would not be very discriminating.

Ideally, a controlled experiment in which the source parameters are known with certainty is the most suitable approach at present. In this case the predicted field could be compared with that observed and the accuracy of the model assessed, while an estimate of the nature of the uncertainties in predicting source parameters by forcing a match of the fields could also be made. While the required control is, almost by definition, absent from occurrences of spontaneous rupture, some degree of control is present in the case of shock induced rupture associated with underground nuclear testing. Thus, while uncertainties in the source parameters are not totally absent, they are reduced to a relative minimum and it appears that underground nuclear explosions may provide the most controlled experiment available. ⁽¹⁾ Indeed the development of the theory for shock induced tectonic radiation has been, at least in part, motivated by the possibility of its use in a controlled experiment. Thus in the present chapter, many of the applications made are constructed to serve as a means of accurately predicting the radiation field through use of the available nuclear blast data.

The first order of business then is to show that tectonic energy release can and in fact does occur with such an explosion in prestressed media. Next, the detailed evaluation and subsequent comparative study of the radiation field from such a source would follow.

⁽¹⁾ Certainly laboratory modeling of a tectonic source is an alternative. However a realistic model of a tectonic source is non-existent and is probably some few years in the future.

In the present chapter the theoretical phase and amplitude spectrums for shock induced tectonic radiation are computed as is the expected energy release. Using Haskell's static theory for contained underground explosions, (Haskell, 1961), the radius of the rupture zone, as a function of explosive energy, is estimated and a theoretical "scaling law" for tectonic energy release versus explosive energy and initial stress is obtained. The tectonic energy release predicted by this law for several assumed prestress fields and known bomb yields is compared with the observed energy of anomalous radiation⁽¹⁾ from a particular underground explosion experiment. From these considerations, the inevitability of tectonic energy release from explosions in prestressed media is established. Further, the conjecture that all or nearly all of the anomalous radiation observed arises from this particular phenomenon becomes, as a consequence of the relatively low prestress values that are required in order to give an energy release of the order of that observed, highly plausible. Indeed, in view of other supporting evidence such as the occurrence of rather distant associated after-shocks, a conclusion to this effect is almost inescapable. Since the magnitude of the stress field required to explain the anomalous radiation is reasonable, then it is concluded that a controlled comparative study is possible, the only unknown source parameter being the orientation of this initial stress

⁽¹⁾The anomalous radiation is that part of the observed radiation field which cannot be assigned directly to the conversion of the shock wave to a compressional elastic wave.

field. Under these conditions a comparative study of the controlled type desired could be made with minimum uncertainty by varying the orientation of the initial stress field to give the best fit to the observed radiation. Thus, the radiation field computed should provide the means of predicting the detailed nature of the anomalous radiation and in addition the means of deducing the detailed nature of the initial stress field. A study of shock induced radiation can therefore lead to estimates of the prestress condition of the material near the earth's surface in tectonically active regions. Further, the stress field determined in this manner could be used to predict the radiation field from any nearby earthquakes, assuming the initial stress field to be regional in character. In this way a reasonably controlled comparative study of the two types of tectonic source could also be made. In addition one might at least hope that some easily detectible differences between the radiation fields from underground explosions and earthquakes could be substantiated in the course of such a comparative study.

All of the more extensive and detailed applications for continued study are basically related to the preliminary applications considered in this chapter. Some of these projected studies are as follows:

- (1) Numerical computation of the surface wave and forced oscillation excitation for all source models as a function of period and the source parameters for use in comparative studies.

- (2) Extended computations of body wave spectra, with consideration of propagation effects, especially on amplitudes. (Near surface reverberation, dissipation and dispersion effects, interference of the phases, refraction effects, etc.)
- (3) Energy calculations for all source models and comparison with "observed" values.
- (4) Computation of theoretical first motions for P and S waves and comparison with existing theory and observation.
- (5) Comparison of the observed near source static strain with that predicted theoretically.
- (6) Deduction of the rupture zone orientation and dimensions, the rupture velocity and nature of the initial tectonic stress field from measurements of the radiation from rupture sources, utilizing both body wave and surface wave amplitudes and phase information.
- (7) Coupled with (6), a comparison of rupture models in an effort to determine which rupture model best agrees with the amplitude and phase characteristics observed for a given rupture event.
- (8) Investigation of observed source characteristics with respect to epicenter and depth, to ascertain whether fundamental differences in source characteristics occur between different spatial domains.
- (9) Coupled with the comparative studies above, a simultaneous study of uniqueness and error estimation.

By and large these efforts at comparative studies are already

underway, although with greatly simplified source models. An accurate estimation of the source properties, especially the initial stress field, is probably the most important information to be obtained from a comparative study in view of the physical inferences that could be drawn on the basis of such information.

In the context of the above framework of experimental and applied work, the applications of this chapter are an attempt to accomplish the preliminary work required for an approach to any one of the detailed programs contemplated above.

4. 2. The Radiation Field from Natural Tectonic Sources as a Function of the Rupture Dynamics and Geometry

In order to utilize the theoretical predictions expressed in the previous chapter in a practical way, it is necessary to have the capability of expressing the radiation field numerically. Indeed it is imperative that the complicated representation be reduced to a simple and readily available numerical representation for comparison with the observed field if the applications suggested in (4.1) are to be realized. This is accomplished in the present study via a computer program which furnishes the radiation patterns for tectonic sources as predicted by the results of Chapter 3.

In particular the amplitude and phase of the direct radiation field from the propagating rupture source are computed as functions of frequency in terms of the multipole coefficients for the dilatation and rotation. In addition the amplitude at any frequency, or for any range of frequencies, is computed as a function of the azimuthal

angle around the source, providing then a means of completely specifying the directional properties of the field. These numerical results can of course be obtained for any distance and for any combination of initial stress, rupture velocity and so on. Examples are given in the present section to illustrate some of the important properties of the field.

Consider then the radiation patterns to be observed on a plane, corresponding to the surface of the earth, located a distance H away from the point of initial rupture. Two cases will be distinguished in this preliminary study, that is rupture corresponding to purely "strike slip" faulting and to "dip slip" faulting. In the former the direction of rupture propagation is parallel to the earth's surface while in the latter it is normal to and away from the surface. Figure 16 indicates these relationships schematically, wherein a surface azimuth λ and epicentral distance ρ are introduced. The direct radiation field from the source is projected on to this surface and the radiation patterns computed in terms of λ and ρ .

The computation of the source field involves, essentially, the computation of the multipole coefficients given by (3.14.9) or (3.14.11), as is appropriate. Figure 17 gives the amplitudes of the first few of these (i. e., for $\ell = 2, 3, 4$) as functions of frequency while Figure 18 indicates the phase variations. The particular rupture parameters chosen are given in Figure 17. The amplitude and phase characteristics of these coefficients can be described in terms of the ratio of radiated wavelength λ to the length of the

rupture zone a_0 . Here λ is $v_p T$ or $v_s T$, depending on the type of wave in question. Thus for $[a_0/\lambda] \ll 1$ the phases of all the coefficients are nearly constant and equal to zero (or 2π). The amplitudes on the other hand are widely separated and the various coefficients vary as $[a_0/\lambda]^\ell$, essentially. Thus the coefficients with the lowest values of ℓ dominate, that is, those with $\ell = 2$. The field is therefore quite simple in this long wavelength limit since the lowest order multipole completely dominates all others as is indicated in Figure 17. This will manifest itself in the theoretical radiation patterns as well. In the intermediate range where a_0/λ is approaching unity, the other multipole coefficients begin to become comparable to the quadrupole term ($\ell = 2$) and the dependence of the amplitudes on frequency is more complex, although yet approximately the same as in the long period range. The phases in this range vary relatively rapidly, although monotonically. Near $[a_0/\lambda] \sim 1$ a rather rapid transition occurs and a point is reached where the size of the coefficients is nearly the same and the slopes of the curves have decreased indicating, to first order, a power law dependence on the ratio $[a_0/\lambda]$ which is different than in the long period limit. The phase variation is somewhat similar in that a limiting value is approached at short periods. This period range is by far the most interesting in that it shows the effects of rupture growth and the causality effects associated with stress relaxation. The computations were carried out up to the radiation frequency corresponding to wavelengths of about the rupture length.

It should be emphasized that the variations of the coefficients shown in these figures as functions of frequency are to an appreciable extent independent of the rupture dimensions, but strongly dependent on the ratio $[a_0/\lambda]$. In particular the slopes and transition regions for these coefficients as functions of period depend almost entirely on this dimensionless ratio, so that effects can be scaled to represent any rupture length. The magnitudes of the individual multipole coefficients do however increase directly with the length of rupture and the magnitude of the initial stress field.

In order to demonstrate more clearly the nature of the field and its dependence on the rupture parameters, radiation patterns are shown for two extremes in the frequency range and for different orientations of the initial stress field. Thus at a period of 1.25 sec, corresponding for rotational waves to a wavelength such that $a_0/\lambda=0.65$, Figure 19 shows the radiation pattern for the dilatation and rotation components for a strike slip fault at a distance of about 300 km. These patterns show the displacement amplitude and phase as functions of the azimuthal angle around the source. The scale divisions for the amplitude are indicated for each separate radiation pattern. The arrow denotes the direction of rupture propagation and the x and z axes on the plane, representing the earth's surface, are also indicated (See Figure 16.) The depth of source H, is 3 km and the initial stress field is such that the corresponding strain is, in terms of the initial field parameters $s_{ij} = 2e_{ij}$,

$$e_{12} = \frac{1}{2} s_{12} = 0.0005$$

The patterns shown correspond to a superposition of the first four significant multipoles ($\ell = 2, \dots, 5$), and it is evident that at this period the individual multipoles superpose in such a way as to give a rather strong directional asymmetry, in the direction of rupture propagation. Thus with reference to the previous figures (17-18), this case corresponds to a period value at which the multipole coefficients are of comparable magnitude, although the magnitudes decrease with increasing order ℓ . In addition the amplitudes and phases are just such that the field has the expected asymmetry for radiation approaching the rupture dimensions. This property of tectonic sources has in effect been observed by Ben Menahem and Toksöz (1962) as was previously noted.

These particular computations show that both the amplitude and the phase is affected by the rupture growth and from this example and subsequent computations, it is observed that the phase is somewhat more sensitive to rupture growth. The relative magnitudes of dilatation and rotation for this particular case indicate that the dilatation is at least ten times smaller than any of the rotation components. The fact that P wave amplitudes are appreciably smaller than S wave amplitudes for tectonic sources is a well established fact, however the differences do not seemingly amount to so large a factor. However the spectral character of the P and S body phases is not known with any high degree of certainty, indeed little precise work has been done, so detailed conformation of this particular

aspect of the results may come when more detailed investigations are performed. It is, however, undoubtedly true that if a density change were incorporated or if the initial hydrostatic field were accounted for in the theory, then a larger dilatation field would result.

Of the field components shown, the rotational components (Ω_1 and Ω_3) corresponding to vertically polarized shear waves (SV) are large compared to the other motions. This result is dependent on the orientation of the initial shear field relative to the rupture.

Figure 20 shows the effect of a change in orientation of the initial shear field. In this case the only parameter changed from the previous computation in Figure 19 is the initial strain, taken as $e_{23} = 0.0005$. In this case it is interesting to note that asymmetrical radiation occurs, but that the largest motion, corresponding to Ω_1 , is in the opposite direction to the rupture propagation. Thus constructive interference may occur either in the direction of rupture propagation or opposite to this direction. Both the phase and amplitude of Ω_1 show this effect. Ben Menahem's (1961) "directivity function" indicates a similar result for surface waves generated by a moving line source. All the other motions have "normal" directional properties and it appears then that SH and SV waves from the same source can show, simultaneously, opposing directional asymmetries. The affect is undoubtedly due to the propagation of the rupture zone but nevertheless depends on the relative orientation of the prestress with respect to the rupture zone, since this affect was not manifested in Figure 19. The phenomenon is further complicated by the dependence

on the rupture velocity.

Figure 21 shows the radiation patterns for the same rupture parameters as before but with yet a different orientation of the stress field. In this case the component Ω_2 of the rotation is larger than all others indicating large SH wave generation. Constructive interference occurs in a direction opposite to the direction of rupture propagation for this rotational component while the components for SV type motion and dilatation are normally directional and of nearly equal magnitude. From the three sets of radiation patterns in Figures 19 through 21 it is evident that the properties of the radiation field are strongly dependent upon the orientation of the initial stress field with respect to the rupture and the surface of measurement.

Figure 22 corresponds to the radiation patterns of Figure 19 for longer period radiation. In this case $[a_0/\lambda] \sim 0.16$ and so, corresponds to the intermediate range of frequencies where the quadrupole term is beginning to dominate the other multipole contributions. It is clear that the amplitude variation has lost most of its asymmetry at this longer period. A close inspection of the patterns does show a residual asymmetry along the line of rupture propagation, but it is slight. The phase asymmetry is observed to be somewhat more pronounced than that of the amplitudes. Figure 23 shows the radiation of 5 sec period for a stress distribution corresponding to that of Figure 21, with the other rupture parameters the same as well. Again the effect of the rupture propagation is slight.

It is clear from comparisons at these two periods then, that

at longer periods the tectonic source has essentially the properties of a simple quadrupole. The effects of rupture growth or propagation however continuously manifest themselves, becoming more and more pronounced at the higher frequencies. In particular, the volume effects of stress relaxation and rupture propagation for the model considered become noticeable for frequencies such that $[a_0/\lambda] > 2\pi$, that is, such that $ka_0 > 1$ where k is the wave number appropriate to the type of radiation in question. This phenomenon is well within the range of seismic observation and indeed for large earthquakes corresponds to the frequency range of maximum observed energy.

Figure 24 shows the radiation patterns for "dip slip" rupture, where the rupture propagation is away from the plane over which the field is projected as in Figure 16. The rupture parameters are the same as in the previous examples except for the orientation of the rupture. The stress field is taken to correspond to that considered in Figures 19 and 22. Thus it is clear that even at this relatively short period, there is no observed asymmetry due to rupture propagation. The reason for this is easy to visualize since the enhanced radiation amplitude is either in the direction of rupture growth or opposite to it and when projected on the plane normal to this direction cannot be seen. In a spherical earth however the asymmetry would be observed at distances such that the normal to the surface of observation is not coincident with the direction of rupturing.

In any event, it is clear that "dip slip" rupturing will appear, in terms of its radiation pattern, to be considerably different than

than "strike slip" rupturing. This implies that the effect of the rupture orientation with respect to the normal to the surface over which the field is observed, strongly affects the observed field symmetry.

The nature of the radiation field from a tectonic source is then, as is observed, most strongly influenced by the magnitude and orientation of the initial stress field and the rate and orientation of the rupture propagation. The examples of the present section have served to illustrate these properties in detail, but most important for future work is the existence of the means for rapid automatic computation of the multipole coefficients. Thus, coupled with the expansions given in section 2.8 and the theoretical considerations for the boundary value problem in layered earth models of section 2.2, these results can be used to compute the excitation of oscillation spectra for the earth in a relatively straightforward manner. Such computations then lead to comparisons with the observed spectrums and estimates of the initial stress and rupture parameters. On the other hand the present results can be used directly for prediction and comparison of body wave radiation.

4.3. Energy From Tectonic Sources

It has already been shown in section 3.8 that an estimate for the bounds on the energy E_r radiated from a tectonic source is given by

$$\frac{1}{2} \iiint_{V_1} \sigma_{ij}^* e_{ij}^* d\tau \leq E_r \leq \frac{1}{2} \iiint_{V_1} \sigma_{ij}^* e_{ij}^* d\tau + \iiint_{V_0} \mu e_{ij}^{(0)} e_{ij}^{(0)} d\tau \quad (4.3.1)$$

This relation will be used to compute the energy release due to shock induced rupture in a prestressed medium (Press and Archambeau, 1962).

Let the initial displacement field be

$$\underline{u}^{(0)} = s_{12} y \hat{e}_1 \quad (4.3.2)$$

and in this case the prestress is a pure shear field such that

$$\sigma_{12} = \mu s_{12}$$

The appropriate boundary value problem is that given by (3.7.6) and the general solution given by Love (1944) is, from (3.7.8)

$$\underline{u}^* = (B + Cr^2) \left(\frac{\partial}{\partial x_1}, \frac{\partial}{\partial x_2}, \frac{\partial}{\partial x_3} \right) \frac{x_1 x_2}{r^5} - \frac{3\lambda + 8\mu}{3(\lambda + \mu)} C \left(\frac{x_2}{r^3}, \frac{x_1}{r^3}, 0 \right) \quad (4.5.3)$$

where B and C are constants given by

$$B = \frac{3(\lambda + \mu)}{9\lambda + 14\mu} R^5 s_{12}^2, \quad C = - \frac{3(\lambda + \mu)}{9\lambda + 14\mu} R^3 s_{12}^2 \quad (4.3.4)$$

with R the rupture radius.

The strain differences e_{ij}^* are easily shown to have the form

$$e_{ij}^* = \frac{5BP_{ij}(\theta, \phi)}{r^5} + \frac{5CQ_{ij}(\theta, \phi)}{r^3} \quad (4.3.5)$$

where r , θ and ϕ are spherical coordinates and the matrices P_{ij} and Q_{ij} are given in the Appendix 10. On the other hand the initial strain is of course just

$$e_{12}^{(0)} = \frac{1}{2} s_{12} \quad (4.3.6)$$

in this case.

Substitution of these relations for the strains into the energy integrals of (4.5.1) yields upon integration

$$\frac{\mu s_{12}^2}{2} \left(\frac{4}{3} \pi R^3 \right) f\left(\frac{\mu}{\lambda}\right) \leq E_r \leq \frac{\mu s_{12}^2}{2} \left(\frac{4}{3} \pi R^3 \right) [1 + f\left(\frac{\mu}{\lambda}\right)] \quad (4.3.7)$$

with

$$f\left(\frac{\mu}{\lambda}\right) = \frac{378 + 1596\left(\frac{\mu}{\lambda}\right) + 1568\left(\frac{\mu}{\lambda}\right)^2}{576 + 1764\left(\frac{\mu}{\lambda}\right) + 1372\left(\frac{\mu}{\lambda}\right)^2}$$

The function $f\left(\frac{\mu}{\lambda}\right)$ is a rather slowly varying function of the ratio $\frac{\mu}{\lambda}$ and has bounds

$$\frac{2}{3} \leq f\left(\frac{\mu}{\lambda}\right) \leq 1.14$$

For the most common situation $\lambda \simeq \mu$ and

$$f(1) = 0.957 \simeq 1.0$$

Thus it would seem that about an equal amount of energy is released

from outside the rupture due to relaxation as was originally stored within the spherical rupture zone. Thus the bounds on the tectonic energy released are, approximately, between the total shear strain energy originally stored within the rupture zone and twice that value. As a conservative estimate, E_r will be taken as the lower bound, the energy originally stored within the rupture volume being at least in part assumed lost to the coherent radiation field. Thus for this induced rupture phenomenon the tectonic energy release is, approximately

$$E_r \simeq \frac{\mu_s^2}{2} \left(\frac{4}{3} \pi R^3 \right) f \left(\frac{\mu}{\lambda} \right) \quad (4.3.8)$$

It is clear from this expression that the energy release is critically dependent upon the volume of the rupture region created by the explosion. In the following section an estimate of the value of R for a given explosive energy will be made based on the static theory proposed by Haskell (1961). It can be seen that the likelihood of an appreciable tectonic energy release is critically dependent upon this estimate.

The energy release associated with natural rupture in the earth is likewise computed in the same manner, that is using (4.3.1) with the appropriate expressions for ellipsoidal rupture. The expressions given in section 3.14 for the equilibrium field in the neighborhood of such a rupture are appropriate, the integrations being straightforward but tedious. This particular computation will be left for future consideration.

4.4. Scaling Laws for Tectonic Energy Release Associated with Explosive Sources

The evidence in favor of the occurrence of appreciable tectonic energy release from several nuclear explosions has accumulated from a number of studies since the initial study of this possibility by Press and Archambeau (1961). These authors, following suggestions of the possibility by Porzel (1959) and Latter (1960), estimated the energy release by use of formula (4.3.8) and concluded, tentatively, that while such release of energy undoubtedly did occur, its affect on the radiation field observed would be small. It now appears that the magnitude of the affect was underestimated and that certain features of the radiation field are strongly affected.

The original phenomenon observed which suggested tectonic stress release was the large SH wave motion in the radiation field from some underground explosions of large energy, in particular the Ranier nuclear explosion. Since it is not difficult to show that no radiation of this sort would be generated by an ideal explosive source in a layered earth model, it was naturally concluded that some appreciable departure from the idealized model was responsible. A number of possibilities are apparent, in particular

- (1) Mode conversion of compressional or SV type motions along the path due to lateral inhomogeneities within the medium.
- (2) Strong inhomogeneities of structure or in the yield characteristics of the material in the source region leading to mode conversion essentially within the source volume itself.

- (3) Tectonic energy release due to stress relaxation in the elastic zone around the shock induced rupture volume.
- (4) Tectonic energy release due to secondary rupture arising from the existence of a weak zone and pre-existing stress which, when coupled to the pressure field from the explosion, results in failure (fracture) along the weak zone ("triggering of an earthquake").

The first of these possibilities was considered unlikely by Press and Archambeau inasmuch as the travel times of the SH phases indicated that they originated within the neighborhood of the explosion. In addition the abrupt initial motion associated with these waves is not indicative of mode conversion along a long path. Finally, the fact that many air explosions and earthquakes having almost no SH motion have been observed, indicates that very little mode conversion occurs along paths within the earth.

It is more difficult to choose among the remaining three. The second of the possibilities corresponds to the residue of all non linear behavior not inconsistent with the observation of SH motion generation within or very near the source volume. As such it is difficult to conclusively eliminate or, on the other hand, to accept on the basis of the available evidence. A different tactic may be adopted however, and that is to show that all the observations including SH wave radiation are consistent with tectonic energy release. Indeed tectonic release must occur, the question being only whether the affect is large enough to explain all the observations.

The necessity of tectonic release follows from the fact that the region in which the explosions took place is known to be tectonically active and numerous earthquakes have occurred nearby. From the previous theoretical considerations it follows that introduction of a cavity or crushed zone, as is associated with such an explosion, into a prestressed medium must result in the release of strain energy in the form of elastic waves.

The essential qualitative observations concern first, the fact that aftershocks have been observed from the near vicinity of the explosions (Press 1963). This indicates first the existence of a tectonic stress field which was probably a shear field since failure occurs most readily in this case, and second that a large and drastic readjustment must have occurred in this field resulting in creep phenomenon and eventually further rupture. In addition, Hoy (1963) has observed displacements within an active fault zone in the vicinity of one of the large detonations (37kT yield). In particular the motion was such as to create a vertical scarp with maximum displacement of 3 inches which could be traced 6000' north and 10,000' south from the point on the rupture closest to the explosion point, which was 3300' east of the fault. Thus the movement in the fracture zone centered at a point 2000' south of the point nearest the shot point rather than at this point. In addition the displacement on the fracture was down on the side toward the shot consistent with previous tectonic movement. If the movement had been due solely to the shock wave from the source, one would expect the displacement to have centered at

the point closest to the shot and that the motion would have been, if anything, upward on the side towards the shot since the explosion was centered at a depth of nearly 1500 ft. Hoy thus suggests tectonic stress release on essentially these grounds. In this case it would appear that both (3) and (4) of the possibilities listed occurred.

Not in all other cases in which anomalous SH wave radiation occurred was secondary rupture of this sort observed, but in such cases (3) alone could serve to explain the phenomenon.

More quantitatively, P waves observed from these explosions always show compressional form as expected for a purely explosive source. The release of tectonic energy is consistent with this observation inasmuch as the P wave has been shown to be much smaller than the SH motion for certain stress distributions associated with spontaneous rupture. This will also be shown to hold for shock induced rupture in the following section. Thus large SH wave motion can be produced, having in fact energies much larger than the energy associated with the observed P wave, without affecting to any discernible degree, the compressional first motions for the P waves from such a composite source.

Toksöz, Ben Menahem and Harkrider (1964) and Brune (1963) observed that the surface wave radiation patterns, in particular Rayleigh waves, from a number of underground nuclear explosions showed clear evidence of quadrupole radiation. Thus, in addition to the existence of SH motion, such as short period Love waves, the Rayleigh type surface waves also exhibit an anomalous component.

It has been shown in section 3.13 that shock induced tectonic radiation exhibits just such quadrupole radiation. In the following section detailed numerical examples are worked out which show these properties and that this particular type of tectonic source has no asymmetry due to rupture propagation as does spontaneous rupture. Thus due to this difference, the possibility of distinguishing between secondary rupture and shock induced rupture as the major source of the anomalous radiation exists. Toksöz, Ben Menahem and Harkrider have in fact shown that the observed Rayleigh radiation can be described by the superposition of a symmetric compression source and a symmetric quadrupole, suggesting shock induced tectonic release.

The observations are then consistent with the tectonic release hypothesis. It is difficult to conceive of a nonlinear mechanism at the source which could explain these observations so well. The final conclusive acceptance can come only with many observations of the different manifestations of tectonic release, however the evidence cited above, by itself, seems quite strong. Theoretical estimates concerning the expected energy release from particular explosions exhibiting anomalous radiation provide the final conclusive evidence, from the viewpoint of the present study. In particular, these energy considerations, given below, show that ample radiation energy can be derived from tectonic release due to shock induced rupture for initial stresses of the order expected in the earth's crust. Coupled with the dynamical results obtained in 3.13 and the following section,

this mechanism of stress release is accepted as being the process responsible for the observations. Consequently the energy release formulas obtained below are intended to serve as scaling laws for the prediction of energy release for additional work, as suggested in 4.1.

The non-linear phenomenon giving rise to a rupture zone has been described in numerous reports and publications (e.g. Haskell (1961), Bishop (1963)). Figure 25 furnishes a schematic representation of the zones of non-linear behavior around the explosion. The zonal radii used have been chosen to correspond, approximately, with those employed by Haskell while the division into zones of behavior is a modification of Bishop's detailed description. From the viewpoint of the present study, the rupture radius, which is denoted as R_2 here, is the parameter of interest.

Haskell's application of a modified Coulomb-Mohr yield criteria to the rupture phenomenon gives an estimate of R_2 in terms of the other source parameters. This estimate is given in terms of the following set of equations.

$$\left(\frac{R_o}{R_1}\right) = \left[1 - \frac{3k(\sigma_1 + P_o)}{\mu(3-k)} \left(\frac{R_2}{R_1}\right)^3 - \frac{3(\sigma_1 + P_o)}{(3\lambda + 2\mu)} \left\{ 1 + \frac{4k}{3-k} \left(\frac{R_2}{R_1}\right)^3 - \frac{3(1+k)}{3-k} \left(\frac{R_2}{R_1}\right)^m \right\} \right]^{1/3} \quad (4.4.1)$$

$$W = \frac{4\pi R_o^3}{3(\gamma-1)} \left(\frac{R_1}{R_o}\right)^{3\gamma} \left[\frac{3(1+k)}{3-k} (\sigma_1 + P_o) \left(\frac{R_2}{R_1}\right)^m - \sigma_1 \right] \quad (4.4.2)$$

$$P = \frac{3(\gamma-1)}{4\pi R_o^2} W \left(\frac{R_o}{R_1} \right)^{3\gamma} \quad (4.4.3)$$

where

R_o = Vaporized cavity radius

R_1 = Final cavity radius after compression of the medium

R_2 = Radius of the rupture zone

W = Explosive yield in ergs (1 kiloton $\equiv 4.2 \times 10^{19}$ ergs $\equiv 10^{12}$ calories)

P = Final cavity pressure

P_o = Initial hydrostatic pressure within the medium, at the shot point (overburden pressure)

λ, μ = Elastic constants of the medium

γ = Ratio of specific heats of the gas formed within the cavity

$k = \sin \phi$; $\tan \phi$ = Coefficient of internal friction on internal yield surfaces within the medium

$\phi_1 = \phi_o - p \tan \phi$; σ_o = Related to the uniaxial tensile strength of the material, σ_T , by $\sigma_o = \frac{1}{2} \sigma_T (1 + \sin \phi) / \sin \phi$

p = Fluid pressure in the pore spaces within the material

$m = 4k / (1 + k)$

In order to obtain R_2 from a given explosion event it is evident that knowledge of a considerable number of source and medium parameters is required. It happens that many of these can be measured directly or in general deduced from independent theoretical considerations. Thus the procedure followed in the present study was to assume knowledge of all the parameters except R_2 , P and the

friction parameter k . For this starting condition an automatic computational scheme (I. B. M. 7090 Program) was adopted using (4.4.1).

In detail, a particular set of values of k were chosen and for each k a range of values of the ratio R_2/R_1 was also chosen. Then the corresponding values of the ratio R_0/R_1 were computed from (4.4.1) for a particular k and for all the set of ratios R_2/R_1 . In each case W and P values were also computed from (4.4.2) and (4.4.3). This procedure was repeated for each k value. When the computed values of R_2/R_1 and W were equal to the known values for the explosion a solution was obtained and the corresponding values of k and R_2 were duly recorded.

The particular example of interest in the present study is the Ranier explosion since the parameters required are known and since tectonic energy was apparently released. In addition Haskell gives the appropriate parameters as follows:

Ranier Nuclear Explosion, after Haskell (1961)

$$R_1 = 18.9 \text{ m.}$$

$$R_0 = 2.3 \text{ m.}$$

$$P_0 = 4.724 \times 10^7 \text{ dynes/cm}^2$$

$$\mu = 5.38 \times 10^9 \text{ dynes/cm}^2$$

$$\lambda = 9.5 \times 10^9 \text{ dynes/cm}^2$$

$$\gamma = 1.2$$

$$\sigma_1 = -2.36 \times 10^7 \text{ dynes/cm}^2 \quad (\sigma_0 = 0)$$

$$W = 7.11 \times 10^{19} \text{ ergs (1.7 kT)}$$

Using the procedure outlined above, the values $k = 0.1$ and $R_2 = 312$ m. were obtained for this explosion. Figure 26 shows the manner in which the appropriate k value can be obtained. In this figure all the curves of constant k are for R_1 fixed at 18.9 m., so that this will relate R_0 to W via equation (4.4.1) and (4.4.2). For a known yield energy W and radius R_0 then the proper value of k may be chosen.

With this k value, R_2 may be obtained as in Figure 27. The two Figures 26 and 27 show the procedure graphically, while in practice it is carried out automatically by the computer. Figure 28 shows the appropriate final cavity pressure for this explosion.

Haskell obtained $k = 0.1$ from near field displacement measurements and noted that the value was lower than what might be expected. However if the material was prestressed it would tend to fracture more easily under shock and the net effect might be to give a low value for k when observations of the displacement field are used. Even if this were the case, the k value so obtained would be appropriate for the estimate of R_2 since a low value of k leads to larger R_2 values which would be expected as the prestress would favor easier fracturing. Under conditions of prestress it would be expected that the rupture zone would be somewhat asymmetric (ellipsoidal) due to easier rupture in a preferred direction. This effect is probably small however and will be ignored here.

Having obtained the rupture radius from Haskell's theory it is only necessary to use the value R_2 in equation (4.3.8) in order to

obtain an estimate of the tectonic energy release for various assumed values of the prestress field. It is worth noting however, that ideally the theory considered in (4.3) is appropriate to the region within the "quasi-elastic" plastic boundary, as indicated in Figure 25, in view of the boundary condition of vanishing traction imposed at the rupture boundary. The boundary conditions used by Haskell are not inconsistent with this condition and the use of a Coulomb-Mohr criterion implies that the material has the mechanical properties of a "nearly incoherent granular aggregate." In this case R_2 as obtained from Haskell's approach should be quite near the value appropriate to the plastic zone boundary, although it would, if anything, probably be somewhat larger than the true plastic radius. It is also to be noted, however, that the radial cracking in the zone beyond the plastic region would also lead to stress release so that an additional contribution from this region would arise. For example, use of Bishop's calculated yield curves applied to the Ranier explosion gives limits for the radius of the radial cracking zone of from 366 m. to 488 m. Taking all these factors into account, use of the value R_2 in the relation for the tectonic energy release ought to give a fairly good estimate for the energy.

Thus, added to the automatic procedure for the computation of R_2 , k and P previously outlined, the value of E_s was computed for each trial value of R_2 by the formula

$$E_s = \frac{\mu_s^2}{2} \left(\frac{4}{3} \pi R_2^3 \right) f \left(\frac{\mu}{\lambda} \right) \quad (4.4.4)$$

along with W , the corresponding explosion yield. Thus when W assumes the value appropriate to the particular explosion under consideration, the proper value of E_s will be obtained. Figure 29 indicates the nature of the computation for the case appropriate to the Ranier nuclear test. The three curves correspond to the three k constant curves considered in Figures 26 through 28. Thus for the Ranier explosion, with the proper value of W and using the appropriate curve along which $k = 0.1$, the value $E_s = 3.6 \times 10^{18}$ ergs is obtained when the prestress field is taken to have the representative value of 5.38×10^7 dynes/cm² (53.8 bars). In order to compare this energy in the radiation field with that contributed directly by the shock wave from the blast, the equivalent seismic magnitude (M_o) is computed via the relation

$$M_o = \frac{\log(\beta W) - 9.4}{2.14} \quad (4.4.5)$$

Here β represents the efficiency factor for the conversion of the total bomb yield energy into seismic energy. In the computations of Figure 29 this was taken as 0.05, which is an over-estimate. The resulting magnitudes M_o are given on the scale at the top of the Figure opposite to W while on the scale opposite to E_s , the seismic magnitudes M_s appropriate to the tectonic energy release are given. These are computed using

$$M_s = \frac{\log E_s - 9.4}{2.14} \quad (4.4.6)$$

A line along which M_s and M_o are equal then gives the points where the radiation field is made up equally of tectonic and explosive contributions. It is seen that the point appropriate to the Ranier shot lies nearly on this equipartition line. Thus the theory predicts a 50 % contribution to the radiation field from tectonic stress release for this assumed prestress. About this much anomalous radiation energy was observed from this test.

Griggs and Press (1961) have given values of β , appearing in (4.4.5), estimated from observations of a large number of explosions in various environments. From their estimates $\beta = 0.001$ is considered most appropriate to an explosion like that of Ranier. Thus, if this value is assumed and if the prestress is varied so as to give a tectonic yield about equal to the direct seismic energy from the shock wave, then a more accurate estimate of the prestress can be obtained. Figure 30 shows the result of varying the prestress for the curve $k = 0.1$ of the previous Figure. The strain parameter s_{12} is twice the usually defined strain so that the stress is

$$\sigma_{12} = 2\mu e_{12} = \mu s_{12}$$

With this more appropriate value of β , then the stress corresponding to equipartition of energy is $\sigma_{12} = 1.56 \times 10^7$ dynes/cm² or approximately 15 bars. Perturbations of the various parameters toward values which tend to be more conservative (i. e. decreasing R_2 and increasing β) yet consistent with the observations, $\sigma_{12} \sim 25$ bars.

It appears then that tectonic release did occur for the example studied and that the prestress of the material in shear was probably of the order of 20 bars. This value is well within the levels of stress that are usually associated with tectonically active regions and well below the estimates of the crustal shear strength of 300 bars (e. g. Kaula (1963)).

4.5. Anomalous Tectonic Radiation from an Explosive Source in a Homogeneously Prestrained Medium and Comparisons with Spontaneous Rupture

Using a computational program essentially identical to that employed for spontaneous rupture, the radiation patterns and source spectrums for induced rupture were computed. The choice of rupture parameters was made to correspond roughly to the Ranier explosion previously treated. In addition the choice of the spontaneous rupture parameters in the examples of section 4.3 are such that they are roughly comparable, in terms of total energy, to the examples of the present section. The formulas utilized in the present computation are those given in section 3.13. Thus the means of rapidly computing the radiation field for any induced tectonic source is provided by this program.

Figure 31 gives the amplitude spectrums of the quadrapole coefficients in 31a, and 31b. the spectrums of the dilatation and rotation components at an epicentral distance of 344 km and an azimuth of 60° are also given. The distance and azimuthal angles are measured

as for the "dip slip" rupture in Figure 16b. As was the case for spontaneous rupture, the multipole coefficient spectrums can be described in terms of a dimensionless parameter, in this case obviously $[R_o/\lambda]$, where R_o is the rupture radius. Precisely the same sort of description of the spectrum applies, that is for $[R_o/\lambda] \ll 1$ these quadrupole coefficients follow a dependence which is approximately $[R_o/\lambda]^4$. When $[R_o/\lambda]$ approaches unity a transition occurs and for short periods such that $[R_o/\lambda] \geq 1$ an essentially different power law dependence approximates the spectrums. The exact expressions are of course given in section 3.13. The frequency range shown in 31a is such that the variation at $R_o/\lambda \sim 1$ is not apparent since the radius is small, of the order of 300 meters.

Comparison of these spectrums with those for the spontaneous tectonic source in 4.2, Figure 17, shows that while the tectonic energy release is comparable in the two cases, the multipole spectrums have a different distribution with period. That is the spontaneous rupture source multipole spectrums show a variation and change of slope at longer periods than do the induced rupture coefficients. Essentially the spontaneous rupture will appear to have more energy at the longer periods than will the induced rupture source of the same energy due to this difference. This is seen to be associated with the difference in the characteristic source dimensions.

The potential spectrums in 31b begin to show an amplitude slope change at the short periods. This characteristic is primarily a propagational effect rather than a property of the source and occurs

similarly for the spontaneous rupture source as well. In particular the spherical Hankel functions in the solutions show a dependence on frequency and distance which is proportional to $(kr)^{-1}$, so that especially for $(kr) > 1$, the higher frequencies will be observed to suffer an attenuation proportional to ω^{-1} . The value κ is k_p for the dilatation and k_s for the rotation components and due to the higher value of the compressional velocity in the medium, the effects of propagation will manifest themselves at higher frequencies for Θ compared to $\underline{\Omega}$, as can be observed from 31b.

Figure 32 shows the quadrupole phases for the induced source. The variation is not unlike that for the spontaneous rupture source. One observes however that the induced source is purely a quadrupole and that no superposition of multipoles is involved. Thus the induced source will not show any asymmetry as did the spontaneous rupture and physically this is just due to the symmetry of the rupture volume. Similar symmetry would also be expected for bilateral spontaneous rupture treated in section 3.11.

Thus Figure 33 shows the expected quadrupole pattern for a particular initial stress and for rupture parameters appropriate to the Ranier experiment. The depth of the source is however taken at 3 km rather than at about 0.3 km as would be appropriate for the Ranier explosion. Figure 34 shows the effect of a change in stress orientation, the radiation patterns being drastically changed from those of the previous Figure. Figure 35 shows yet another

prestress case, while Figure 36 shows the affect of a small change in the stress properties on the radiation patterns. Thus comparing Figures 35 and 36 gives an indication of the sensitivity of the radiation to rather small changes in the initial prestress. One observes that the dependence of the field, as a function of azimuth, is indeed very sensitive to the nature of the initial prestress.

In all these computations only the radiation from the tectonic release has been considered and the Figures show only this contribution to the field. It is necessary of course to add to this, the direct field from the explosion itself. This will result in the superposition of a spherically symmetric dilatational contribution to the dilatation due to tectonic release. Since most of the tectonic energy is seen to be in the rotational field and since the scaling procedure of the previous section has shown that the energies in the explosive-tectonic contributions are usually about equal, then it follows that the affect of tectonic release on the direct dilatation field from the explosion itself is small. As was previously remarked this is consistent with the observations. The dilatation pattern will therefore be very nearly circular.

The quadrapole nature of this induced tectonic radiation is consistent with the observations of the field by Toksöz, Harkrider and Ben Menahem. It is evident that the "dip slip" radiation pattern (Figure 24) has characteristics similar to that for induced rupture. However in a spherical earth the effects of rupture propagation would show up for the "dip slip" case while this would not be the case for

the induced rupture. In addition, the added dilatation field from the shock wave would provide a difference in the dilatational components of the two types of source. Consequently, one may conclude that while the fields from the spontaneous rupture and induced rupture-explosive sources have some similarities, there are nevertheless the strong differences predicted that provide the means of differentiating between them.

The clear possibility of secondary rupture under prestress conditions requires however that this conclusion be taken with some obvious provisions. Thus the theory shows that for instances in which secondary rupture is a factor, the differences in the field properties of the two sources will be more subtle. In this case more detailed application of the present theory is called for in order to delineate all the possible differences. However even at the present stage, the theory suggests a dilatational component of the field which is essentially characteristic of an explosion, that is uniformly compressional. This however depends on the size of secondary rupture, or in other words on the size of the prestress field.

In any case it seems clear that with ample instrumental coverage with respect to azimuth and distance, the tectonic source field can provide detailed information concerning the initial prestress field at the source. Analysis of the spectrums and azimuthal properties of the various types of motion will indicate the degree of coverage necessary but it is evident that precise estimates of the tectonic stress will require more detailed work than has previously been attempted.

Chapter 5

CONCLUSIONS

5.1. A Resume of Results and Conclusions

The theoretical results and conclusions of Chapter 2 are summarized in section 2.10 and need not be considered further here. The important physical inferences to be drawn from the formal theory given have, in any event, been incorporated in the subsequent developments of this study.

From a review of the microscopic characteristics of rupture and with due regard to the experimental evidence, it is concluded that the processes leading to rupture in the earth can best be described microscopically in terms of dislocation phenomenon. The mechanism is essentially quantization of the stress field in the form of dislocations with interactions between dislocations giving the material a finite strength at low stresses. As the tectonic forces become larger an unstable generation of dislocations and dislocation movement occurs which is manifested macroscopically as creep. At this stage the creep strength of the material has been exceeded. Since dislocations tend to be self generating then once the processes have been initiated it tends to concentrate and a "weak zone" develops. Several possibilities of rupture can be distinguished depending on the thermodynamic state of the material. At low temperatures and pressures the relative immobility of the dislocations suggests dislocation accumulation at inhomogeneities with stress accumulation and eventual

fracture or shear melting. At higher temperatures and pressures phase change associated with the unstable generation of dislocations and vacancies is considered most likely.

The continuum mechanical models of the rupture phenomenon which are introduced are at least consistent with the microscopic hypotheses of rupture and embody the essential properties of the medium in parametric form, particularly its stress condition. While no attempt is made to show any uniqueness between the phase change hypothesis of rupture and the theoretical models proposed, nor does it seem possible to do so, the models are considered to most closely represent an expanding phase change (melting) phenomenon.

The mathematical treatment accorded the tectonic source is based on the standard method of treating an initial value problem. It is concluded that this description provides the only means of completely specifying the radiation field from tectonic rupturing, including its time dependence. The theory is in total best described as a relaxation theory and this relaxation concept is considered to be an accurate description of the physical origins of the radiation field.

Applications of the theory to the detailed description of the radiation field from tectonic sources in layered models of the earth is shown to be feasible and straightforward. It is concluded that an application of the theory for the experimental determination of the prestress condition of the material in the vicinity of a rupture is possible and that the induced rupture theory can provide the means of obtaining stress information from explosive sources.

From the examples of radiation from spontaneous and induced tectonic sources and in view of the large number of source parameters which affect the radiation field, it is concluded that more complete and detailed analysis of the field than has previously been the case, is required in order to form precise estimates of the source parameters.

The preliminary applications of the theory show that the spontaneous rupture source has a directional asymmetry as would be expected and that constructive enhancement of the amplitude of the radiation field can occur either in the forward or backward directions along the axis of rupture propagation. The asymmetry is frequency dependent and is shown to diminish with increasing period. The spontaneous rupture source has a quadrupole azimuthal distribution at wavelengths long compared to the maximum rupture dimension. The radiation field is shown to be strongly dependent on rupture orientation with respect to the stress field and the surface of the earth. In particular "dip slip" radiation is shown to be quite different than "strike slip" rupture radiation due simply to orientation. It is concluded that these properties are in general agreement with the observations, although detailed experimental work is required for full and detailed confirmation.

Consideration of induced rupture associated with explosions leads to the conclusion that such an effect occurs and is responsible for the major part of the anomalous radiation observed from nuclear underground explosions. In particular detailed investigation of the

Ranier nuclear test suggests that a prestress of the order of 20 bars was the origin of the observed anomalous radiation from this explosion. In the course of this investigation scaling laws for tectonic energy release from primary shock induced rupture are obtained and are considered applicable to other such explosions.

REFERENCES

Aki, K., Study of Love and Rayleigh waves from earthquakes with fault plane solutions or with known faulting.

Part 1. A phase difference method based on a new model of earthquake source.

Part 2. Application of the phase difference method.

Part 3. Table of source phase differences between Rayleigh and Love waves.

Bull. Seism. Soc. Am., 54, 2, Apr. 1964.

Balakina, L. M., E. F. Savarensky and A. V. Vvedenskaya, On determination of earthquake mechanism, Physics and Chemistry of the Earth, Edited by L. H. Ahrens, et al. Vol. 4, 211-238, 1961.

Benioff, H., Earthquakes and rock creep, Bull. Seism. Soc. Am., 41, 31-62, 1951.

Benioff, H., Source wave forms of three earthquakes, Bull. Seism. Soc. Am., (in press).

Ben-Menahem, A., Radiation of Seismic surface-waves from finite moving sources, Bull. Seism. Soc. Am., 51, 3, 401-435, 1961.

Ben-Menahem, A., Radiation of Seismic body waves from a finite moving sources, Journ. of Geophys. Res., 67, No. 1, 1962.

Ben-Menahem, A., Operational representation of the addition theorems for spherical waves, Journ. of Math. and Physics, XLI, No. 3, 1962.

Ben-Menahem, A., and M. N. Toksoz, Source mechanism from the spectra of long-period seismic surface waves 1. The Mongolian earthquake of Dec. 4, 1957, Journ. of Geophys. Res., 67, 1943-1955, 1962.

Bishop, R. H., Spherical shock waves from underground explosions, Close-in Phenomena of Buried Explosions, Sandia Corp. Project No. 14.041.00, May 1, 1963.

Byerly, P., and J. De Noyer, Energy in earthquakes as computed from geodetic observations, Contributions in Geophysics 1, 17, Pergamon Press, 1958.

- Chinnery, M. A., Some physical aspects of earthquake mechanism, Journ. of Geophys. Res., 65, 1960.
- Chinnery, M. A., The deformation of the ground around surface faults, Bull. Seism. Soc. Am., 51, 1961.
- Cottrell, A. H., Dislocations and plastic flow in Crystals, Oxford Univ. Press, 1953.
- Dash, W. C., Evidence of dislocation jogs in deformed silicon, J. Appl. Physics, 29, 705-709, April 1958.
- deHoop, A. T., Representation theorems for the displacement in an elastic solid and their application to elastodynamic diffraction theory, Doctoral Dissertation, Delft, 1958.
- Droste, S., and R. Teisseyre, The mechanism of earthquakes according to dislocation theory, Sci. Rep. Tohoku Univ. Ser. 5, Geophys. II, Nr. 1, 1959.
- Droste, S., and R. Teisseyre, The theory of the dislocation Process and its application to the Pacific region, Bull. Seism. Soc. Am., 50, 57-70, 1960.
- Duvall, G. E., Concepts of shock wave propagation, Bull. Seism. Soc. Am., 52, No. 4, 869-893, Oct. 1962.
- Erdelyi, A., W. Magnus, F. Oberhettinger, and F. G. Tricomi, Bateman Manuscript Project, Calif. Inst. of Tech., Tables of Integral Transforms (I.T.) Vol. 1-2, McGraw-Hill Book Co., 1954.
- Erdelyi, A., W. Magnus, F. Oberhettinger and F. G. Tricomi, Higher Transcendental Functions, Bateman Manuscript Project, Calif. Inst. of Tech., McGraw-Hill Book Co., 1953, (H.T.F.)
- Eshelby, I. D., F. C. Frank, F. R. N. Nabarro, The equilibrium of linear Arrays of dislocations, Phil. Mag., 41, 351-364, 1951.
- Ewing, W. M., W. S. Jardetzky, and F. Press, Elastic waves in layered media, McGraw-Hill Book Co., New York, 1957.
- Friedel, J., Les Dislocations, Paris, Gauthier Villars, 1956.
- Friedman, B., and J. Russek, Addition theorems for spherical waves, Quart. App. Math, 12, 13-23, 1954.

- Gilbert, F., and G. J. F. MacDonald, Free oscillations of the earth: I Toroidal oscillations, Journ. of Geophys. Res., 1960.
- Griffiths, A. A., The phenomena of rupture and flow in solids, Phil. Trans. Roy. Soc., A, 221, 163-198, 1921.
- Griggs, D., and J. Handin, Observations on fracture and a hypothesis of earthquakes, Rock Deformation; A Symposium, The Geol. Soc. of Am., Memoir 79, 1960.
- Griggs, D. T., and F. Press, Probing the earth with nuclear explosions, Journ. of Geophys. Res., 66, 1, Jan. 1961.
- Harkrider, D. G., Thesis, Calif. Inst. of Tech., 1963, Part II Rayleigh and Love waves from sources in a multilayered elastic half-space.
- Harkrider, D. G., Surface waves in multilayered elastic media I. Rayleigh and Love waves from buried sources in a multilayered elastic half-space, Bull. Seism. Soc. Am., 54, 2, Apr. 1964.
- Haskell, N. A., The dispersion of surface waves on multilayered media, Bull. Seism. Soc. Am., 43, 17-34, 1953.
- Hobson, E. W., The theory of spherical and ellipsoidal harmonics, Cambridge Univ. Press, 1931.
- Honda, H., The mechanism of the earthquakes, Science Reports, Tohoku Univ. Ser. 5, Geophys. 9, Suppl. 1957.
- Honda, H., Earthquake mechanism and seismic waves, Geophys. Notes, Vol. 15, Suppl., Tokyo Univ., 1962.
- Housner, G., Properties of strong ground motion earthquakes, Bull. Seism. Soc. Am., 45, 199, 1955.
- Hoy, R. B., Induced Faulting, Bull. Seism. Soc. Am., 53, 4, July, 1963.
- Jackson, J. D., Classical Electrodynamics, John Wiley and Sons, 1962.
- Jeffreys, H., and B. Jeffreys, Methods of Mathematical Physics, Cambridge Univ. Press, 1956.
- Kaula, W. M., Elastic models of the mantle corresponding to variations in the external gravity field, NASA, Goddard Space Flight Center, 1963.

- Keilis-Borok, V., On estimation of the displacement in an earthquake source and of source dimensions, Annali di Geofisica, Vol. XII, 2, 1959.
- Keilis-Borok, V., Investigation of the mechanism of earthquakes, Soviet Res. in Geophys., 4, American Geophysical Union, Consultants Bureau New York, 1960.
- Knopoff, L., Diffraction of elastic waves, Journ. Acoust. Soc. Am., 28, 217-220, 1956.
- Knopoff, L., Energy release in earthquakes, Geophys. Journ. 1, 44-52, 1958.
- Knopoff, L., and F. Gilbert, Radiation from a strike-slip fault, Bull. Seism. Soc. Am., 49, 163-178, 1959.
- Knopoff, L., and F. Gilbert, First motions from seismic sources, Bull. Seism. Soc. Am., 50, 117-134, 1960.
- Koehler, J. S., and F. Seitz, The nature of dislocations in ideal single crystals, Dislocations in Metals, Edited by M. Cohen, AIME, 1954.
- Landau, L. D., and E. M. Lifshitz, Theory of Elasticity, Addison-Wesley, 1951.
- Latter, A., Personal communication, 1960.
- Love, A. E. H., A treatise on the mathematical theory of elasticity, Dover, 1944.
- Mason, W. P., Physical Acoustics and the properties of solids, Van Nostrand, 1958.
- Morse, P. M., and H. Feshbach, Methods of theoretical physics, McGraw-Hill, 1953.
- Mott, N. F., Theory of fracture of metals, International Union of Theoretical and Applied Mechanics, Colloquium on the Deformation and Flow of Solids, 53-58, Madrid, Spring-Verlag, Berlin-Göttingen, 1956.
- Nabarro, F. R. N., The synthesis of elastic dislocation fields, Phil. Mag. 122, 1224-1231, 1951.
- Nakano, H., Notes on the nature of the forces which give rise to the earthquake motions, Seism. Bull. Centr. Met., Obs. Japan, 1, 92-120, 1923.

- Orowan, E., Dislocations and mechanical properties, Dislocations in Metals, Edited by M. Cohen, AIME, 1954.
- Orowan, E., Mechanism of seismic faulting, Rock Deformation, A Symposium, The Geological Society of America, Memoir 79, 1960.
- Porzel, F. B., Close-in time of arrival measurements and hydrodynamic yield, Univ. Calif. Rad. Lab. Report 5675, 28-49, 1959.
- Press, F., A. Ben-Menahem, and M. N. Toksoz, Experimental determination of earthquake fault length and rupture velocity, Journ. Geophys. Res., 66, 3471-3485, 1961.
- Press, F., and C. B. Archambeau, Release of tectonic strain by underground nuclear explosions, Journ. of Geophys. Res., 67, 1, 1962.
- Press, F., Personal communication, 1963.
- Read, W. T., Dislocations in crystals, McGraw-Hill Book Co., 1953.
- Reid, H. F., Physics of the Earth, VI, 100, 1933.
- Richards, P. I., Manual of Mathematical Physics, Pergamon Press, 1959.
- Sato, Y., Transformations of wave-functions related to the transformations of coordinate systems, I., Bull. Earthquake Res. Inst., 28, 1950.
- Seitz, F., The physics of metals, McGraw-Hill Book Co., 1943.
- Sneddon, I. N., Fourier Transforms, McGraw-Hill Book Co., 1951.
- Sokolnikoff, I. S., Mathematical Theory of elasticity, McGraw-Hill Book Co., 1956.
- Steketee, I. A., Some geophysical applications of elasticity theory of dislocations, Canadian Journ. of Phys. 36, 1168-1198, 1958.
- Sternberg, E., and R. A. Eubanks, On stress functions for elastokinetics and the integration of the repeated wave equation, Quart, Appl. Math., 15, 149, 1957.

- Stratton, J. A., Electromagnetic Theory, McGraw-Hill Book Co., 1941.
- Toksoz, M. N., D. G. Harkrider, and A. Ben-Menahem, Determination of source parameters by amplitude equalization of seismic surface waves, II Release of tectonic strain by underground nuclear explosions, (in preparation,) 1964.
- Teisseyre, R., Dynamic and time relations of the dislocation theory of earthquakes, Acta Geoph. Pol. 1960.
- Weertman, J., Continuum distribution of dislocations on faults with finite friction, (in press) Cont. 1249, Div. of Geol. Sciences, Calif. Inst. of Tech., Pasadena.

APPENDIX 1
MULTIPOLE COEFFICIENTS

In the following, use is made of the equations (2.3.6) and (2.3.7) of the text to compute the multipole coefficients $\alpha_{n+1,m}^{(i_0)}$, $\beta_{n+1,m}^{(i_0)}$, $\gamma_{n+1,m}^{(i_0)}$, and $\delta_{n+1,m}^{(i_0)}$ with $i_0 = 1, 2, 3$, for the two cases $n = 0$ and $n = 1$. The equations to be used are

$$\frac{\rho^{(n+1)}}{r^{n+2}} \sum_{n=0}^{m+1} (\alpha_{n+1,m} \cos m\phi, \beta_{n+1,m} \sin m\phi) P_{n+1}^m(\cos \theta) = \frac{(-1)^{n+1}}{n!} R^{(n+1)}(i_0 \dots i_n) \frac{\partial^{(n+1)} r^{-1}}{\partial x_{i_0} \dots \partial x_{i_n}} \quad (1-1)$$

$$\frac{\rho^{(n+1)}}{r^{n+2}} \sum_{n=0}^{m+1} (\gamma_{n+1,m}^{(i_0)} \cos m\phi, \delta_{n+1,m}^{(i_0)} \sin m\phi) P_{n+1}^m(\cos \theta) = \frac{(-1)^{n+1}}{n!} \epsilon_{i_0 j k} R^{(n+1)}(j, i_1 \dots i_n) \frac{\partial^{(n+1)} r^{-1}}{\partial x_k \partial x_{i_1} \dots \partial x_{i_n}}$$

where

$$\rho^{(n+1)} = (n+1) \left\{ \sum_{i_0=1}^3 \dots \sum_{i_n=1}^3 [R^{(n+1)}(i_0 \dots i_n)]^n \right\}^{\frac{1}{2}} \quad (1-2)$$

$$R^{(n+1)}(i_0 \dots i_n) = \iiint_{\hat{v}} R_{i_0} x'_{i_1} \dots x'_{i_n} d\hat{v}'$$

(a) Case $n = 0$

From the first equation of (1-1), one has for $n = 0$

$$P^{(1)} \sum_{m=0}^1 [\alpha_{1m} \cos m\phi + \beta_{1m} \sin m\phi] P_1^m(\cos \theta) / r^2 =$$

$$- \left[R^{(1)}_{(1)} \frac{\partial r^{-1}}{\partial x_1} + R^{(1)}_{(2)} \frac{\partial r^{-1}}{\partial x_2} + R^{(1)}_{(3)} \frac{\partial r^{-1}}{\partial x_3} \right]$$

or, in terms of trigonometric functions

$$P^{(1)} [\alpha_{10} \cos \theta] + P^{(1)} [\alpha_{11} \cos \theta \sin \theta + \beta_{11} \sin \phi \sin \theta] =$$

$$R^{(1)}_{(1)} \sin \theta \cos \phi + R^{(1)}_{(2)} \sin \theta \sin \phi + R^{(1)}_{(3)} \cos \theta$$

Thus we obtain

$$\alpha_{10} = \frac{R^{(1)}_{(3)}}{\rho^{(1)}} ; \quad \alpha_{11} = \frac{R^{(1)}_{(1)}}{\rho^{(1)}} ; \quad \beta_{11} = \frac{R^{(1)}_{(2)}}{\rho^{(1)}} \quad (1-3)$$

From the second of the equations (1-1), one has three equations given by

$$P^{(i)} \frac{\delta^{(i_0)}(\theta, \phi)}{r^2} = \frac{\rho^{(1)}}{r^2} \sum_{m=0}^1 [\gamma_{1m}^{(i_0)} \cos m\phi + \delta_{1m}^{(i_0)} \sin m\phi] P_1^m(\cos \theta)$$

$$= - \epsilon_{i_0 j k} P^{(j)} \frac{\partial r^{-1}}{\partial x_k}$$

with $i_0 = 1, 2, 3$. And so for $i_0 = 1$

$$\frac{\rho^{(1)}}{r^2} \left\{ \gamma_{10}^{(1)} \cos \theta + \gamma_{11}^{(1)} \cos \phi \sin \theta + \delta_{11}^{(1)} \sin \phi \sin \theta \right\} =$$

$$\frac{1}{r^2} \left\{ R^{(1)}(2) \cos \theta - R^{(1)}(3) \sin \theta \sin \phi \right\}$$

From which one gets

$$\gamma_{10}^{(1)} = \frac{R^{(1)}(2)}{\rho^{(1)}} ; \gamma_{11}^{(1)} = 0 ; \delta_{11}^{(1)} = -\frac{R^{(1)}(3)}{\rho^{(1)}} \quad (1-4)$$

For $i_0 = 2$

$$\frac{\rho^{(1)}}{r^2} \left\{ \gamma_{10}^{(2)} \cos \theta + (\gamma_{11}^{(2)} \cos \phi + \delta_{11}^{(2)} \sin \phi) \sin \theta \right\} =$$

$$\frac{1}{r^2} \left\{ R^{(1)}(3) \sin \theta \cos \phi - R^{(1)}(1) \cos \theta \right\}$$

Hence

$$\gamma_{10}^{(2)} = \frac{-R^{(1)}(1)}{\rho^{(1)}} ; \gamma_{11}^{(2)} = \frac{R^{(1)}(3)}{\rho^{(1)}} ; \delta_{11}^{(2)} = 0 \quad (1-5)$$

And finally for $i_0 = 3$

$$\frac{\rho^{(1)}}{r^2} \left\{ \gamma_{10}^{(3)} \cos \theta + (\gamma_{11}^{(3)} \cos \phi + \delta_{11}^{(3)} \sin \phi) \sin \theta \right\} =$$

$$\frac{1}{r^2} \left\{ R^{(1)}(1) \sin \theta \sin \phi - R^{(1)}(2) \sin \theta \cos \phi \right\}$$

so that

$$\gamma_{10}^{(3)} = 0 \quad ; \quad \gamma_{11}^{(3)} = \frac{R^{(1)}(2)}{\rho^{(1)}} \quad ; \quad \delta_{11}^{(3)} = \frac{R^{(1)}(1)}{\rho^{(1)}} \quad (1-6)$$

Collecting these results for easy reference gives the array

$$\begin{array}{cccc} \alpha_{10} = \frac{R^{(1)}(3)}{\rho^{(1)}} & \gamma_{10}^{(1)} = \frac{R^{(1)}(2)}{\rho^{(1)}} & \gamma_{10}^{(2)} = -\frac{R^{(1)}(1)}{\rho^{(1)}} & \gamma_{10}^{(3)} = 0 \\ \alpha_{11} = \frac{R^{(1)}(1)}{\rho^{(1)}} & \gamma_{11}^{(1)} = 0 & \gamma_{11}^{(2)} = \frac{R^{(1)}(3)}{\rho^{(1)}} & \gamma_{11}^{(3)} = \frac{R^{(1)}(2)}{\rho^{(1)}} \\ \beta_{11} = \frac{R^{(1)}(2)}{\rho^{(1)}} & \delta_{11}^{(1)} = -\frac{R^{(1)}(3)}{\rho^{(1)}} & \delta_{11}^{(2)} = 0 & \delta_{11}^{(3)} = \frac{R^{(1)}(1)}{\rho^{(1)}} \end{array} \quad (1-7)$$

For the special case of the horizontally directed force field ($R_1 \neq 0, R_2 = R_3 = 0$) as a source, one has $R^{(1)}(2) = R^{(1)}(3) = 0$ and the only non-vanishing coefficients are, in this case

$$\alpha_{11} = 1 \quad , \quad \gamma_{10}^{(2)} = -1 \quad , \quad \delta_{11}^{(3)} = 1$$

For the vertically directed force field

$$R^{(1)}(1) = R^{(1)}(2) = 0$$

and the non-vanishing coefficients are

$$\alpha_{10} = 1 \quad , \quad \delta_{11}^{(1)} = -1 \quad , \quad \gamma_{11}^{(2)} = 1$$

These simple cases are often used, most recently by Ben-Menahem (1961) and Harkrider (1963), to construct more general sources or to

compute the effect of a particular source on the amplitudes of the waves in a layered medium.

(b) Case n = 1

For the dipole moments, the first of the equations (1-1) takes the form

$$\begin{aligned} \rho^{(2)} \frac{S_2(\theta, \phi)}{r^3} = & \left[R^{(2)}_{(1,1)} \frac{\partial^2 r^{-1}}{\partial x_1^2} + R^{(2)}_{(1,2)} \frac{\partial^2 r^{-1}}{\partial x_1 \partial x_2} + R^{(2)}_{(1,3)} \frac{\partial^2 r^{-1}}{\partial x_1 \partial x_3} \right] \\ & + \left[R^{(2)}_{(2,1)} \frac{\partial^2 r^{-1}}{\partial x_2 \partial x_1} + R^{(2)}_{(2,2)} \frac{\partial^2 r^{-1}}{\partial x_2^2} + R^{(2)}_{(2,3)} \frac{\partial^2 r^{-1}}{\partial x_2 \partial x_3} \right] \quad (1-8) \\ & + \left[R^{(2)}_{(3,1)} \frac{\partial^2 r^{-1}}{\partial x_3 \partial x_1} + R^{(2)}_{(3,2)} \frac{\partial^2 r^{-1}}{\partial x_3 \partial x_2} + R^{(2)}_{(3,3)} \frac{\partial^2 r^{-1}}{\partial x_3^2} \right] \end{aligned}$$

For the computation of these multipole coefficients, the following identity is useful

$$\left(\frac{\partial^2 r^{-1}}{\partial x_i \partial x_j} \right) = \begin{pmatrix} (3 \sin^2 \theta \cos^2 \phi - 1)/r^3 & (3 \sin^2 \theta \sin \phi \cos \phi)/r^3 & (3 \sin \theta \cos \theta \cos \phi)/r^3 \\ (3 \sin^2 \theta \sin \phi \cos \phi)/r^3 & (3 \sin^2 \theta \sin^2 \phi - 1)/r^3 & (3 \sin \theta \cos \theta \sin \phi)/r^3 \\ (3 \sin \theta \cos \theta \cos \phi)/r^3 & (3 \sin \theta \cos \theta \sin \phi)/r^3 & (3 \cos^2 \theta - 1)/r^3 \end{pmatrix}$$

Using this identity in the right side of (1-8) and expanding the left side of (1-8) in trigonometric functions gives

$$\begin{aligned} & \rho^{(2)} \left[\frac{\alpha_{20}}{2} (3 \cos^2 \theta - 1) + \alpha_{21} (3 \sin \theta \cos \theta \cos \phi) + \beta_{21} (3 \sin \theta \cos \theta \sin \phi) \right. \\ & \left. + \alpha_{22} (3 \sin^2 \theta \cos^2 \phi - 3 \sin^2 \theta \sin^2 \phi) + 2\beta_{22} (3 \sin^2 \theta \sin \phi \cos \phi) \right] = \\ & R_{(1,1)}^{(2)} [3 \sin^2 \theta \cos^2 \phi - 1] + [R_{(1,2)}^{(2)} + R_{(2,1)}^{(2)}] [3 \sin^2 \theta \sin \phi \cos \phi] + \\ & [R_{(1,3)}^{(2)} + R_{(3,1)}^{(2)}] [3 \sin \theta \cos \theta \cos \phi] + R_{(2,2)}^{(2)} [3 \sin^2 \theta \sin^2 \phi - 1] + \\ & [R_{(2,3)}^{(2)} + R_{(3,2)}^{(2)}] [3 \sin \theta \cos \theta \sin \phi] + R_{(3,3)}^{(2)} [3 \cos^2 \theta - 1] \end{aligned}$$

From this expansion one gets immediately

$$\begin{aligned} \alpha_{21} &= \frac{R_{(1,3)}^{(2)} + R_{(3,1)}^{(2)}}{\rho^{(2)}} \quad ; \quad \beta_{21} = \frac{R_{(2,3)}^{(2)} + R_{(3,2)}^{(2)}}{\rho^{(2)}} \\ \beta_{22} &= \frac{R_{(1,2)}^{(2)} + R_{(2,1)}^{(2)}}{2 \rho^{(2)}} \end{aligned} \quad (1-9)$$

Further, the remaining terms on the right side of the expression may be recombined by use of the identity $\nabla^2(\frac{1}{r}) = 0$, while the identity

$$3 \sin^2 \theta \cos^2 \phi - 3 \sin^2 \theta \sin^2 \phi = 2 (3 \sin^2 \theta \cos^2 \phi - 1) + (3 \cos^2 \theta - 1)$$

may be used with the remaining terms on the left side and the reduced equation becomes

$$\begin{aligned} & \rho^{(2)} \left\{ \left(\frac{\alpha_{20}}{2} + \alpha_{22} \right) (3 \cos^2 \theta - 1) + 2\alpha_{22} (3 \sin^2 \theta \cos^2 \phi - 1) \right\} = \\ & [R_{(1,1)}^{(2)} - R_{(2,2)}^{(2)}] (3 \sin^2 \theta \cos^2 \phi - 1) + [R_{(3,3)}^{(2)} - R_{(2,2)}^{(2)}] (3 \cos^2 \theta - 1) \end{aligned}$$

Thus

$$\alpha_{22} = \frac{R_{(1,1)}^{(2)} - R_{(2,2)}^{(2)}}{2 \rho^{(2)}} \quad (1-10)$$

which in turn yields

$$\chi_{20} = \frac{R^{(2)}_{(3,3)} - R^{(2)}_{(1,1)}}{\rho^{(2)}} + \frac{R^{(2)}_{(3,3)} - R^{(2)}_{(2,2)}}{\rho^{(2)}} \quad (1-11)$$

From the second of the equations (1-1), one has the following set of equations which determine the remaining coefficients

$$\begin{aligned} \frac{\rho^{(2)}}{r^3} \mathcal{S}_2^{(1)}(\theta, \phi) &= \frac{R^{(2)}_{(2,1)}}{r^3} (3 \sin \theta \cos \theta \cos \phi) + \left[\frac{R^{(2)}_{(2,2)} - R^{(2)}_{(3,3)}}{r^3} \right] \times \\ &(3 \sin \theta \cos \theta \sin \phi) - \frac{R^{(2)}_{(3,1)}}{r^3} (3 \sin^2 \theta \sin \phi \cos \phi) + \frac{R^{(2)}_{(2,3)}}{r^3} (3 \cos^2 \theta - 1) \\ &- \frac{R^{(2)}_{(3,2)}}{r^3} (3 \sin^2 \theta \sin^2 \phi - 1) \end{aligned} \quad (1-12)$$

$$\begin{aligned} \frac{\rho^{(2)}}{r^3} \mathcal{S}_2^{(2)}(\theta, \phi) &= \frac{1}{r^3} \left\{ R^{(2)}_{(3,1)} (3 \sin^2 \theta \cos^2 \phi - 1) + [R^{(2)}_{(3,3)} - R^{(2)}_{(1,1)}] \right. \\ &(3 \sin \theta \cos \theta \cos \phi) + R^{(2)}_{(3,2)} (3 \sin^2 \theta \sin \phi \cos \phi) \\ &\left. - R^{(2)}_{(1,2)} (3 \sin \theta \cos \theta \sin \phi) - R^{(2)}_{(1,3)} (3 \cos^2 \theta - 1) \right\} \end{aligned} \quad (1-13)$$

$$\begin{aligned} \frac{\rho^{(2)}}{r^3} \mathcal{S}_2^{(3)}(\theta, \phi) &= \frac{1}{r^3} \left\{ [R^{(2)}_{(1,1)} - R^{(2)}_{(2,2)}] [3 \sin^2 \theta \sin \phi \cos \phi] + R^{(2)}_{(1,2)} (3 \sin^2 \theta \sin^2 \phi - 1) \right. \\ &- R^{(2)}_{(2,1)} (3 \sin^2 \theta \cos^2 \theta - 1) + R^{(2)}_{(1,3)} (3 \sin \theta \cos \theta \sin \phi) - \\ &\left. R^{(2)}_{(2,3)} (3 \sin \theta \cos \theta \cos \phi) \right\} \end{aligned} \quad (1-14)$$

Using the identity

$$\begin{aligned} \frac{\rho^{(2)}}{r^3} \mathcal{S}_2^{(j)}(\theta, \phi) &= \frac{\rho^{(2)}}{r^3} \left\{ \left[\frac{\chi_{20}^{(j)}}{2} + \frac{\chi_{22}^{(j)}}{1} \right] (3 \cos^2 \theta - 1) + \chi_{21}^{(j)} (3 \sin \theta \cos \theta \cos \phi) \right. \\ &+ \mathcal{S}_{21}^{(j)} (3 \sin \theta \cos \theta \sin \phi) + 2 \chi_{22}^{(j)} (3 \sin^2 \theta \cos^2 \phi - 1) \\ &\left. + 2 \mathcal{S}_{22}^{(j)} (3 \sin^2 \theta \sin \phi \cos \phi) \right\} \end{aligned}$$

with $j = 1, 2, 3$, to expand the left sides of these equations, the desired multipole coefficients may be obtained after minor manipulations using trigonometric identities previously introduced. These coefficients are, along with those already mentioned

$$\underline{i_0 = 1} \tag{1-15}$$

$$\begin{aligned} \gamma_{10}^{(1)} &= \frac{2R^{(2)}(2,3) + R^{(2)}(3,2)}{\rho^{(2)}} & \delta_{11}^{(1)} &= \frac{R^{(2)}(2,2) - R^{(2)}(3,3)}{\rho^{(2)}} \\ \gamma_{11}^{(1)} &= R^{(2)}(2,1) / \rho^{(2)} & \delta_{12}^{(1)} &= -\frac{R^{(2)}(3,1)}{2\rho^{(2)}} \\ \gamma_{12}^{(1)} &= R^{(2)}(3,2) / 2\rho^{(2)} \end{aligned}$$

$$\underline{i_0 = 2} \tag{1-16}$$

$$\begin{aligned} \gamma_{10}^{(2)} &= -\frac{2R^{(2)}(1,3) + R^{(2)}(3,1)}{\rho^{(2)}} & \delta_{11}^{(2)} &= -\frac{R^{(2)}(1,2)}{\rho^{(2)}} \\ \gamma_{11}^{(2)} &= \frac{R^{(2)}(3,3) - R^{(2)}(1,1)}{\rho^{(2)}} & \delta_{12}^{(2)} &= \frac{R^{(2)}(3,2)}{2\rho^{(2)}} \\ \gamma_{12}^{(2)} &= \frac{R^{(2)}(3,1)}{2\rho^{(2)}} \end{aligned}$$

$$\underline{i_0 = 3} \tag{1-17}$$

$$\begin{aligned} \gamma_{10}^{(3)} &= \frac{R^{(2)}(2,1) - R^{(2)}(1,2)}{\rho^{(2)}} & \delta_{11}^{(3)} &= \frac{R^{(2)}(1,3)}{\rho^{(2)}} \\ \gamma_{11}^{(3)} &= -\frac{R^{(2)}(2,3)}{\rho^{(2)}} & \delta_{12}^{(3)} &= \frac{R^{(2)}(1,1) - R^{(2)}(2,2)}{2\rho^{(2)}} \\ \gamma_{12}^{(3)} &= -\frac{R^{(2)}(2,1) + R^{(2)}(3,1)}{2\rho^{(2)}} \end{aligned}$$

$$\text{and} \tag{1-18}$$

$$\alpha_{11} = \frac{R^{(2)}(1,3) + R^{(2)}(3,1)}{P^{(2)}}$$

$$\beta_{11} = \frac{R^{(2)}(2,3) + R^{(2)}(3,2)}{P^{(2)}}$$

$$\alpha_{12} = \frac{R^{(2)}(1,1) - R^{(2)}(2,2)}{2 P^{(2)}}$$

$$\beta_{12} = \frac{R^{(2)}(1,2) + R^{(2)}(2,1)}{2 P^{(2)}}$$

$$\alpha_{10} = \frac{R^{(2)}(3,3) - R^{(2)}(1,1)}{P^{(2)}} + \frac{R^{(2)}(3,3) - R^{(2)}(2,2)}{P^{(2)}}$$

APPENDIX 2

A THEOREM FOR HARMONIC FUNCTIONS

Let $\chi(\underline{r}')$ be a harmonic function in a region R , where $r' \neq 0$. Thus $\chi(\underline{r}')$ satisfies the Laplace equation in R

$$\nabla^2 \chi = 0 \tag{2-1}$$

and is of the form

$$\chi(\underline{r}') = \left(\frac{1}{r'}\right)^{n+1} Y_n(\theta', \phi') \tag{2-2}$$

If S is a spherical enclosing R with center at the point P (see Figure 37.) and of radius $r^* < r$, then one has immediately from the mean value theorem for harmonic functions (Brand, p. 240)

$$\chi(\underline{r}) = \frac{1}{4\pi r^{*2}} \iint_S \chi(\underline{r}') d\sigma ; \quad r^* < r \tag{2-3}$$

On the other hand, consider a spherical surface of radius $r^* > r$ about the point P , then let R be the region between this surface, call it S , and a second spherical surface S_0 of radius $r_0^* > r^* > r$. (See Figure 37., permit S as shown to expand to contain (o) , but to be within S_0).

Now, Green's second identity gives, for any two functions χ and ψ , continuous up to their second derivatives in R

$$\iiint_R [\chi \nabla^2 \psi - \psi \nabla^2 \chi] d\tau = \iint_{S+S_0} \left[\chi \frac{d\psi}{dn} - \psi \frac{d\chi}{dn} \right] d\sigma$$

dn the normal to $d\sigma$

Taking χ as in (2-1) and ψ to be harmonic in R as well, then $\nabla^2 \psi = \nabla^2 \chi = 0$, and

$$\iint_{S+S_0} \left[\chi \frac{d\psi}{dn} - \psi \frac{d\chi}{dn} \right] ds = 0 \quad (2-4)$$

Now, considering χ as represented by (2-2) with $n \geq 1$, note that

$$|\chi| \leq \frac{K}{R^{n+1}} \quad ; \quad \left| \frac{d\chi}{dn} \right| \leq \frac{K'}{R^{n+2}} \left(\frac{R^*}{R'} \right) \quad ; \quad n \geq 1 \quad (2-5)$$

Hence first choosing $\psi = 1$, then from (2-4)

$$\iint_S \left(\frac{d\chi}{dn} \right) ds + \iint_{S_0} \left(\frac{d\chi}{dn} \right) ds = 0 \quad (2-6)$$

However, using the bounds given by (2-5)

$$0 \leq \left| \iint_{S_0} \left(\frac{d\chi}{dn} \right) ds \right| \leq \left(\frac{1}{R_0^*} \right)^n \iint_0^{2\pi} \int_0^\pi \frac{K'}{\left[\left(\frac{R}{R_0^*} \right)^2 + 1 + 2 \left(\frac{R}{R_0^*} \right) \cos \gamma' \right]^{1/2+3/2}} d\theta d\phi'$$

where γ' denotes the angle between \underline{r} and \underline{r}'_0 . Now, allowing $|r'_0| \rightarrow \infty$ in this expression gives

$$0 \leq \lim_{R_0^* \rightarrow \infty} \left| \iint_{S_0} \left(\frac{d\chi}{dn} \right) ds \right| \leq \lim_{R_0^* \rightarrow \infty} \left(\frac{M}{R_0^* n} \right) \rightarrow 0 \quad ; \text{ for } n \geq 1$$

Therefore

$$\iint_{S_0} \left(\frac{d\chi}{dn} \right) ds = 0 \quad (2-7)$$

for S_0 taken to infinity. Therefore from (2-6)

$$\iint_S \left(\frac{d\chi}{dn} \right) ds = 0 \quad (2-8)$$

Now, taking $\psi = \frac{1}{r^*}$, then from (2-4) and using (2-7) and (2-8)

$$\iint_S \chi \frac{d}{dn} \left(\frac{1}{r^*} \right) ds + \iint_{S_0} \chi \frac{d}{dn} \left(\frac{1}{r^*} \right) ds = 0$$

But

$$\frac{d}{dn} \left(\frac{1}{r^*} \right) = - \frac{d}{dr^*} \left(\frac{1}{r^*} \right) = \left(\frac{1}{r^*} \right)^2$$

and so

$$\left(\frac{1}{r^*} \right)^2 \iint_S \chi ds + \left(\frac{1}{r_0^*} \right)^2 \iint_{S_0} \chi ds = 0$$

Now since $|\chi| \leq K(r')^{-n-1}$, then after permitting S_0 to recede to infinity

$$\iint_S \chi ds = 0 \quad , \quad r^* > R \quad (2-9)$$

Consequently, for harmonic functions $\chi = Y_n(\theta', \phi')/r^{n+1}$, $n \geq 1$

$$\iint_S \chi ds = \begin{cases} 4\pi r^{*2} \chi(r) & ; r^* < R \\ 0 & ; r^* > R \end{cases} \quad (2-10)$$

APPENDIX 3

TRANSFORMATIONS OF THE STATIC SOURCE FIELD

Observing from the diagram in Figure 38. that

$$r^2 = r_0^2 + r'^2 - 2r_0r' \cos \theta' \quad , \quad \phi = \phi'$$

then one may write the static potentials in the form

$$\mathcal{J}^{(1)}(r) = \frac{r^2}{8\pi(\lambda+2\mu)} \sum_{n=1}^{\infty} \frac{\rho^{(n)}}{r^{n+1}} S_n(\theta, \phi)$$

$$\underline{\Psi}^{(1)}(r) = \frac{r^2}{8\pi\mu} \sum_{n=1}^{\infty} \frac{\rho^{(n)}}{r^{n+1}} \underline{S}_n(\theta, \phi)$$

and consider the effect of the transformation on the solid harmonics of the form $(\frac{1}{r})^{n+1} S_n(\theta, \phi)$. However, since $\phi = \phi'$, it is clear that one need consider only the transformation of $(\frac{1}{r})^{n+1} P_n^m(\cos \theta)$.

From Hobson, p. 140, and Sato (1953), one has

$$\frac{P_n^m(\cos \theta)}{r^{n+1}} = \frac{1}{r'^{n+1}} \sum_{s=0}^{\infty} (-1)^s \frac{(n-m+s)!}{s!(n-m)!} \left(\frac{r_0}{r'}\right)^s P_{n+s}^m(\cos \theta'); \quad r_0 < r'$$

$$\frac{P_n^m(\cos \theta)}{r^{n+1}} = \frac{(-1)^{n+1}}{r_0^{n+1}} \sum_{s=0}^{\infty} (-1)^s \frac{(n+s)!}{(m+s)!(n-m)!} \left(\frac{r'}{r_0}\right)^s P_s^m(\cos \theta'); \quad r_0 > r'$$

Thus, for example

$$\mathcal{J}^{(1)}(\underline{r}') = \frac{1}{8\pi(\lambda+2\mu)} \left\{ 1 + \left(\frac{r_0}{r'}\right)^2 - 2\left(\frac{r_0}{r'}\right) \cos \theta' \right\} \sum_{n=1}^{\infty} \frac{\rho^{(n)}}{r'^{n-1}} \left[\sum_{m=0}^n (\alpha_{nm} \cos m\phi' + \beta_{nm} \sin m\phi') \right. \\ \left. \times \sum_{s=0}^{\infty} (-1)^s \frac{(n-m+s)!}{s!(n-m)!} \left(\frac{r_0}{r'}\right)^s P_{n+s}^m(\cos \theta') \right] ; r' > r_0$$

$$\mathcal{J}^{(1)}(\underline{r}') = \frac{1}{8\pi(\lambda+2\mu)} \left\{ 1 + \left(\frac{r'}{r_0}\right)^2 - 2\left(\frac{r'}{r_0}\right) \cos \theta' \right\} \sum_{n=1}^{\infty} \frac{\rho^{(n)}}{r_0^{n-1}} \left[\sum_{m=0}^n (\alpha_{nm} \cos m\phi' + \beta_{nm} \sin m\phi') \right. \\ \left. \sum_{s=0}^{\infty} (-1)^{n+s+1} \frac{(n+s)!}{(m+s)!(n-m)!} \left(\frac{r'}{r_0}\right)^s P_s^m(\cos \theta') \right] ; r' > r_0$$

Further, the recursion relation (Hobson, p. 290)

$$(2n+1)\mu P_n^m(\mu) - (n-m+1)P_{n+1}^m(\mu) - (n+m)P_{n-1}^m(\mu) = 0$$

can be used to remove the $\cos \theta' P_{n+s}^m(\cos \theta')$ factor from the above equations. Therefore

$$\mathcal{J}^{(1)}(\underline{r}') = \frac{1}{8\pi(\lambda+2\mu)} \sum_{n=0}^{\infty} \frac{\rho^{(n+1)}}{r_0^n} \left[\sum_{m=0}^{n+1} (\alpha_{n+1,m} \cos m\phi' + \beta_{n+1,m} \sin m\phi') \sum_{s=0}^{\infty} (-1)^s \frac{(n-m+s+1)!}{s!(n-m+1)!} \right. \\ \left. \times \left(\frac{r_0}{r'}\right)^{n+s} \left[P_{n+s+1}^m(\cos \theta') + \left(\frac{r_0}{r'}\right)^2 P_{n+s+1}^m(\cos \theta') - 2 \left\{ \frac{(n+s-m+2)}{2n+2s+3} P_{n+s+2}^m(\cos \theta') + \frac{(n+s+m+1)}{2n+2s+3} \right. \right. \right. \\ \left. \left. \times P_{n+s}^m(\cos \theta') \right\} \right] ; r' > r_0$$

and

$$\mathcal{J}^{(1)}(\underline{r}') = \frac{1}{8\pi(\lambda+2\mu)} \sum_{n=0}^{\infty} \frac{\rho^{(n+1)}}{r_0^n} \left[\sum_{m=0}^{n+1} \left(\alpha_{n+1,m} \cos m\varphi' + \beta_{n+1,m} \sin m\varphi' \right) \sum_{s=0}^{\infty} (-1)^{s+m+n+2} \right. \\ \left. \times \frac{(n+m+s+1)!}{(2m+s)!(n-m+1)!} \left(\frac{r'}{r_0} \right)^{m+s} \left[P_{m+s}^m(\cos\theta') + \left(\frac{r'}{r_0} \right)^2 P_{m+s}^m(\cos\theta') - 2 \left\{ \frac{s+1}{2s+2m+1} \right\} P_{s+m+1}^m(\cos\theta') \right. \right. \\ \left. \left. + \left(\frac{s+2m}{2s+2m+1} \right) P_{s+m-1}^m(\cos\theta') \right] \right] \quad ; \quad r' < r_0$$

With similar expressions for each of the components of the vector potential $\underline{\Psi}^{(1)}(\underline{r})$. (Here, $P_n^m(\cos\theta') = 0$, if $m > n$ and also

$$P_{-1}^0(\cos\theta') \equiv 0 \quad).$$

A convenient form for the transformed field is, for example

$$\mathcal{J}^{(1)}(\underline{r}') = \frac{1}{8\pi(\lambda+2\mu)} \sum_{l=0}^{\infty} \sum_{k=0}^l \left\{ a_{lk}^{(1)}(r') \cos k\varphi + b_{lk}^{(1)}(r') \sin k\varphi \right\} P_l^k(\cos\theta') \quad (3-1)$$

Thus it is necessary to contract the expressions obtained to the form (3-1). This is most easily accomplished by using the orthogonality properties of the Legendre functions $P_l^k(\cos\theta')$ and the trigonometric functions. The necessary relations for the Legendre functions are summarized by

$$\int_0^\pi P_n^m(\cos\theta') P_l^m(\cos\theta') \sin\theta' d\theta' = \frac{2}{2m+1} \frac{(n+m)!}{(n-m)!} \delta_{nl}$$

$$\delta_{nl} \equiv \begin{cases} 0 & , n \neq l \\ 1 & , n = l \end{cases}$$

Thus, equation (3-1) to the previous expressions obtained for $\mathcal{D}^{(1)}(\underline{r}')$, multiplying both sides of the resulting equation by $\cos k\phi' P_l^k(\cos \theta')$ or $\sin k\phi' P_l^k(\cos \theta')$ and integrating over θ' and ϕ' in each case, one gets for G_{lk} when $r' > r_0$

$$a_{lk}(r') = \sum_{n=0}^{\infty} \frac{\rho^{(n+1)}}{r_0^n} \alpha_{n+1,k} \sum_{s=0}^{\infty} (-1)^s \frac{(n-k+s+1)!}{5!(n-k+1)!} \left(\frac{r_0}{r'}\right)^{n+s} \left[\left(1 + \left(\frac{r_0}{r'}\right)^2\right) \delta_{n+s+1,l} - 2\left(\frac{r_0}{r'}\right) \left\{ \frac{(n+s-k+2)}{(2n+2s+3)} \delta_{n+s+2,l} + \frac{(n+s+k+1)}{(2n+2s+3)} \delta_{n+s,l} \right\} \right] ; r' > r_0$$

Thus, combining terms gives

$$a_{lk}(r') = \left(\frac{r_0}{r'}\right)^{l-1} a_{lk}^{(0)} + \left(\frac{r_0}{r'}\right)^{l+1} a_{lk}^{(1)} \tag{3-2}$$

where

$$a_{lk}^{(0)} = \sum_{n=k-1}^{l-1} \frac{\rho^{(n+1)}}{r_0^n} (-1)^{l-n-1} \frac{(l-k)!}{(l-n)!(n-k+1)!} \left[1 + 2\left(\frac{l-n-1}{2l-1}\right) \right] \alpha_{n+1,k} \tag{3-3}$$

$$a_{lk}^{(1)} = \sum_{n=k-1}^l \frac{\rho^{(n+1)}}{r_0^n} (-1)^{l-n-1} \frac{(l-k+1)!}{(l-n)!(n-k+1)!} \left[\frac{l-n}{l-k+1} + 2\left(\frac{l+k+1}{2l-1}\right) \right] \alpha_{n+1,k}$$

for $r' > r_0$.

In these and following expressions the usual conventions for summations are employed. That is, none of the integers n, l, k may be negative, so that for $k = 0$ in (3-3), the summation index $n = 0$ at the lower limit. In addition, the sum is empty if the upper limit is negative. Finally, $1 \geq k$ by the definition of the Legendre functions.

In the case $r' < r_0$,

$$a_{lk}(r') = \sum_{n=0}^{\infty} \frac{\rho^{(n+1)}}{r_0^n} \left[\sum_{m=0}^{n+l} \alpha_{n+1,m} \delta_{m,k} \sum_{s=0}^{\infty} (-1)^{s+n+m+2} \frac{(n+m+s+1)!}{(2m+s)!(n-m+1)!} \left(\frac{r'}{r_0}\right)^{m+s} \right. \\ \left. \times \left\{ \left(1 + \left(\frac{r'}{r_0}\right)^2\right) \delta_{l,m+2} - 2\left(\frac{r'}{r_0}\right) \left[\frac{(5+1)}{(25+2m+1)} \delta_{l,m+5+1} + \frac{(5+2m)}{(25+2m+1)} \delta_{l,m+5-1} \right] \right\} \right]$$

from which, by combining factors, one gets

$$a_{lk}(r') = \left(\frac{r'}{r_0}\right)^l a_{lk}^{(2)} + \left(\frac{r'}{r_0}\right)^{l+2} a_{lk}^{(3)} \quad (3-4)$$

where

$$a_{lk}^{(2)} = \sum_{n=k-1}^{\infty} \frac{\rho^{(n+1)}}{r_0^n} (-1)^{n+l} \frac{(n+l+1)!}{(l+k)!(n-k+1)!} \left[1 + 2 \frac{(l^2-k^2)}{(n+l+1)(2l-1)} \right] \alpha_{n+1,k} \quad (3-5)$$

$$a_{lk}^{(3)} = \sum_{n=k-1}^{\infty} \frac{\rho^{(n+1)}}{r_0^n} (-1)^{n+l} \frac{(n+l+1)!}{(l+k)!(n-k+1)!} \left[1 + 2 \frac{(n+l+2)}{2l+3} \right] \alpha_{n+1,k}$$

By the same procedure, the function $b_{lk}(r')$ is

$$b_{lk}(r') = \left(\frac{r_0}{r'}\right)^{l-1} b_{lk}^{(0)} + \left(\frac{r_0}{r'}\right)^{l+1} b_{lk}^{(1)} \quad ; \quad r' > r_0 \quad (3-6)$$

$$b_{lk}^{(0)} = \sum_{n=k-1}^{l-1} \frac{\rho^{(n+1)}}{r_0^n} (-1)^{l-n-1} \frac{(l-k)!}{(l-n)!(n-k+1)!} \left[1 + 2 \frac{(l-n-1)}{2l-1} \right] \beta_{n+1,k}$$

$$b_{lk}^{(1)} = \sum_{n=k-1}^l \frac{\rho^{(n+1)}}{r_0^n} (-1)^{l-n-1} \frac{(l-k+1)!}{(l-n)!(n-k+1)!} \left[\frac{(l-n)}{(l-k+1)} + 2 \frac{(l+k+1)}{2l-1} \right] \beta_{n+1,k} \quad (3-7)$$

$$b_{lk}(r') = \left(\frac{r'}{r_0}\right)^l b_{lk}^{(2)} + \left(\frac{r'}{r_0}\right)^{l+2} b_{lk}^{(3)} \quad ; \quad r' < r_0 \quad (3-8)$$

$$b_{lk}^{(2)} = \sum_{n=k-1}^{\infty} \frac{\rho^{(n+1)}}{r_0^n} (-1)^{n+l} \frac{(n+l+1)!}{(l+k)!(n-k+1)!} \left[1 + 2 \frac{(l^2 - k^2)}{(n+l+1)(2l-1)}\right] \beta_{n+1,k} \quad (3-9)$$

$$b_{lk}^{(3)} = \sum_{n=k-1}^{\infty} \frac{\rho^{(n+1)}}{r_0^n} (-1)^{n+l} \frac{(n+l+1)!}{(l+k)!(n-k+1)!} \left[1 + 2 \frac{(n+l+2)}{2l+3}\right] \beta_{n+1,k}$$

The vector potential $\underline{\psi}^{(1)}(\underline{r})$ may be attacked in exactly the same way, by considering each Cartesian component separately.

Thus, for the i th component

$$\psi_i^{(1)}(R) = \frac{1}{8\pi\mu} \sum_{l=0}^{\infty} \left[\sum_{k=0}^l (i c_{lk}(r') \cos k\phi' + i d_{lk}(r') \sin k\phi') P_l^k(\cos\theta') \right] \quad (3-10)$$

where the functions $i c_{lk}(r')$ and $i d_{lk}(r')$ are, by a repetition of the computations for $a_{lk}(r')$ and $b_{lk}(r')$

$$i c_{lk}(r') = \left(\frac{r_0}{r'}\right)^{l-1} i c_{lk}^{(0)} + \left(\frac{r_0}{r'}\right)^{l+1} i c_{lk}^{(1)} \quad ; \quad r' > r_0 \quad (3-11)$$

$$i c_{lk}^{(0)} = \sum_{n=k-1}^{l-1} \frac{\rho^{(n+1)}}{r_0^n} (-1)^{l-n-1} \frac{(l-k)!}{(l-n)!(n-k+1)!} \left[1 + 2 \frac{(l-n-1)}{2l-1}\right] \gamma_{n+1,k}^{(0)} \quad (3-12)$$

$$i c_{lk}^{(1)} = \sum_{n=k-1}^l \frac{\rho^{(n+1)}}{r_0^n} (-1)^{l-n-1} \frac{(l-k+1)!}{(l-n)!(n-k+1)!} \left[\frac{(l-n)}{(l-k+1)} + 2 \frac{(l+k+1)}{2l-1} \right] \gamma_{n+1,k}^{(0)}$$

and

$${}_i C_{lk}(r') = \left(\frac{r'}{r_0}\right)^l {}_i C_{lk}^{(2)} + \left(\frac{r'}{r_0}\right)^{l+2} {}_i C_{lk}^{(3)} ; r' < r_0 \quad (3-13)$$

$${}_i C_{lk}^{(2)} = \sum_{n=k-1}^{\infty} \frac{\rho^{(n+1)}}{r_0^n} (-1)^{n+l} \frac{(n+l+1)!}{(l+k)!(n-k+1)!} \left[1 + 2 \frac{(l^2 - k^2)}{(n+l+1)(2l-1)} \right] \gamma_{n+1,k}^{(i)} \quad (3-14)$$

$${}_i C_{lk}^{(3)} = \sum_{n=k-1}^{\infty} \frac{\rho^{(n+1)}}{r_0^n} (-1)^{n+l} \frac{(n+l+1)!}{(l+k)!(n-k+1)!} \left[1 + 2 \frac{(n+l+2)}{2l+3} \right] \gamma_{n+1,k}^{(i)}$$

Likewise, the functions ${}_i d_{lk}(r')$ are given by

$${}_i d_{lk}(r') = \left(\frac{r_0}{r'}\right)^{l-1} {}_i d_{lk}^{(0)} + \left(\frac{r_0}{r'}\right)^{l+1} {}_i d_{lk}^{(1)} ; r' > r_0 \quad (3-15)$$

$${}_i d_{lk}^{(0)} = \sum_{n=k-1}^{l-1} \frac{\rho^{(n+1)}}{r_0^n} (-1)^{l-n-1} \frac{(l-k)!}{(l-n)!(n-k+1)!} \left[1 + 2 \frac{(l-n-1)}{2l-1} \right] \delta_{n+1,k}^{(i)} \quad (3-16)$$

$${}_i d_{lk}^{(1)} = \sum_{n=k-1}^l \frac{\rho^{(n+1)}}{r_0^n} (-1)^{l-n-1} \frac{(l-k+1)!}{(l-n)!(n-k+1)!} \left[\frac{l-n}{l-k+1} + 2 \frac{(l+k+1)}{2l-1} \right] \delta_{n+1,k}^{(i)}$$

$${}_i d_{lk}(r') = \left(\frac{r'}{r_0}\right)^l {}_i d_{lk}^{(2)} + \left(\frac{r'}{r_0}\right)^{l+2} {}_i d_{lk}^{(3)} ; r' < r_0 \quad (3-17)$$

$${}_i d_{lk}^{(2)} = \sum_{n=k-1}^{\infty} \frac{\rho^{(n+1)}}{r_0^n} (-1)^{n+l} \frac{(n+l+1)}{(l+k)!(n-k+1)!} \left[1 + 2 \frac{(l^2 - k^2)}{(n+l+1)(2l-1)} \right] \delta_{n+1,k}^{(i)} \quad (3-18)$$

$${}_i d_{lk}^{(3)} = \sum_{n=k-1}^{\infty} \frac{\rho^{(n+1)}}{r_0^n} (-1)^{n+l} \frac{(n+l+1)!}{(l+k)!(n-k+1)!} \left[1 + 2 \frac{(n+l+2)}{2l+3} \right] \delta_{n+1,k}^{(i)}$$

The potentials may thus be written as

$$\mathcal{J}^{(1)}(\underline{r}') = \begin{cases} \frac{1}{8\pi(\lambda+2\mu)} \left[\sum_{l=0}^{\infty} \left(\frac{R_0}{R'}\right)^{l-1} {}_0S_l(\theta, \varphi') + \sum_{l=0}^{\infty} \left(\frac{R_0}{R'}\right)^{l+1} {}_1S_l(\theta', \varphi') \right]; R' > R_0 \\ \frac{1}{8\pi(\lambda+2\mu)} \left[\sum_{l=0}^{\infty} \left(\frac{R'}{R_0}\right)^l {}_2S_l(\theta, \varphi) + \sum_{l=0}^{\infty} \left(\frac{R'}{R_0}\right)^{l+2} {}_3S_l(\theta', \varphi') \right]; R' < R_0 \end{cases} \quad (3-19)$$

$$\Psi_i(\underline{r}') = \begin{cases} \frac{1}{8\pi\mu} \left[\sum_{l=0}^{\infty} \left(\frac{R_0}{R'}\right)^{l-1} \mathcal{S}_l^{(i)}(\theta, \varphi') + \sum_{l=0}^{\infty} \left(\frac{R_0}{R'}\right)^{l+1} \mathcal{S}_l^{(i)}(\theta', \varphi') \right]; R' > R_0 \\ \frac{1}{8\pi\mu} \left[\sum_{l=0}^{\infty} \left(\frac{R'}{R_0}\right)^l \mathcal{S}_l^{(i)}(\theta, \varphi) + \sum_{l=0}^{\infty} \left(\frac{R'}{R_0}\right)^{l+2} \mathcal{S}_l^{(i)}(\theta', \varphi') \right]; R' < R_0 \end{cases}$$

where

$${}_pS_l(\theta, \varphi') = \sum_{k=0}^l (a_{pk}^{(p)} \cos k\varphi' + b_{pk}^{(p)} \sin k\varphi') P_l^k(\cos \theta) ; p=0,1,2,3 \quad (3-20)$$

$${}_p\mathcal{S}_l^{(i)}(\theta, \varphi') = \sum_{k=0}^l (i c_{pk}^{(p)} \cos k\varphi' + i d_{pk}^{(p)} \sin k\varphi') P_l^k(\cos \theta) ; p=0,1,2,3$$

Finally, the displacement field $\underline{u}^{(1)}(\underline{r})$ expressed as spherical components in the translated coordinate system r', θ', φ' is obtained using the formulas of the Appendix 4 (e. g., see equation 4-7). Thus, by an application of the equations (4-7) of Appendix 4,

$$\begin{aligned}
 u_{\pi'} = & \left\{ \begin{aligned}
 & -\frac{1}{8\pi\kappa_0} \sum_{l=0}^{\infty} \sum_{p=0}^1 \left(\frac{\kappa_0}{\kappa'}\right)^{l+2p} \left[\frac{l+2p-1}{\lambda+2\mu} \frac{1}{p} S_l(\theta', \varphi') + \frac{1}{\mu} \left\{ (\sin\varphi' \frac{\partial}{\partial\theta'} + \cos\varphi' \cot\theta' \frac{\partial}{\partial\varphi'}) \right. \right. \\
 & \left. \left. + S_l^{(1)}(\theta', \varphi') + \left(\sin\varphi' \cot\theta' \frac{\partial}{\partial\varphi'} - \cos\varphi' \frac{\partial}{\partial\theta'} \right) S_l^{(2)}(\theta', \varphi') - \frac{\partial}{\partial\varphi'} S_l^{(3)}(\theta', \varphi') \right\} \right] ; \kappa' > \kappa_0 \\
 & -\frac{1}{8\pi\kappa_0} \sum_{l=0}^{\infty} \sum_{p=2}^3 \left(\frac{\kappa'}{\kappa_0}\right)^{l+2p-5} \left[\frac{l+2p-1}{\lambda+2\mu} \frac{1}{p} S_l(\theta', \varphi') + \frac{1}{\mu} \left\{ (\sin\varphi' \frac{\partial}{\partial\theta'} + \cos\varphi' \cot\theta' \frac{\partial}{\partial\varphi'}) \right. \right. \\
 & \left. \left. + S_l^{(1)}(\theta', \varphi') + \left(\sin\varphi' \cot\theta' \frac{\partial}{\partial\varphi'} - \cos\varphi' \frac{\partial}{\partial\theta'} \right) S_l^{(2)}(\theta', \varphi') - \frac{\partial}{\partial\varphi'} S_l^{(3)}(\theta', \varphi') \right\} \right] ; \kappa' < \kappa_0
 \end{aligned} \right.
 \end{aligned}
 \tag{3-21}$$

$$\begin{aligned}
 u_{\theta} = & \left\{ \begin{aligned}
 & \frac{1}{8\pi\kappa_0} \sum_{l=0}^{\infty} \sum_{p=0}^1 \left(\frac{\kappa_0}{\kappa'}\right)^{l+2p} \left[\frac{1}{\lambda+2\mu} \left(\frac{\partial}{\partial\theta'}\right) \frac{1}{p} S_l(\theta', \varphi') + \frac{1}{\mu} \left\{ (\cos\varphi' \frac{\partial}{\partial\varphi'} - (l+2p-1)\sin\varphi' \right. \right. \\
 & \left. \left. + S_l^{(1)}(\theta', \varphi') + \left(\sin\varphi' \frac{\partial}{\partial\varphi'} + (l+2p-1)\cos\varphi' \right) S_l^{(2)}(\theta', \varphi') + \left(\cot\theta' \frac{\partial}{\partial\varphi'} \right) S_l^{(3)}(\theta', \varphi') \right\} \right] ; \kappa' > \kappa_0 \\
 & \frac{1}{8\pi\kappa_0} \sum_{l=0}^{\infty} \sum_{p=2}^3 \left(\frac{\kappa'}{\kappa_0}\right)^{l+2p-5} \left[\frac{1}{\lambda+2\mu} \left(\frac{\partial}{\partial\theta'}\right) \frac{1}{p} S_l(\theta', \varphi') + \frac{1}{\mu} \left\{ (\cos\varphi' \frac{\partial}{\partial\varphi'} - (l+2p-4)\sin\varphi' \right. \right. \\
 & \left. \left. + S_l^{(1)}(\theta', \varphi') + \left(\sin\varphi' \frac{\partial}{\partial\varphi'} + (l+2p-4)\cos\varphi' \right) S_l^{(2)}(\theta', \varphi') + \left(\cot\theta' \frac{\partial}{\partial\varphi'} \right) S_l^{(3)}(\theta', \varphi') \right\} \right] ; \kappa' < \kappa_0
 \end{aligned} \right.
 \end{aligned}
 \tag{3-22}$$

$$\begin{aligned}
 & \frac{1}{8\pi k_0} \sum_{l=0}^{\infty} \sum_{p=0}^l \left(\frac{k_0}{k'}\right)^{l+2p} \left[\frac{1}{\lambda+2\mu} \left(\frac{1}{\sin\theta} \frac{\partial}{\partial\theta}\right)_{p,l} S(\theta',\varphi') - \frac{1}{\mu} \left\{ (l+2p-1) \cos\theta' \cos\varphi' + \right. \\
 & \left. \sin\theta' \cos\varphi' \frac{\partial}{\partial\theta'} \right\} \sum_{p,l}^{(1)} S(\theta',\varphi') + \left\{ (l+2p-1) \cos\theta' \sin\varphi' + \sin\theta' \sin\varphi' \frac{\partial}{\partial\theta'} \right\} \sum_{p,l}^{(2)} S(\theta',\varphi') + \\
 & \left. \left(\cos\theta' \frac{\partial}{\partial\theta'} - (l+2p-1) \sin\theta' \right) \sum_{p,l}^{(3)} S(\theta',\varphi') \right\}; \quad \pi' > k_0 \\
 & \frac{1}{8\pi k_0} \sum_{l=0}^{\infty} \sum_{p=2}^3 \left(\frac{k_0}{k'}\right)^{l+2p-5} \left[\frac{1}{\lambda+2\mu} \left(\frac{1}{\sin\theta} \frac{\partial}{\partial\theta}\right)_{p,l} S(\theta',\varphi') - \frac{1}{\mu} \left\{ (l+2p-4) \cos\theta' \cos\varphi' + \right. \\
 & \left. \sin\theta' \cos\varphi' \frac{\partial}{\partial\theta'} \right\} \sum_{p,l}^{(1)} S(\theta',\varphi') + \left\{ (l+2p-4) \cos\theta' \sin\varphi' + \sin\theta' \sin\varphi' \frac{\partial}{\partial\theta'} \right\} \sum_{p,l}^{(2)} S(\theta',\varphi') \\
 & \left. + \left(\cos\theta' \frac{\partial}{\partial\theta'} - (l+2p-4) \sin\theta' \right) \sum_{p,l}^{(3)} S(\theta',\varphi') \right\}; \quad \pi' < k_0 \tag{3-23}
 \end{aligned}$$

APPENDIX 4

TRANSFORMATION OF THE VECTOR DISPLACEMENT FIELD
TO CURVILINEAR COORDINATES

Consider the displacement field given by

$$\underline{u} = \nabla\phi + \nabla\times\Psi \quad (4-1)$$

In terms of general curvilinear coordinates (ξ^1, ξ^2, ξ^3) , where the metric elements are defined by⁽¹⁾

$$ds^2 = h_i^2 (d\xi^i)^2 = g_{ii} (d\xi^i)^2 ; dv = h_1 h_2 h_3 d\xi^1 d\xi^2 d\xi^3$$

$$g_{ii} = \frac{\partial x_m}{\partial \xi^i} \frac{\partial x_n}{\partial \xi^i} \delta_{mn} ; h_i = \sqrt{g_{ii}} ; \delta_{mn} = \begin{cases} 0, & m \neq n \\ 1, & m = n \end{cases} \quad (4-2)$$

one has the following relations

$$\nabla\phi = \frac{1}{h_1} \frac{\partial\phi}{\partial\xi^1} \hat{n}_1 + \frac{1}{h_2} \frac{\partial\phi}{\partial\xi^2} \hat{n}_2 + \frac{1}{h_3} \frac{\partial\phi}{\partial\xi^3} \hat{n}_3$$

$$\nabla \cdot \underline{\Psi} = \frac{1}{h_1 h_2 h_3} \left\{ \frac{\partial}{\partial\xi^1} (h_2 h_3 \bar{\Psi}_1) + \frac{\partial}{\partial\xi^2} (h_1 h_3 \bar{\Psi}_2) + \frac{\partial}{\partial\xi^3} (h_1 h_2 \bar{\Psi}_3) \right\} \quad (4-3)$$

$$\nabla\times\underline{\Psi} = \frac{\hat{n}_i}{h_j h_k} \epsilon_{ijk} \frac{\partial}{\partial\xi^j} (h_k \bar{\Psi}_k)$$

$$\nabla^2\phi = \frac{1}{h_1 h_2 h_3} \left\{ \frac{\partial}{\partial\xi^1} \left(\frac{h_2 h_3}{h_1} \frac{\partial\phi}{\partial\xi^1} \right) + \frac{\partial}{\partial\xi^2} \left(\frac{h_3 h_1}{h_2} \frac{\partial\phi}{\partial\xi^2} \right) + \frac{\partial}{\partial\xi^3} \left(\frac{h_1 h_2}{h_3} \frac{\partial\phi}{\partial\xi^3} \right) \right\}$$

⁽¹⁾The summation convention is used throughout.

where $\bar{\psi}_k$ are the so-called "physical components" of the vector $\underline{\psi}$, that is the orthogonal projections of the vector $\underline{\psi}$ on the unit vectors \hat{h}_k of the basic system.

Finally, between the Cartesian (rectangular) components of the vector $\underline{\psi}$, denoted by ψ_i , and the components $\bar{\psi}_i$ in the general curvilinear system, we have the relationship (Morse and Feshback, Vol. 1, p. 29),

$$\bar{\psi}_i = \left(\frac{1}{h_j}\right) \psi_k \frac{\partial x^k}{\partial \xi^i} \delta_{ij} \quad (4-4)$$

Let δ and ψ_i , the Cartesian components of $\underline{\psi}$, be assumed expressed in terms of the curvilinear coordinates ξ^k . Then the displacement field \underline{u} is, in terms of the curvilinear coordinates and rectangular components of $\underline{\psi}$

$$\bar{u} = \frac{1}{h_i} \frac{\partial \phi}{\partial \xi^i} \hat{n}_i + \frac{\hat{n}_i}{h_j h_k} \epsilon_{ijk} \frac{\partial}{\partial \xi^j} \left(\psi_l \frac{\partial x^l}{\partial \xi^i} \right) \quad (4-5)$$

Thus,

$$\bar{u}_1 = \left(\frac{1}{h_1}\right) \frac{\partial \phi}{\partial \xi^1} + \left(\frac{1}{h_2 h_3}\right) \left\{ \frac{\partial}{\partial \xi^2} \left(\psi_1 \frac{\partial x^1}{\partial \xi^3} + \psi_2 \frac{\partial x^2}{\partial \xi^3} + \psi_3 \frac{\partial x^3}{\partial \xi^3} \right) - \frac{\partial}{\partial \xi^3} \left(\psi_1 \frac{\partial x^1}{\partial \xi^2} + \psi_2 \frac{\partial x^2}{\partial \xi^2} + \psi_3 \frac{\partial x^3}{\partial \xi^2} \right) \right\}$$

$$\bar{u}_2 = \left(\frac{1}{h_2}\right) \frac{\partial \phi}{\partial \xi^2} + \left(\frac{1}{h_1 h_3}\right) \left\{ \frac{\partial}{\partial \xi^3} \left(\psi_1 \frac{\partial x^1}{\partial \xi^1} + \psi_2 \frac{\partial x^2}{\partial \xi^1} + \psi_3 \frac{\partial x^3}{\partial \xi^1} \right) - \frac{\partial}{\partial \xi^1} \left(\psi_1 \frac{\partial x^1}{\partial \xi^3} + \psi_2 \frac{\partial x^2}{\partial \xi^3} + \psi_3 \frac{\partial x^3}{\partial \xi^3} \right) \right\}$$

$$\bar{u}_3 = \left(\frac{1}{h_3}\right) \frac{\partial \phi}{\partial \xi^3} + \left(\frac{1}{h_1 h_2}\right) \left\{ \frac{\partial}{\partial \xi^1} \left(\psi_1 \frac{\partial x^1}{\partial \xi^2} + \psi_2 \frac{\partial x^2}{\partial \xi^2} + \psi_3 \frac{\partial x^3}{\partial \xi^2} \right) - \frac{\partial}{\partial \xi^2} \left(\psi_1 \frac{\partial x^1}{\partial \xi^1} + \psi_2 \frac{\partial x^2}{\partial \xi^1} + \psi_3 \frac{\partial x^3}{\partial \xi^1} \right) \right\} \quad (4-6)$$

where here again, the bar over the components of \underline{u} indicates components along the basis vectors in the curvilinear system.

Consider the spherical and cylindrical coordinate systems.

For the first of these

$$\begin{array}{lll} x^1 = r \sin \theta \cos \phi & h_1 = h_r = 1 & \xi^1 = r \\ x^2 = r \sin \theta \sin \phi & h_2 = h_\theta = r & \xi^2 = \theta \\ x^3 = r \cos \theta & h_3 = h_\phi = r \sin \theta & \xi^3 = \phi \end{array}$$

$$\left\{ \frac{\partial x^j}{\partial \xi^k} \right\} = \begin{pmatrix} \sin \theta \cos \phi & r \cos \theta \cos \phi & -r \sin \theta \sin \phi \\ \sin \theta \sin \phi & r \cos \theta \sin \phi & r \sin \theta \cos \phi \\ \cos \theta & -r \sin \theta & 0 \end{pmatrix}$$

And therefore we have

$$\begin{aligned} \bar{u}_1 = u_r = \frac{\partial \psi}{\partial r} - \frac{1}{r \sin \theta} \left\{ (\sin \phi \sin \theta \frac{\partial}{\partial \theta} + \cos \phi \cos \theta \frac{\partial}{\partial \phi}) \psi_1 \right. \\ \left. + (\sin \phi \cos \theta \frac{\partial}{\partial \theta} - \cos \phi \sin \theta \frac{\partial}{\partial \phi}) \psi_2 - (\sin \theta \frac{\partial}{\partial \phi}) \psi_3 \right\} \end{aligned}$$

$$\begin{aligned} \bar{u}_2 = u_\theta = \frac{1}{r} \frac{\partial \psi}{\partial \theta} + \frac{1}{r \sin \theta} \left\{ (\sin \theta \cos \phi \frac{\partial}{\partial \phi} + r \sin \theta \sin \phi \frac{\partial}{\partial r}) \psi_1 \right. \\ \left. + (\sin \theta \sin \phi \frac{\partial}{\partial \phi} - r \sin \theta \cos \phi \frac{\partial}{\partial r}) \psi_2 + (\cos \theta \frac{\partial}{\partial \phi}) \psi_3 \right\} \end{aligned}$$

$$\begin{aligned} \bar{u}_3 = u_\phi = \frac{1}{r \sin \theta} \frac{\partial \psi}{\partial \phi} + \frac{1}{r} \left\{ (r \cos \theta \cos \phi \frac{\partial}{\partial r} - \sin \theta \cos \phi \frac{\partial}{\partial \theta}) \psi_1 \right. \\ \left. + (r \cos \theta \sin \phi \frac{\partial}{\partial r} - \sin \theta \sin \phi \frac{\partial}{\partial \theta}) \psi_2 - (r \sin \theta \frac{\partial}{\partial r} + \cos \theta \frac{\partial}{\partial \theta}) \psi_3 \right\} \end{aligned}$$

In the cylindrical system

$$\begin{aligned} x^1 &= \rho \cos \phi & h_1 &\equiv h_\rho = 1 & \xi^1 &= \rho \\ x^2 &= \rho \sin \phi & h_2 &\equiv h_\phi = \rho & \xi^2 &= \phi \\ x^3 &= z & h_3 &\equiv h_z = 1 & \xi^3 &= z \end{aligned} \quad \left\{ \frac{\partial x^j}{\partial \xi^k} \right\} = \begin{pmatrix} \cos \phi & -\rho \sin \phi & 0 \\ \sin \phi & \rho \cos \phi & 0 \\ 0 & 0 & 1 \end{pmatrix}$$

and the displacements in cylindrical coordinates become

$$\begin{aligned} \bar{u}_1 \equiv u_\rho &= \frac{\partial v}{\partial \rho} + \frac{1}{\rho} \left\{ \rho \sin \phi \frac{\partial \psi_1}{\partial z} - \rho \cos \phi \frac{\partial \psi_2}{\partial z} + \frac{\partial \psi_3}{\partial \phi} \right\} \\ \bar{u}_2 \equiv u_\phi &= \frac{1}{\rho} \frac{\partial v}{\partial \phi} + \cos \phi \frac{\partial \psi_1}{\partial z} + \sin \phi \frac{\partial \psi_2}{\partial z} - \frac{\partial \psi_3}{\partial \rho} \\ \bar{u}_3 \equiv u_z &= \frac{\partial v}{\partial z} + \frac{1}{\rho} \left\{ (\rho \sin \phi \frac{\partial}{\partial \rho} + \cos \phi \frac{\partial}{\partial \phi}) \psi_1 + (\rho \cos \phi \frac{\partial}{\partial \rho} + \sin \phi \frac{\partial}{\partial \phi}) \psi_2 \right\} \end{aligned} \quad (4-8)$$

As an application of these relations, the static displacement field expressed by the potentials (equation (2.5.5) of the text)

$$\begin{aligned} \varphi^{(i)}(r) &= \frac{1}{8\pi(\lambda+2\mu)} \sum_{n=0}^{\infty} \frac{\rho^{(n+1)}}{r^n} S_{n+1}(\theta, \phi) \\ \psi_i^{(i)}(r) &= \frac{1}{8\pi\mu} \sum_{n=0}^{\infty} \frac{\rho^{(n+1)}}{r^n} S_{n+1}^{(i)}(\theta, \phi); \quad i=1,2,3 \end{aligned}$$

appropriate to the primary field from a general volume source is, in terms of spherical coordinates and components of \underline{u} ,

$$u_r = -\frac{1}{8\pi} \sum_{n=0}^{\infty} \frac{P^{(n+1)}}{r^{n+1}} \left[\frac{1}{\lambda+2\mu} (n S_{n+1}(\theta, \phi) + \frac{1}{\mu} \left\{ (\sin\phi \frac{\partial}{\partial\theta} + \cos\phi \cot\theta \frac{\partial}{\partial\phi}) S_{n+1}^{(1)}(\theta, \phi) + (\sin\phi \cot\theta \frac{\partial}{\partial\phi} - \cos\phi \frac{\partial}{\partial\theta}) \times S_{n+1}^{(2)}(\theta, \phi) - \left(\frac{\partial}{\partial\phi}\right) S_{n+1}^{(3)}(\theta, \phi) \right\} \right]$$

$$u_\theta = \frac{1}{8\pi} \sum_{n=0}^{\infty} \frac{P^{(n+1)}}{r^{n+1}} \left[\frac{1}{\lambda+2\mu} (n S_{n+1}(\theta, \phi)) + \frac{1}{\mu} \left\{ (\sin\phi \frac{\partial}{\partial\theta} + \cos\phi \cot\theta \frac{\partial}{\partial\phi}) S_{n+1}^{(1)}(\theta, \phi) + (\sin\phi \frac{\partial}{\partial\phi} + n \cos\phi) S_{n+1}^{(2)} + (\cot\theta \frac{\partial}{\partial\phi}) S_{n+1}^{(3)}(\theta, \phi) \right\} \right]$$

$$u_\phi = \frac{1}{8\pi} \sum_{n=0}^{\infty} \frac{P^{(n+1)}}{r^{n+1}} \left[\frac{1}{\lambda+2\mu} \left(\frac{1}{\sin\theta} \frac{\partial}{\partial\phi} \right) S_{n+1}(\theta, \phi) - \frac{1}{\mu} \left\{ (n \cos\theta \cos\phi + \sin\theta \cos\phi \frac{\partial}{\partial\theta}) S_{n+1}^{(1)}(\theta, \phi) + (n \cos\theta \sin\phi + \sin\theta \sin\phi \frac{\partial}{\partial\theta}) S_{n+1}^{(2)}(\theta, \phi) + \left(\cos\theta \frac{\partial}{\partial\theta} - n \sin\theta \right) S_{n+1}^{(3)}(\theta, \phi) \right\} \right]$$

APPENDIX 5

SOLUTION COEFFICIENTS FOR EXPANDING
ELLIPSOIDAL RUPTURE MODELS

The form of the solution for the expanding rupture model (m = 1) is given by the equation (3.11.20) of the text. The multipole coefficients in this solution are given by (3.11.21) as (s ≡ l - n)

$$\begin{aligned} \begin{pmatrix} A_{lk}(\omega) \\ B_{lk}(\omega) \end{pmatrix} &= k_p^2 \frac{\eta_1}{V_p} \sum_{p \geq 0} \left(\frac{2}{V_R}\right)^p \sum_{n=1}^l (-1)^{l-n} \begin{pmatrix} A_{nk}^{(p)} \\ B_{nk}^{(p)} \end{pmatrix} \frac{\Gamma(l-k+1)}{\Gamma(l-n+1)\Gamma(n-k+1)} \\ &\times \left[\int_0^{a_0} \left(\frac{1}{r'}\right)^{n-p-1} {}_1F_1(s+p; s+p+1; -2i\eta_1 k_p r') e^{-ik_p r'} j_l(k_p r') dr' \right. \\ &\left. + a_0^{l-n+p} {}_1F_1(s+p; s+p+1; -2i\eta_1 k_p a_0) \int_0^{R_s} \left(\frac{1}{r'}\right)^{l-1} e^{-ik_p r'} j_l(k_p r') dr' \right] \quad (5-1) \end{aligned}$$

The integrals in this expression will be evaluated and the coefficients A_{lk} and B_{lk} expressed in a convenient form. As in section 2.7 one has from Erdelyi et al. (1954) (I. T. - Vol. 1, p. 328),

$$\int_0^1 (1-x)^\mu e^{\pm iax} J_\nu(ax) x^{\nu-1} dx = \frac{a^\nu B(\nu, \mu+1)}{2^\nu \Gamma(\nu+1)} \times {}_2F_2\left(\nu + \frac{1}{2}, \nu + \frac{1}{2}; \nu + \mu + \frac{1}{2}, \nu + \frac{1}{2}; \pm 2ia\right) \quad (5-2)$$

provided

$$\text{Re}(\mu) > -1, \quad \text{Re}(\nu) > -\text{Re}(\mu)$$

Here $B(x, y)$ denotes the beta function and ${}_2F_2$ is a hypergeometric function. Thus, writing the integrals in (5-1) as

$$\int_0^{a_0} \left(\frac{1}{\pi'}\right)^{n-p-1} {}_1F_1(s+p; s+p+1; -2i\eta, k_R \pi') e^{-ik_p \pi'} J_l(k_p \pi') d\pi'$$

$$= \sum_{q=0}^{\infty} \frac{(s+p)}{(s+p+q)} \frac{(-2i\eta, k_R)^q}{\Gamma(q+1)} \int_0^{a_0} \left(\frac{1}{\pi'}\right)^{n-p-1} e^{-ik_p \pi'} J_l(k_p \pi') d\pi' \quad (5-3)$$

and

$$\int_{a_0}^{R_s} \left(\frac{1}{\pi'}\right)^{l-1} e^{-ik_p \pi'} J_l(k_p \pi') d\pi' = \int_0^{R_s} \left(\frac{1}{\pi'}\right)^{l-1} e^{-ik_p \pi'} J_l(k_p \pi') d\pi'$$

$$- \int_0^{a_0} \left(\frac{1}{\pi'}\right)^{l-1} e^{-ik_p \pi'} J_l(k_p \pi') d\pi' \quad (5-4)$$

then (5-2) may be utilized to evaluate these integrals. ⁽¹⁾ Thus setting the integral in (5-3) equal to I_1 and transforming gives

$$I_1 = \sqrt{\frac{\pi}{2}} \left(\frac{1}{a_0}\right)^{n-p-q-3/2} k_p^{-1/2} \int_0^1 x^{p+q-n+1/2} e^{-i(k_p a_0)x} J_{l+1/2}(k_p a_0 x) dx \quad (5-5)$$

In this case, comparing the parameters with those in (5-2)

(1) Interchange of the order of summation and integration in (5-3) follows from the uniform convergence of the hypergeometric series over the interval $(0, a_0)$.

$$\operatorname{Re}(\mu) = 0 \quad \text{and} \quad \kappa = \rho + q - n + 3/2$$

with $\nu = l + \frac{1}{2}$. Thus the first of the conditions on the integral parameters is satisfied, while the second reduces to the condition

$$l - n > -(p + q + 2)$$

Since $l \geq n$ in all cases, while p and q are both non-negative, then clearly the second of the conditions is satisfied. Thus

$$I_1 = \sqrt{\frac{\pi}{2}} \left(\frac{1}{a_0}\right)^{n-p-q-2} (k_p a_0)^l \frac{B(l-n+p+q+2, 1)}{2^{l+1/2} \Gamma(l+3/2)} \quad (5-6)$$

$${}_2F_2(l+1, 5+p+q+2; 5+p+q+3, 2l+2; -2ik_p a_0)$$

where $s \equiv l - n$ and $k_p = \frac{\omega}{v_p}$. However, using the identities

$$B(x, y) = \frac{\Gamma(x)\Gamma(y)}{\Gamma(x+y)}$$

$$\Gamma(n+k) = \frac{\sqrt{\pi} \Gamma(2n)}{2^{2n-1} \Gamma(n)}$$

in (5-6) reduces the result to

$$I_1 = (2k_p a_0)^l a_0^{\rho+q-n+2} \sum_{\kappa=0}^{\infty} \frac{\Gamma(l+\kappa+1)}{\Gamma(2l+\kappa+2)} \left(\frac{1}{5+p+q+\kappa+2}\right) \times \frac{(-2ik_p a_0)^\kappa}{\Gamma(\kappa+1)} \quad (5-7)$$

This series result is convergent for all values of the argument $k_p a_0$.

Thus finally one has

$$\int_0^{a_0} \left(\frac{1}{R'}\right)^{n-p-1} {}_1F_1(s+p; s+p+1; -2i\gamma, k_p a_0) e^{-i k_p R'} J_{\frac{1}{2}}(k_p R') dR' = (2k_p a_0)^l a_0^{2n+2}$$

$$\sum_{q=0}^{s+p} \frac{(s+p)}{(s+p+q)} \frac{(-2i\gamma k_p a_0)^q}{\Gamma(q+1)} \sum_{n=0}^{\infty} \frac{\Gamma(l+n+1)}{\Gamma(2l+n+2)} \left(\frac{1}{l-n+p+q+n+2}\right) \frac{(-2i k_p a_0)^n}{\Gamma(n+1)}$$

(5-8)

The result is equivalent to a generalized hypergeometric series (Erdelyi, 1954; H. T. F. - Vol. 1).

Turning to the second integral (5-4) and setting it equal to I_2 , one has after transforming

$$I_2 = \sqrt{\frac{\pi}{2}} k_p^{-1/2} \left[\left(\frac{1}{R_s}\right)^{l-3/2} \int_0^1 e^{-i(k_p R_s)x} J_{l+1/2}(k_p R_s x) x^{1/2-l} dx \right. \\ \left. - \left(\frac{1}{a_0}\right)^{l-3/2} \int_0^1 e^{-i(k_p a_0)x} J_{l+1/2}(k_p a_0 x) x^{1/2-l} dx \right]$$

(5-9)

It is easy to verify that the conditions associated with (5-2) are satisfied and therefore

$$I_2 = \sqrt{\frac{\pi}{2}} \frac{B(2,1) k_p^l}{2^{l+1/2} \Gamma(l+3/2)} \left[R_s^2 F_2(l+1, 2; 3, 2l+2; -2i k_p R_s) \right. \\ \left. - a_0^2 F_2(l+1, 2; 3, 2l+2; -2i k_p a_0) \right]$$

(5-10)

This expression may be rearranged to a form suitable for computation by use of the definitions of the various functions involved. In particular one has

$$I_2 = -(2k_p)^{l-2} \sum_{k=0} \frac{\Gamma(l+k+1)}{\Gamma(2l+k+2)} \left(\frac{1}{\pi+2}\right) \left[1 - \left(\frac{a_0}{R_s}\right)^{\pi+2}\right] \frac{(-2ik_p R_s)^{\pi+2}}{\Gamma(\pi+1)} \quad (5-11)$$

Replacing the integrals in (5-1) by the series expansion of (5-8) and (5-11) gives, after minor rearrangement

$$\begin{aligned} \begin{pmatrix} A_{lk}(\omega) \\ B_{lk}(\omega) \end{pmatrix} &= -\frac{\eta_l}{4V_p} (2k_p a_0)^l \sum_{p \geq 0} \left(\frac{2a_0}{V_e}\right)^p \sum_{n=1}^l (-1)^{l-n} \begin{pmatrix} A_{nk}^{(p)} \\ B_{nk}^{(p)} \end{pmatrix} \frac{\Gamma(l-k+1)}{\Gamma(l-n+1)\Gamma(n-k+1)} \\ &\left(\frac{1}{a_0}\right)^n \sum_{q=0} \frac{(l-n+p)}{(l-n+p+q)} \left[E_l^{(1)}(\gamma, \delta; 0; k_p a_0) + E_l^{(1)}(\gamma, 0; a_0; k_p R_s) \right] \frac{(-2i\eta_l k_p a_0)^q}{\Gamma(q+1)} \end{aligned} \quad (5-12)$$

where $\gamma = l - n + p + q$ and

$$E_l^{(1)}(\mu, \delta; R_0; \kappa R) = \sum_{k=0} \frac{\Gamma(l+k+1)}{\Gamma(2l+k+2)} \left(\frac{1}{\gamma+k+2}\right) \left[1 - \left(\frac{R_0}{R}\right)^{\gamma+k+2}\right] \frac{(-2i\kappa R)^{\gamma+k+2}}{\Gamma(\gamma+k+1)}$$

The coefficients are essentially sums of generalized hypergeometric functions of two variables.

APPENDIX 6

SOLUTION COEFFICIENTS FOR PROPAGATING RUPTURE MODELS

The form of the solution coefficients for the propagating rupture models ($m = 2, 3$), in the case

$$1/10 \leq \alpha_0^m < 1/2$$

are given by the equation (3.12.38) with

$$d_m = \left(\frac{1 - \alpha_0^m}{1 - 2\alpha_0^m} \right)$$

and $s = l - n$, as

$$\begin{aligned} \begin{pmatrix} A_{lk}(\omega) \\ B_{lk}(\omega) \end{pmatrix} &= \frac{k_p^2 \eta_m}{V_p} \sum_{p \geq 0} \left(\frac{1}{V_k} \right)^p \sum_{h=1}^l (-1)^{l-h} \frac{(l-h)!}{(n-h)!} \begin{pmatrix} A_{nk}^{(p)} \\ B_{nk}^{(p)} \end{pmatrix} \sum_{j=0}^{l-n} \left(\frac{\alpha_0^m}{a_0} \right)^j \\ &\times \frac{(1-2\alpha_0^m)^{l-n-j}}{\Gamma(l-n-j+1)\Gamma(j+1)} \left\{ \left(\frac{1-\alpha_0^m}{1-2\alpha_0^m} \right)^{s+p+j} \int_0^{R_0^{(m)}} \left(\frac{1}{r'} \right)^{n-p-j-1} {}_1F_1(s+p+j; s+p+j+1; -i\eta_m k_p r') \right. \\ &\left. e^{-ik_p r'} \int_{R_0^{(m)}}^{R_1^{(m)}} (k_p r') dr' + (g_m a_0)^{s+p+j} \int_{R_0^{(m)}}^{R_1^{(m)}} \left(\frac{1}{r'} \right)^{l-1} \left(1 + \frac{h_m r'}{g_m a_0} \right)^{s+p+j} {}_1F_1(s+p+j; s+p+j+1; \right. \\ &\left. -i\eta_m k_p (g_m a_0 + h_m r')) e^{-ik_p r'} \int_{R_0^{(m)}}^{R_1^{(m)}} (k_p r') dr' + (2a_0)^{s+p+j} {}_1F_1(s+p+j; s+p+j+1; \right. \\ &\left. -2i\eta_m k_p a_0) \int_{R_1^{(m)}}^{R_s} \left(\frac{1}{r'} \right)^{l-1} e^{-ik_p r'} \int_{R_0^{(m)}}^{R_1^{(m)}} (k_p r') dr' \right. \end{aligned} \end{aligned}$$

(6-1)

The evaluation of the integrals in this expression is carried out in the same manner as was the case in Appendix 5. Indeed one has

immediately from the previous appendix

$$\int_{R_1^{(m)}}^{R_5} \left(\frac{1}{R'}\right)^{l-1} e^{-ik_p R'} j_l(k_p R') dR' = -(2k_p)^{l-2} \sum_{\pi=0}^{l-2} \frac{\Gamma(l+\pi+1)}{\Gamma(2l+\pi+2)} \left(\frac{1}{R_5}\right)^{\pi+2} \left[1 - \left(\frac{R_1^{(m)}}{R_5}\right)^{\pi+2}\right] \times \frac{(-2ik_p R_5)^{\pi+2}}{\Gamma(\pi+1)} \quad (6-2)$$

The remaining integrals in (6-1) can be put in the form

$$\int_0^{R_0^{(m)}} \left(\frac{1}{R'}\right)^{n-p-j-1} {}_1F_1(s+p+j; s+p+j+1; -i\eta_m d m k_e R') e^{-ik_p R'} j_l(k_p R') dR' = \sum_{q=0}^{\infty} \frac{(s+p+j)}{(s+p+j+q)} \frac{(-i\eta_m d m k_e)^q}{\Gamma(q+1)} \int_0^{R_0^{(m)}} \left(\frac{1}{R'}\right)^{n-p+q-j-1} e^{-ik_p R'} j_l(k_p R') dR' \quad (6-3)$$

$$\int_{R_0^{(m)}}^{R_1^{(m)}} \left(\frac{1}{R'}\right)^{l-1} \left(1 + \frac{h_m R'}{g_m a_0}\right)^{s+p+j} {}_1F_1(s+p+j; s+p+j+1; -i\eta_m k_e (g_m a_0 + h_m R')) \times e^{-ik_p R'} j_l(k_p R') dR' = \sum_{q=0}^{\infty} \frac{(s+p+j)}{(s+p+j+q)} \frac{(-i\eta_m g_m k_e a_0)^q}{\Gamma(q+1)} \times \int_{R_0^{(m)}}^{R_1^{(m)}} \left(\frac{1}{R'}\right)^{l-1} \left(1 + \frac{h_m R'}{g_m a_0}\right)^{s+p+q+j} e^{-ik_p R'} j_l(k_p R') dR' = \sum_{q=0}^{\infty} \frac{(s+p+j)}{(s+p+j+q)} \frac{(-i\eta_m g_m k_e a_0)^q}{\Gamma(q+1)} \sum_{N=0}^{s+p+q-j} \frac{(s+j+p+q)!}{(s+j+p+q-N)! N!} \left(\frac{h_m}{g_m}\right)^N \left(\frac{1}{a_0}\right)^N \times \int_{R_0^{(m)}}^{R_1^{(m)}} \left(\frac{1}{R'}\right)^{l-N-1} e^{-ik_p R'} j_l(k_p R') dR' \quad (6-4)$$

In both cases the interchange of summation and integration order follows from the uniform convergence of the power series representing the hypergeometric functions. The series convergence is uniform over the entire range of r' , $(0, \infty)$, so that no restriction need be

placed on the frequency parameters k_R and k_p .

Denoting the first of these integrals by I_1 , and utilizing (5-2) of the previous Appendix, then

$$I_1 \equiv \int_0^{R_0^{(m)}} \left(\frac{1}{R'}\right)^{n-p-q-j-1} e^{-ik_p R'} J_j(k_p R') dR' = -(2k_p R_0^{(m)})^{l-2} (R_0^{(m)})^{-n+p+q+j}$$

$$\times \sum_{\pi=0} \frac{\Gamma(l+\pi+1)}{\Gamma(2l+\pi+2)} \left(\frac{1}{l-n+p+q+j+\pi+2}\right) \frac{(-2ik_p R_0^{(m)})^{\pi+2}}{\Gamma(\pi+1)} \quad (6-5)$$

where it is easy to show that the conditions for the application of (5-2) are satisfied by I_1 . Similarly

$$I_2 \equiv \int_{R_0^{(m)}}^{R_1^{(m)}} \left(\frac{1}{R'}\right)^{l-N-1} e^{-ik_p R'} J_l(k_p R') dR' = (2k_p)^l \left[(R_1^{(m)})^{N+2} \sum_{\pi=0} \frac{\Gamma(l+\pi+1)}{\Gamma(2l+\pi+2)} \right.$$

$$\left. \left(\frac{1}{\pi+N+2}\right) \frac{(-2ik_p R_1^{(m)})^\pi}{\Gamma(\pi+1)} - (R_0^{(m)})^{N+2} \sum_{\pi=0} \frac{\Gamma(l+\pi+1)}{\Gamma(2l+\pi+2)} \left(\frac{1}{\pi+N+2}\right) \frac{(-2ik_p R_0^{(m)})^\pi}{\Gamma(\pi+1)} \right]$$

Or, upon rearrangement

$$I_2 = -(2k_p)^{l-2} (R_1^{(m)})^N \sum_{\pi=0} \frac{\Gamma(l+\pi+1)}{\Gamma(2l+\pi+2)} \left(\frac{1}{\pi+N+2}\right) \left\{ 1 - \left(\frac{R_0^{(m)}}{R_1^{(m)}}\right)^{\pi+N+2} \right\}$$

$$\times \frac{(-2ik_p R_1^{(m)})^{\pi+2}}{\Gamma(\pi+1)} \quad (6-6)$$

Finally, (6-3) and (6-4) become

$$\int_0^{\pi_0^{(m)}} \left(\frac{1}{\pi'}\right)^{n-p-j-1} {}_1F_1(s+p+j; s+p+j+1; -i\eta_m d_m k_p \pi') e^{-ik_p \pi'} j_l(k_p \pi') d\pi' =$$

$$-(2k_p)^{l-2} \sum_{q=0}^{s+p+j} \frac{(s+p+j)}{(s+p+q+j)} \frac{(-i\eta_m d_m k_p \pi_0^{(m)})^q}{\Gamma(q+1)} (\pi_0^{(m)})^{l+p+j-n} \times$$

$$\times \sum_{\kappa=0}^{\infty} \frac{\Gamma(l+\kappa+1)}{\Gamma(2l+\kappa+2)} \left(\frac{1}{\alpha+\kappa+2}\right) \frac{(-2ik_p \pi_0^{(m)})^{\kappa+2}}{\Gamma(\kappa+1)} \quad (6-7)$$

and

$$\int_{\pi_0^{(m)}}^{\pi_1^{(m)}} \left(\frac{1}{\pi'}\right)^{l-1} \left(1 + \frac{k_p \pi'}{g_m a_0}\right)^{s+p+d} {}_1F_1(s+p+j; s+p+j+1; -i\eta_m k_p (g_m a_0 + k_p \pi'))$$

$$\times e^{-ik_p \pi'} j_l(k_p \pi') d\pi' = -(2k_p)^{l-2} \sum_{q=0}^{s+p+d} \frac{(s+p+d)}{(s+p+d+q)} \frac{(-i\eta_m k_p a_0)^q}{\Gamma(q+1)}$$

$$\times \sum_{N=0}^{\alpha} \frac{\Gamma(\alpha+1)}{\Gamma(\alpha-N+1)} \left(\frac{k_m \pi_1^{(m)}}{g_m a_0}\right)^N / \Gamma(N+1) \sum_{\kappa=0}^{\infty} \frac{\Gamma(l+\kappa+1)}{\Gamma(2l+\kappa+2)} \left(\frac{1}{\kappa+N+2}\right) \times$$

$$\times \left[1 - \left(\frac{\pi_0^{(m)}}{\pi_1^{(m)}}\right)^{\kappa+N+2}\right] \frac{(-2ik_p \pi_1^{(m)})^{\kappa+2}}{\Gamma(\kappa+1)} \quad (6-8)$$

with $\alpha = l - n + p + q + j$. Therefore introducing these results into (6-1), noting that (from 3.12.30 and 3.12.14)

$$\left(\frac{k_m \pi_1^{(m)}}{g_m a_0}\right) = 2/g_m - 1$$

and rearranging, one has the results given by the equations (3.12.40) through (3.12.42) of the text.

APPENDIX 7

STRESS-STRAIN RELATIONS IN ELLIPSOIDAL COORDINATES
AS FUNCTIONS OF THE HARMONIC POTENTIALS ϕ AND $\underline{\omega}$

The curvilinear components of the stress tensor (or strain tensor) may be expressed in terms of the Cartesian components of stress as (Love, 1944)

$$\bar{\sigma}_{ij} = \alpha_{ik} \sigma_{kl} \alpha_{lj}^T \quad (7-1)$$

where, in the notation of the Appendix 4, $\bar{\sigma}_{ij}$ denotes the curvilinear stress components, σ_{kl} the Cartesian components and

$$\alpha_{ik} = \begin{pmatrix} \frac{1}{h_1} \frac{\partial X_1}{\partial \xi_1} & \frac{1}{h_2} \frac{\partial X_2}{\partial \xi_1} & \frac{1}{h_3} \frac{\partial X_3}{\partial \xi_1} \\ \frac{1}{h_1} \frac{\partial X_1}{\partial \xi_2} & \frac{1}{h_2} \frac{\partial X_2}{\partial \xi_2} & \frac{1}{h_3} \frac{\partial X_3}{\partial \xi_2} \\ \frac{1}{h_1} \frac{\partial X_1}{\partial \xi_3} & \frac{1}{h_2} \frac{\partial X_2}{\partial \xi_3} & \frac{1}{h_3} \frac{\partial X_3}{\partial \xi_3} \end{pmatrix} \quad (7-2)$$

$$\alpha_{lj}^T = \alpha_{jl}$$

where the h_j are the metric elements for an orthogonal curvilinear system. From these same relations, the strain tensor has the explicit form

$$\bar{e}_{ii} = \left(\frac{1}{h_i^2} \right) \frac{\partial X_k}{\partial \xi_i} \frac{\partial u_k}{\partial \xi_i} \quad (7-3)$$

$$\bar{e}_{ij} = \frac{1}{2h_i h_j} \left(\frac{\partial X_k}{\partial \xi_i} \frac{\partial u_k}{\partial \xi_j} + \frac{\partial X_k}{\partial \xi_j} \frac{\partial u_k}{\partial \xi_i} \right)$$

where summation over the repeated index k is implied.

Adopting Hobson's notation and coordinate relationships for ellipsoidal coordinates, then (Hobson, 1931)

$$\begin{aligned} X_1 &= \frac{\rho \mu \nu}{kh}, & X_2 &= \frac{\sqrt{\rho^2 - h^2} \sqrt{\mu^2 - h^2} \sqrt{h^2 - \nu^2}}{h \sqrt{k^2 - h^2}} \\ X_3 &= \frac{\sqrt{\rho^2 - k^2} \sqrt{k^2 - \mu^2} \sqrt{k^2 - \nu^2}}{k \sqrt{k^2 - h^2}} \end{aligned} \tag{7-4}$$

where (ρ, μ, ν) replace the previous general curvilinear coordinates (ξ_1, ξ_2, ξ_3) and

$$\begin{aligned} k &\leq \rho < \infty \\ h &\leq \mu \leq k \\ -h &\leq \nu \leq h \end{aligned}$$

with h and k arbitrary constants such that

$$k > h$$

In terms of the semi-axes of the focal ellipsoid

$$\begin{aligned} h^2 &= a^2 - b^2 \\ k^2 &= a^2 - c^2 \end{aligned}$$

The ellipsoidal system is orthogonal, so the metric elements h_j , $j = 1, 2, 3$, are

$$h_1 = \left[\frac{(\rho^2 - \mu^2)(\rho^2 - \nu^2)}{(\rho^2 - h^2)(\rho^2 - k^2)} \right]^{1/2} ; h_2 = \left[\frac{(\rho^2 - \mu^2)(\mu^2 - \nu^2)}{(\mu^2 - h^2)(k^2 - \mu^2)} \right]^{1/2}$$

$$h_3 = \left[\frac{(\rho^2 - \nu^2)(\mu^2 - \nu^2)}{(h^2 - \nu^2)(k^2 - \nu^2)} \right]^{1/2}$$

(7-5)

The partial derivatives $(\partial X_i / \partial \xi_j)$ are then

$$\left\{ \frac{\partial X_i}{\partial \xi_j} \right\} = \begin{pmatrix} \frac{\mu \nu}{hk} & \frac{\rho \sqrt{\mu^2 - h^2} \sqrt{h^2 - \nu^2}}{h \sqrt{\rho^2 - h^2} \sqrt{k^2 - h^2}} & \frac{\rho \sqrt{k^2 - \mu^2} \sqrt{k^2 - \nu^2}}{k \sqrt{\rho^2 - k^2} \sqrt{k^2 - h^2}} \\ \frac{\rho \nu}{kh} & \frac{\mu \sqrt{\rho^2 - h^2} \sqrt{h^2 - \nu^2}}{h \sqrt{\mu^2 - h^2} \sqrt{k^2 - h^2}} & \frac{-\mu \sqrt{\rho^2 - k^2} \sqrt{k^2 - \nu^2}}{k \sqrt{k^2 - \mu^2} \sqrt{k^2 - h^2}} \\ \frac{\rho \mu}{hk} & \frac{-\nu \sqrt{\rho^2 - h^2} \sqrt{\mu^2 - h^2}}{h \sqrt{h^2 - \nu^2} \sqrt{k^2 - h^2}} & \frac{-\nu \sqrt{\rho^2 - k^2} \sqrt{k^2 - \mu^2}}{k \sqrt{k^2 - \nu^2} \sqrt{k^2 - h^2}} \end{pmatrix} \quad (7-6)$$

where the index i is the row index and j the column index.

From these relationships, the ellipsoidal components of stress may be expressed in terms of Cartesian components of stress, $\sigma_{ij}^{(0)}$, as

$$\begin{aligned} \sigma_{\rho\rho}^{(0)} &= \frac{(\rho^2 - h^2)(\rho^2 - k^2)}{(\rho^2 - \mu^2)(\rho^2 - \nu^2)} \left[\left(\frac{\mu \nu}{kh} \right)^2 \sigma_{11}^{(0)} + \rho^2 \left\{ \frac{(\mu^2 - h^2)(h^2 - \nu^2)}{h^2(\rho^2 - h^2)(k^2 - h^2)} \right\} \sigma_{22}^{(0)} \right. \\ &\quad \left. + \rho^2 \frac{(k^2 - \mu^2)(k^2 - \nu^2)}{k^2(\rho^2 - k^2)(k^2 - h^2)} \sigma_{33}^{(0)} + 2\rho^2 \left\{ \frac{\sqrt{\mu^2 - h^2} \sqrt{k^2 - \mu^2} \sqrt{h^2 - \nu^2} \sqrt{k^2 - \nu^2}}{k^2 h \sqrt{\rho^2 - k^2} \sqrt{\rho^2 - h^2} (k^2 - h^2)} \right\} \sigma_{23}^{(0)} \right] \\ &\quad \left. + 2\rho \left\{ \frac{\mu \nu \sqrt{\mu^2 - h^2} \sqrt{h^2 - \nu^2}}{k h^2 \sqrt{\rho^2 - h^2} \sqrt{k^2 - h^2}} \right\} \sigma_{12}^{(0)} + 2\rho \left\{ \frac{\mu \nu \sqrt{k^2 - \mu^2} \sqrt{k^2 - \nu^2}}{h k^2 \sqrt{\rho^2 - k^2} \sqrt{k^2 - h^2}} \right\} \sigma_{13}^{(0)} \right] \end{aligned}$$

$$\begin{aligned}
 \sigma_{\rho\mu}^{(0)} &= \left[\frac{(\rho^2-h^2)(\rho^2-k^2)(\mu^2-h^2)(k^2-\mu^2)}{(\rho^2-\mu^2)(\rho^2-\nu^2)(\mu^2-\nu^2)} \right]^{1/2} \left[\frac{\rho\mu\nu^2}{h^2k^2} \sigma_{11}^{(0)} + \rho\mu \frac{h^2-\nu^2}{h^2(k^2-h^2)} \sigma_{22}^{(0)} \right. \\
 &\quad - \rho\mu \frac{k^2-\nu^2}{k^2(k^2-h^2)} \sigma_{33}^{(0)} + \left\{ \frac{\mu^2\nu\sqrt{\rho^2-h^2}\sqrt{h^2-\nu^2}}{h^2k\sqrt{\mu^2-h^2}\sqrt{k^2-h^2}} + \frac{\rho^2\nu\sqrt{\mu^2-h^2}\sqrt{h^2-\nu^2}}{h^2k\sqrt{\rho^2-h^2}\sqrt{k^2-h^2}} \right\} \sigma_{12}^{(0)} \\
 &\quad - \left\{ \frac{\mu^2\nu\sqrt{\rho^2-k^2}\sqrt{k^2-\nu^2}}{hk^2\sqrt{k^2-\mu^2}\sqrt{k^2-h^2}} - \frac{\rho^2\nu\sqrt{k^2-\mu^2}\sqrt{k^2-\nu^2}}{hk^2\sqrt{\rho^2-k^2}\sqrt{k^2-h^2}} \right\} \sigma_{13}^{(0)} + \left\{ \frac{\rho\mu}{hk} \frac{\sqrt{\rho^2-h^2}}{\sqrt{\mu^2-h^2}} \right. \\
 &\quad \left. \frac{\sqrt{h^2-\nu^2}\sqrt{k^2-\mu^2}\sqrt{k^2-\nu^2}}{\sqrt{\rho^2-k^2}(k^2-h^2)} - \frac{\rho\mu\sqrt{\rho^2-k^2}\sqrt{k^2-\nu^2}\sqrt{\mu^2-h^2}\sqrt{h^2-\nu^2}}{hk\sqrt{\rho^2-h^2}\sqrt{k^2-\mu^2}(k^2-h^2)} \right\} \sigma_{23}^{(0)} \\
 \sigma_{\rho\nu}^{(0)} &= \left[\frac{(\rho^2-h^2)(\rho^2-k^2)(h^2-\nu^2)(k^2-\nu^2)}{(\rho^2-\nu^2)^2(\rho^2-\mu^2)(\mu^2-\nu^2)} \right]^{1/2} \left[\frac{\rho\mu^2\nu}{h^2k^2} \sigma_{11}^{(0)} - \rho\nu \frac{(\mu^2-h^2)}{h^2(k^2-h^2)} \sigma_{22}^{(0)} \right. \\
 &\quad - \rho\nu \frac{(k^2-\mu^2)}{k^2(k^2-h^2)} \sigma_{33}^{(0)} + \left\{ \rho^2\mu \frac{\sqrt{\mu^2-h^2}\sqrt{h^2-\nu^2}}{h^2k\sqrt{\rho^2-h^2}\sqrt{k^2-h^2}} - \nu^2\mu \frac{\sqrt{\rho^2-h^2}\sqrt{\mu^2-h^2}}{h^2k\sqrt{h^2-\nu^2}\sqrt{k^2-h^2}} \right\} \\
 &\quad \sigma_{12}^{(0)} + \left\{ \rho^2\mu \frac{\sqrt{k^2-\mu^2}\sqrt{k^2-\nu^2}}{hk^2\sqrt{\rho^2-k^2}\sqrt{k^2-h^2}} - \mu\nu^2 \frac{\sqrt{\rho^2-k^2}\sqrt{k^2-\mu^2}}{hk^2\sqrt{k^2-\nu^2}\sqrt{k^2-h^2}} \right\} \sigma_{13}^{(0)} \\
 &\quad - \left\{ \rho\nu \frac{\sqrt{\mu^2-h^2}\sqrt{h^2-\nu^2}\sqrt{\rho^2-k^2}\sqrt{k^2-\mu^2}}{hk\sqrt{\rho^2-h^2}\sqrt{k^2-\nu^2}\sqrt{k^2-h^2}} + \rho\nu \frac{\sqrt{\rho^2-h^2}\sqrt{\mu^2-h^2}\sqrt{k^2-\mu^2}\sqrt{k^2-\nu^2}}{hk\sqrt{h^2-\nu^2}\sqrt{\rho^2-k^2}\sqrt{k^2-h^2}} \right\} \sigma_{23}^{(0)} \\
 &\hspace{20em} (7-7)
 \end{aligned}$$

The Cartesian stress components $\sigma_{ij}^{(0)}$ will in the present application denote the initial stress field, which will be taken to be constant, so that $\sigma_{\rho\rho}^{(0)}$, etc., denote the initial stress field in ellipsoidal coordinates.

The equilibrium displacement field, \underline{u}^* , appropriate to the boundary value problem associated with the stress relaxation around an ellipsoidal rupture boundary is given by harmonic potentials ϕ and ω , as

$$\underline{u}^* = \nabla(\phi + \underline{r} \cdot \underline{\omega}) - 4(1-\sigma) \underline{\omega}$$

$$\nabla^2 \phi = 0, \quad \nabla^2 \omega_k = 0, \quad k=1, 2, 3$$

The ellipsoidal components of the vector displacement field are obtained from

$$\bar{u}_i^* = \frac{1}{h_i} \left[\frac{\partial \phi}{\partial \xi_i} + \chi_l \frac{\partial \omega_l}{\partial \xi_i} - 3 \left(1 - \frac{4}{3} \sigma \right) \omega_l \frac{\partial \chi_l}{\partial \xi_i} \right] \quad (7-8)$$

where \bar{u}_i denotes the curvilinear components of the vector and the summation convention applies to the repeated index l . The ω_l denote the Cartesian components of the vector potential $\underline{\omega}$.

The ellipsoidal components of the strain (or stress) tensor can be expressed in terms of the harmonic potentials ϕ and ω_k by means of (7-8) and (7-3). Thus, for the strain components

$$\begin{aligned} e_{\rho\rho}^* = & \left[\frac{(\rho^2-h^2)(\rho^2-k^2)}{(\rho^2-\mu^2)(\rho^2-\nu^2)} \right] \left\{ \frac{\partial^2 \phi}{\partial \rho^2} - 2\rho \left(\frac{1}{\rho^2-\nu^2} + \frac{1}{\rho^2-\mu^2} + \frac{1}{\rho^2-h^2} - \right. \right. \\ & \left. \left. \frac{1}{\rho^2-k^2} \right) \frac{\partial \phi}{\partial \rho} + \mu\nu \left[\frac{\rho}{kh} \frac{\partial^2 \omega_1}{\partial \rho^2} - \frac{2\rho^2}{kh} \left(\frac{1}{\rho^2-\nu^2} + \frac{1}{\rho^2-\mu^2} - \frac{1}{\rho^2-k^2} \right. \right. \right. \\ & \left. \left. - \frac{1}{\rho^2-h^2} \right) \frac{\partial \omega_1}{\partial \rho} + 2(3-4\sigma) \frac{\rho}{kh} \left(\frac{1}{\rho^2-\nu^2} + \frac{1}{\rho^2-\mu^2} - \frac{1}{\rho^2-k^2} - \frac{1}{\rho^2-h^2} \right) \omega_1 \right. \\ & \left. - \frac{2(1-2\sigma)}{kh} \frac{\partial \omega_1}{\partial \rho} \right] + \sqrt{\mu^2-h^2} \sqrt{h^2-\nu^2} \left[\frac{\sqrt{\rho^2-h^2}}{h\sqrt{k^2-h^2}} \frac{\partial^2 \omega_2}{\partial \rho^2} + \right. \\ & \left. (3-4\sigma) \frac{h}{\sqrt{k^2-h^2} \sqrt{\rho^2-h^2} (\rho^2-h^2)} \omega_2 - 2\rho \left(\frac{1}{\rho^2-\nu^2} + \frac{1}{\rho^2-\mu^2} - \frac{1}{\rho^2-h^2} \right) \right. \\ & \left. \left(\frac{\sqrt{\rho^2-h^2}}{h\sqrt{k^2-h^2}} \frac{\partial \omega_2}{\partial \rho} - (3-4\sigma) \frac{\rho}{h\sqrt{\rho^2-h^2} \sqrt{k^2-h^2}} \omega_2 \right) - 2(1-2\sigma) \right] \end{aligned}$$

$$\frac{\rho}{h \sqrt{\rho^2 - h^2} \sqrt{k^2 - h^2}} \frac{\partial \omega_2}{\partial \rho} \Big] + \sqrt{k^2 - \mu^2} \sqrt{k^2 - \nu^2} \left[\frac{\sqrt{\rho^2 - k^2}}{k \sqrt{k^2 - h^2}} \frac{\partial^2 \omega_2}{\partial \rho^2} + \right. \\ (3-4\sigma) \frac{k}{\sqrt{k^2 - h^2} \sqrt{\rho^2 - k^2} (\rho^2 - k^2)} \omega_3 - 2\rho \left(\frac{1}{\rho^2 - \nu^2} + \frac{1}{\rho^2 - \mu^2} - \frac{1}{\rho^2 - k^2} \right) \\ \left. \left(\frac{\sqrt{\rho^2 - k^2}}{k \sqrt{k^2 - h^2}} \frac{\partial \omega_3}{\partial \rho} - (3-4\sigma) \frac{\rho}{k \sqrt{k^2 - h^2} \sqrt{\rho^2 - k^2}} \omega_3 \right) - \right. \\ \left. 2(1-2\sigma) \frac{\rho}{k \sqrt{k^2 - h^2} \sqrt{\rho^2 - k^2}} \omega_3 \right] \quad (7-9)$$

$$e_{\rho\mu}^* = \left[\frac{(\mu^2 - h^2)(k^2 - \mu^2)(\rho^2 - h^2)(\rho^2 - k^2)}{(\rho^2 - \mu^2)^2 (\rho^2 - \nu^2)(\mu^2 - \nu^2)} \right]^{1/2} \left\{ \frac{\partial^2 \phi}{\partial \mu \partial \rho} + \frac{\mu}{\rho^2 - \mu^2} \frac{\partial \phi}{\partial \rho} - \right. \\ \frac{\rho}{\rho^2 - \mu^2} \frac{\partial \phi}{\partial \mu} + \mu \nu \left[\frac{\rho}{kh} \frac{\partial^2 \omega_1}{\partial \mu \partial \rho} - \frac{(3-4\sigma)}{kh} \frac{\omega_1}{\mu} + \frac{\mu}{\rho^2 - \mu^2} \frac{\rho}{kh} \frac{\partial \omega_1}{\partial \rho} \right. \\ \left. - \frac{(3-4\sigma)}{kh} \frac{\mu}{\rho^2 - \mu^2} \omega_1 - \frac{\rho}{\rho^2 - \mu^2} \frac{\rho}{kh} \frac{\partial \omega_1}{\partial \mu} + \frac{3-4\sigma}{kh} \frac{\rho}{\rho^2 - \mu^2} \frac{\rho}{\mu} \omega_1 \right. \\ \left. - (1-2\sigma) \frac{\rho}{kh} \frac{\omega_1}{\mu} - \frac{1-2\sigma}{kh} \frac{\partial \omega_1}{\partial \mu} \right] + \sqrt{\mu^2 - h^2} \sqrt{h^2 - \nu^2} \left[\frac{\sqrt{\rho^2 - h^2}}{h \sqrt{k^2 - h^2}} \frac{\partial^2 \omega_2}{\partial \rho \partial \mu} \right. \\ \left. - \frac{(3-4\sigma)}{h \sqrt{k^2 - h^2}} \left(\frac{\rho \mu}{(\mu^2 - h^2) \sqrt{\rho^2 - h^2}} \right) \omega_2 + \frac{\mu}{\rho^2 - \mu^2} \left(\frac{\sqrt{\rho^2 - h^2}}{h \sqrt{k^2 - h^2}} \right) \frac{\partial \omega_2}{\partial \rho} - \right. \\ (3-4\sigma) \frac{\mu}{\rho^2 - \mu^2} \left(\frac{\rho}{h \sqrt{\rho^2 - h^2} \sqrt{k^2 - h^2}} \right) \omega_2 - \frac{\rho}{\rho^2 - \mu^2} \left(\frac{\sqrt{\rho^2 - h^2}}{h \sqrt{k^2 - h^2}} \right) \frac{\partial \omega_2}{\partial \mu} \\ \left. + (3-4\sigma) \frac{\rho}{\rho^2 - \mu^2} \left(\frac{\mu \sqrt{\rho^2 - h^2}}{h \sqrt{k^2 - h^2} (\mu^2 - h^2)} \right) \omega_2 - (1-2\sigma) \left(\frac{\mu \sqrt{\rho^2 - h^2}}{h (\mu^2 - h^2) \sqrt{k^2 - h^2}} \right) \frac{\partial \omega_2}{\partial \rho} \right. \\ \left. - (1-2\sigma) \left(\frac{\rho}{h \sqrt{\rho^2 - h^2} \sqrt{k^2 - h^2}} \right) \frac{\partial \omega_2}{\partial \mu} \right] + \left(\sqrt{k^2 - \mu^2} \sqrt{k^2 - \nu^2} \right) \quad (7-10)$$

$$\left[\frac{\sqrt{\rho^2 - k^2}}{k \sqrt{k^2 - h^2}} \frac{\partial^2 \omega_3}{\partial \rho \partial \mu} + \frac{(3-4\sigma)}{k \sqrt{k^2 - h^2}} \left(\frac{\rho \mu}{\sqrt{\rho^2 - k^2} (k^2 - \mu^2)} \right) \omega_3 \right. \\ \left. + \frac{\mu}{\rho^2 - \mu^2} \left(\frac{\sqrt{\rho^2 - k^2}}{k \sqrt{k^2 - h^2}} \right) \frac{\partial \omega_3}{\partial \rho} - (3-4\sigma) \frac{\mu}{\rho^2 - \mu^2} \left(\frac{\rho}{k \sqrt{k^2 - h^2}} \right) \right. \\ \left. \left(\frac{1}{\sqrt{\rho^2 - k^2}} \right) \omega_3 - \frac{\rho}{\rho^2 - \mu^2} \left(\frac{\sqrt{\rho^2 - k^2}}{k \sqrt{k^2 - h^2}} \right) \frac{\partial \omega_3}{\partial \mu} - (3-4\sigma) \right. \\ \left. \left(\frac{\rho}{\rho^2 - \mu^2} \right) \left(\frac{\mu \sqrt{\rho^2 - k^2}}{k \sqrt{k^2 - h^2} (k^2 - \mu^2)} \right) \omega_3 - (1-2\sigma) \left(\frac{\rho}{k \sqrt{\rho^2 - k^2}} \right) \right. \\ \left. \left(\frac{1}{k^2 - h^2} \right) \frac{\partial \omega_3}{\partial \mu} + (1-2\sigma) \left(\frac{\mu \sqrt{\rho^2 - k^2}}{k \sqrt{k^2 - h^2} (k^2 - \mu^2)} \right) \frac{\partial \omega_3}{\partial \rho} \right] \left. \right\}$$

$$e_{\rho\nu}^* = \left[\frac{(h^2 - \nu^2)(k^2 - \nu^2)(\rho^2 - h^2)(\rho^2 - k^2)}{(\rho^2 - \nu^2)^2 (\rho^2 - \mu^2)(\mu^2 - \nu^2)} \right]^{\frac{1}{2}} \left\{ \frac{\partial^2 \phi}{\partial \rho \partial \nu} + \frac{\nu}{\rho^2 - \nu^2} \frac{\partial \phi}{\partial \rho} \right. \\ \left. - \frac{\rho}{\rho^2 - \nu^2} \frac{\partial \phi}{\partial \nu} + \mu \nu \left[\frac{\rho}{hk} \frac{\partial^2 \omega_1}{\partial \rho \partial \nu} - \frac{(3-4\sigma)}{hk} \frac{\omega_1}{\nu} + \right. \right. \\ \left. \frac{\nu}{\rho^2 - \nu^2} \left(\frac{\rho}{hk} \right) \frac{\partial \omega_1}{\partial \rho} - \frac{(3-4\sigma)}{kh} \frac{\nu}{\rho^2 - \nu^2} \omega_1 - \left(\frac{\rho}{\rho^2 - \nu^2} \right) \right. \\ \left. \left(\frac{\rho}{kh} \right) \frac{\partial \omega_1}{\partial \nu} + \frac{(3-4\sigma)}{kh} \left(\frac{\rho}{\rho^2 - \nu^2} \right) \frac{\rho}{\nu} \omega_1 - \right. \\ \left. \frac{(1-2\sigma)}{kh} \frac{\partial \omega_1}{\partial \nu} - \frac{(1-2\sigma)}{kh} \left(\frac{\rho}{\nu} \right) \frac{\partial \omega_1}{\partial \rho} \right] + \left(\sqrt{\mu^2 - h^2} \sqrt{h^2 - \nu^2} \right) \\ \left[\frac{\sqrt{\rho^2 - h^2}}{h \sqrt{k^2 - h^2}} \frac{\partial^2 \omega_2}{\partial \rho \partial \nu} + \frac{(3-4\sigma)}{h \sqrt{k^2 - h^2}} \left(\frac{\rho}{\sqrt{\rho^2 - h^2}} \right) \frac{\nu}{h^2 - \nu^2} \omega_2 + \right.$$

$$\begin{aligned}
 & \frac{v}{\rho^2 - v^2} \left(\frac{\sqrt{\rho^2 - h^2}}{h \sqrt{k^2 - h^2}} \right) \frac{\partial \omega_3}{\partial \rho} - \frac{(3-4\sigma)}{h \sqrt{k^2 - h^2}} \frac{\rho \sqrt{\rho^2 - h^2}}{\rho^2 - v^2} \left(\frac{v}{h^2 - v^2} \right) \omega_2 \\
 & - (1-2\sigma) \frac{\rho}{h \sqrt{\rho^2 - h^2} \sqrt{k^2 - h^2}} \frac{\partial \omega_2}{\partial v} + (1-2\sigma) \frac{\sqrt{\rho^2 - h^2}}{h \sqrt{k^2 - h^2}} \left(\frac{v}{h^2 - v^2} \right) \\
 & \left(\frac{\partial \omega_2}{\partial \rho} \right) \left. \right] + \sqrt{k^2 - v^2} \sqrt{k^2 - h^2} \left[\frac{\sqrt{\rho^2 - k^2}}{k \sqrt{k^2 - h^2}} \frac{\partial^2 \omega_3}{\partial \rho \partial v} + \frac{(3-4\sigma)}{k \sqrt{k^2 - h^2}} \left(\frac{\rho}{\sqrt{\rho^2 - k^2}} \right) \right. \\
 & \left. \left(\frac{v}{k^2 - v^2} \right) \omega_3 + \frac{v}{\rho^2 - v^2} \left(\frac{\sqrt{\rho^2 - k^2}}{h \sqrt{k^2 - h^2}} \right) \frac{\partial \omega_3}{\partial \rho} - \frac{(3-4\sigma)}{k \sqrt{k^2 - h^2}} \left(\frac{\rho}{\sqrt{\rho^2 - k^2}} \right) \right. \\
 & \left. \left(\frac{v}{\rho^2 - v^2} \right) \omega_3 - \frac{\rho}{(\rho^2 - v^2)} \left(\frac{\sqrt{\rho^2 - k^2}}{k \sqrt{k^2 - h^2}} \right) \frac{\partial \omega_3}{\partial \rho} - \frac{(3-4\sigma)}{k \sqrt{k^2 - h^2}} \right. \\
 & \left. \left(\frac{\rho}{\rho^2 - v^2} \right) \left(\frac{v}{k^2 - v^2} \right) (\sqrt{\rho^2 - k^2}) \omega_3 - (1-2\sigma) \left(\frac{\rho}{k \sqrt{k^2 - h^2} \sqrt{\rho^2 - k^2}} \right) \right. \\
 & \left. \left(\frac{\partial \omega_3}{\partial v} \right) + (1-2\sigma) \frac{\sqrt{\rho^2 - k^2}}{k \sqrt{k^2 - h^2}} \left(\frac{v}{k^2 - v^2} \right) \right. \\
 & \left. \left(\frac{\partial \omega_3}{\partial \rho} \right) \right] \left. \right\}
 \end{aligned}$$

(7-11)

The complete relationship between the equilibrium state of the medium and the potentials previously defined is given by

$$\nabla^2 \underline{u}^* + \frac{1}{1-2\sigma} \nabla (\nabla \cdot \underline{u}^*) = 0$$

$$\underline{u}^* = \nabla(\phi + \underline{r} \cdot \underline{\omega}) - 4(1-\sigma)\underline{\omega}$$

with $\nabla^2 \phi = 0$, $\nabla^2 \underline{\omega} = 0$

(7-12)

From these relations, one has for the dilatation and rotation

$$\theta^* = -2(1-2\sigma)\nabla \cdot \underline{\omega}$$

$$\underline{\Omega}^* = -2(1-\sigma)\nabla \times \underline{\omega}$$

(7-13)

In terms of the ellipsoidal coordinates the dilatation

$$\theta^* = e_{\rho\rho} + e_{\mu\mu} + e_{\nu\nu}$$

is

$$\begin{aligned} \theta^* = & \frac{-2(1-2\sigma)}{(\rho^2-\mu^2)(\rho^2-\nu^2)} \left[\mu\nu \left\{ \frac{\rho}{kh} (2\rho^2 - h^2 - k^2) \omega_1 + \frac{(\rho^2-h^2)(\rho^2-k^2)}{kh} \right. \right. \\ & \left. \left. \left(\frac{\partial \omega_1}{\partial \rho} \right) + \frac{\rho}{kh} \frac{(k^2+h^2-2\mu^2)}{(\mu^2-\nu^2)} (\rho^2-\nu^2) \omega_1 + \frac{\rho}{kh} \frac{(\mu^2-h^2)}{\mu} \right. \right. \\ & \left. \left. \left(\frac{(k^2-\mu^2)(\rho^2-\nu^2)}{(\mu^2-\nu^2)} \right) \frac{\partial \omega_1}{\partial \mu} - \frac{\rho}{kh} \frac{(h^2+k^2-2\nu^2)(\rho^2-\mu^2)}{(\mu^2-\nu^2)} \omega_1 + \right. \right. \\ & \left. \left. \frac{\rho}{kh} \frac{(h^2-\nu^2)(k^2-\nu^2)(\rho^2-\mu^2)}{\nu(\mu^2-\nu^2)} \frac{\partial \omega_1}{\partial \nu} \right\} + \left(\sqrt{\mu^2-h^2} \sqrt{h^2-\nu^2} \right) \right. \\ & \left. \left\{ \frac{(2\rho^2-k^2)\sqrt{\rho^2-h^2}}{h\sqrt{k^2-h^2}} \omega_2 + \frac{\rho(\rho^2-k^2)\sqrt{\rho^2-h^2}}{h\sqrt{k^2-h^2}} \frac{\partial \omega_2}{\partial \rho} + \frac{(k^2-2\mu^2)(\rho^2-\nu^2)}{(\mu^2-\nu^2)} \right. \right. \\ & \left. \left. \frac{\sqrt{\rho^2-h^2}}{\sqrt{k^2-h^2}} \omega_2 + \frac{\mu(k^2-\mu^2)(\rho^2-\nu^2)\sqrt{\rho^2-h^2}}{(\mu^2-\nu^2)h\sqrt{k^2-h^2}} \frac{\partial \omega_2}{\partial \mu} - \right. \right. \end{aligned}$$

$$\begin{aligned}
 & \left. \frac{(k^2 - 2v^2)(\rho^2 - \mu^2)\sqrt{\rho^2 - h^2}}{(\mu^2 - v^2)h\sqrt{k^2 - h^2}} \omega_2 - \frac{v(k^2 - v^2)\sqrt{\rho^2 - h^2}(\rho^2 - \mu^2)}{(\mu^2 - v^2)h\sqrt{k^2 - h^2}} \frac{\partial \omega_2}{\partial v} \right\} + \\
 & (\sqrt{k^2 - \mu^2}\sqrt{k^2 - v^2}) \left\{ \frac{(2\rho^2 - h^2)\sqrt{\rho^2 - k^2}}{k\sqrt{k^2 - h^2}} \omega_3 + \frac{\rho(\rho^2 - h^2)\sqrt{\rho^2 - k^2}}{k\sqrt{k^2 - h^2}} \frac{\partial \omega_3}{\partial \rho} \right. \\
 & - \frac{(2\mu^2 - h^2)\sqrt{\rho^2 - k^2}(\rho^2 - v^2)}{(\mu^2 - v^2)k\sqrt{k^2 - h^2}} \omega_3 - \frac{\mu(\mu^2 - h^2)\sqrt{\rho^2 - k^2}(\rho^2 - v^2)}{(\mu^2 - v^2)k\sqrt{k^2 - h^2}} \frac{\partial \omega_3}{\partial \mu} \\
 & \left. - \frac{(h^2 - 2v^2)(\rho^2 - \mu^2)\sqrt{\rho^2 - k^2}}{k\sqrt{k^2 - h^2}(\mu^2 - v^2)} \omega_3 - \frac{v(h^2 - v^2)(\rho^2 - \mu^2)\sqrt{\rho^2 - k^2}}{k\sqrt{k^2 - h^2}(\mu^2 - v^2)} \frac{\partial \omega_3}{\partial v} \right\} \quad (7-14)
 \end{aligned}$$

From the expressions (7-7) and (7-9) through (7-14) the boundary conditions expressing the continuity of stress and the vanishing of the tractions at an ellipsoidal rupture boundary, $\rho = \text{const.}$, may be set down. These relations are, in terms of the previously expressed stresses and strains

$$\sigma_{\rho\mu}^* = \sigma_{\rho\mu}^{(0)} \quad , \quad \sigma_{\rho v}^* = \sigma_{\rho v}^{(0)} \quad , \quad \sigma_{\rho\rho}^* = \sigma_{\rho\rho}^{(0)} \quad (7-15)$$

when $\rho = \rho_0$, ρ_0 a constant and equal to the semi-major axis of the ellipsoidal rupture boundary. Here

$$\sigma_{\rho\mu}^* = 2\mu e_{\rho\mu}^* \quad , \quad \sigma_{\rho v}^* = 2\mu e_{\rho v}^* \quad , \quad \sigma_{\rho\rho}^* = \lambda \theta^* + 2\mu e_{\rho\rho}^*$$

where λ and μ are, of course, the elastic moduli and the strains and dilatation are given by the previous equations.

APPENDIX 8
ELLIPSOIDAL HARMONICS

Laplace's equation for ϕ (or ω_k) can be put in the form (Hobson, 1931)

$$(\mu^2 - \nu^2) \frac{\partial^2 \phi}{\partial \xi^2} + (\rho^2 - \nu^2) \frac{\partial^2 \phi}{\partial \eta^2} + (\rho^2 + \mu^2) \frac{\partial^2 \phi}{\partial \zeta^2} = 0 \quad (8-1)$$

where ρ , μ , and ν are the ellipsoidal coordinates defined in Appendix 7 and

$$\xi = \int_k^\rho \frac{d\rho}{\sqrt{\rho^2 - h^2} \sqrt{\rho^2 - k^2}} \quad ; \quad \eta = \int_h^\mu \frac{d\mu}{\sqrt{\mu^2 - h^2} \sqrt{k^2 - \mu^2}} \quad (8-2)$$

$$\zeta = \int_0^\nu \frac{d\nu}{\sqrt{h^2 - \nu^2} \sqrt{k^2 - \nu^2}}$$

solutions of (8-1) are (internal harmonics)

$$\phi(\rho, \mu, \nu) = E(\rho) E(\mu) E(\nu) \quad (8-3a)$$

where the functions E all satisfy Lamé equations

$$\begin{aligned} (z^2 - h^2)(z^2 - k^2) \frac{d^2 E(z)}{dz^2} + z(z^2 - h^2 - k^2) \frac{dE(z)}{dz} \\ + ((h^2 + k^2)\rho - n(n+1)z^2) E(z) = 0 \end{aligned} \quad (8-3b)$$

The solutions for all three functions may be found from a consideration of Lamé's equation and the solutions for E fall into four

distinct classes of the form (Hobson, 1931)

$$\begin{aligned}
 K(z) &= a_0 z^n + a_1 z^{n-2} + \dots \\
 L(z) &= \sqrt{z^2 - k^2} (a_0 z^{n-1} + a_1 z^{n-3} + \dots) \\
 M(z) &= \sqrt{z^2 - k^2} (a_0 z^{n-1} + a_1 z^{n-3} + \dots) \\
 N(z) &= \sqrt{z^2 - k^2} \sqrt{z^2 - k^2} (a_0 z^{n-2} + a_1 z^{n-4} + \dots)
 \end{aligned}
 \tag{8-4}$$

The Lamé functions constituting the four different classes of solutions can be shown to give $(2n + 1)$ distinct functions of degree n , that is, it is possible to choose p in (8-3) in $(2n+1)$ ways so that the resulting solutions are single valued, finite and continuous over a sphere of radius r . The number of functions in each class for a given n are as follows

$$K(z): \begin{cases} 1 + \frac{1}{2}n & \text{functions if } n \text{ is even} \\ \frac{1}{2}(n+1) & \text{functions if } n \text{ is odd} \end{cases}$$

$$L(z): \begin{cases} \frac{1}{2}n & \text{functions if } n \text{ is even} \\ \frac{1}{2}(n-1) & \text{functions if } n \text{ is odd} \end{cases}$$

$$M(z): \begin{cases} \frac{1}{2}n & \text{functions if } n \text{ is even} \\ \frac{1}{2}(n-1) & \text{functions if } n \text{ is odd} \end{cases}$$

$$N(z): \begin{cases} \frac{1}{2}n & \text{functions if } n \text{ is even} \\ \frac{1}{2}(n+1) & \text{functions if } n \text{ is odd} \end{cases}$$

These functions are related to the tesseral harmonics by

$$P_n^{2m}(\cos \theta) \cos 2m\phi = \sum \alpha K(\mu) K(\nu)$$

$$P_n^{2m+1}(\cos \theta) \cos (2m+1)\phi = \sum \alpha L(\mu) L(\nu)$$

$$P_n^{2m}(\cos \theta) \sin 2m\phi = \sum \alpha N(\mu) N(\nu)$$

$$P_n^{2m+1}(\cos \theta) \sin (2m+1)\phi = \sum \alpha M(\mu) M(\nu)$$

where the α 's are constants and where the number of terms in each sum is the number of functions in each class.

The solution

$$\Phi(\rho, \mu, \nu) = \sum_{n=1}^{2n+1} \beta_n E_n(\rho) E_n(\mu) E_n(\nu) \quad (8-5)$$

possesses the same degree of generality as does

$$\Phi(r, \theta, \phi) = \sum_{m=0}^n r^n P_n^m(\cos \theta) [a_m \cos m\phi + b_m \sin m\phi]$$

for the internal harmonics in spherical coordinates.

The coefficients in the polynomials in (8-4) are determined by substituting the solutions given by (8-4) into the differential equation (8-3), then equating the coefficients of powers of z to zero and finally, requiring that there be only a finite number of non-zero coefficients a_r , $r = 0, 1, \dots$, the total number being n , for $K(z)$, $n-1$, for $L(z)$ and $M(z)$ and $n-2$ for $N(z)$. In this way the acceptable values of the parameters p are determined in terms of the parameters h and k . The

details are treated by Hobson, Chapter XI.

The following summary gives the Lamé functions for $n = 0, 1, 2, 3$ along with the internal ellipsoidal harmonics which may be constructed from them. This list is sufficient for the present study.

(1) $n = 0$

Only $K(z)$ exists and it is a constant. Thus

$$\Phi_0'(\rho, \mu, \nu) \equiv E_0'(\rho) E_0'(\mu) E_0'(\nu) = 1 \quad (8-6)$$

(2) $n = 1$

$$K(z) = z, \quad L(z) = \sqrt{z^2 - k^2}, \quad M(z) = \sqrt{k^2 - z^2}$$

Thus

$$\begin{aligned} \Phi_1' &\equiv E_1'(\rho) E_1'(\mu) E_1'(\nu) = \rho \mu \nu \\ \Phi_1^2 &\equiv E_1^2(\rho) E_1^2(\mu) E_1^2(\nu) = \sqrt{\rho^2 - k^2} \sqrt{k^2 - \mu^2} \sqrt{k^2 - \nu^2} \\ \Phi_1^3 &\equiv E_1^3(\rho) E_1^3(\mu) E_1^3(\nu) = \sqrt{\rho^2 - k^2} \sqrt{\mu^2 - k^2} \sqrt{k^2 - \nu^2} \end{aligned} \quad (8-7)$$

(3) $n = 2$

(a) $K(z)$ functions

Following the procedure mentioned for choosing the values of p for an acceptable set of K functions, one has

$$K(z) = \mu^2 + \frac{1}{6} (p-4) \alpha$$

with p having the two values

$$P = 2(1 \pm \sqrt{1 + 3\beta/\alpha^2}) = (p_1, p_2)$$

where

$$\alpha = h^2 + k^2, \quad \beta = h^2 k^2$$

(b) L, M, N functions

$$M(z) = z \sqrt{k^2 - z^2}, \quad L(z) = z \sqrt{z^2 - h^2}, \quad N(z) = \sqrt{k^2 - z^2} \sqrt{z^2 - h^2}$$

Thus one has the following set of harmonic functions

$$\begin{aligned} \Phi_2^1 \equiv E_2^1(p) E_2^1(\mu) E_2^1(v) &= \left\{ p^2 + \frac{1}{6}(p_1 - 4)\alpha \right\} \left\{ \mu^2 + \frac{1}{6}(p_1 - 4)\alpha \right\} \\ &\quad \times \left\{ v^2 + \frac{1}{6}(p_1 - 4)\alpha \right\} \end{aligned}$$

$$\begin{aligned} \Phi_2^2 \equiv E_2^2(p) E_2^2(\mu) E_2^2(v) &= \left\{ p^2 + \frac{1}{6}(p_2 - 4)\alpha \right\} \left\{ \mu^2 + \frac{1}{6}(p_2 - 4)\alpha \right\} \\ &\quad \times \left\{ v^2 + \frac{1}{6}(p_2 - 4)\alpha \right\} \end{aligned}$$

$$\Phi_2^3 \equiv E_2^3(p) E_2^3(\mu) E_2^3(v) = \{ p\mu v \} \sqrt{p^2 - h^2} \sqrt{\mu^2 - h^2} \sqrt{h^2 - v^2}$$

$$\Phi_2^4 \equiv E_2^4(p) E_2^4(\mu) E_2^4(v) = \{ p\mu v \} \sqrt{p^2 - h^2} \sqrt{h^2 - \mu^2} \sqrt{h^2 - v^2}$$

$$\begin{aligned} \Phi_2^5 \equiv E_2^5(p) E_2^5(\mu) E_2^5(v) &= \sqrt{p^2 - h^2} \sqrt{p^2 - h^2} \sqrt{h^2 - \mu^2} \sqrt{\mu^2 - h^2} \\ &\quad \times \sqrt{h^2 - v^2} \sqrt{h^2 - v^2} \end{aligned} \quad (8-8)$$

(4) n = 3

(a) K functions

$$K(z) = z^3 + \frac{1}{10} (p-9)\alpha z$$

with the two values of p (p_1 and p_2) given by

$$\alpha^2 (p-1)(p-9) + 60\beta = 0$$

(b) L functions

$$L(z) = \sqrt{z^2 - k^2} \left[z^2 + \frac{1}{10} \{ (p-4) \alpha - 5k^2 \} \right]$$

with the two values of p (p_3 and p_4) given by

$$(\alpha p^2 - k^2) (\alpha (p-4) - 5k^2) + 20\beta = 0$$

(c) M functions

$$M(z) = \sqrt{k^2 - z^2} \left(z^2 + \frac{1}{10} [(p-4) \alpha - 5k^2] \right)$$

with the two values of p (p_5 and p_6) given by

$$(\alpha p - k^2) (\alpha (p-4) - 5k^2) + 20\beta = 0$$

(d) N functions

$$N(z) = z \sqrt{k^2 - z^2} \sqrt{z^2 - k^2}$$

Then :

$$\Phi_3^1 = \left\{ p^3 + \frac{1}{10} (p_1-9) \alpha p \right\} \left\{ \mu^3 + \frac{1}{10} (p_1-9) \alpha \mu \right\} \left\{ v^3 + \frac{1}{10} (p_1-9) \alpha v \right\}$$

$$\Phi_3^2 = \left\{ p^3 + \frac{1}{10} (p_2-9) \alpha p \right\} \left\{ \mu^3 + \frac{1}{10} (p_2-9) \alpha \mu \right\} \left\{ v^3 + \frac{1}{10} (p_2-9) \alpha v \right\}$$

$$\begin{aligned} \Phi_3^3 &= \sqrt{p^2 - k^2} \sqrt{\mu^2 - k^2} \sqrt{k^2 - v^2} \left(p^2 + \frac{1}{10} [(p_3-4) \alpha - 5k^2] \right) \\ &\quad \times \left(\mu^2 + \frac{1}{10} [(p_3-4) \alpha - 5k^2] \right) \left(v^2 + \frac{1}{10} [(p_3-4) \alpha - 5k^2] \right) \end{aligned}$$

$$\begin{aligned} \Phi_3^4 &= \sqrt{p^2 - k^2} \sqrt{\mu^2 - k^2} \sqrt{k^2 - v^2} \left[p^2 + \frac{1}{10} \{ (p_4-4) \alpha - 5k^2 \} \right] \\ &\quad \times \left[\mu^2 + \frac{1}{10} \{ (p_4-4) \alpha - 5k^2 \} \right] \left[v^2 + \frac{1}{10} \{ (p_4-4) \alpha - 5k^2 \} \right] \end{aligned}$$

$$\begin{aligned} \Phi_3^5 &= \sqrt{p^2 - k^2} \sqrt{k^2 - \mu^2} \sqrt{k^2 - v^2} \left[p^2 + \frac{1}{10} \{ (p_5-4) \alpha - 5k^2 \} \right] \\ &\quad \times \left[\mu^2 + \frac{1}{10} \{ (p_5-4) \alpha - 5k^2 \} \right] \left[v^2 + \frac{1}{10} \{ (p_5-4) \alpha - 5k^2 \} \right] \end{aligned}$$

$$\phi_3^6 = \sqrt{\rho^2 - k^2} \sqrt{k^2 - \mu^2} \sqrt{k^2 - v^2} \left[\rho^2 + \frac{1}{10} \{ (\rho^2 - 4) \alpha - 5k^2 \} \right]$$

$$\times \left[\mu^2 + \frac{1}{10} \{ (\rho^2 - 4) \alpha - 5k^2 \} \right] \left[v^2 + \frac{1}{10} \{ (\rho^2 - 4) \alpha - 5k^2 \} \right]$$

$$\phi_3^7 = \rho \mu v \sqrt{\rho^2 - k^2} \sqrt{\rho^2 - h^2} \sqrt{k^2 - \mu^2} \sqrt{\mu^2 - h^2}$$

$$\times \sqrt{k^2 - v^2} \sqrt{h^2 - v^2}$$

(8-9)

External harmonics, which vanish as ρ becomes infinite, may be generated from Lamé functions of the second kind. These latter functions may be obtained from the previous solutions $E_n^{(\sigma)}(\rho)$ by the usual procedures (Ince, 1926 or Hobson, 1931) as

$$F_n^{(\sigma)}(\rho) = (2n+1) E_n^{(\sigma)}(\rho) \int_{\rho}^{\infty} \frac{d\rho}{\{ E_n^{(\sigma)}(\rho) \}^2 \sqrt{\rho^2 - h^2} \sqrt{\rho^2 - k^2}} \quad (8-10)$$

These functions are important for the applications of the present study. For the cases $n = 0, 1$ the functions are

(1) $n = 0$

$$F_0'(\rho) = \int_{\rho}^{\infty} \frac{d\rho}{\sqrt{\rho^2 - h^2} \sqrt{\rho^2 - k^2}} \quad (8-11)$$

(2) n = 1

$$F_1'(p) = 3p \int_p^\infty \frac{dp}{p^2 \sqrt{p^2 - h^2} \sqrt{p^2 - k^2}}$$

$$F_1^2(p) = 3 \sqrt{p^2 - k^2} \int_p^\infty \frac{dp}{\sqrt{p^2 - h^2} (p^2 - k^2)^{3/2}} \quad (8-12)$$

$$F_1^3(p) = 3 \sqrt{p^2 - h^2} \int_p^\infty \frac{dp}{\sqrt{p^2 - k^2} (p^2 - h^2)^{3/2}}$$

and similarly, higher order functions may be constructed from (8-10) and the previous solutions for $E_n^{(\sigma)}(p)$.

Thus, external harmonic functions, analogous to those in spherical coordinates are

$$\phi(\rho, \mu, \nu) = \sum_{n=0}^{\infty} \sum_{\sigma=1}^{2n+1} \alpha_n^{(\sigma)} F_n^{(\sigma)}(\rho) E_n^{(\sigma)}(\mu) E_n^{(\sigma)}(\nu) \quad (8-13)$$

APPENDIX 9
EXPANSION OF ELLIPSOIDAL HARMONICS IN
TERMS OF SPHERICAL HARMONICS

The relationship of an ellipsoidal harmonic to spherical harmonics is given by Hobson (1931) in the operational form

$$\mathcal{C}_n^\sigma(x, y, z) = \left\{ 1 - \frac{D^2}{2(2n-1)} + \frac{D^4}{2 \cdot 4(2n-1)(2n-3)} - \dots \right\} H_n^m(x, y, z) \quad (9-1)$$

for internal harmonics, where

$$\mathcal{C}_n^\sigma(x, y, z) \equiv E_n^{(\sigma)}(\rho) E_n^{(\sigma)}(\mu) E_n^{(\sigma)}(z) \quad (9-2)$$

$$H_n^m(x, y, z) \equiv r^n P_n^m(\cos \theta) \begin{pmatrix} \cos m\phi \\ \sin m\phi \end{pmatrix}$$

with

$$D^2 \equiv a^2 \frac{\partial^2}{\partial x^2} + b^2 \frac{\partial^2}{\partial y^2} + c^2 \frac{\partial^2}{\partial z^2}$$

$$m = \begin{cases} \sigma/2, & \text{if } \sigma \text{ is even} \\ \frac{1}{2}(\sigma-1), & \text{if } \sigma \text{ is odd} \end{cases}$$

and where $\cos m\phi$ is used if σ is even and $\sin m\phi$ if σ is odd.

Here a, b, c are the semi-axes of the ellipsoid.

For the external harmonics Hobson's results may be put in the form

$$\mathcal{C}_n^\sigma(x, y, z) = \left(\frac{2}{2n+1} \right) \left\{ 1 + \frac{D^2}{2(2n+3)} + \frac{D^4}{2 \cdot 4(2n+3)(2n+5)} + \dots \right\} \frac{H_n^m(x, y, z)}{r^{2n+1}} \quad (9-3)$$

where

$$\mathcal{G}_n^{(\sigma)}(x, y, z) \equiv F_n^{(\sigma)}(\rho) E_n^{(\sigma)}(\mu) E_n^{(\sigma)}(\nu) \quad (9-4)$$

is an external ellipsoidal harmonic.

In the present application of these relationships the potential functions of interest have the form

$$\begin{aligned} \omega_i = & C_i^{(1)} F_1^{(1)}(\rho) \mu \nu + C_i^{(2)} F_1^{(2)}(\rho) \sqrt{k^2 - \mu^2} \sqrt{k^2 - \nu^2} \\ & + C_i^{(3)} F_1^{(3)}(\rho) \sqrt{\mu^2 - h^2} \sqrt{h^2 - \nu^2} \end{aligned} \quad (9-5)$$

Thus the potential ω_i is, in spherical coordinates, obtained from the relations

$$F_1^{(1)}(\rho) \mu \nu = \frac{2}{3} \left\{ 1 + \frac{D^2}{2 \cdot 5} + \frac{D^4}{2 \cdot 4(5)(7)} + \dots \right\} \frac{1}{R^2} P_1^0(\cos \theta)$$

$$F_1^{(2)}(\rho) \sqrt{k^2 - \mu^2} \sqrt{k^2 - \nu^2} = \frac{2}{3} \left\{ 1 + \frac{D^2}{2 \cdot 5} + \frac{D^4}{2 \cdot 4(5)(7)} + \dots \right\} \frac{1}{R^2} P_1^1(\cos \theta) \sin \phi$$

$$F_1^{(3)}(\rho) \sqrt{\mu^2 - h^2} \sqrt{h^2 - \nu^2} = \frac{2}{3} \left\{ 1 + \frac{D^2}{2 \cdot 5} + \frac{D^4}{2 \cdot 4(5)(7)} + \dots \right\} \frac{1}{R^2} P_1^1(\cos \theta) \cos \phi \quad (9-6)$$

The computations may be simplified by performing the differential operations in Cartesian coordinates. Thus observing that⁽¹⁾

(1) Hobson's choice of coordinates, employed in Appendices 7 and 8, will be adopted here also. When applied to the theory of the text the results may be reinterpreted in terms of the conventional system employed therein.

$$\frac{1}{R^2} P_1^0(\cos\theta) = \frac{x}{R^3} \quad \Rightarrow \quad \frac{1}{R^2} P_1^1(\cos\theta) \begin{pmatrix} \cos m\phi \\ \sin m\phi \end{pmatrix} = \frac{1}{R^3} \begin{pmatrix} y \\ z \end{pmatrix}$$

and that these functions satisfy Laplaces equation so

$$D^2 H_1^m(x, y, z) = \left\{ (a^2 - c^2) \frac{\partial^2}{\partial x^2} + (b^2 - c^2) \frac{\partial^2}{\partial y^2} \right\} H_1^m(x, y, z)$$

for example, then (9-6) can be put in the form

$$F_1^1(\rho) \mu \nu = \frac{2}{3} \left\{ 1 - \frac{1}{10} \left[(a^2 - b^2) \frac{\partial^2}{\partial y^2} + (a^2 - c^2) \frac{\partial^2}{\partial z^2} \right] + \frac{1}{280} \left[(a^2 - b^2) \frac{\partial^2}{\partial y^2} + (a^2 - c^2) \frac{\partial^2}{\partial z^2} \right]^2 - \dots \right\} \left(\frac{x}{R^3} \right)$$

$$F_1^2(\rho) \sqrt{k^2 - \mu^2} \sqrt{k^2 - \nu^2} = \frac{2}{3} \left\{ 1 + \frac{1}{10} \left[(a^2 - c^2) \frac{\partial^2}{\partial x^2} + (b^2 - c^2) \frac{\partial^2}{\partial y^2} \right] + \frac{1}{280} \left[(a^2 - c^2) \frac{\partial^2}{\partial x^2} + (b^2 - c^2) \frac{\partial^2}{\partial y^2} \right]^2 + \dots \right\} \left(\frac{z}{R^3} \right)$$

$$F_1^3(\rho) \sqrt{\mu^2 - k^2} \sqrt{h^2 - \nu^2} = \frac{2}{3} \left\{ 1 + \frac{1}{10} \left[(a^2 - b^2) \frac{\partial^2}{\partial x^2} - (b^2 - c^2) \frac{\partial^2}{\partial z^2} \right] + \frac{1}{280} \left[(a^2 - b^2) \frac{\partial^2}{\partial x^2} - (b^2 - c^2) \frac{\partial^2}{\partial z^2} \right]^2 + \dots \right\} \left(\frac{y}{R^3} \right)$$

Carrying out the indicated operations, one has finally

$$\begin{aligned} F_1^1(\rho) \mu \nu &= \frac{2}{3} \left(\frac{x}{R^3} \right) - \frac{1}{5} \left(\frac{1}{R^4} \right) \left[(a^2 - b^2) \left(\frac{5xy^2}{R^3} - \frac{x}{R} \right) + (a^2 - c^2) \left(\frac{5xz^2}{R^3} - \frac{x}{R} \right) \right] \\ &+ \left(\frac{5}{140} \right) \frac{1}{R^6} \left[(a^2 - b^2)^2 \left(\frac{3x}{R} - \frac{42xy^2}{R^3} + \frac{63xy^4}{R^5} \right) \right. \\ &+ 2(a^2 - b^2)(a^2 - c^2) \left(\frac{x}{R} - \frac{7x(y^2 + z^2)}{R^3} + \frac{63xy^2z^2}{R^5} \right) \\ &\left. + (a^2 - c^2)^2 \left(\frac{3x}{R} - \frac{42xz^2}{R^3} + \frac{63xz^4}{R^5} \right) \right] + O\left(\frac{1}{R^8}\right) \end{aligned}$$

(9-7)

$$\begin{aligned}
 F_1^2(\rho) \sqrt{k^2 - \mu^2} \sqrt{k^2 - \nu^2} &= 2/3 \left(\frac{z}{R^3} \right) + \frac{1}{5} \left(\frac{1}{R^4} \right) \left[(a^2 - c^2) \left(\frac{5xz^2}{R^3} - \frac{z}{R} \right) + (b^2 - c^2) \right. \\
 &\left. \left(\frac{5y^2z}{R^3} - \frac{z}{R} \right) \right] + \left(\frac{5}{140} \right) \frac{1}{R^6} \left[(a^2 - c^2)^2 \left(\frac{3z}{R} - \frac{42x^2z}{R^3} + \frac{63z^3}{R^5} \right) + 2(a^2 - c^2)(b^2 - c^2) \right. \\
 &\left. \left(\frac{z}{R} - \frac{7z(x^2 + y^2)}{R^3} + \frac{63z^3}{R^5} \right) + (b^2 - c^2)^2 \left(\frac{3z}{R} - \frac{42zy^2}{R^3} + \frac{63zy^4}{R^5} \right) \right] + O\left(\frac{1}{R^8}\right)
 \end{aligned}
 \tag{9-8}$$

$$\begin{aligned}
 F_1^3(\rho) \sqrt{\mu^2 - h^2} \sqrt{h^2 - \nu^2} &= 2/3 \left(\frac{y}{R^3} \right) + \frac{1}{5} \left(\frac{1}{R^4} \right) \left[(a^2 - b^2) \left(\frac{5x^2y}{R^3} - \frac{y}{R} \right) - (b^2 - c^2) \right. \\
 &\left. \left(\frac{5yz^2}{R^3} - \frac{y}{R} \right) \right] + \left(\frac{5}{140} \right) \frac{1}{R^6} \left[(a^2 - b^2) \left(\frac{3y}{R} - \frac{42x^2y}{R^3} + \frac{63y^3}{R^5} \right) - 2(a^2 - b^2)(b^2 - c^2) \right. \\
 &\left. \left(\frac{y}{R} - \frac{7y(x^2 + z^2)}{R^3} + \frac{63y^3}{R^5} \right) + (b^2 - c^2)^2 \left(\frac{3y}{R} - \frac{42yz^2}{R^3} + \frac{63yz^4}{R^5} \right) \right] \\
 &+ O\left(\frac{1}{R^8}\right)
 \end{aligned}
 \tag{9-9}$$

The results have been carried out sufficiently far that all terms which are likely to be of importance in any practical application, including the present, are included. It is clear that all the harmonics of a given order n can be obtained from one of their number by interchanges of x , y and z , as would be expected.

APPENDIX 10

STRAIN COEFFICIENTS P_{ij} , Q_{ij}

$$\{P_{ij}\} : \quad P_{ij} = P_{ji}$$

$$P_{11} = 7 \sin^4 \theta \cos^3 \phi \sin \phi - (3/2) \sin^2 \theta \sin 2\phi$$

$$P_{12} = (1/5) - \sin^2 \theta + (7/4) \sin^4 \theta \sin^2 2\phi$$

$$P_{22} = 7 \sin^4 \theta \sin^3 \phi \cos \phi - (3/2) \sin^2 \theta \sin 2\phi$$

$$P_{23} = 7 \sin^3 \theta \cos \theta \sin^2 \phi \cos \phi - (1/2) \sin 2\theta \cos \phi$$

$$P_{33} = (7/8) \sin^2 2\theta \sin 2\phi - (1/2) \sin^2 \theta \sin 2\phi$$

$$P_{13} = 7 \sin^3 \theta \cos \theta \cos^2 \phi \sin \phi - (1/2) \sin 2\theta \sin \phi$$

$$\{Q_{ij}\} : \quad Q_{ij} = Q_{ji}$$

$$Q_{11} = 5 \sin^4 \theta \cos^3 \phi \sin \phi - [(2\lambda + \mu)/2(\lambda + \mu)] \sin^2 \theta \sin 2\phi$$

$$Q_{12} = (5/4) \sin^4 \theta \sin^2 2\phi - [\lambda/2(\lambda + \mu)] \sin^2 \theta - \frac{\mu}{3(\lambda + \mu)}$$

$$Q_{22} = 5 \sin^4 \theta \sin^3 \phi \cos \phi - [(2\lambda + \mu)/2(\lambda + \mu)] \sin^2 \theta \sin 2\phi$$

$$Q_{23} = 5 \sin^3 \theta \cos \theta \sin^2 \phi \cos \phi - [\lambda/4(\lambda + \mu)] \sin 2\theta \cos \phi$$

$$Q_{33} = (5/8) \sin^2 2\theta \sin 2\phi - (1/2) \sin^2 \theta \sin 2\phi$$

$$Q_{13} = 5 \sin^3 \theta \cos \theta \cos^2 \phi \sin \phi - [\lambda/4(\lambda + \mu)] \sin 2\theta \sin \phi$$

APPENDIX II

TABLE OF SYMBOLS AND SPECIAL FUNCTIONS

<u>Symbol</u>	<u>Definition</u>	<u>First Introduced in Equation or Section</u>
λ	Lamé (elastic) constant	2. 2. 1
μ	Rigidity	2. 2. 1
ρ	Density	2. 2. 1
$\underline{f} = \rho \underline{f}$	Body force, source term	2. 2. 1
B_τ	Source boundary	2. 2
Φ	Scalar source potential	2. 2. 4
\underline{B}	Vector source potential	2. 2. 4
(r', θ', ϕ')	Source coordinates	2. 2
(r, θ, ϕ)	General (observers) coordinates	2. 2
$r^* = \underline{r} - \underline{r}' $	Distance from source point to an arbitrary point	2. 2
\underline{u}	Elastic displacement field	2. 2. 1
δ	Scalar displacement potential	2. 2. 5
$\underline{\psi}$	Vector displacement potential	2. 2. 5
v_p	Compressional (primary) wave velocity	2. 2. 5
v_s	Shear (secondary) wave velocity	2. 2. 5
$\Theta = \nabla \cdot \underline{u}$	Dilatation	2. 2. 8
$\underline{\Omega} = \frac{1}{2} \nabla \times \underline{u}$	Rotation vector	2. 2. 8
χ	General scalar potential	2. 2. 10
\underline{r}_0	Source coordinates	2. 2. 11
t_0	Source time	2. 2. 11

<u>Symbol</u>	<u>Definition</u>	<u>First Introduced in Equation or Section</u>
$G(\underline{r}, t/\underline{r}_0, t_0)$	Green's Function for the scalar wave equation	2. 2. 12
$\mathfrak{S}(\underline{r}_0, t_0)$	Generalized source function	2. 2. 11
τ^*	Space-connected source time (delay time for volume relaxation)	2. 2. 11
χ_j	Generalized scalar potential for the jth layer	2. 2. 13
$\chi_j^{(0)}$	Scalar potential of homogeneous wave equation in the jth layer	2. 2. 13
$\chi_n^{(1)}$	Scalar potential for the source field in the nth (source) layer	2. 2. 13
ω	"angular frequency"	2. 2. 15
k_1, k_2, k_3	Wave number components	2. 2. 15
$\kappa_j = \omega/v_j$	Special "wave number" notation involving body wave velocities, v_j , in layered earth models	2. 2. 15
k	Wave number magnitude	2. 2. 16
$\delta(x)$	Dirac delta function	2. 2. 18
$\delta_1(x-y)$	$\delta_1(x-y) = \frac{\partial}{\partial y} \delta(x-y)$ Delta function derivative	2. 2. 18
$\mathcal{F}\{ \}$	Fourier transform operator	2. 2
$\tilde{x}(\omega) = \mathcal{F}\{x(t)\}$	Fourier transformed function of time	2. 2
τ_1^*, τ_2^*	Delay times appropriate to compressional and shear type potentials	2. 2. 22
k_p, k_s, κ	$k_p = \omega/v_p, k_s = \omega/v_s,$ $\kappa = k_p$ or k_s	2. 2. 27
\underline{u}^*	Initial displacement field	2. 2. 27

<u>Symbol</u>	<u>Definition</u>	<u>First Introduced in Equation or Section</u>
\mathcal{R}	Static source function	2.3.2
$S(t)$	Source time function	2.3.1
ϵ_{ijk}	$\epsilon_{ijk} = \begin{cases} +1 & i, j, k \text{ even permutation} \\ & \text{of } 1, 2, 3 \\ -1 & \text{odd permutation} \\ 0 & \text{one indice equals another} \end{cases}$	2.3
\hat{e}_i	Basis vectors, $i = 1, 2, 3$	2.3
$R^{(n+1)}(i_0 \dots i_n)$	Multipole (integral) moments	2.3.4
$\rho^{(n+1)}(\omega)$	"Multipole magnitude"	2.3.7
$s_n^{(i)}(\theta, \phi)$	Spherical surface harmonic	2.3.8
$\Omega(kr)$	"Propagation function"	2.6.4
$r^F_s(a_1 \dots a_r; b_1 \dots b_s; x)$	General hyper-geometric function	2.6.4
$S_n(\theta, \phi)$	Spherical surface harmonic	2.7
\mathcal{R}_s	Effective source volume radius	2.7
$\mathcal{G}(m , \mu ; p, n, \nu)$	Transformation coefficient	2.8.2
$(n)!!$	"Double factorial"; $(n)!! = n(n-2) \dots \left(\frac{2}{1}\right)$	2.8
δ_{nm}	Kroeneker delta function $\delta_{nm} = \begin{cases} 0, & n \neq m \\ 1, & n = m \end{cases}$	2.8.4 2.8
$G_{lk}(r', \omega), C_{lk}^{(j)}(r', \omega)$	Multipole coefficients for potentials in a translated coordinate system	2.8.4
$P_n^m(\xi)$	Associated Legendre function (Ferrers definition)	2.2
$\overline{P}_n^m(\xi)$	Associated Legendre function (Hobson's definition)	2.8.7
$P_n^{(m)}(\xi)$	mth derivative of the Legendre polynomial $P_n(\xi)$	2.8.7

<u>Symbol</u>	<u>Definition</u>	<u>First Introduced in Equation or Section</u>
$Y_n^a(x, y, z)$	Solid harmonic	2. 9. 3
$S_{\mu, \nu}(z)$	Lommel's function	2. 9. 4
$\sigma_{ij}^{(0)}, \underline{u}^{(0)}$	Initial tectonic prestress field and associated displacement	3. 7. 1
$\sigma_{ij}^{(1)}, \underline{u}^{(1)}$	Tectonic stress field in the presence of a rupture and associated displacement	3. 7. 2a
$B(\tau)$	Surface of the rupture	3. 7. 2b
\underline{n}	Unit vector normal to B	3. 7. 2b
w_s	Energy density released at a point due to elastic relaxation	3. 7. 3
σ_{ij}^*	The change in the stress equilibrium value due to creation of a rupture	3. 7. 4
\underline{u}^*	Displacement change associated with σ_{ij}^*	3. 7. 6
$\sigma = \frac{\lambda}{2(\lambda + \mu)}$	Poisson's ratio	3. 7. 6
τ	Source time variable	3. 7
\underline{G}	Galerkin vector	3. 7. 9
Θ^*	Dilatation associated with the change in stress σ_{ij}^*	3. 7. 14
Ω^*	Rotation vector associated with σ_{ij}^*	3. 7. 14
$\phi, \underline{\omega}$	Harmonic scalar and vector potentials associated with an elastic equilibrium field	3. 7. 16
$\mathcal{S}^*, \underline{\psi}^*$	Biharmonic scalar and vector potentials associated with σ_{ij}^*	3. 7. 18
$W^{(0)}$	Initial strain energy of a pre-stressed medium	3. 8. 1
$W^{(1)}$	Final strain energy of stressed medium after creation of a rupture	3. 8. 1

<u>Symbol</u>	<u>Definition</u>	<u>First Introduced in Equation or Section</u>
δW^*	Change in potential energy of a stressed medium due to creation of a rupture ($W^{(0)} - W^{(1)}$)	3.8.1
$e_{ij}^{(0)}, e_{ij}^{(1)}$	Strains associated with prestress $\sigma_{ij}^{(0)}$ and final stress $\sigma_{ij}^{(1)}$	3.8
e_{ij}^*	Strain difference associated with σ_{ij}^*	3.8
V_0	Rupture volume	3.8
V_1	Volume of the medium or finite body exterior to the rupture volume V_0	3.8
V	Volume of the prestressed medium	3.8
F_i	Total force, tectonic and otherwise, within the stressed medium	3.8
τ_{ij}, ϵ_{ij}	Total stress and strain within a rupture volume, including that due to plasticity	3.8.7
\mathcal{E}	Energy required for phase change and fracture associated with rupturing	3.8.7
γ_{ij}^*	Shear stress within the rupture volume V_0	3.8.8
E_r	Lower bound of energy released as seismic radiation due to rupture	3.8.11
$\left. \begin{array}{l} u_i(\underline{r}, t/\tau) \\ \sigma_{ij}(\underline{r}, t/\tau) \end{array} \right\}$	Dynamical displacement and stress fields associated with incremental rupture as functions of observer time t and a source time τ	3.9.1
$\left. \begin{array}{l} y_i(\underline{r}, t/\tau) \\ \tau_{ij}(\underline{r}, t/\tau) \end{array} \right\}$	Relative dynamical displacement and stress associated with incremental rupture	3.9.1
$\left. \begin{array}{l} \Theta(\underline{r}, t/\tau) \\ \Omega(\underline{r}, t/\tau) \end{array} \right\}$	Dilatation and rotation corresponding to the relative displacement and stresses y_i, τ_{ij} ("physical potentials")	3.9.4

<u>Symbol</u>	<u>Definition</u>	<u>First Introduced in Equation or Section</u>
$\mathfrak{D}(\underline{r}, t/\tau)$ $\underline{\Psi}(\underline{r}, t/\tau)$	Displacement potentials associated with the relative displacement y_i	3.9.6
$\Theta^*(\underline{r}, \tau)$ $\Omega^*(\underline{r}, \tau)$	Initial values for dilatation and rotation due to incremental rupture ("relaxation potentials")	3.9
$\mathfrak{D}^*(\underline{r}, \tau)$ $\underline{\Psi}^*(\underline{r}, \tau)$	Initial values for the displacement potentials due to incremental rupture	3.9
Φ, χ	Generalized potentials representing either the "physical potentials" or the displacement potentials	3.9
$\Phi^*(\underline{r}, \tau)$ $\chi^*(\underline{r}, \tau)$	Initial values corresponding to the generalized potentials describing incremental rupture radiation	3.9
τ_k	Particular value of the source time τ	3.9
$\delta\tau$	Infinitesimal interval of source time	3.9.7
$\zeta(\underline{r}, t)$	Minimum distance from the rupture surface to the point at \underline{r}	3.9.8
$\delta\Phi^*$ $\delta\chi_j^*$	Discontinuous changes in the generalized potentials corresponding to a change in equilibrium due to incremental rupture	3.9.12
$\mathcal{R}(\tau)$	Region exterior to the rupture surface $B(\tau)$	3.9.13
$\delta_n(t)$	n th derivative of the Dirac delta function	3.9.14
$\delta\underline{u}^*$	Discontinuous change in the displacement corresponding to a change in equilibrium due to incremental rupture	3.9
Ω	Solid angle	3.9.19
$R(\Omega, \tau)$	Radial distance to the rupture surface	3.9.19

<u>Symbol</u>	<u>Definition</u>	<u>First Introduced in Equation or Section</u>
$\left. \begin{array}{l} \Phi(\underline{r}, t) \\ \chi_j(\underline{r}, t) \end{array} \right\}$	Generalized potentials for rupture radiation	3.10.2
τ_o	Source time at the end of rupture	3.10.2
$S(\tau - \tau_o)$	The step function defining the time interval of rupturing	3.10.2
v_R	Velocity of the rupture front (Rate of rupture expansion)	3.10.3
a_o, b_o, c_o	Semi-axes of the final rupture ellipsoid	3.10.3
$a(\tau), b(\tau), c(\tau)$	Semi-axes of an expanding or propagating rupture ellipsoid	3.10.3
(r'', θ'', ϕ'')	Spherical coordinates in a system translating with the rupture	3.10.7
$\left. \begin{array}{l} \alpha_{nm}(\tau) \\ \beta_{nm}(\tau) \end{array} \right\}$	Source time dependent multipole coefficients for the harmonic initial value Θ^*	3.10.7
$\left. \begin{array}{l} \gamma_{nm}^{(j)}(\tau) \\ \delta_{nm}^{(j)}(\tau) \end{array} \right\}$	Source time dependent multipole coefficients for the harmonic initial value Ω_j^*	3.10.7
(r', θ', ϕ')	Spherical coordinates in a system fixed at the point of initial rupture	3.10.8
$d(\tau)$	Separation of the origins of the fixed source coordinates and that translating with the rupture	3.10.8
d_o	Final separation of fixed and moving coordinate systems after rupture	3.10.11
$\Gamma_m(\theta', \phi')$	"Angular delay factor" associated with the distance function ζ	3.10.12a
$\left. \begin{array}{l} \eta_m(\theta', \phi') \\ \xi_m(\theta', \phi') \end{array} \right\}$	Angular delay factors $\eta_m = 1 - (v_R/v_p)\Gamma_m$ $\xi_m = 1 - (v_R/v_s)\Gamma_m$	3.10.14

<u>Symbol</u>	<u>Definition</u>	<u>First Introduced in Equation or Section</u>
t_p^*, t_s^*	Delay times for causality effects for p and s type potentials	3.10.14
$R(\tau)$	Radius of a propagating spherical rupture	3.10.17
a_o	Form factor for the rupture shape, ratio of the rupture length at $\tau_o/2$ to the final length at τ_o	3.10.23
Θ_1^*, Θ_2^*	Relaxation potentials, corresponding to Θ^* in the two spatial domains $r' > d(\tau)$ and $r' < d(\tau)$ respectively	3.11.2
$A_{nm}(\omega)$ $B_{nm}(\omega)$	Multipole expansion coefficients for the dilatation field due to rupture	3.11.10
$C_{nm}^{(j)}(\omega)$ $D_{nm}^{(j)}(\omega)$	Multipole expansion coefficients for the rotation field due to rupture	3.11.10
$\tilde{\Theta}^{(1)}(\underline{r}, \omega)$ $\tilde{\Omega}^{(1)}(\underline{r}, \omega)$	Fourier transforms of the dilation and rotation fields due to rupture (source radiation)	3.11.10
$A_{nm}^{(p)}, B_{nm}^{(p)}$	Coefficients in the expansion in $(\tau)^p$	3.11.15
$j C_{nm}^{(p)}, j D_{nm}^{(p)}$	Coefficients in the $(\tau)^p$ series for $\gamma_{nm}^{(j)}(\tau)$ and $\delta_{nm}^{(j)}(\tau)$	3.11
$\begin{Bmatrix} x \\ y \end{Bmatrix}$	Row matrix: (x y)	3.11.16
$\begin{pmatrix} x \\ y \end{pmatrix}$	Column matrix	3.11.16
$G_{lk}(\omega), \beta_{lk}(\omega)$	Multipole coefficients for the dilatation field due to rupture	3.11.20
$C_{lk}^{(j)}(\omega), \beta_{lk}^{(j)}(\omega)$	Multipole coefficients for the rotation field due to rupture	3.11.22
k_R	$k_R = \omega/v_R$	3.11.23
$E_\ell^{(1)}(\mu, \gamma; x; by)$	"Modified hypergeometric function"	3.11.25

<u>Symbol</u>	<u>Definition</u>	<u>First Introduced in Equation or Section</u>	
a_o^m	Form factor for propagating ruptures	3.12.3	
β_m	space partition parameters	3.12.12	
f_m	$f_m \equiv (1-2a_o^m)/2a_o^m$	3.12.13	
h_m, g_m	Space partition parameters	3.12.13	
$(1)\Omega_j^*, (2)\Omega_j^*$	Relaxation potentials corresponding to Ω_j^* in the two spatial domains $r' > d(\tau)$ and $r' < d(\tau)$ respectively	3.12.21	
$r_o^{(m)}, r_1^{(m)}$	Space partition radii for the propagating rupture source	3.12.30	
d_m	$d_m \equiv (1-a_o^m)/(1-2a_o^m)$	3.12.40	
$r_2^{(m)}$	Space partition radius for the propagating rupture source) ($a_o^m < 1/10$)	3.12.44	
b_m	$b_m \equiv 1/(1-a_o^m)$	3.12.45	
R_o	Shock induced rupture radius	3.13.3	
(ρ, μ, ν)	Ellipsoidal coordinates		3.14 Appendix 7
$F_n^\sigma(z)$	External ellipsoidal harmonic	3.14.18	Appendix 8
$E_n^\sigma(z)$	Internal ellipsoidal harmonic	3.14.18	Appendix 8

FIGURE CAPTIONS

- Figure 1 Source and receiver coordinate relationships.
- Figure 2 Partition of space about an observation point P.
- Figure 3 Schematic representations of (a) Growing and (b) Propagating ruptures at source times τ_1 and τ_2 , with Q a source point, P the receiver point and $f(z)$ the minimum distance from the source point to the rupture surface $B(\tau)$. (E - rupture envelope).
- Figure 4 Basic types of "macroscopic" and "microscopic" dislocations. (a) An edge dislocation of an elastic body. Slip perpendicular to the dislocation line (Orowan, 1954). (b) A screw dislocation of an elastic body. Slip parallel to the dislocation line. (Orowan, 1954). (c) An edge dislocation in a crystalline lattice showing the position of an impurity atom (I). (Mason, 1958). (d) A screw dislocation in a crystalline lattice (simple cubic structure). (Mason, 1958).
- Figure 5 Frank-Read dislocation source showing various phases of the motion of a dislocation under a stress field, where a new loop and a second pinned dislocation are produced. T_{13} is the total stress on the dislocation during the motion. (Mason, 1958).

- Figure 6 Partitioning of the region about the final rupture envelope for the radiation volume V_1 .
- Figure 7 Spatial relations for a rupture in a prestrained medium.
- Figure 8 Coordinate relationships between the system O^{11} translating with the rupture and the fixed system O^1 with origin at the point of initial rupture. (Unilateral growing rupture shown).
- Figure 9 Growing or expanding ellipsoidal rupture model. Final rupture axes: $a_o, b_o < a_o, c_o \ll b_o$.
- Figure 10 Propagating rupture models (unilateral ruptures). (a) Model $m = 2$, propagating spherical rupture with an ellipsoidal rupture envelope. Axes a_o, b_o, b_o, a_o . (b) Model $m = 3$, propagating ellipsoidal rupture with ellipsoidal rupture envelope. Axes $a_o, b_o < a_o, c_o \ll b_o$.
- Figure 11 Regions of anomolous (delayed) relaxation for the three rupture models at particular stages of rupture. (a) Expanding ellipsoidal rupture ($m = 1$). (b) Propagating spherical rupture ($m = 2$). (c) Propagating ellipsoidal rupture ($m = 3$).
- Figure 12 Angular delay factors $\eta_m(\theta', \phi')$ for expanding and propagating ellipsoidal and spherical ruptures. (a) η_2 for the propagating spherical rupture. (b) η_1 for equilateral expanding ellipsoidal rupture. (c) η_1 for

bilateral expanding ellipsoidal rupture ($d_0 = a_0/4$).

(d) η_1 for unilateral expanding ellipsoidal rupture

(bottom) and η_3 for unilateral propagating ellipsoidal rupture (top). All cases have $b_0/a_0 = 1/4$

Figure 13 Parameters β_m , h_m and g_m for propagating ruptures as functions of the form factor α_0^m , $.1 \leq \alpha_0^m < 1/2$.

Figure 14 Space-time partitioning for propagating rupture sources.

(a) Spatial partitioning as a function of the source form factor α_0^m .

1. Region in which: $(r'/a_0) > (\beta_m + 1)\alpha_0^m$

2. Region in which:

$$(1 - 2\alpha_0^m)^2 / 4\alpha_0^m < (r'/a_0) < (\beta_m + 1)\alpha_0^m$$

3. Region in which:

$$0 \leq (r'/a_0) < (1 - 2\alpha_0^m)^2 / 4\alpha_0^m$$

(b) Source time partition for $\alpha_0^m = 1/8$, a representative case. The exact curve is given for comparison.

1. Region: $(\frac{1 - \alpha_0^m}{1 - 2\alpha_0^m}) \frac{r'}{V_R} < \tau \leq \frac{2a_0}{V_R}$

2. Region: $0 \leq \tau < (\frac{1 - \alpha_0^m}{1 - 2\alpha_0^m}) \frac{r'}{V_R}$

3. Region: $g_m(\frac{a_0}{V_R}) + h_m(\frac{r'}{V_R}) < \tau \leq \frac{2a_0}{V_R}$

4. Region: $0 \leq \tau < g_m(\frac{a_0}{V_R}) + h_m(\frac{r'}{V_R})$

5. Region: $0 \leq \tau \leq \frac{2a_0}{V_R}$

Figure 15 General translations of coordinates to the center of the earth for spontaneous rupture models. (\underline{R} denotes the rupture direction or major axis of the rupture direction or major axis of the rupture ellipsoid which is always taken in the Z direction in the source coordinates).

Figure 16 Coordinate relationships for (a) "Strike slip and (b) "dip slip" ruptures.

λ - surface azimuth
 r, θ, ϕ - source coordinates

P - point of observation

V_R - rupture propagation velocity vector

H - depth of source

Figure 17 Amplitude spectrums of the rotational multipole coefficient $C_{\ell l}^{(j)}$ and the dilatational coefficients A_{12}, B_{12} for $l = 2, 3, 4$. Cases shown are for equal components of the initial stress field, \underline{e} . $S_{12} = S_{23} = S_{13} = .001$. The rupture parameters are

$$a_o = 1.5 \text{ km} \quad V_R = 1.656 \text{ km/sec}$$

$$b_o = .2 \text{ km} \quad V_p = 3.2 \text{ km/sec}$$

$$H = 3 \text{ km} \quad V_s = 1.84 \text{ km/sec}$$

$$R_s = 3 \text{ km}$$

Higher order multipoles become significant at the shorter periods due to propagation of the rupture.

- Figure 18 Phase of multipole coefficients for spontaneous rupture. Source parameters as in Figure (17).
- Figure 19 Spontaneous rupture radiation patterns (strike slip") for (a) dilatation Θ (b) rotation component Ω_1 (c) rotation component Ω_2 (d) rotation component Ω_3 . Rupture parameters as in Figure (17). Scale divisions indicated.
- Figure 20 Spontaneous rupture radiation patterns (strike slip") for (a) dilatation Θ (b) rotation component Ω_1 (c) rotation component Ω_2 (d) rotation component Ω_3 . Rupture parameters as in Figure (17). Scale divisions indicated. The case shown is the same as in Figure (19) except for a change in the stress orientation.
- Figure 21 Spontaneous rupture radiation patterns ("strike slip") for (a) dilatation Θ (b) rotation component Ω_1 (c) rotation component Ω_2 (d) rotation component Ω_3 . Rupture parameters as in Figure (17). Scale divisions indicated. The case shown is the same as in Figures (19) and (20) except for a change in the stress orientation.
- Figure 22 Spontaneous rupture radiation patterns ("strike slip") for (a) dilatation Θ (b) rotation component Ω_1 (c) rotation component Ω_2 (d) rotation component Ω_3 . Rupture parameters as in Figure (17). Scale divisions indicated. The case shown is the same as Figure (19) except for

the longer period of the radiation.

Figure 23 Spontaneous rupture radiation patterns ("strike slip") for (a) dilatation Θ (b) rotation component Ω_1 , (c) rotation component Ω_2 (d) rotation component Ω_3 . Rupture parameters as in Figure (17). Scale divisions indicated. The case shown is the same as Figure (21) except for the longer period of the radiation.

Figure 24 Spontaneous rupture radiation patterns ("dip slip") for (a) dilatation Θ (b) rotation component Ω_1 , (c) rotation component Ω_2 (d) rotation component Ω_3 . Rupture parameters as in Figure (17). Scale divisions indicated. The case shown is the same as that in Figure (19) except for the change in the rupture orientation.

Figure 25 Schematic representation of the various zones of non-linear behavior in the vicinity of an explosive source. (Not to scale).

R_0 - vaporization radius

R_1 - final cavity radius

R_2 - flow zone radius

Figure 26 Curves $k = \text{const.}$ plotted with W and R_0 variable. Other source and medium parameters held constant with values appropriate to the Ranier nuclear explosion in Tuff.

Figure 27 Radius of the zone of flow and crushing (R_2) versus radius of vaporization (R_0) for various values of the internal friction parameter (k). Other source and medium parameters held fixed at values appropriate to the Ranier nuclear explosion.

Figure 28 Final cavity pressure (P) versus "initial cavity" radius R_0 (radius of vaporization) for various values of the internal friction coefficient k . Other source and medium parameters held fixed at values appropriate to the Ranier nuclear test.

Figure 29 Strain energy release E_s versus explosive energy for various values of the internal friction coefficient k . Initial stress field $\sigma_{12} = 5.38 \times 10^7$ dynes/cm². R_1 fixed, but R_0 allowed to vary with W . Other parameters held fixed at values appropriate to the Ranier nuclear explosion.

Figure 30 Strain energy release E_s versus explosive energy for various values of initial strain. Internal friction constant $k = .1$, and held fixed. R_1 fixed, but R_0 varies with W . Other parameters held fixed with values appropriate to the Ranier explosion. Initial stress values: $\sigma_{12} = 53.8$ bars, 26.9 bars, 15.6 bars, 13.45 bars.

Figure 31 Amplitude spectrums for induced rupture. (a) multipole coefficients normalized by division by S_{ij} the strain parameters, plotted as a function of period in the range 1-100 sec. (b) Amplitude spectrums of the dilatation and rotation components at 344 km with $\Theta = 60^\circ$.

Source parameters:

$$\begin{array}{ll} R_o = .3 \text{ km} & V_R = 3.5 \text{ km/sec} \\ R_s = 1.5 \text{ km} & V_p = 3.2 \text{ km/sec} \\ & V_s = 1.84 \text{ km/sec} \end{array}$$

Figure 32 Phase of normalized multipole coefficients A_{2m} , B_{2m} (Dilatation) and $c_{2m}^{(j)}$, $D_{2m}^{(j)}$ (rotation) for the induced rupture. Parameters as in Figure (31).

Figure 33 Shock induced rupture radiation patterns for (a) Dilatation Θ (b) Rotation component Ω_1 (c) Rotation component Ω_2 (d) Rotation component Ω_3 . Rupture parameters as in Figure (31).

Figure 34 Shock induced rupture radiation patterns for (a) Dilatation Θ (b) Rotation component Ω_1 (c) Rotation component Ω_2 (d) Rotation component Ω_3 . Rupture parameters as in Figure (31). The case shown is the same as that in Figure 33 except for a change in the stress orientation.

- Figure 35 Shock induced rupture radiation patterns for (a) Dilatation Θ (b) Rotation component Ω_1 , (c) Rotation component Ω_2 (d) Rotation component Ω_3 . Rupture parameters as in Figure (31). The case shown is the same as that in Figures (33) and (34) except for the differences in stress orientation.
- Figure 36 Shock induced rupture radiation patterns for (a) Dilatation Θ (b) Rotation component Ω_1 , (c) Rotation component Ω_2 (d) Rotation component Ω_3 . Rupture parameters as in Figure (31). The case shown is the same as that in Figure (35) except for a small change in the prestress.
- Figure 37 Partition of space about an observation point and the surfaces of integrations and S_o .
- Figure 38 Translation of coordinates from O (source) to O' (arbitrary origin).

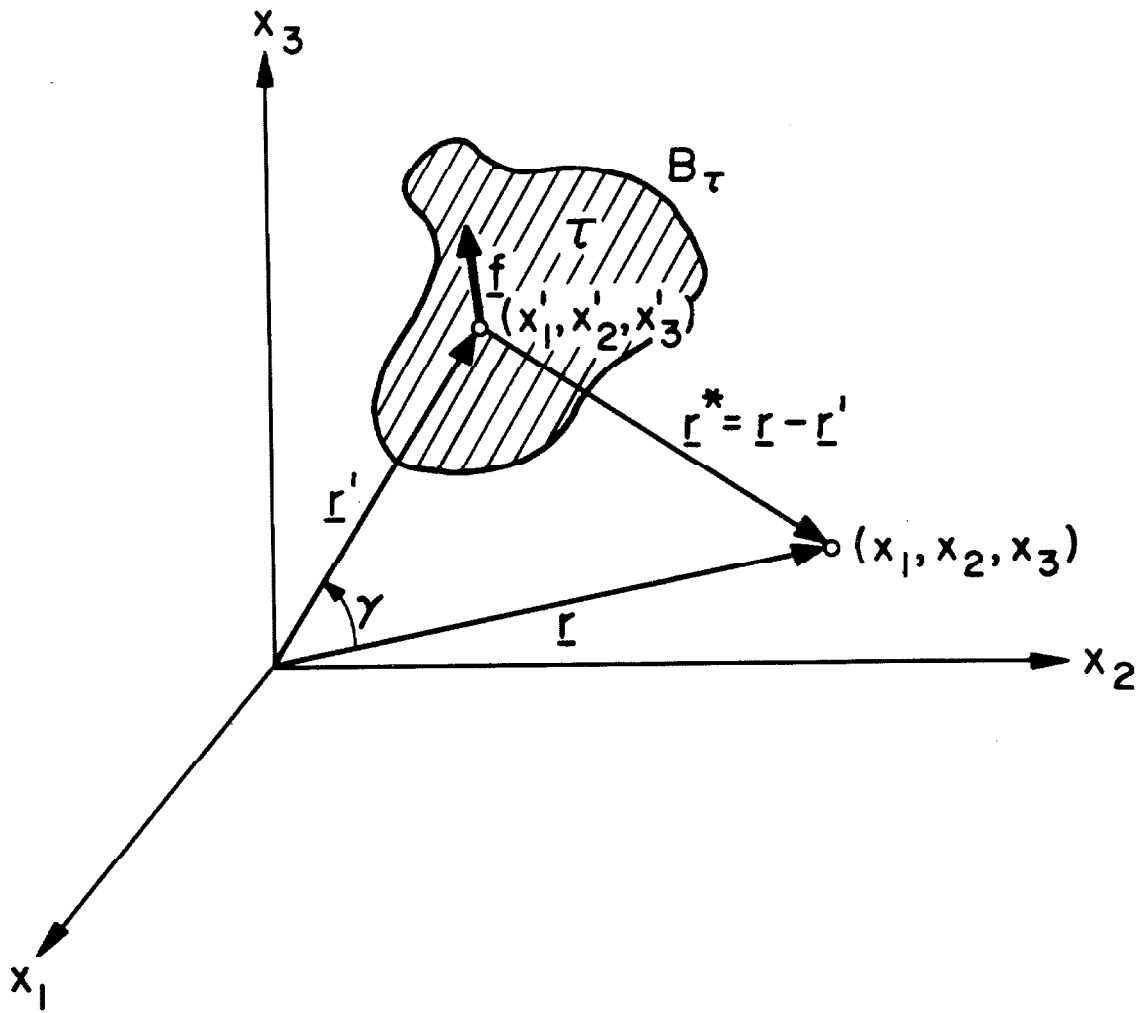


Fig. 1

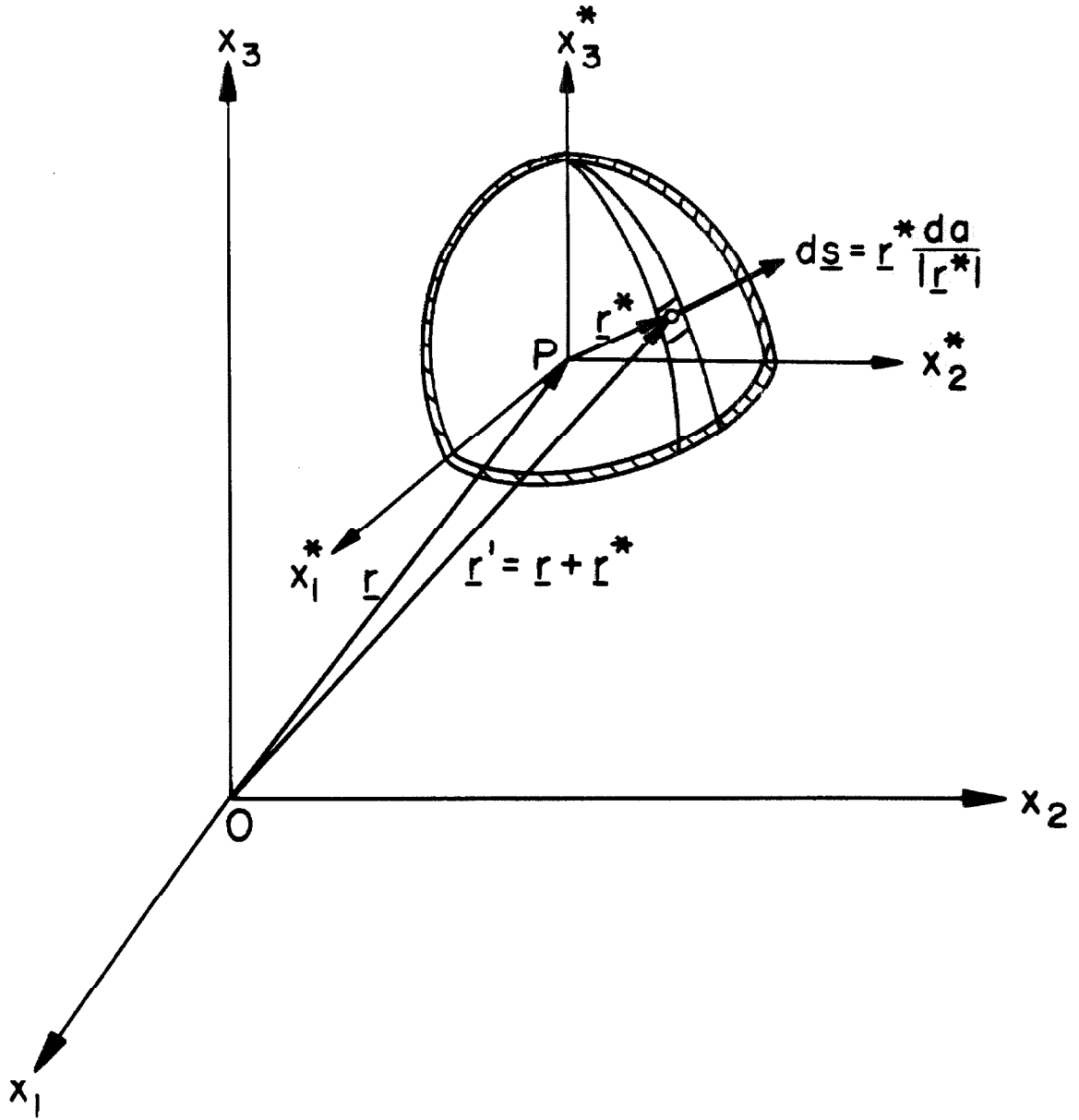


Fig. 2

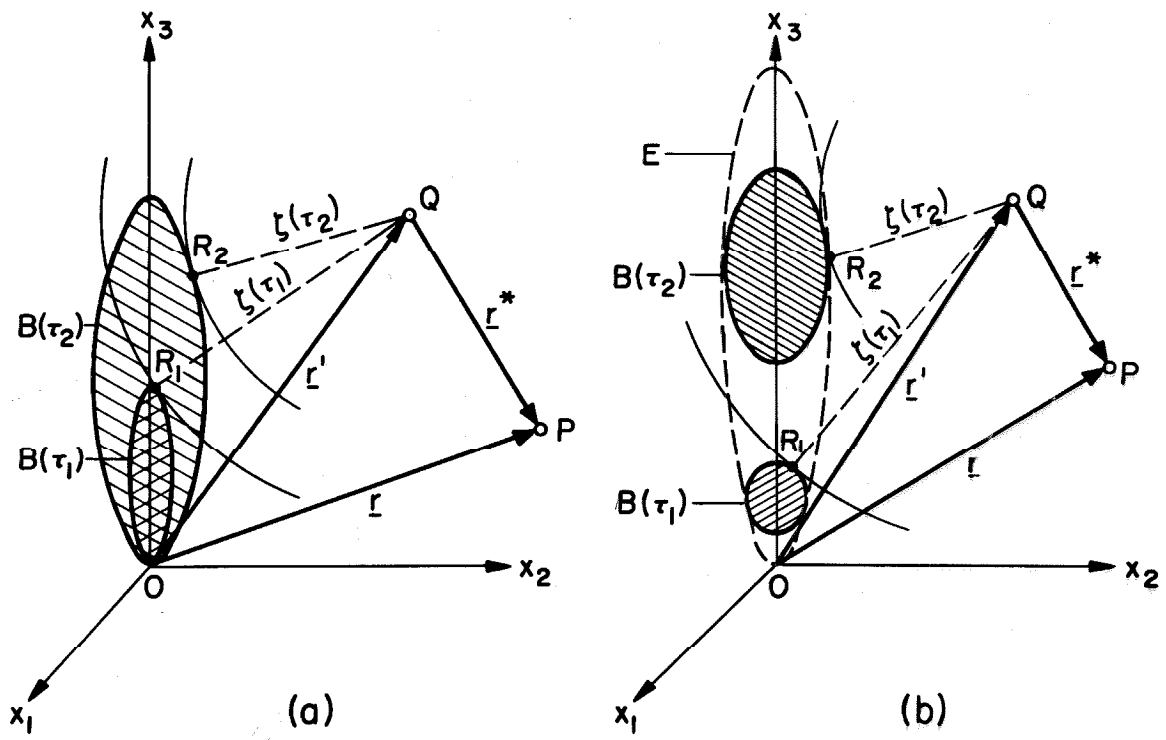
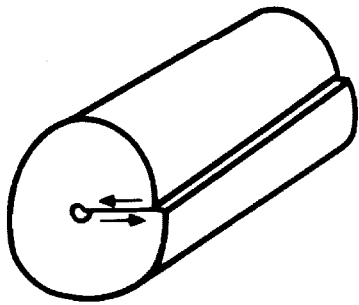
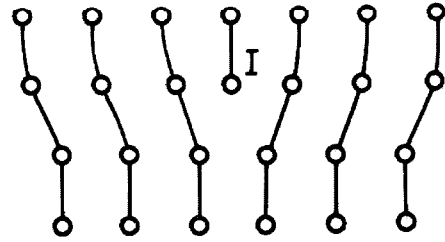


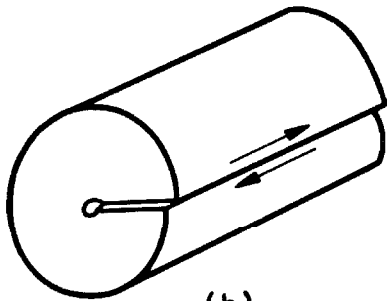
Fig. 3



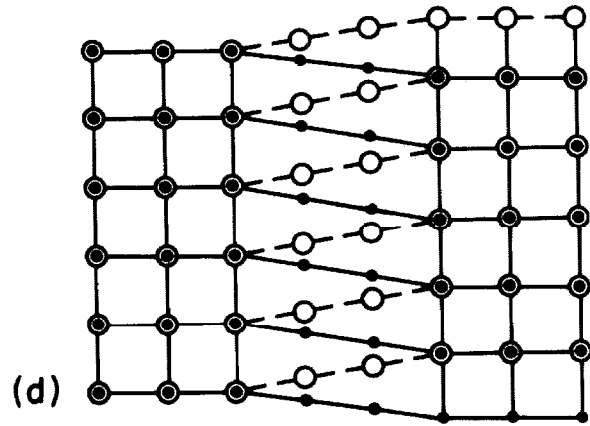
(a)



(c)



(b)



(d)

Fig. 4

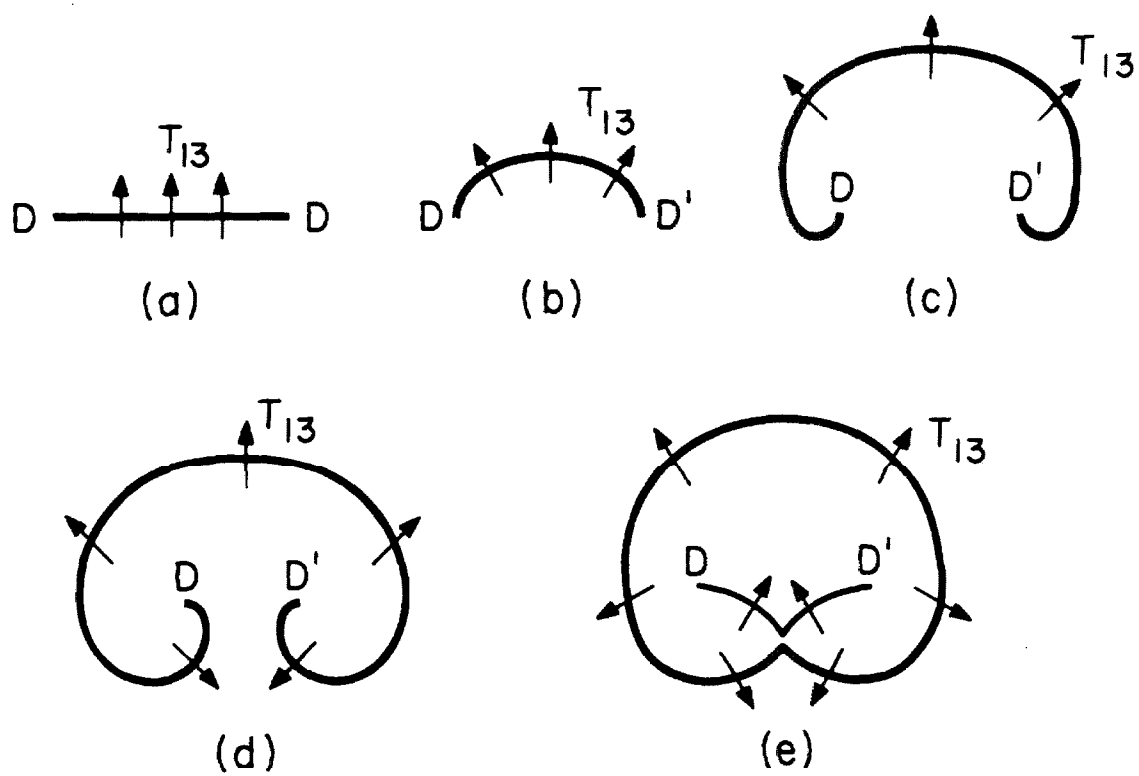


Fig. 5

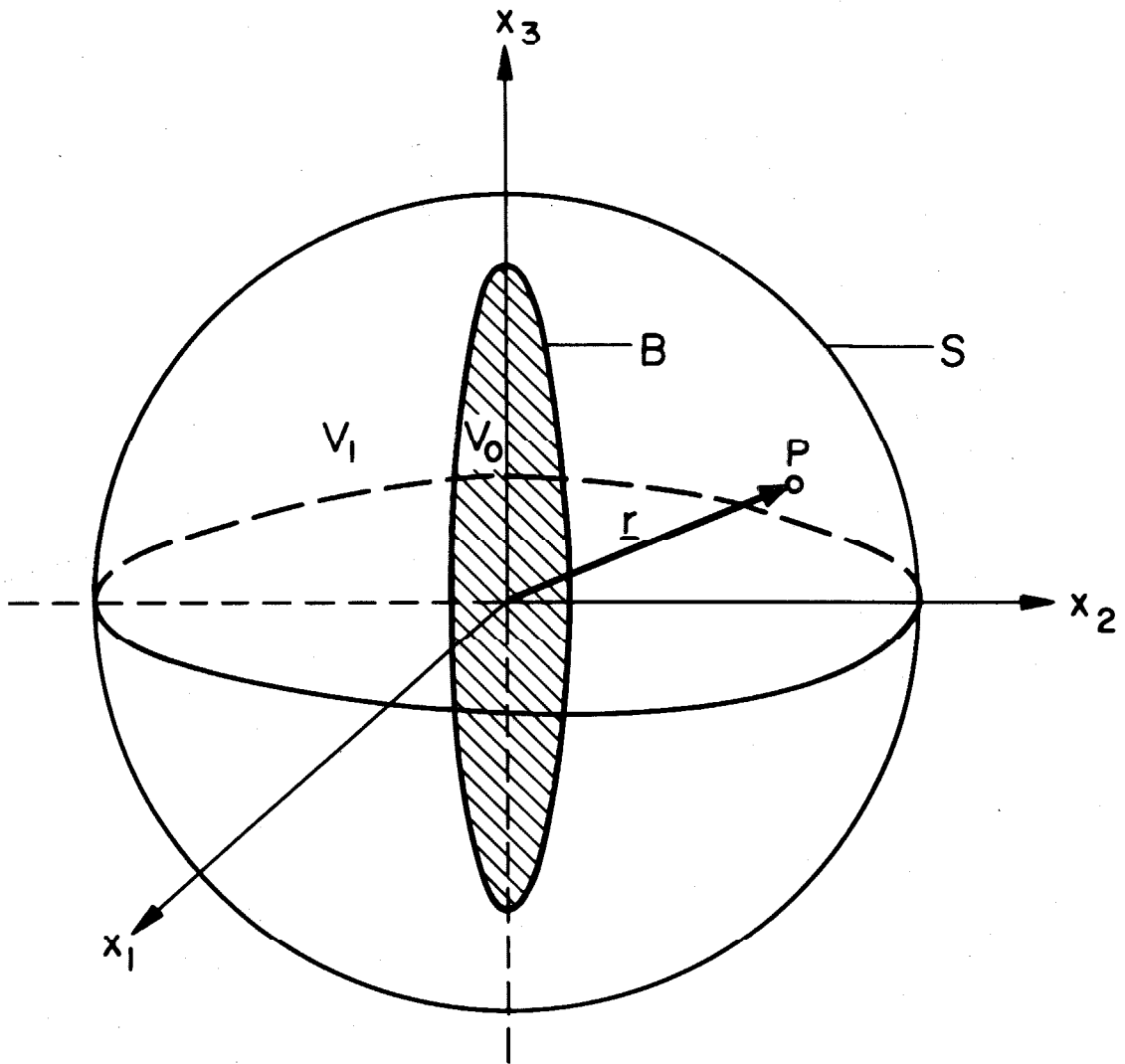


Fig. 6

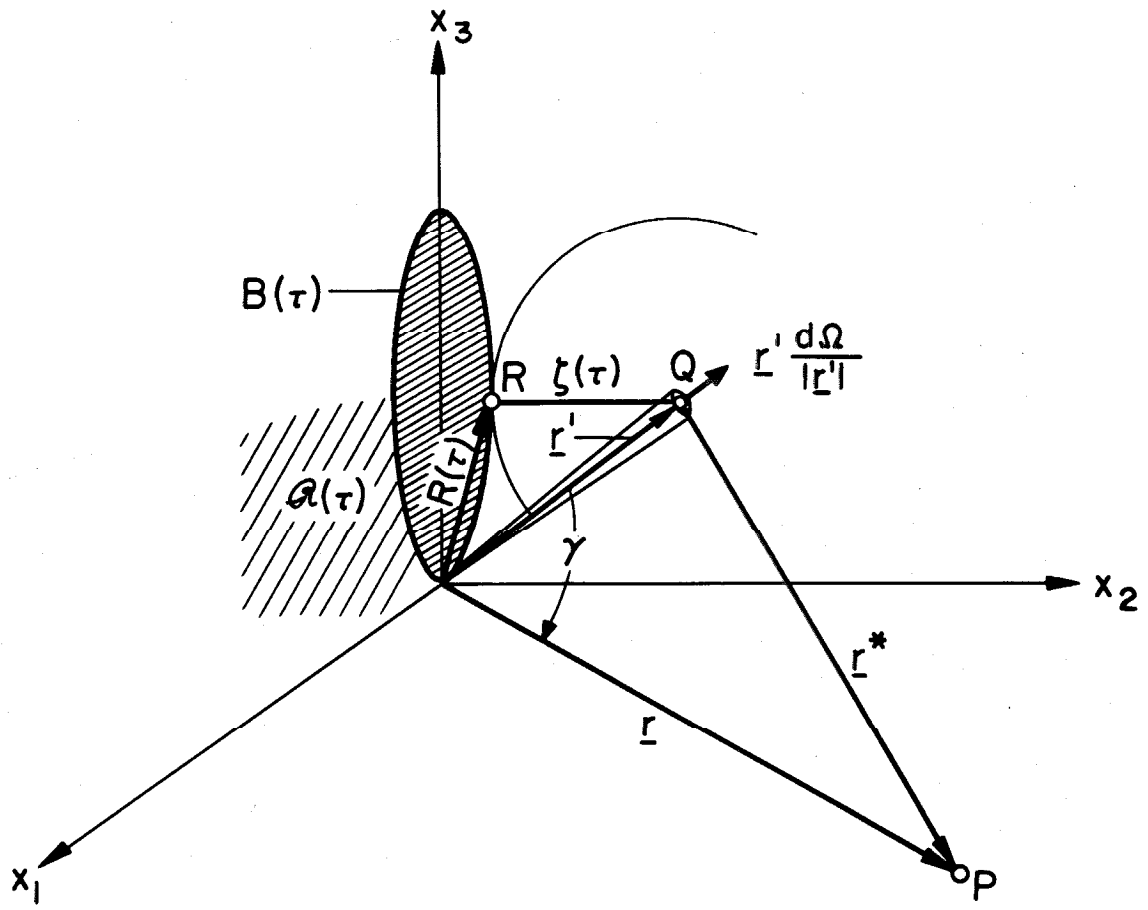


Fig. 7

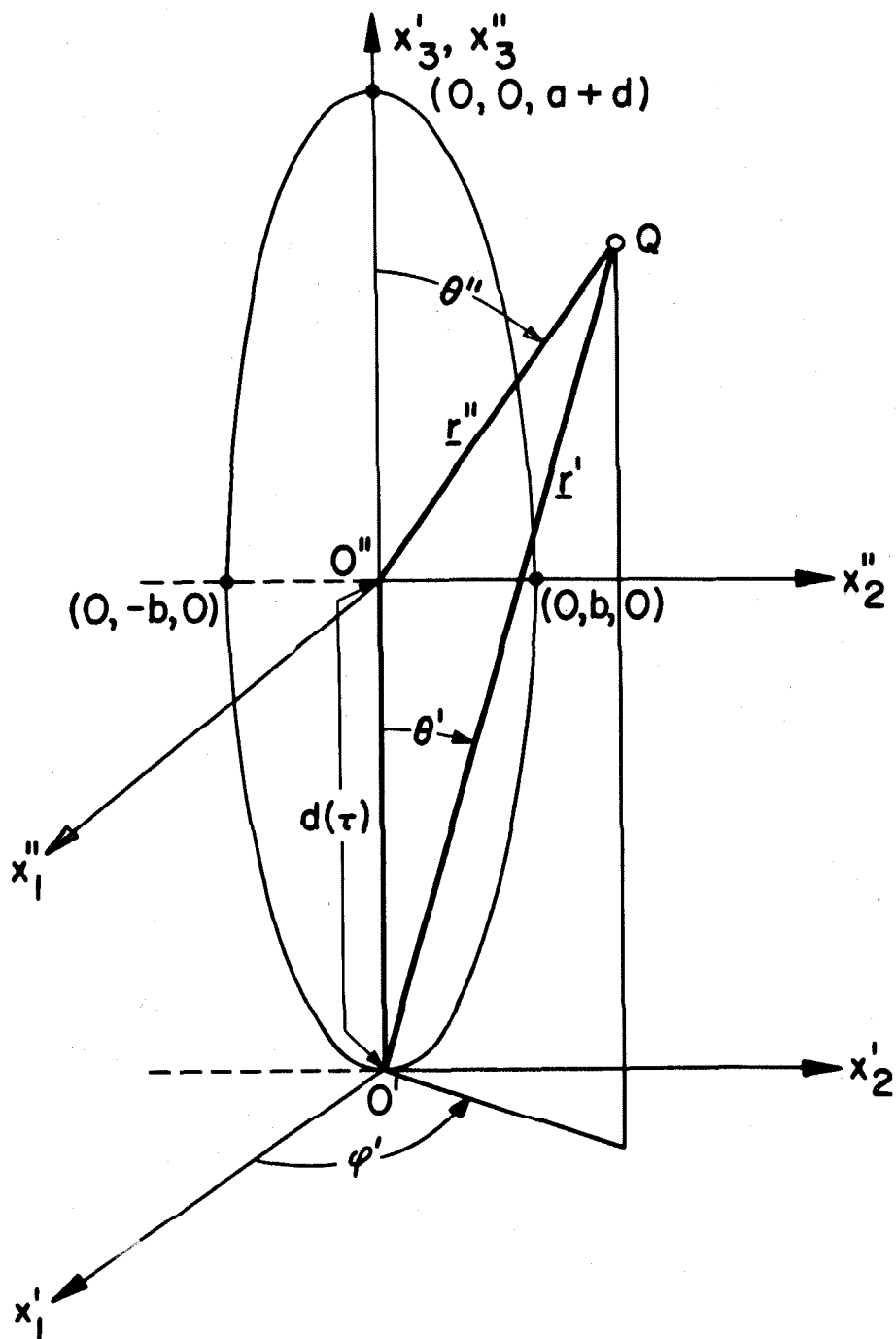


Fig. 8

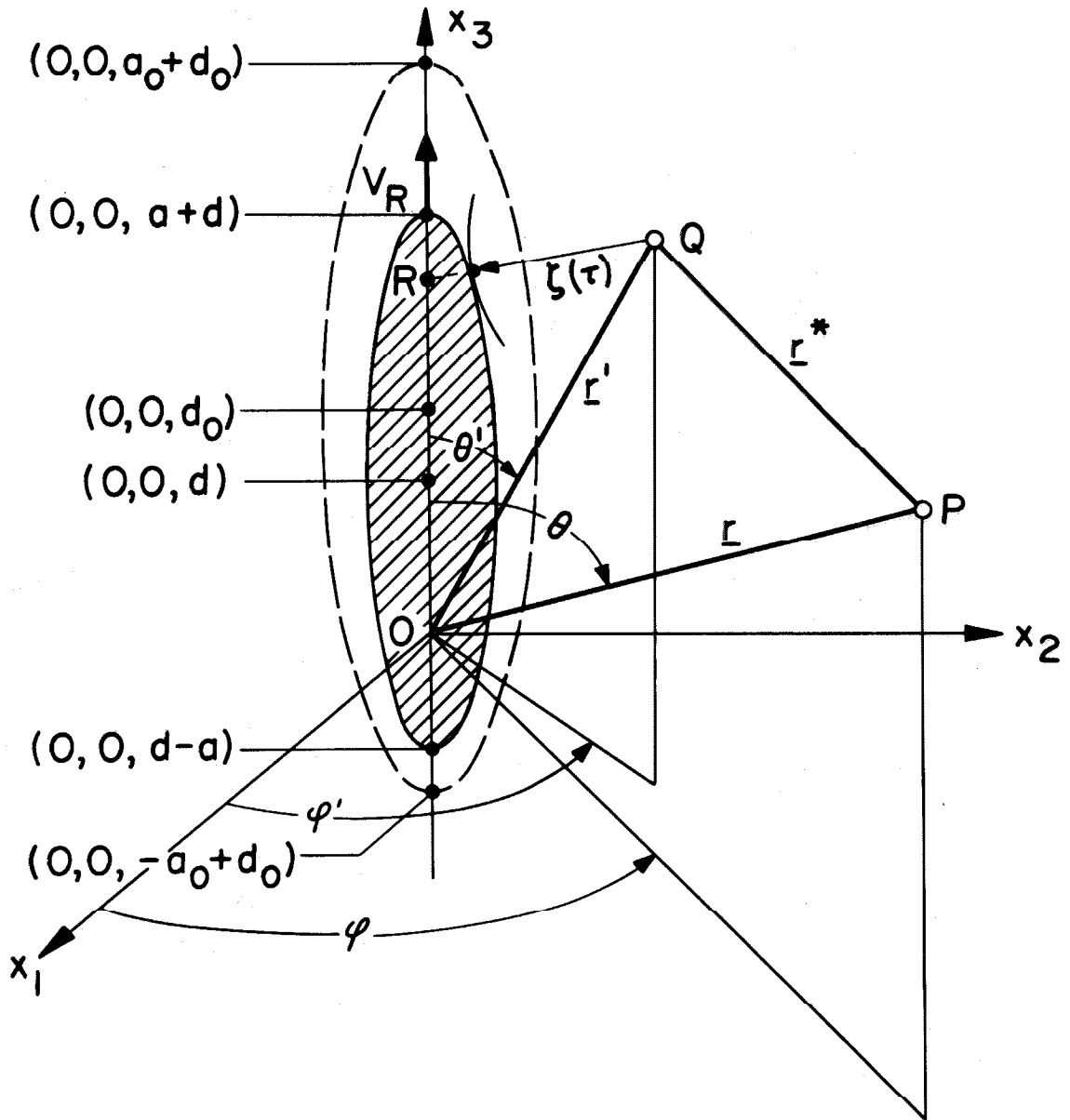
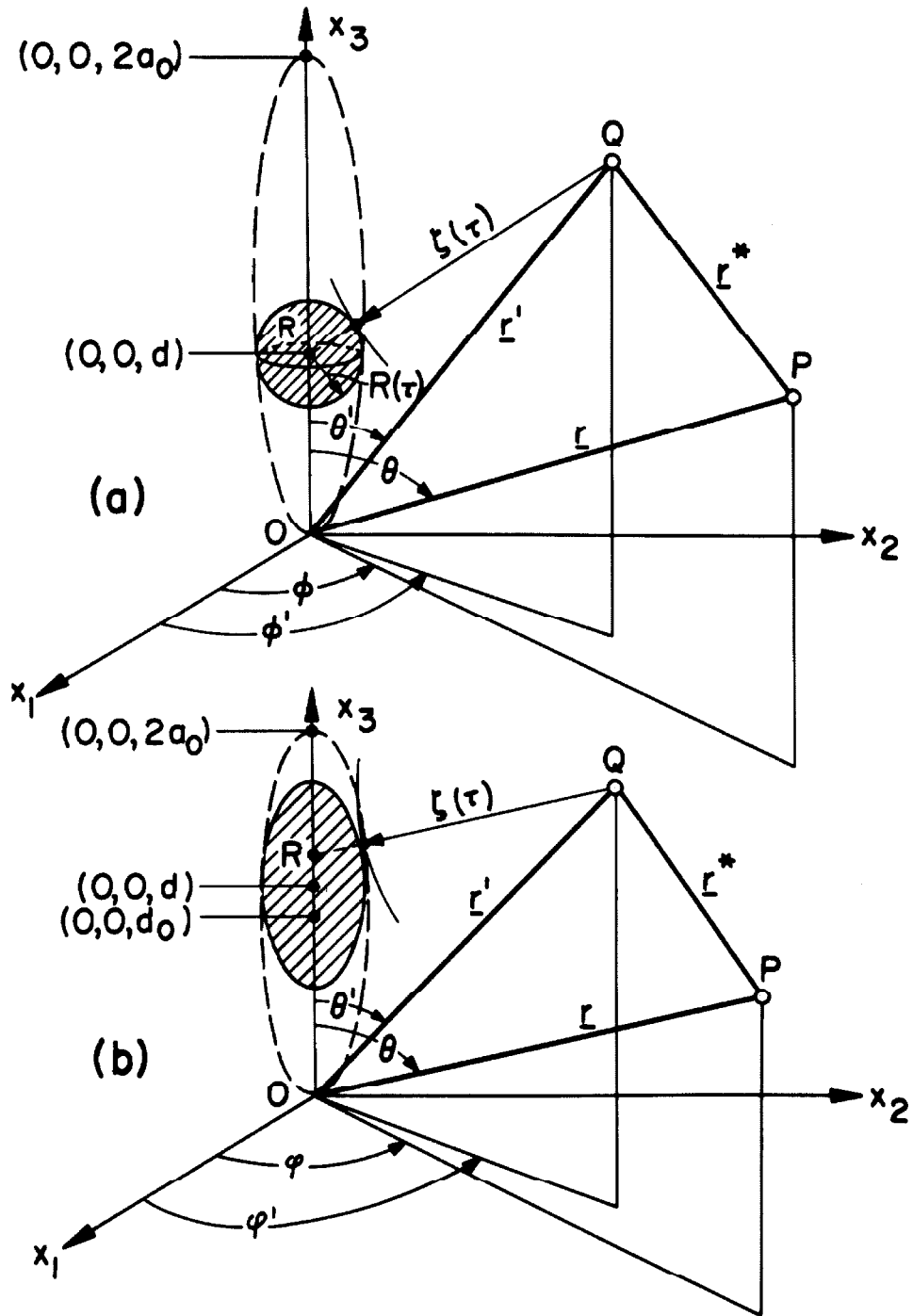


Fig. 9



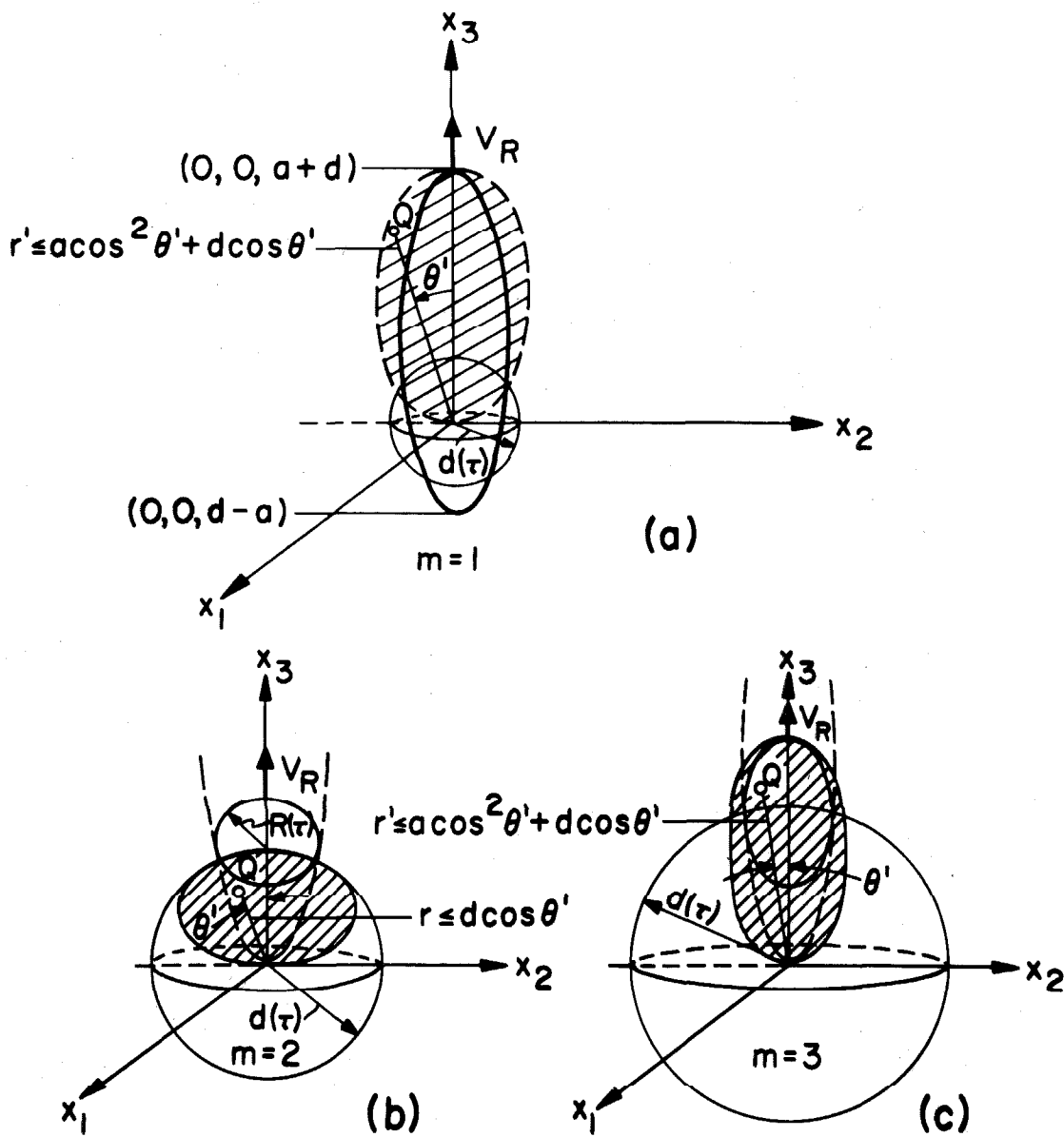


Fig. II

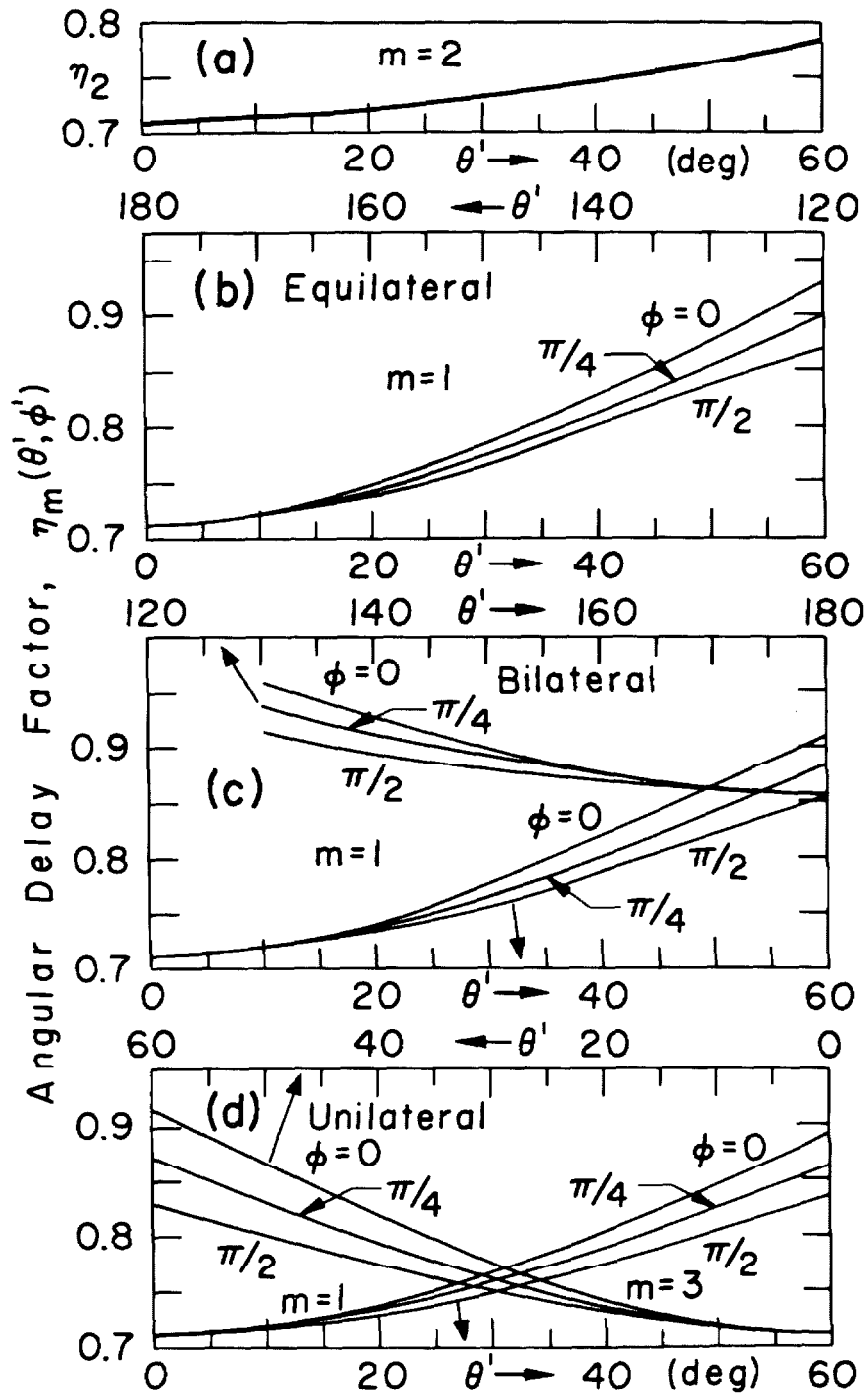


Fig. 12

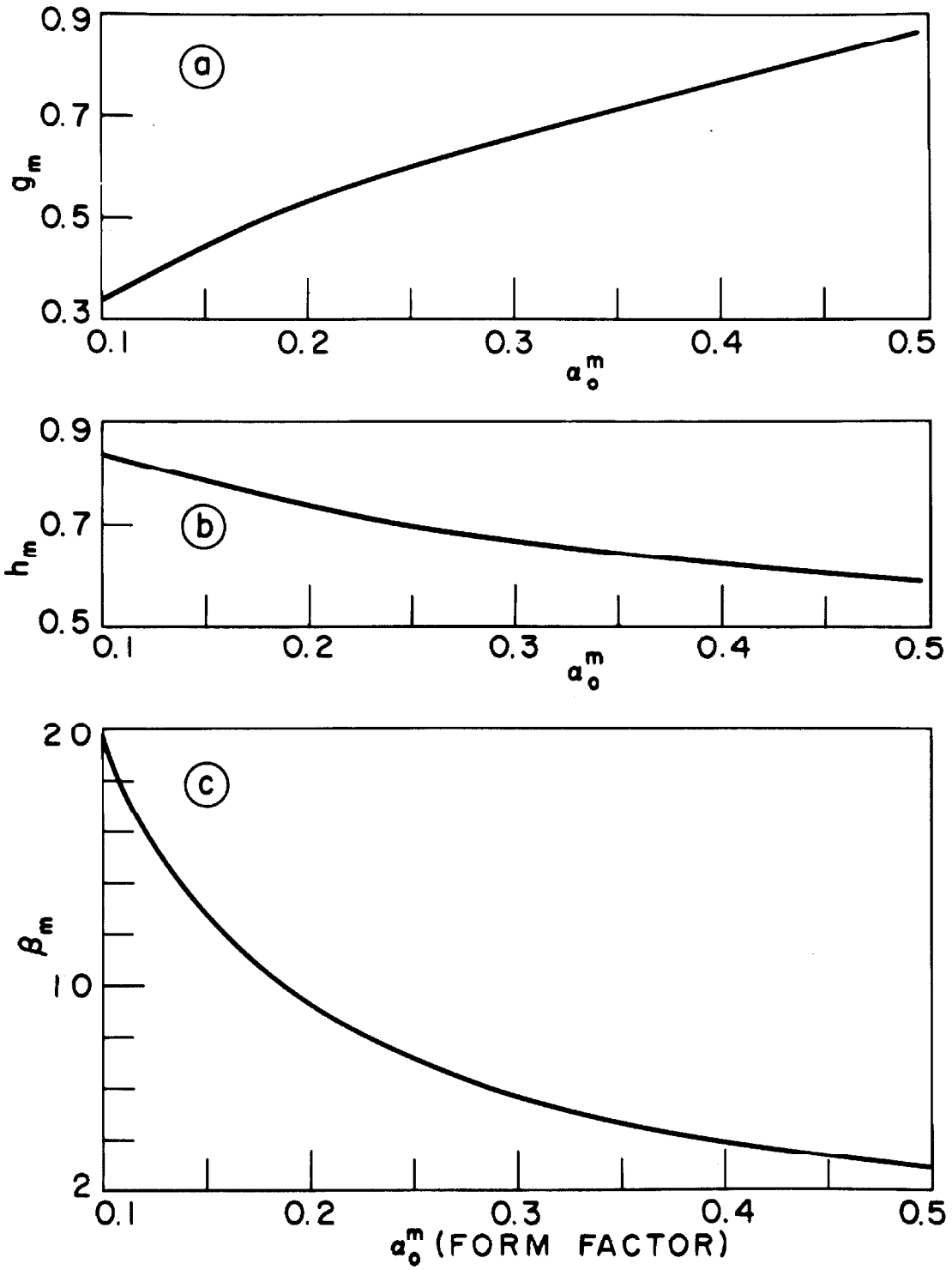


Fig. 13

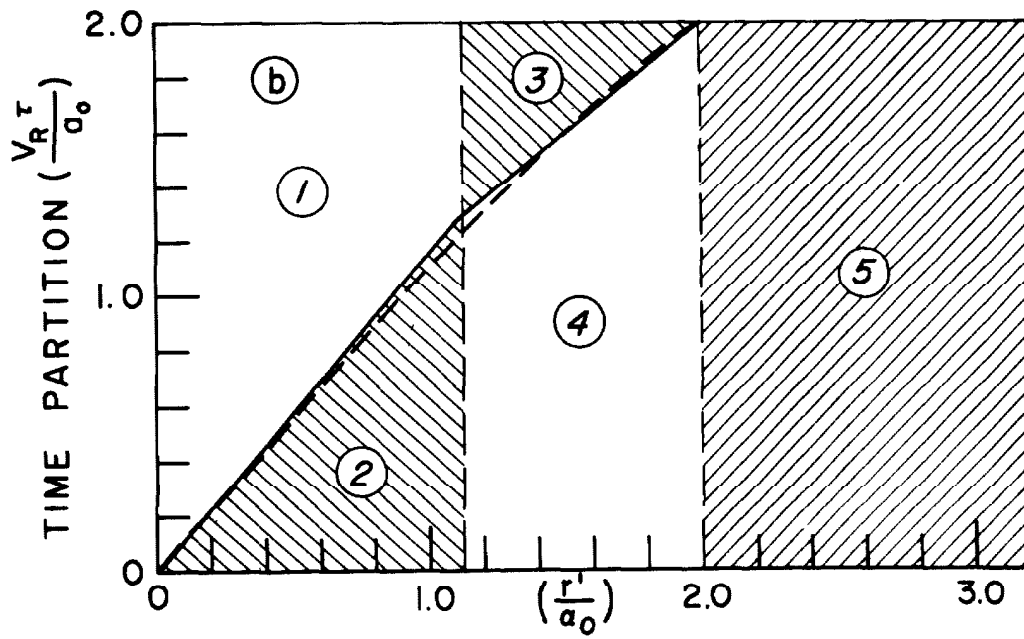
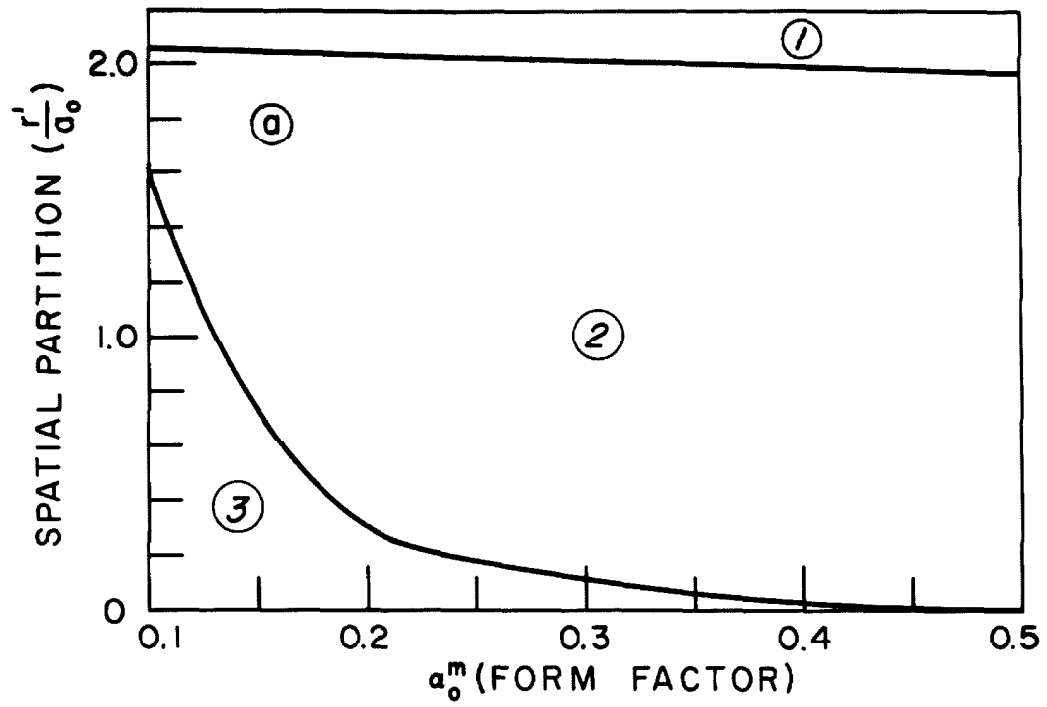


Fig. 14

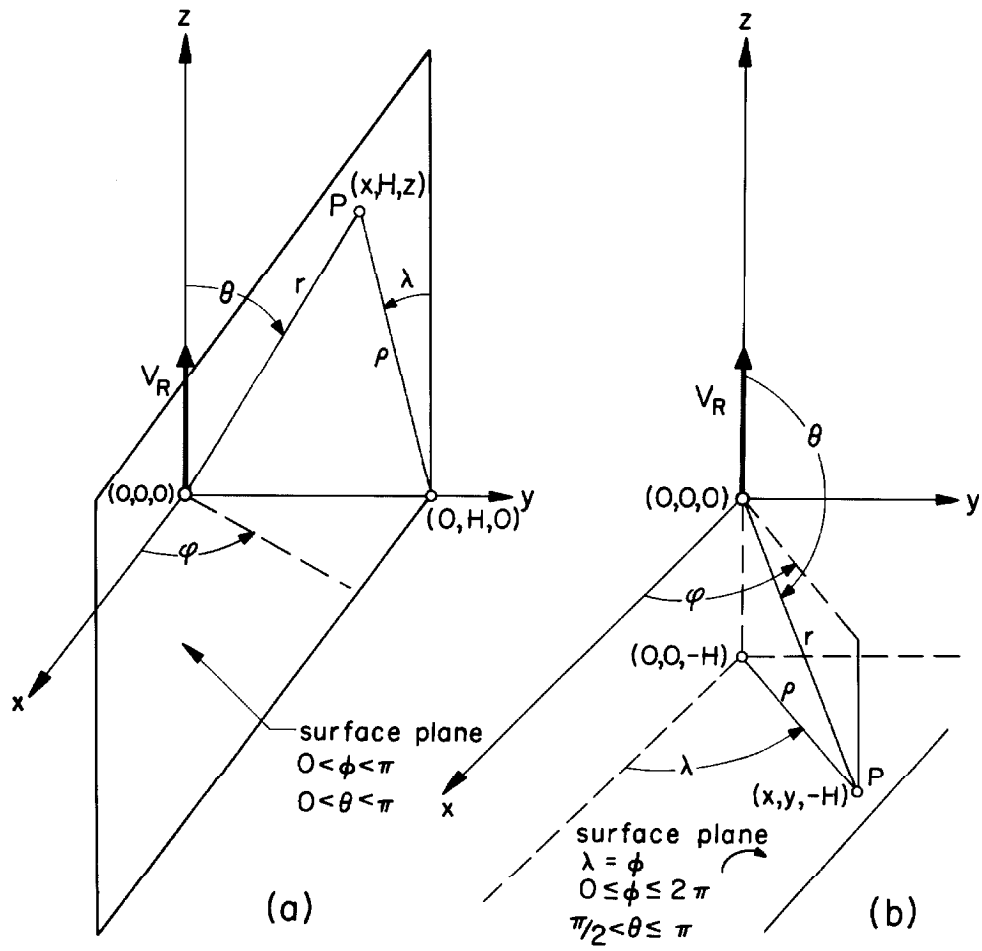


Fig. 16

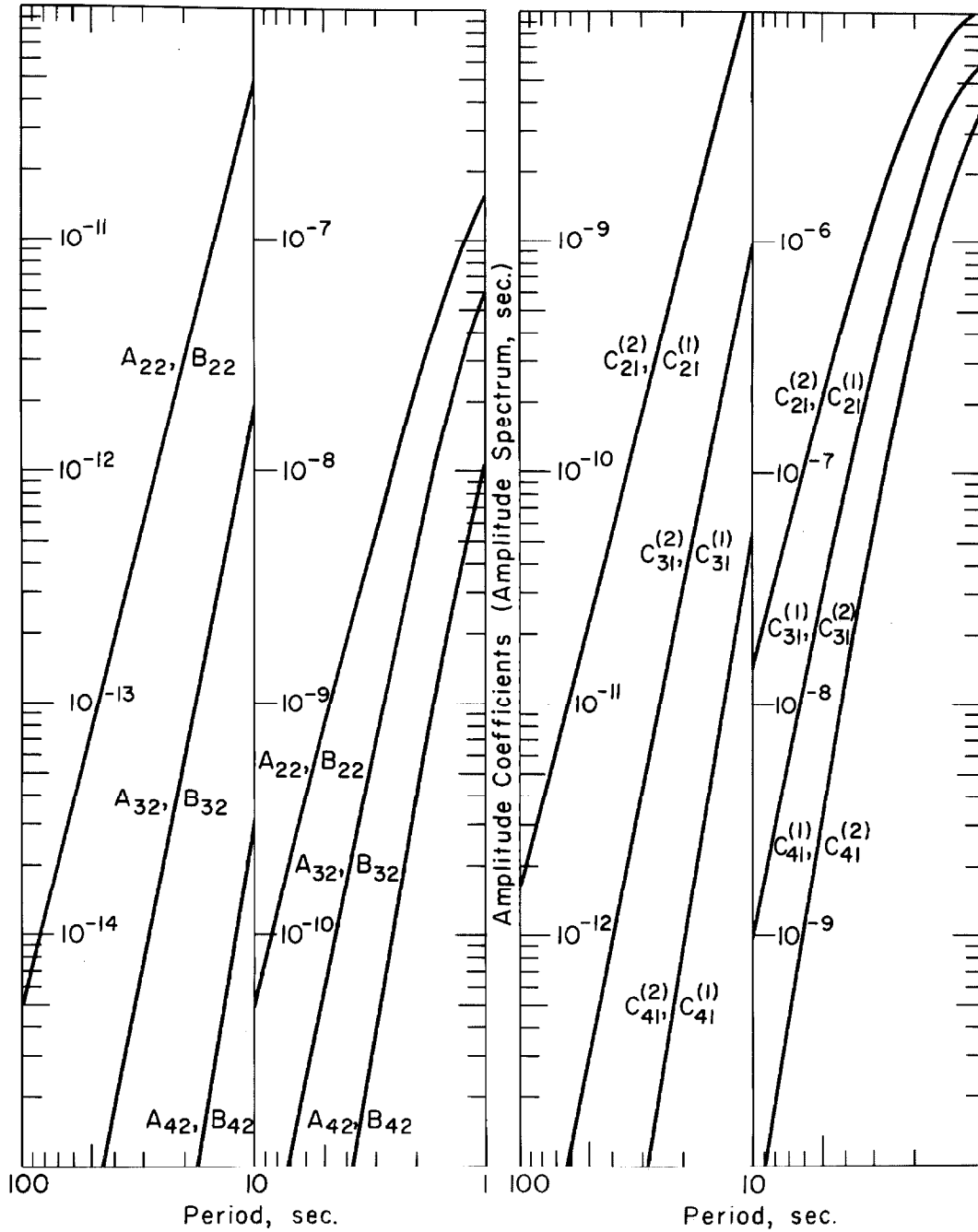


Fig. 17

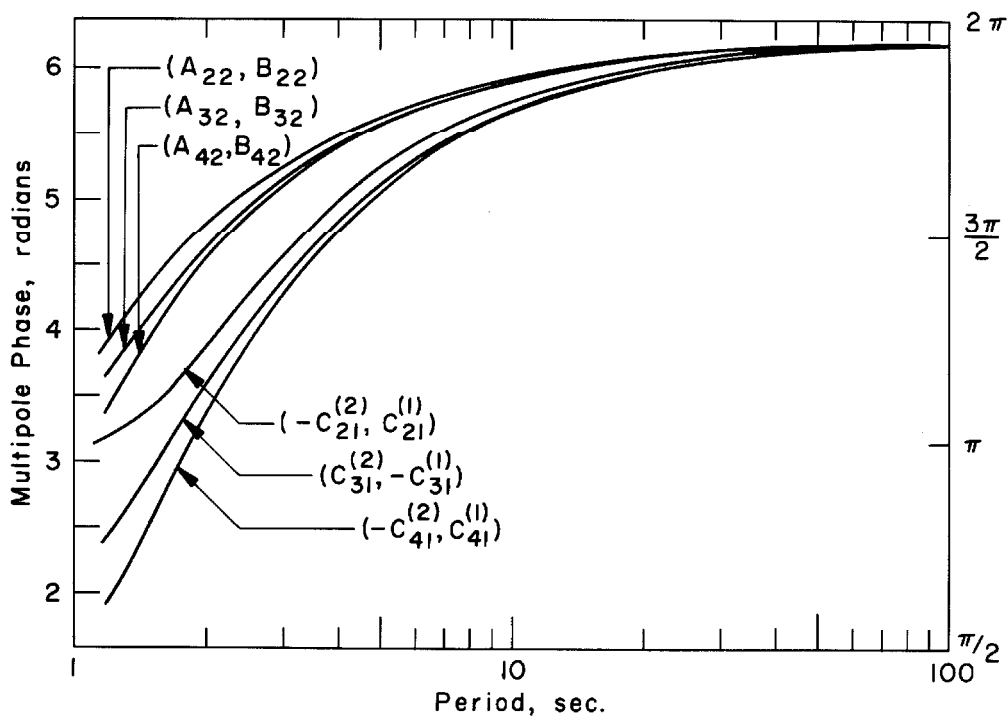


Fig. 18

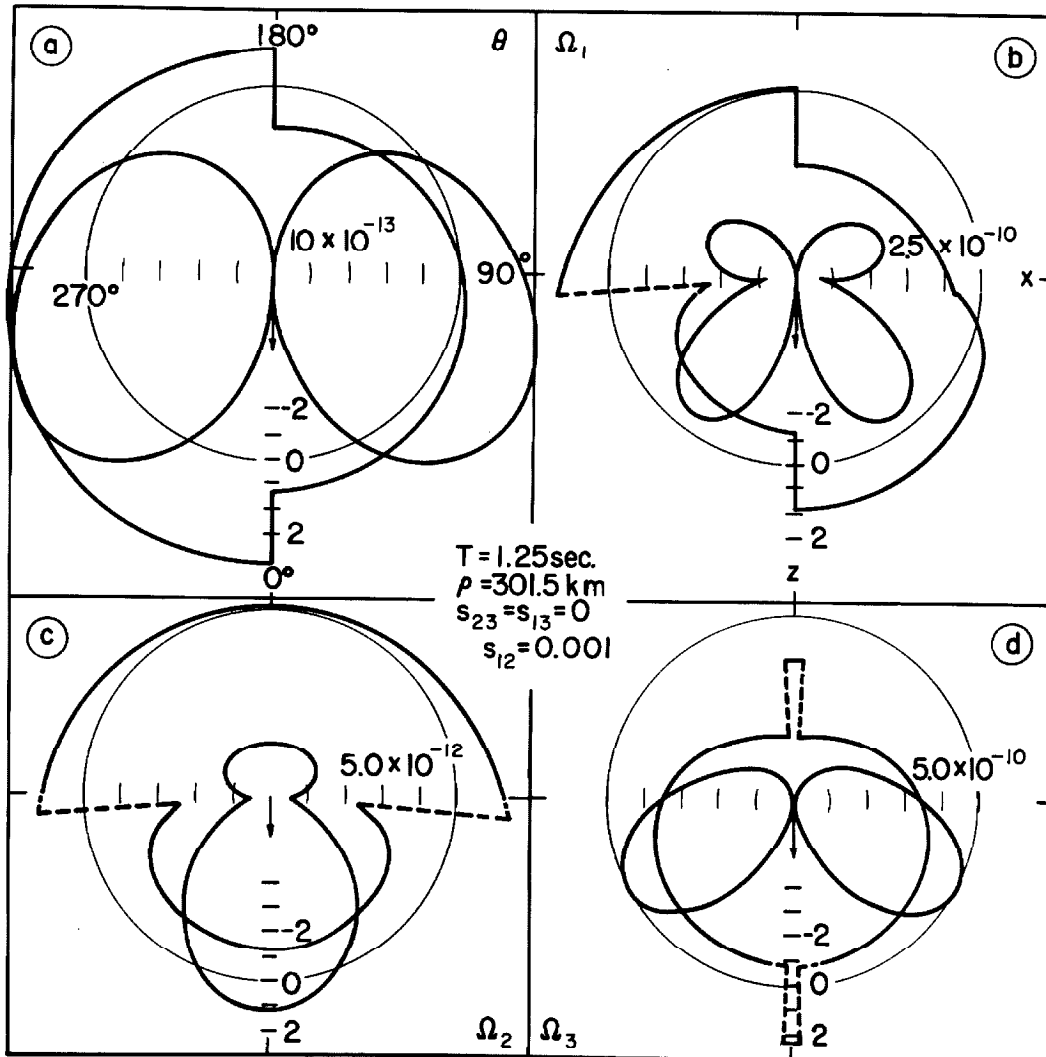


Fig. 15

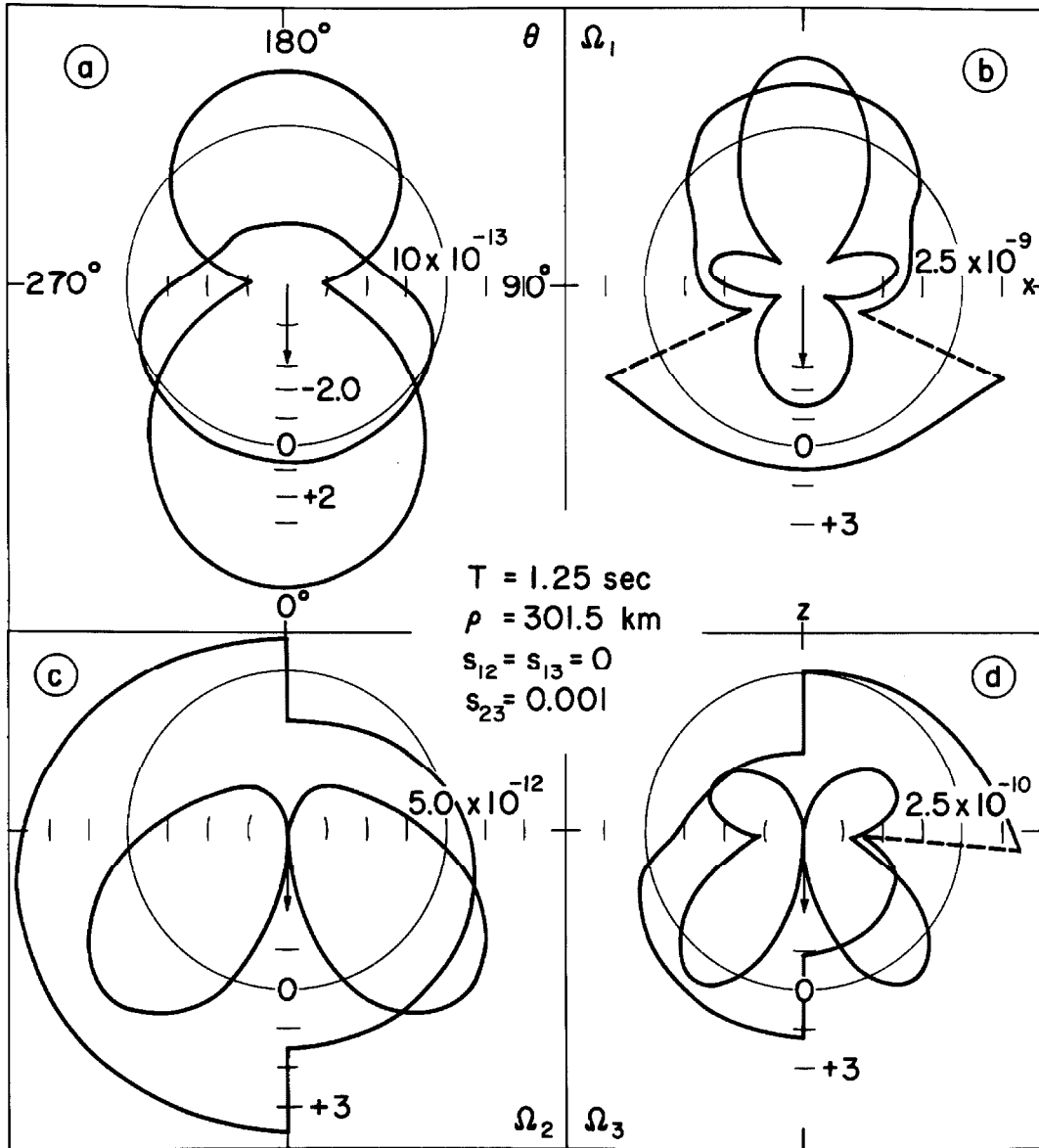


Fig. 20

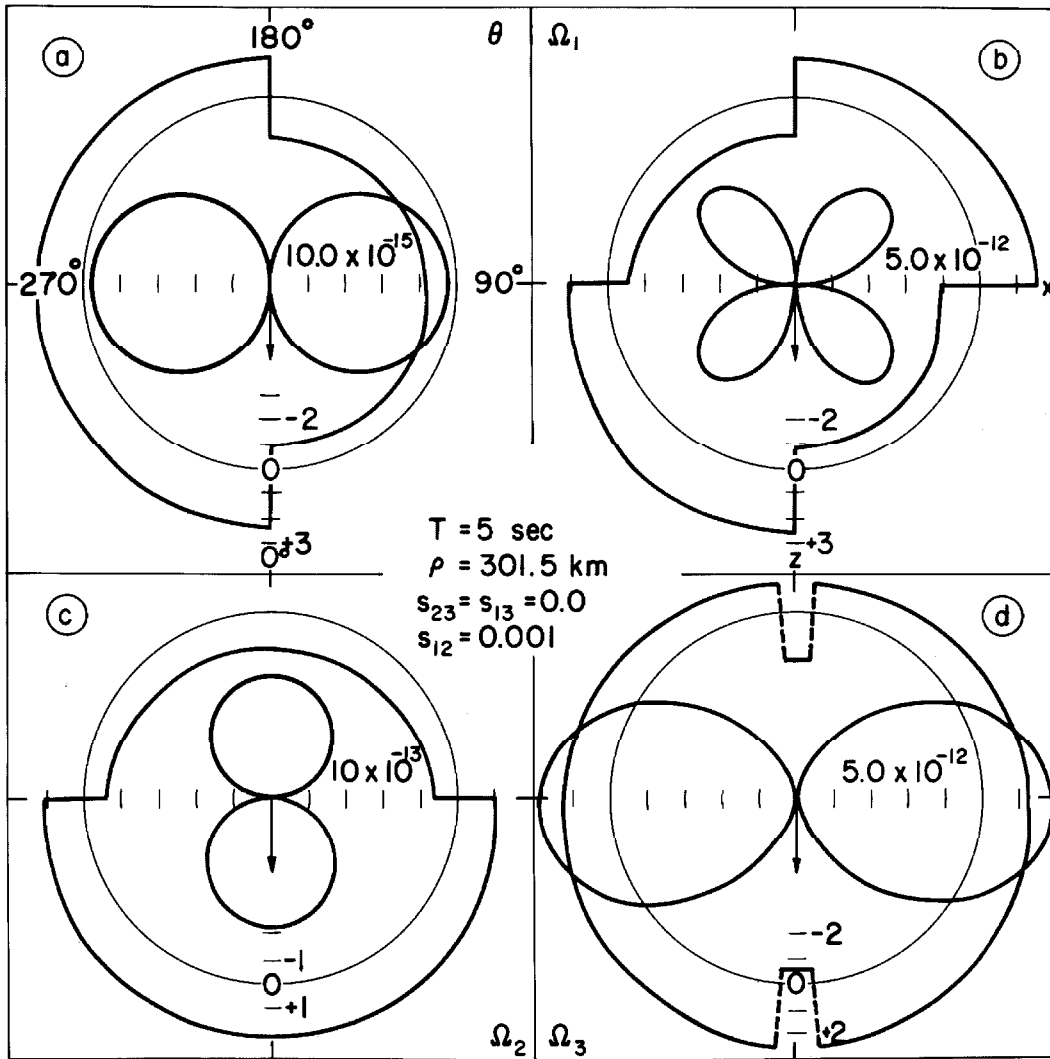


Fig. 22

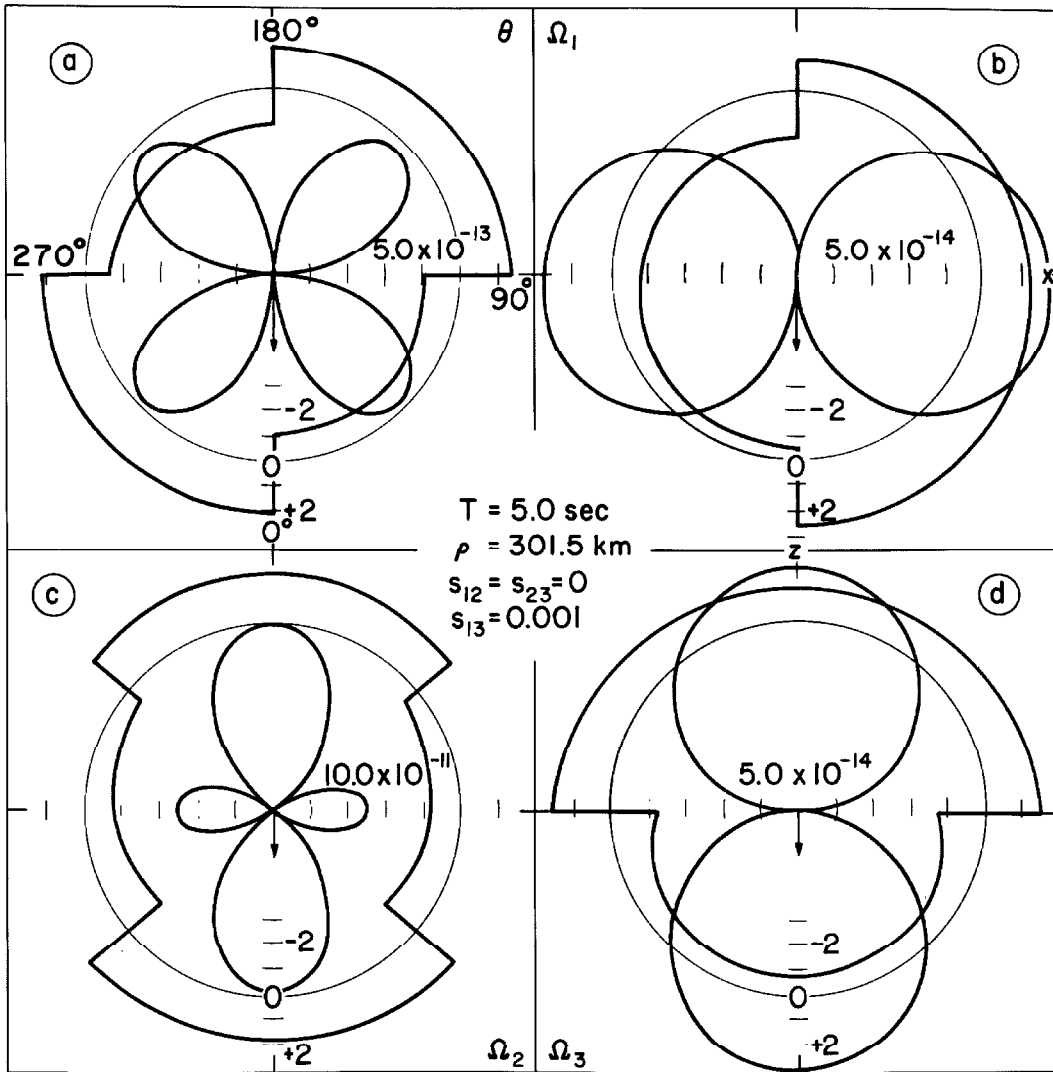


Fig. 23

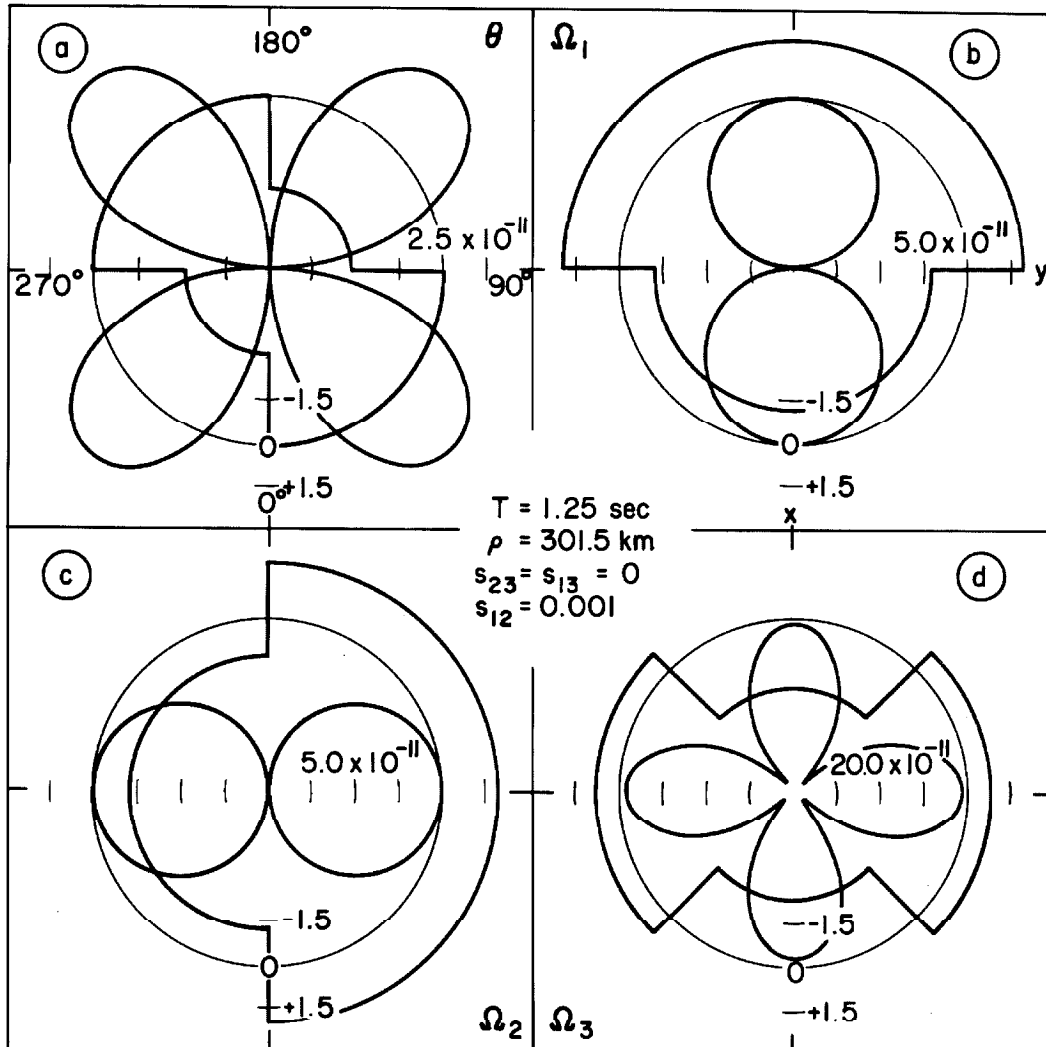


Fig. 24

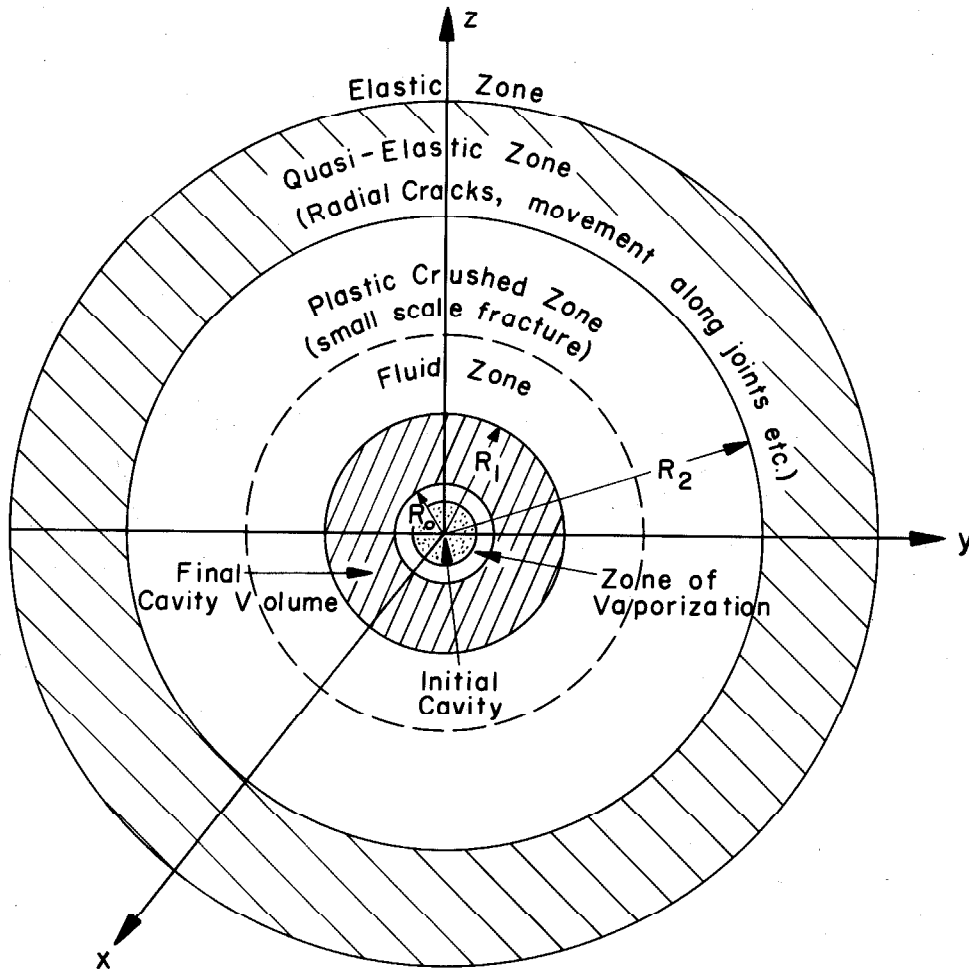


Fig. 25

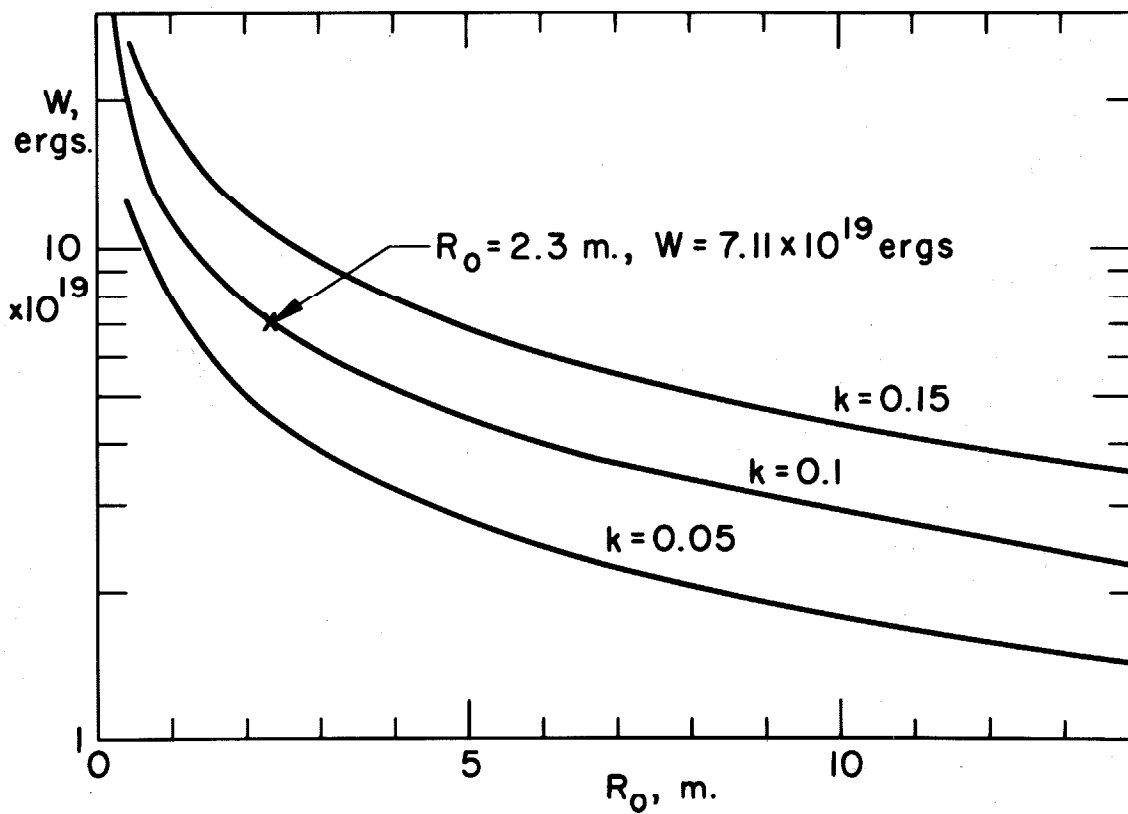


Fig. 26

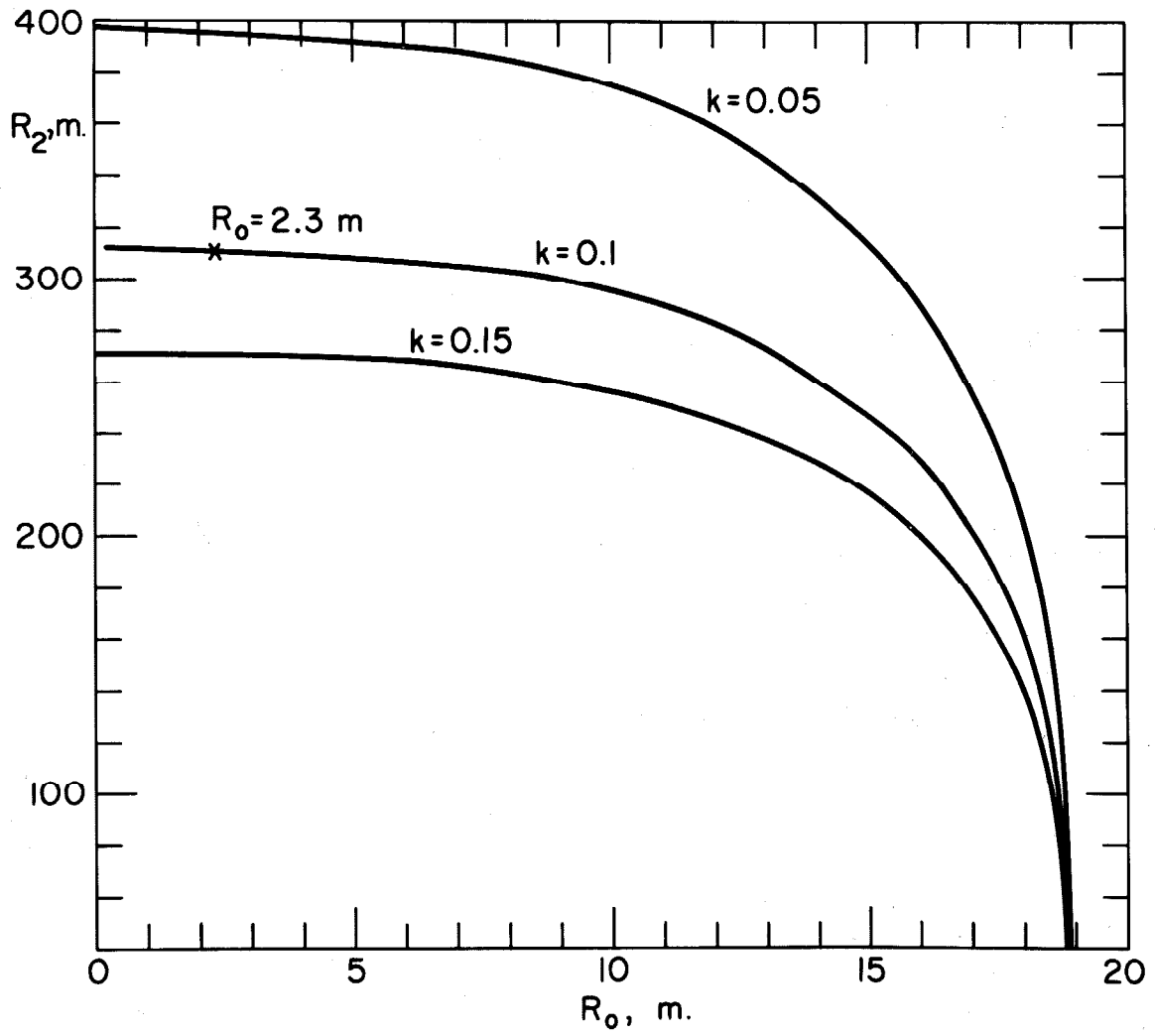


Fig. 27

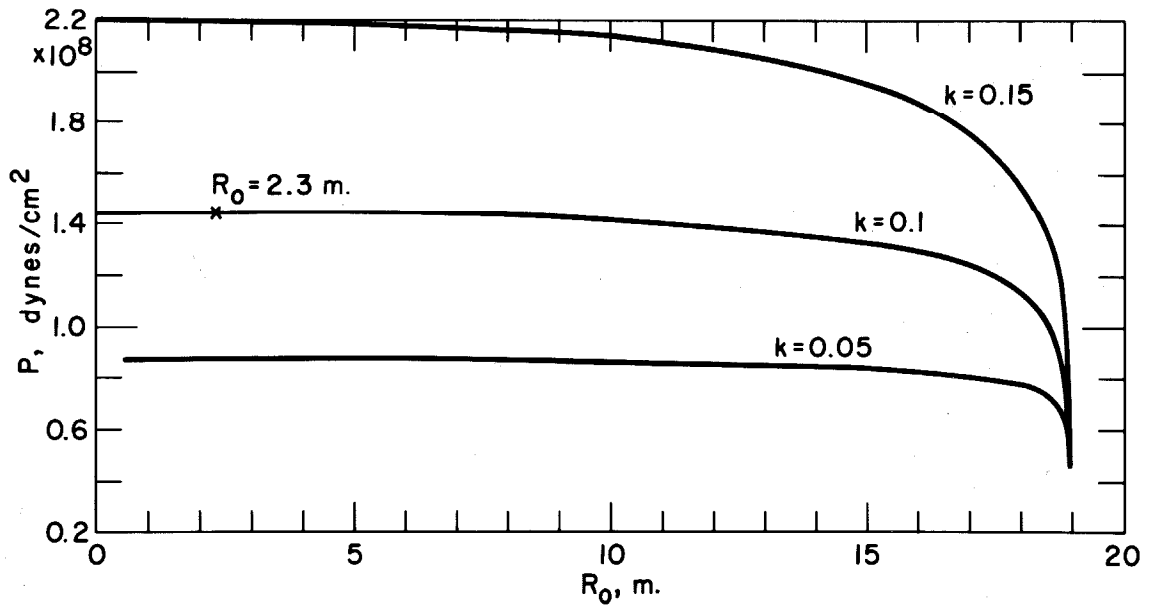


Fig. 28

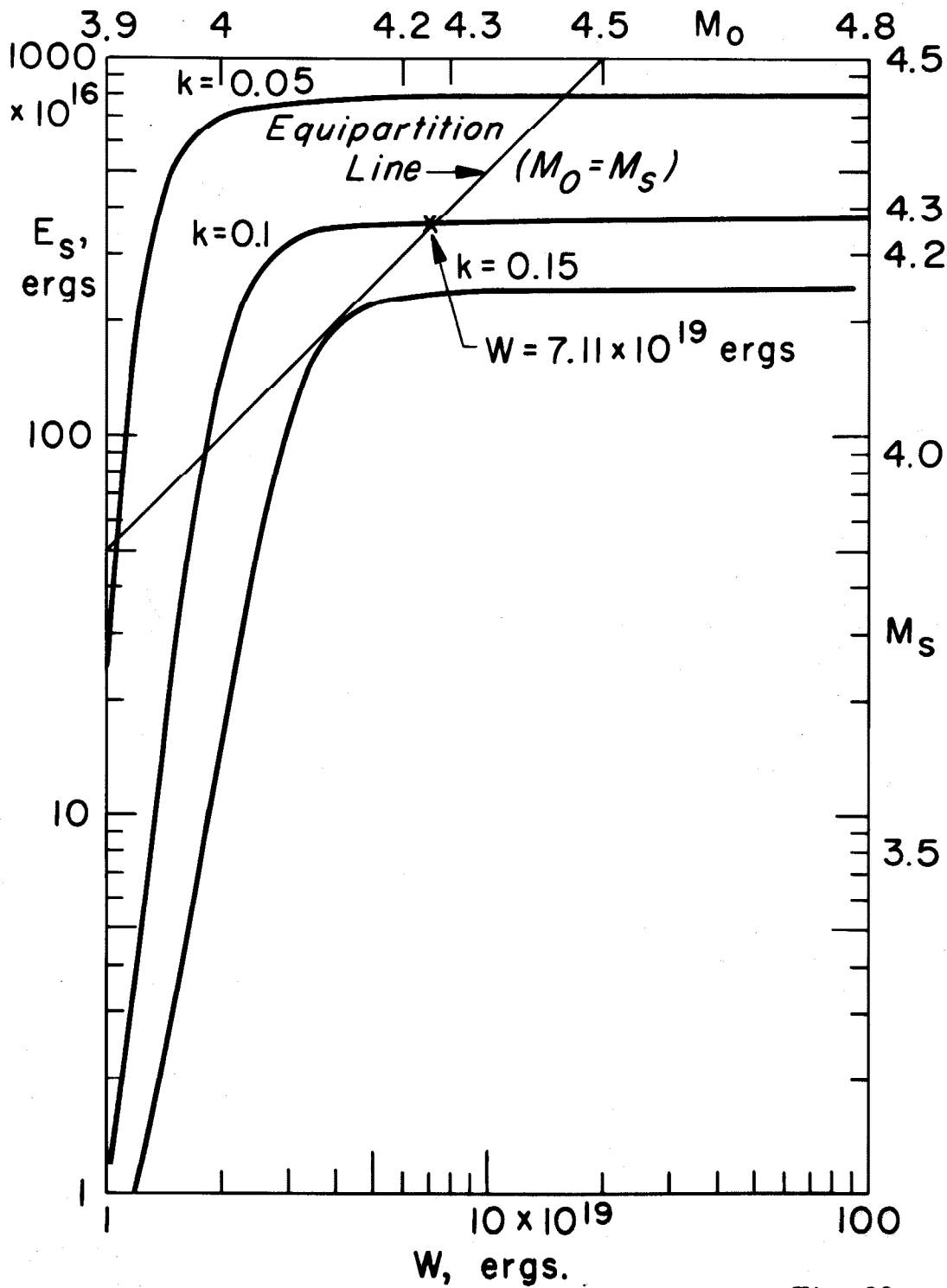


Fig. 29

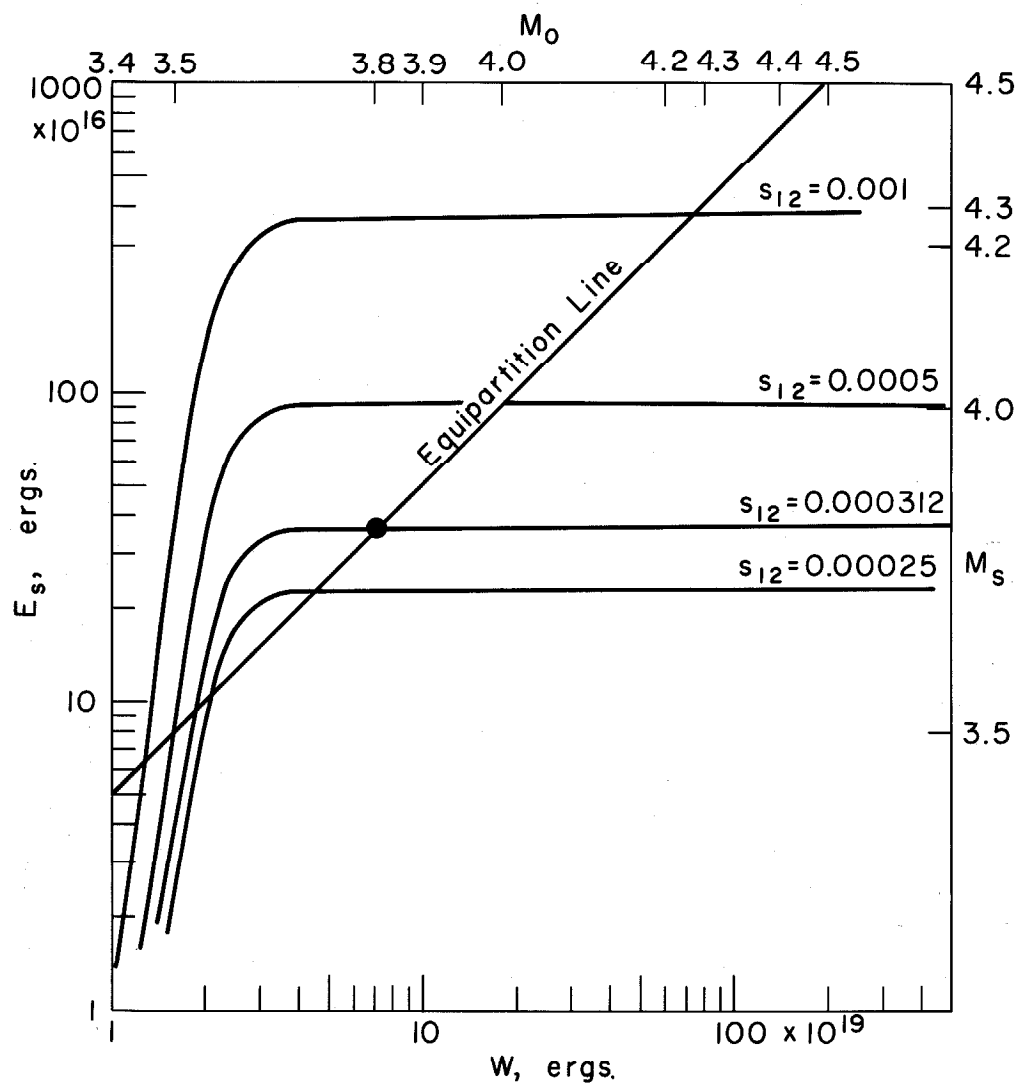


Fig. 30

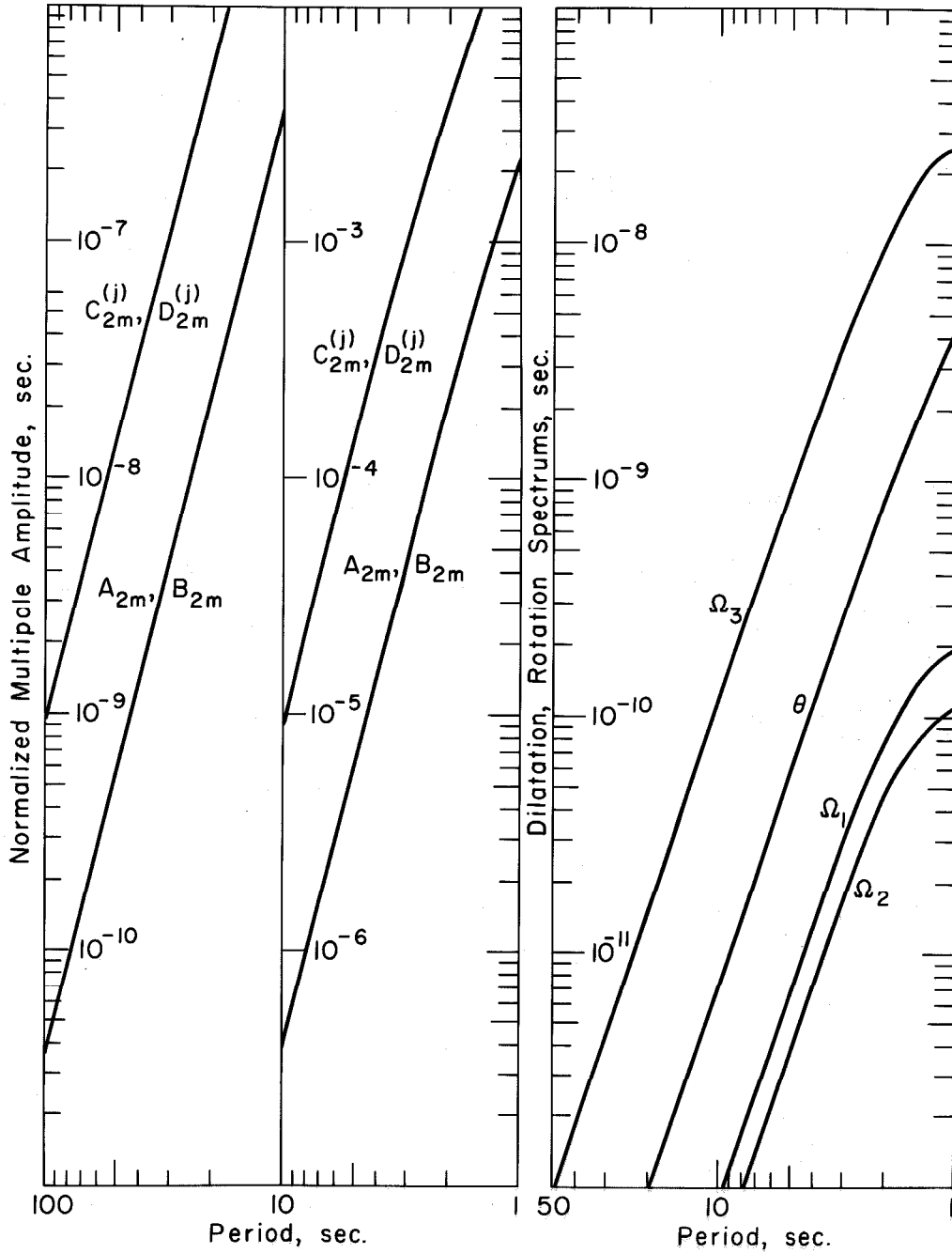


Fig. 31

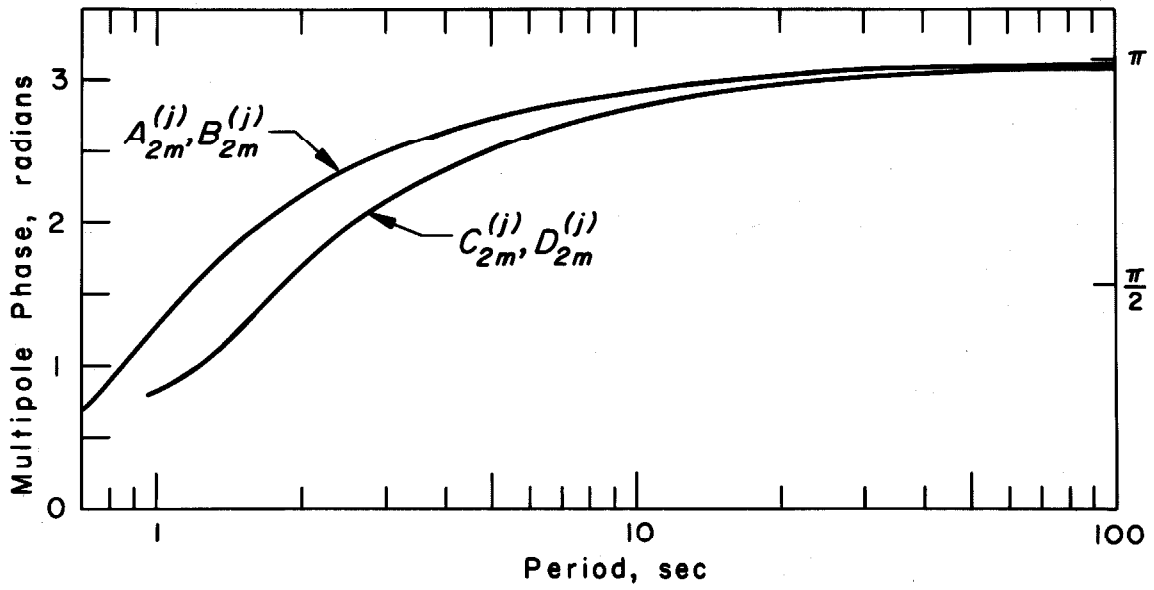


Fig. 32

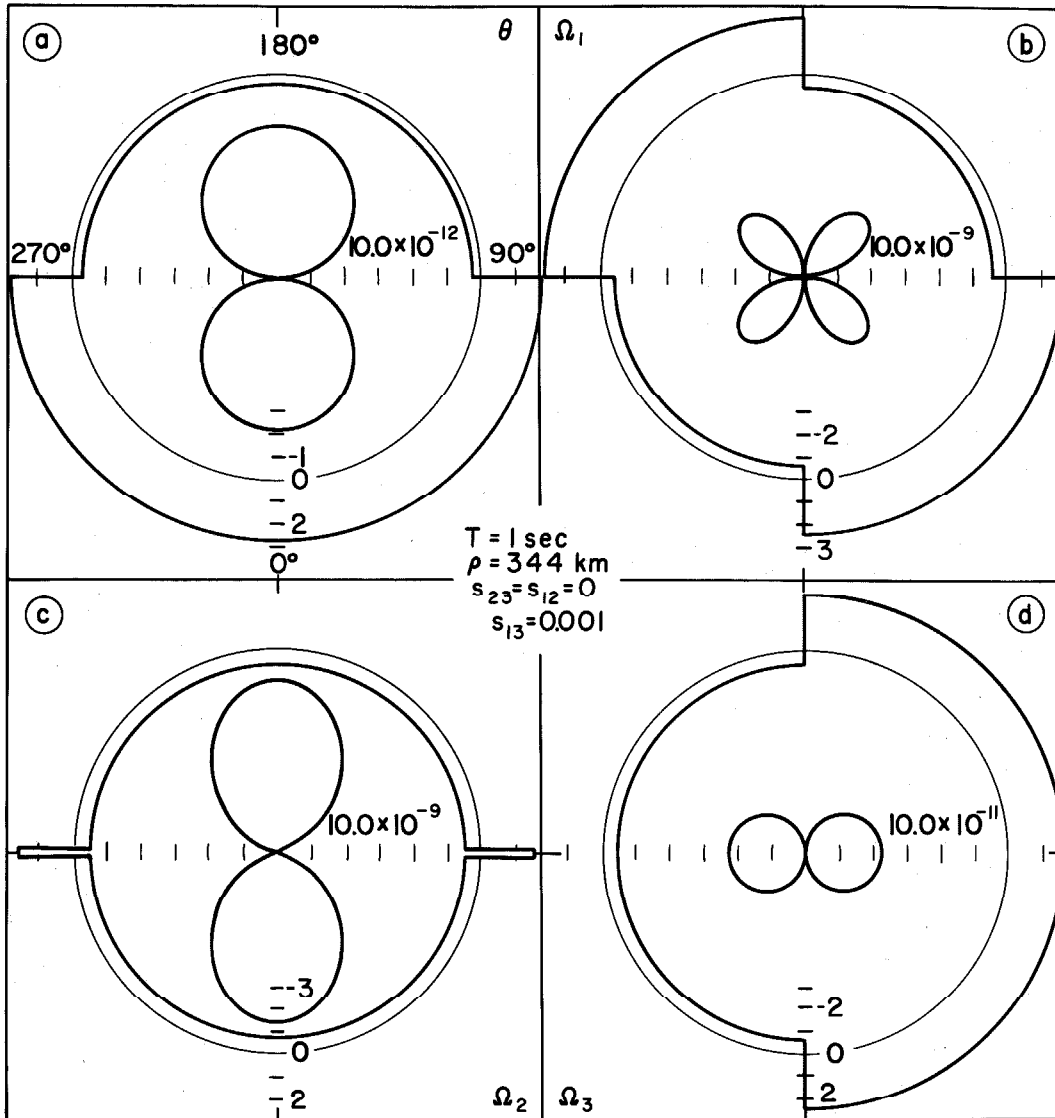


Fig. 33

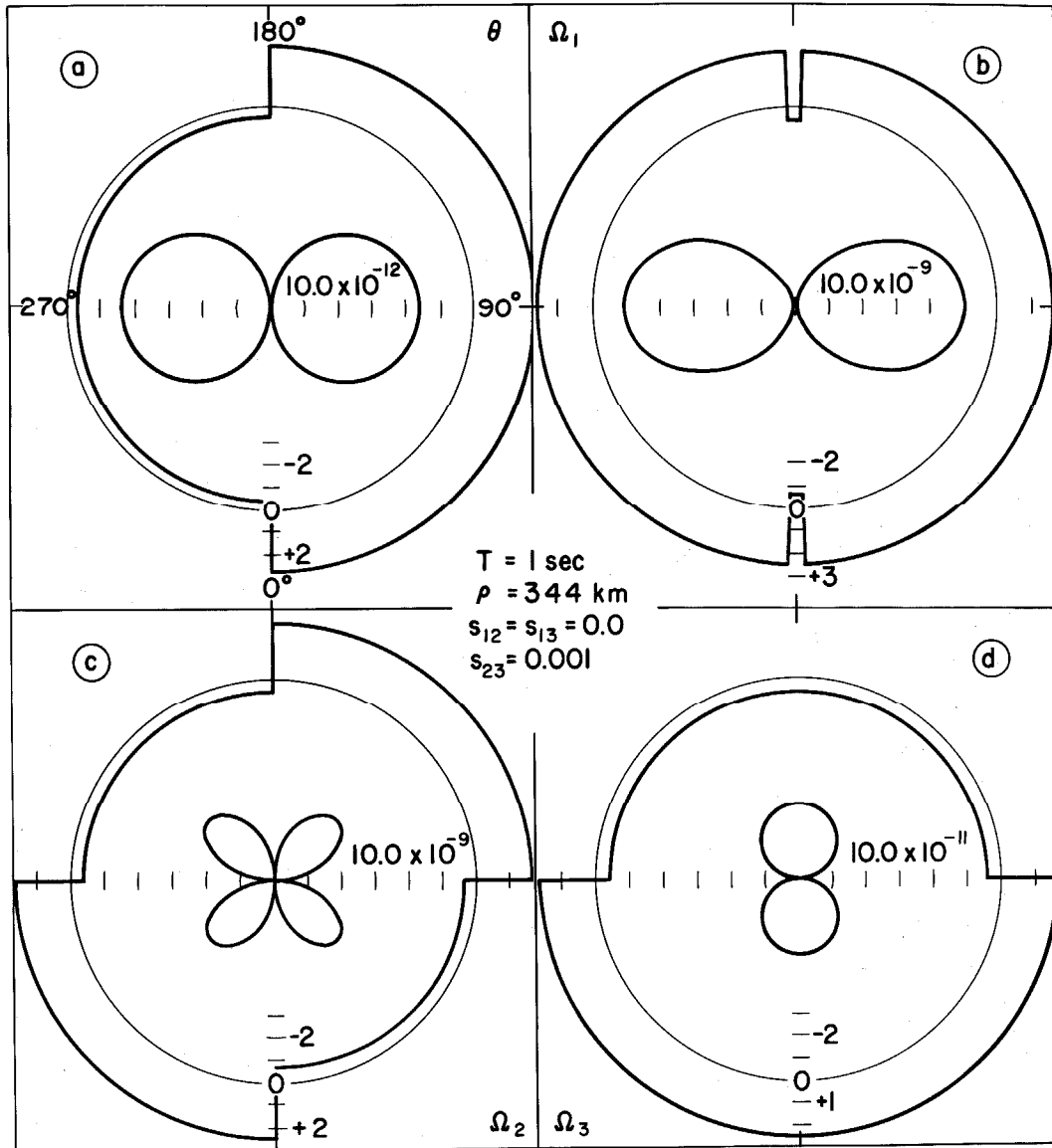


Fig. 34

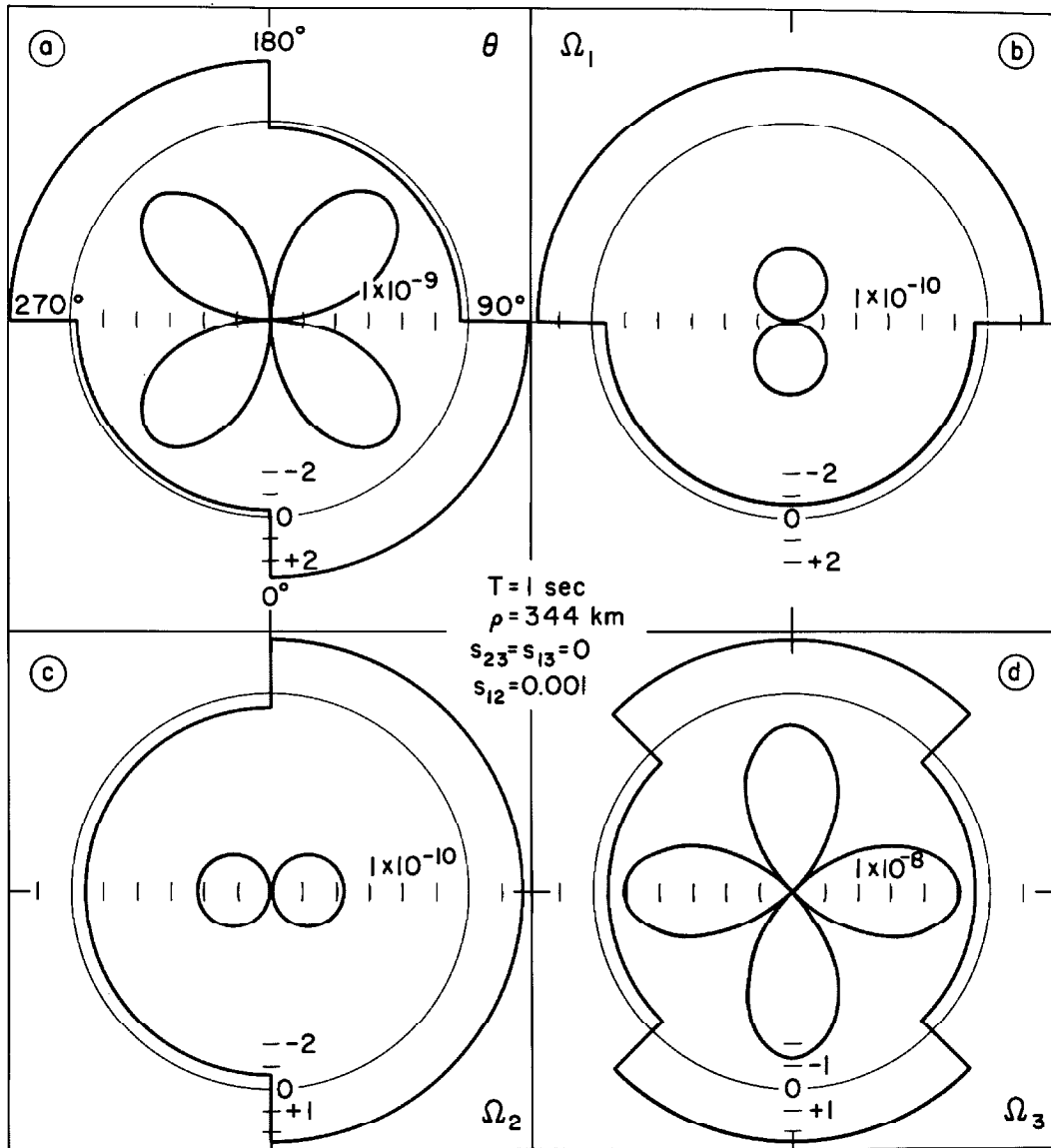


Fig. 35

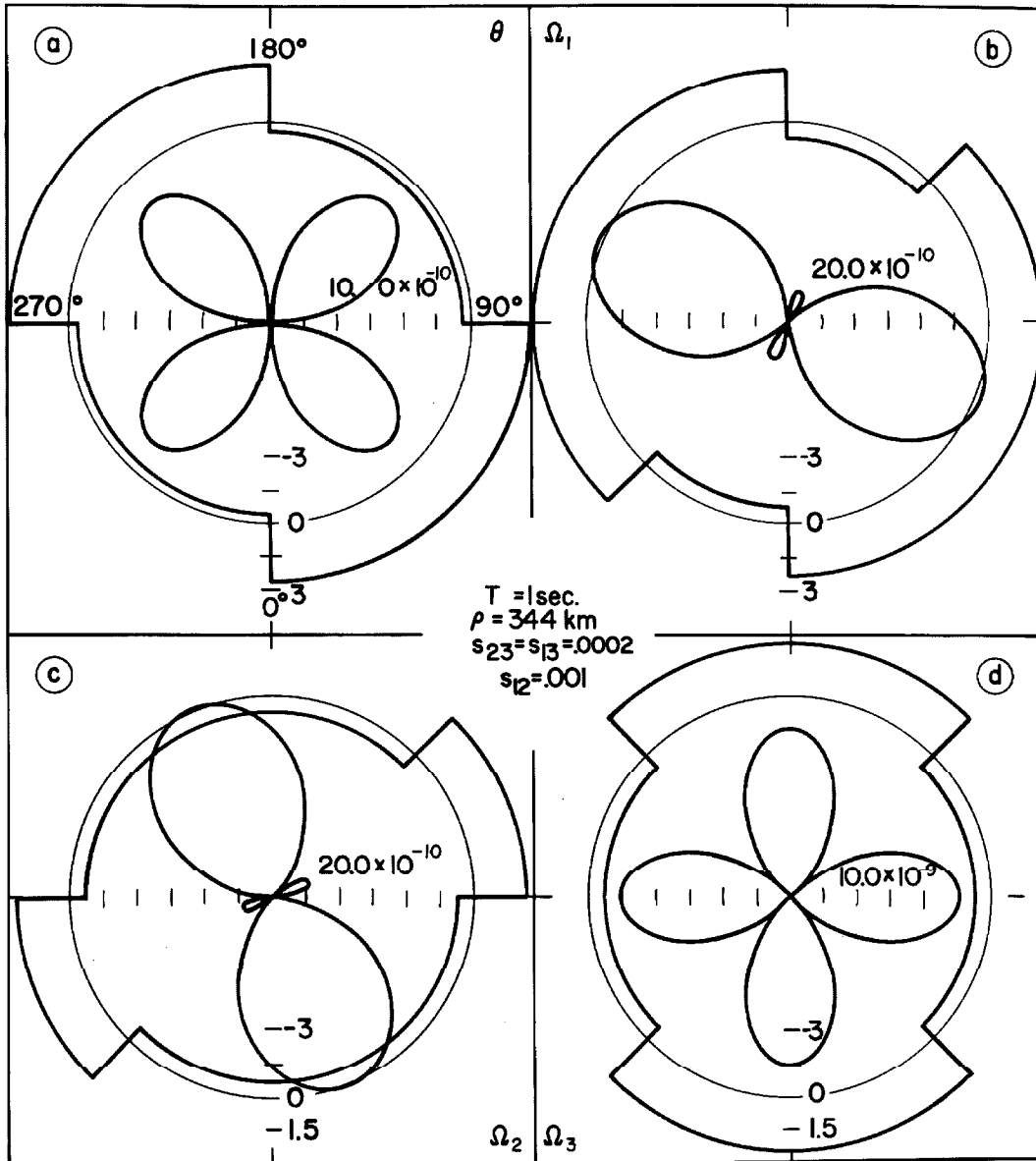


Fig. 36

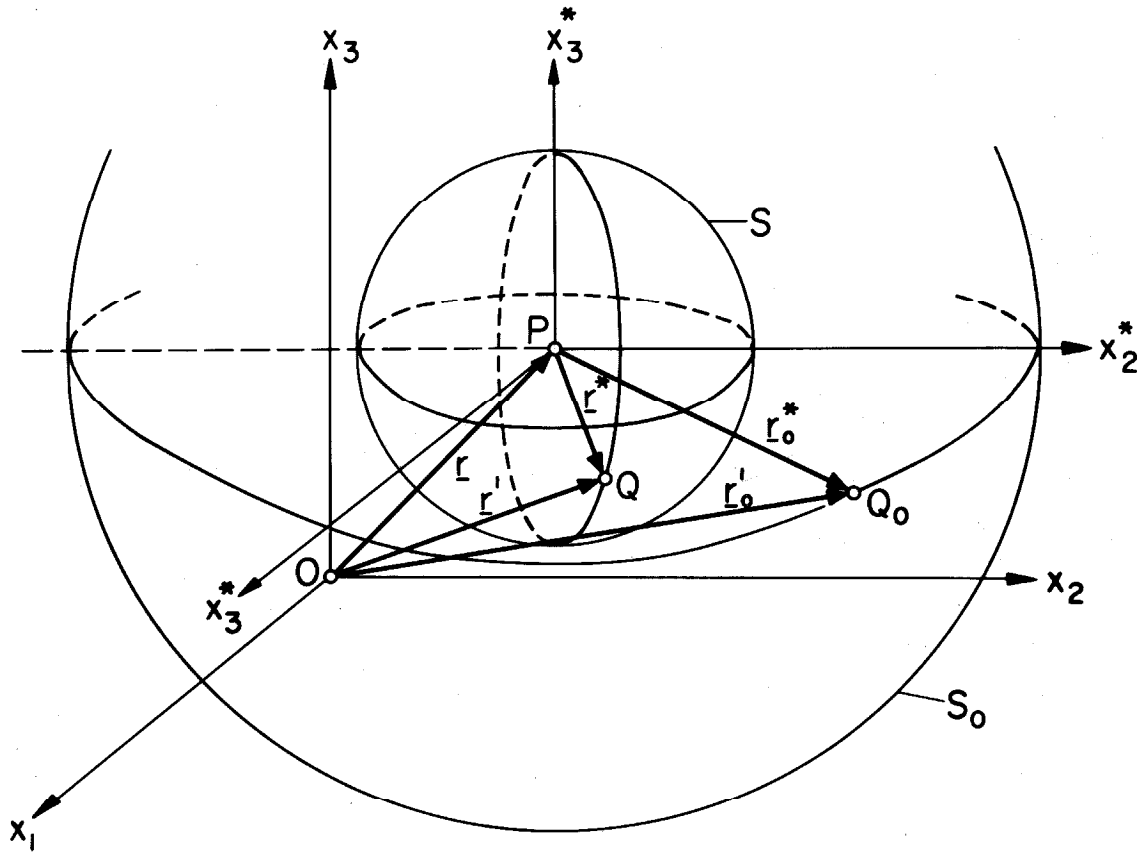


Fig. 37

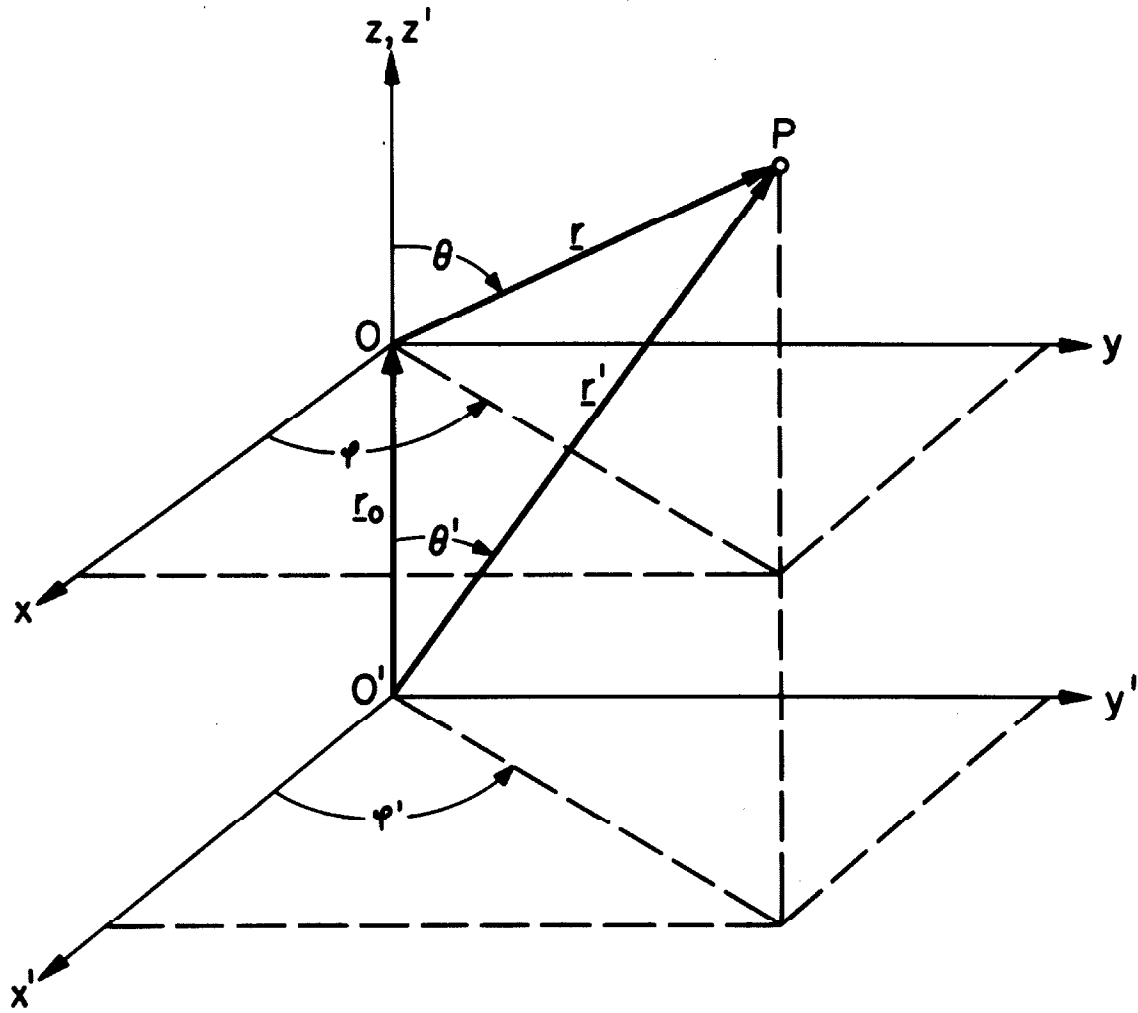


Fig. 38